# ENHANCED HEAVY OIL RECOVERY BY $CO_2$ INJECTION

Seyyed Mehdi Seyyedsar
BSc., MSc.

Submitted for the degree of Doctor of Philosophy in
Petroleum Engineering

Centre for Enhanced Oil Recovery and CO2 Solutions
Institute of Petroleum Engineering
School of Energy, Geoscience, Infrastructure and Society
Heriot-Watt University, Edinburgh
July, 2016

# Abstract

The main objective of this study was to experimentally evaluate the performance of $CO_2$ injection under various conditions of pressure and temperature (variable $CO_2$ density and oil viscosity) as an enhanced oil recovery (EOR) method for heavy oil reservoirs. The parameters that affect the amount of oil recovery by $CO_2$ injection and its underlying mechanisms were investigated. The results of coreflood experiments showed that $CO_2$ injection (i.e. vapour, supercritical, and liquid $CO_2$) can enhance heavy oil recovery. Moreover, the results revealed that the presence of dissolved gas in heavy oil significantly affects the mechanisms of oil recovery. The density of $CO_2$ is found to be a dominant factor determining the impacts of active mechanisms on the process of oil recovery. The dissolution of $CO_2$ in heavy oil and the resultant reduction of oil viscosity is an important mechanism of oil recovery regardless of the properties of $CO_2$. It was observed that the extraction of hydrocarbons plays a crucial role in the process of oil recovery when $CO_2$ is a dense fluid. Additionally, it was demonstrated that the contact of dense $CO_2$ with live heavy oil causes to the instant liberation of methane from the oil. This phenomenon leads to sharp swelling of oil and hence that enhances oil recovery by processes similar to the concept of solution gas drive. The results of compositional analysis of the oil produced in the coreflood experiments revealed that a higher quality oil than the original heavy oil in porous media is recovered by $CO_2$ injection. An important reason for the improvement of the quality of heavy oil is due to the extraction of hydrocarbon compounds by $CO_2$. In the visualisation experiments, it was observed that a significantly mobile oil-rich phase appeared in the $CO_2$-rich phase as a result of oil and $CO_2$ contact in pore spaces. The formation of this new phase is related to the extraction strength of $CO_2$ which causes the accumulation of light and intermediate components of heavy oil in the oil phase, near the interface of oil and $CO_2$. The dissolution of $CO_2$ in oil further facilitates the mobility of this phase by reducing oil viscosity. The results of this study highlight that it is crucial to evaluate the performance of any process of gas injection for EHOR under the actual conditions of the reservoirs.

# Dedication

**To Dad and Mom**,

It’s impossible to thank you adequately for everything you’ve done, for loving me unconditionally …

**تقدیم به پدر و مادر عزیزم**

# Acknowledgements

Firstly, I would like to thank my parents, Abolfazl and Aghdas, and my brother, Jalal, for their endless patience and supporting me during the period of my PhD.

I would like to express my sincere gratitude to my supervisor Professor Mehran Sohrabi for the continuous support of my PhD study and research, for his patience and motivation. His guidance helped me in all the time of research and writing of this thesis.

I greatly appreciate the constructive criticisms of the examiners of my thesis, Dr. Karl Stephen and Professor Ann Muggeridge, which significantly improved the quality of this report.

My sincere thanks go to Dr. Amir Farzaneh, my fellow labmate, for the sleepless nights we were working together, for the invaluable discussions related to our work, and for all the fun we have had in the last two years.

I would like to thank Shaun Ireland, Pantelis Tsolis, Adam Sisson, and Kamran Ahmed for providing support to execute the experimental work.

This research was carried out as a part of the Non-thermal Enhanced Heavy Oil Recovery JIP at Heriot-Watt University. The project was equally funded by Total E&P, ConocoPhillips, CONACyT-SENER-Hidrocarburos - Mexico, Pemex, Wintershall, and Eni, which is gratefully acknowledged.

Last but not least, I would like to thank my friends at Heriot-Watt University.

## Table of Contents

# List of Tables

# List of Figures

# List of Symbols

| | |
|---|---|
| ρ | *Density* |
| °C | *Degrees Centigrade* |
| °F | *Degrees Fahrenheit* |
| cc | *Cubic centimetre* |
| cc/hr | *Cubic centimetres per hour* |
| D | *Darcy* |
| ft. | *Feet* |
| g | *Gram* |
| hr | *Hour(s)* |
| k | *Permeability* |
| $k_r$ | *Relative Permeability* |
| L, µL | *Litre, microlitre* |
| m, nm | *Metre, nanometre* |
| N, mN | *Newton, millinewton* |
| $N_{ca}$ | *Capillary number* |
| Pc | *Capillary pressure* |
| ppm | *Parts per million* |
| psi | *Pounds per square inch* |

# List of Abbreviations

| | |
|---|---|
| API | *American petroleum institute (API gravity)* |
| BPR | *Back-pressure regulator* |
| CSS | *Cyclic steam stimulation* |
| DP | *Differential pressure* |
| DW | *Distilled water* |
| EHG | *Enriched hydrocarbon gas* |
| EHOR | *Enhanced heavy oil recovery* |
| EOR | *Enhanced oil recovery* |
| ESEM | *Environmental scanning electron microscope* |
| FID | *Flame Ionisation detector* |
| HPHT | *High-pressure high-temperature* |
| GC | *Gas chromatography* |
| GOR | *Gas-oil ratio* |
| GWR | *Gas water ratio* |
| ICP | *Inductively coupled plasma* |
| IFT | *Interfacial Tension* |
| MS | *Mass spectrometry* |
| OOIP | *Original oil in place* |
| PV | *Pore volume* |
| SAGD | *Steam-assisted gravity drainage* |
| SCN | *Standard carbon number* |
| Sorw | *Saturation of remaining oil after waterflood* |
| Sorg | *Saturation of remaining oil after gas or liquid $CO_2$ injection* |
| TCD | *Thermal conductivity detector* |
| TDS | *Total dissolved solids* |
| TM | *Trademark* |
| TPV | *Total pore volume* |
| VAPEX | *Vapour extraction* |
| VRG | *Viscosity reducing gas* |
| VRR | *Voidage replacement ratio* |
| WAG | *Water alternating gas* |
| SWAG | *Simultaneous water and gas* |

# List of Publications

1. Seyyedsar S.M., Farzaneh S.A., Sohrabi M., 2015. "Enhanced Heavy Oil Recovery by Intermittent $CO_2$ Injection", SPE Annual Technical Conference and Exhibition, Houston, USA, 28-30 September.
2. Farzaneh S.A., Seyyedsar S.M., Sohrabi M., 2016. "Enhanced Heavy Oil Recovery by Liquid $CO_2$ Injection under Different Injection Strategies", SPE Annual Technical Conference and Exhibition, Dubai, UAE, 26-28 September.
3. Seyyedsar S.M., Farzaneh S.A., Sohrabi M., 2016. "Experimental Investigation of Tertiary $CO_2$ Injection for Enhanced Heavy Oil Recovery", Journal of Natural Gas Science and Engineering, 34(01), pp. 1205-1214.

# CHAPTER 1: OVERVIEW

*A broad overview and motivation of this work are discussed here. In principal, this study addresses the underlying mechanisms of heavy oil recovery by application of $CO_2$ injection. The coreflood experiments were performed under reservoir conditions to truly investigate the impacts of various parameters on enhanced heavy oil recovery. Several visualisation experiments were conducted to understand the pore-scale mechanisms and interactions of the fluids used in the macroscale (coreflood) experiments. In addition, the physical properties of the recovered fluids were measured and compared at various stages of the experiments.*

For many years, the world has relied extensively, and continues to be dependent, on the production of oil as the primary source of transportation fuels. To a significant extent, the development of conventional resources could provide the world's growing demand for oil. However, most of these resources have already reached to an output plateau or they are experiencing a decline in production. In recent years, the advances in fracturing technologies coupled with the technologically advanced horizontal drilling and completion processes revolutionised global energy industry by developing oil production from tight (shale) rocks. However, the recovery performance of these reservoirs declines dramatically and the average recovery factor of these reservoirs is below 10%. In addition, the increase in global energy demand, as well as the depletion of conventional oil reservoirs cause the world, ponder over practical solutions to provide sustainable development.

The estimated volume of technically recoverable heavy oil (including extra-heavy oil) and natural bitumen (often called tar sands or oil sands) in known accumulations is about equal to the Earth's remaining conventional oil reserves. Therefore, the world will still consider heavy oil and natural bitumen resources as the Earth's crucial endowment. Heavy oil is a dense and viscous oil that is chemically characterised by its content of asphaltenes and metals.

The recovery efficiency of primary production for heavy oil reservoirs is generally poor meaning that significant quantities of oil still remain in place. Therefore, heavy oil production almost always requires measures to reduce oil viscosity. Thermal methods, albeit energy-intensive, are mainly utilised to improve recovery factor for heavy oil reservoirs. These methods such as cyclic steam stimulation (CSS) and steam-assisted

gravity drainage (SAGD) can reduce heavy oil viscosity significantly and reservoir pressure is also increased through displacement and partial distillation of the oil. However, because of various technical and economic reasons, many of heavy oil reservoirs are not suitable for thermal recovery processes. Alternative non-thermal recovery methods are, therefore, needed to improve oil recovery from these reservoirs. Non-thermal heavy oil recovery processes mainly enhance oil production by two mechanisms of oil viscosity reduction and or increasing the viscosity of injection fluid. Unlike conventional light oil, heavy oil is considerably more viscous than the displacing fluid (e.g. water and gas). Accordingly, displacement of heavy oil by fluid injection would lead to unfavourable displacement and this obviously represents a huge challenge.

In addition to enhancing conventional oil recovery, $CO_2$ injection offers considerable potential benefits for heavy oil recovery. Although $CO_2$ is not expected to develop miscibility with heavy crude oil, $CO_2$ dissolution in heavy oil can significantly reduce the oil viscosity. However, the process of $CO_2$ dissolution and diffusion in heavy oil is slow and several factors such as the oil viscosity, the density of $CO_2$, the degree of saturation of oil, and reservoir heterogeneity can also adversely affect the mixing process. Thus, $CO_2$ injection is currently perceived not to be a viable technology for enhancing oil recovery from heavy oil reservoirs.

On the other hand, $CO_2$ is the most important gas for controlling Earth's temperature. Carbon dioxide, methane, and halocarbons are greenhouse gases that absorb a wide range of energy from the Sun and Earth and then re-emit it. Some of the re-emitted energy returns to Earth and heats the surface. Overall, $CO_2$ causes about 20% of Earth's greenhouse effect while water vapour and clouds account for about 75%. However, $CO_2$ is the gas that sets the temperature because it controls the amount of water vapour in the atmosphere and thus the size of the greenhouse effect (Schmidt, et al. 2010; Riebeek, 2011).

For several decades, the concentration of the atmospheric $CO_2$ has been increasing on Earth. At the same time, average global temperatures have risen. Global warming would cause to climate change which has significant implications for human health and general wellbeing. Accelerating sea level rise and increased coastal flooding are only one of the major impacts of the global warming. Hence, to mitigate climate change, it is crucial to reduce the anthropogenic $CO_2$ emissions. For this purpose, an attractive solution is to capture $CO_2$ from anthropogenic point sources and store it in geologic formations. Economically, the geologic storage of $CO_2$ would be more attractive when it is injected into the oil reservoirs to enhance oil recovery.

The main objective of this study was to evaluate, experimentally, the performance of $CO_2$ injection under various conditions of pressure and temperature (variable $CO_2$ density and oil viscosity) as an enhanced oil recovery (EOR) method for extra-heavy oil reservoirs at their bubblepoint pressure. Many heavy oil reservoirs have initial pressures higher than the bubblepoint pressures of oil in place. Natural depletion is usually the primary option of oil recovery from a reservoir. However, as the production continued, there is a natural depletion in pressure and hence, it is necessary to support the reservoir pressures by injection of fluids. If the reservoir pressure declines below the bubblepoint, some gas will evolve from the oil solution.

Waterflood is usually the first intervention method to improve recovery factor from oil reservoirs and it is considered by many people in the oil industry as the secondary period of oil production. It is possible that water injection is started from the beginning of oil production from some reservoirs to maintain their pressure. After waterflood, other fluids may also be injected into a reservoir during its lifetime which all would be considered as the tertiary period of oil recovery. However, that may not be the case of all the oil reservoirs, in particular for the cases that sufficient amount of water for injection is not available. In all the fluid flow experiments in this study, the fluid (water or $CO_2$) injection was started immediately after saturating the core with oil at its bubblepoint pressure. Accordingly, the first period of oil recovery will be considered as the secondary period of oil recovery.

Furthermore, the parameters that impact the amount of oil recovery by $CO_2$ injection and its underlying mechanisms were investigated. In addition to fluid characterization and coreflood experiments, the microscopic mechanisms involved in the process of enhanced heavy oil recovery (EHOR) by $CO_2$ injection was investigated by a direct visualisation approach (transparent micromodel and visual-cell).

Oil is generally trapped in deep formations and both temperature and pressure usually increases with depth. Thus, $CO_2$ is mainly a supercritical fluid under the conditions of oil reservoirs. However, $CO_2$ can also be a liquid in several oil reservoirs when their temperature is relatively cold such as the West Sak heavy oil accumulation on Alaska's North Slope (Targac, et al. 2005). To the author's knowledge, no liquid $CO_2$ injection field trials have been reported in the literature for heavy oil reservoirs. Moreover, as the production continued, there is a natural decline in the pressure of the reservoirs. Therefore, when the pressure reduces to low values, $CO_2$ would be a low-density vapour gas in the reservoirs. To understand and evaluate the behaviour of $CO_2$ in its possible states in heavy oil reservoirs, the coreflood experiments were performed at three different

conditions of temperature and pressure, as evident in Figure 1-1. The critical point of $CO_2$ is 1070 *psi* at 31.1˚ *C*. At temperatures and pressures above the critical point, $CO_2$ behaves as a supercritical fluid. In this study, the process of $CO_2$ injection regardless of the state of $CO_2$ will be considered as gas injection because the density of $CO_2$ is always lower than the oil density. Although $CO_2$ at certain conditions is a liquid, it would still be a low viscosity fluid.

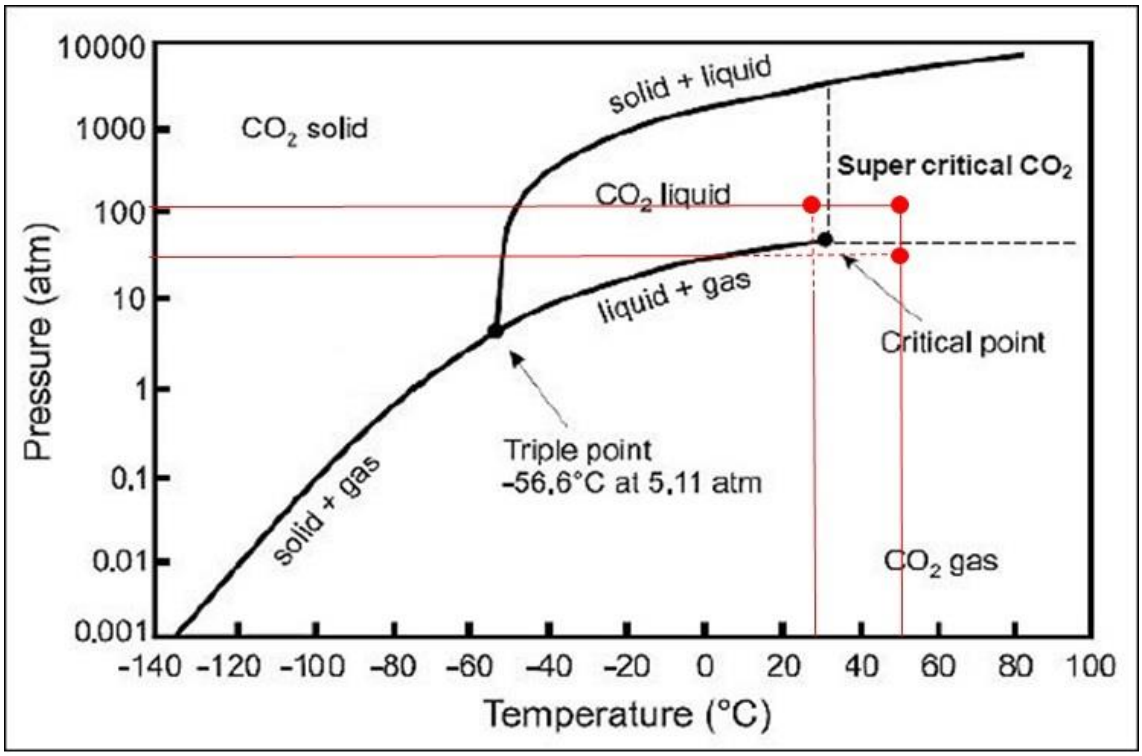


Figure 1-1: Pressure-Temperature phase diagram of pure $CO_2$ and three different conditions (red dots) of the experiments in this study. The black curves indicate the conditions that a change in the state of $CO_2$ takes place, graph adopted from Vermeulen (2011).

The fluid characterization experiments were mainly focused on the effects of solution gas (e.g. methane, $CO_2$) on heavy oil viscosity and oil swelling. Moreover, the impacts of $CO_2$ on the composition of oil under various conditions of pressure, temperature, and injection strategy were investigated. Several injection techniques such as continuous injection, intermittent injection, and water alternating gas (WAG) injection were employed in the coreflood experiments to evaluate the performance of $CO_2$ injection for EHOR under reservoir conditions. The visualisation experiments were performed using a transparent micromodel, to visually investigate the pore-scale displacement mechanisms, and also using a visual-cell setup which was designed to understand the behaviour of $CO_2$ and heavy oil under reservoir conditions.

The results of coreflood experiment showed that $CO_2$ injection under different conditions of pressure and temperature (i.e. vapour, supercritical, and liquid $CO_2$) can significantly improve extra-heavy oil recovery. The main mechanism of oil recovery is the dissolution

and diffusion of $CO_2$ in the oil which increases the mobility of oil in a porous medium. Secondary waterflood for viscous oil recovery resulted in poor sweep efficiency and the presence of water in porous medium also affects the performance of $CO_2$ injection. However, waterflood after a period of properly designed and executed $CO_2$ injection can considerably enhance the recovery factor. Moreover, it was observed that increasing the residence time of $CO_2$ in a porous medium (e.g. intermittent injection) can improve the oil recovery performance of $CO_2$ injection. The effect of $CO_2$ injection rate on the performance of oil production was also evaluated and it was observed that the mechanism of solution gas drive plays an important role in the process of oil recovery before the breakthrough of $CO_2$.

The gas chromatography (GC) analysis of the composition of produced gas during coreflood experiments revealed that the interactions between $CO_2$ and heavy oil led to the liberation of dissolved gas from the oil (e.g. methane). In the visual-cell experiments, it was observed that the contact of $CO_2$ and heavy oil caused the instant extraction of light and intermediate components from the oil. This phenomenon initially led to the swelling of oil which in porous media was noted by the increase of core pressure during the halt periods of intermittent $CO_2$ injection experiments. The compositional analysis of the remaining oil after contact with $CO_2$ revealed that $CO_2$ density is the dominant factor in determining the size of extracted components. Moreover, the effect of extraction by $CO_2$ was not uniformly distributed over the components with different carbon numbers and $CO_2$ has a higher ability to extract some components with certain chemical structure than the other molecules with the same carbon number.

The compositional analysis of core effluent indicated that the concentration of light and intermediate components in the produced oil during periods of $CO_2$ injection was higher than that of the original oil. Additionally, the viscosity of produced oil from the core was measured and compared to that of the original oil. The results show that the oil recovered during the periods of $CO_2$ injection has significantly lower viscosity.

In the micromodel experiments, the formation of a new phase in the $CO_2$-rich stream was observed as a result of $CO_2$ and oil contact in the flow paths of $CO_2$. This oil-rich has a relatively lighter colour than the oil in contact with $CO_2$ and it is significantly mobile in porous media. Because of the extraction strength of dense $CO_2$, an accumulation of light and intermediate components of heavy oil takes place in the oil phase, near the interface of oil and $CO_2$. The dissolution of $CO_2$ in the oil and the resultant oil viscosity reduction and oil swelling facilitates this process. It was also observed that $CO_2$ can reach the oil surrounded by water (either the initial water or the remaining water after a period of

waterflood) by dissolving in the water and diffusing from it into the trapped oil. The nucleation of dense $CO_2$ within the oil (surrounded by water) leads to the extraction of oil components by $CO_2$ and the enlargement of the $CO_2$-rich phase. That is, the growth of $CO_2$-rich phase within the oil surrounded by water results in enlargement of the isolated oil ganglia. This process contributes to additional oil recovery through reconnection of trapped oil and/or by changing the flow path by blocking the main flow paths of $CO_2$.

In this work, *Chapter 2* presents an introduction to the significance of heavy oil resources to supply sustainable stream of energy for the world. Then, various steps and techniques to recover heavy oil are briefly described. The literature review gives a broad overview of the theoretical aspects of heavy oil recovery and the thermal and non-thermal recovery techniques.

*Chapter 3* describes the experimental facilities and the fluids used in this work. The first part of this chapter includes an explanation of the important components of the coreflood apparatus, the micromodel apparatus, and the visual-cell setup. The properties of the core and the fluids (e.g. oil, brine, gas, and surfactant) used in this study are given in this chapter. The results of characterization tests are also presented in this chapter.

*Chapter 4* presents the results of the experiments performed under the condition that $CO_2$ was a liquid fluid. In addition to two coreflood experiments, several visualisation experiments were conducted to investigate the interactions between $CO_2$ and heavy oil under reservoir conditions. The mechanisms involved in these experiments and the impacts of those processes on the performance of oil recovery were evaluated. The compositional analysis of the effluent (e.g. oil, gas) of both coreflood experiments was performed at various periods of the tests. Furthermore, some PVT properties of the fluids were measured or calculated to improve our understanding of the impacts of the parameters affecting the process of heavy oil recovery by $CO_2$.

*Chapter 5* mainly presents the results of three coreflood experiments which were performed to investigate the efficiency of different water and gas injection techniques in the recovery of heavy oil. Two different gas composition were used in these experiments; pure $CO_2$, and an enriched hydrocarbon gas (VRG). Under the conditions of the experiments reported in this chapter, $CO_2$ was a relatively dense fluid and it was in a supercritical state. The impacts of the density of $CO_2$ on the processes contributing to heavy oil production were evaluated by comparing the results of the experiment of this chapter with the results of the experiments reported in the previous chapter. The compositional analysis and measurement of the physical properties of the effluent of the coreflood experiments were also performed and reported in this chapter.

The results of four coreflood experiments, which had been performed at the conditions that $CO_2$ was a low-density (vapour) gas, are presented in *Chapter 6*. By comparing the results of these experiments with those of the experiments reported in the previous chapters, the impacts of the mechanisms involved in the process of oil recovery by $CO_2$ injection were further investigated. In addition, the repeatability of the coreflood experiments reported in this study was evaluated. The compositional analysis and the measurement of the physical properties of the effluent of the coreflood experiments were also performed at several stages of the experiments.

A summary of the results is given in *Chapter 7* followed by conclusions and important findings of this work. Table 1-1 presents the conditions of coreflood experiments as well as the fluids used in those experiments.

Table 1-1 A summary of the coreflood experiments and their conditions in this study.

| # | Chap. | Description | Fluids | Conditions |
|---|---|---|---|---|
| 1 | 4 | Tertiary $CO_2$ Injection | Crude 'C', Liquid $CO_2$, Brine | T = 28° C<br>P= 1500 psi |
| 2 | 4 | Intermittent $CO_2$ Injection | Crude 'C', Liquid $CO_2$, Brine | T = 28° C<br>P= 1500 psi |
| 3 | 5 | Intermittent $CO_2$ Injection | Crude 'C', Supercritical $CO_2$, Brine | T = 50° C<br>P= 1500 psi |
| 4 | 5 | Tertiary $CO_2$ Injection | Crude 'C', Supercritical $CO_2$, Brine | T = 50° C<br>P= 1500 psi |
| 5 | 5 | Intermittent VRG Injection | Crude 'C', VRG, Brine | T = 50° C<br>P= 1500 psi |
| 6 | 6 | Intermittent $CO_2$ Injection | Crude 'C', Vapour $CO_2$, Brine | T = 50° C<br>P= 600 psi |
| 7 | 6 | Tertiary $CO_2$ Injection | Crude 'C' , Vapour $CO_2$, Brine | T = 50° C<br>P= 600 psi |
| 8 | 6 | Secondary $CO_2$ Injection | Crude 'C' , Vapour $CO_2$, Brine | T = 50° C<br>P= 600 psi |
| 9 | 6 | Water alternating $CO_2$ Injection | Crude 'C', Vapour $CO_2$, Brine, Surfactant | T = 50° C<br>P= 600 psi |

# CHAPTER 2: INTRODUCTION

*Heavy oil reservoirs, because of their abundant resources around the world, are regarded as a crucial alternative in propping up the rising demand for oil caused by the depletion of the other oil resources. Heavy oil reservoirs are generally known for their high oil viscosities, low dissolved-gas contents, as well as the low recovery efficiency of natural depletion of these reservoirs. In addition, displacement of heavy oil by fluid injection, even in homogeneous porous media, leads to unstable displacement and viscous fingering. Thus, heavy oil production usually requires measures to reduce the viscosity of oil in the reservoirs. The viscosity of heavy oil can be reduced dramatically by introducing heat into the reservoirs and hence thermal methods have been generally utilised to enhance oil recovery from heavy oil reservoirs. However, these methods are not always feasible options in all the heavy oil reservoirs. Significant reduction in heavy oil viscosity also takes place as a result of $CO_2$ dissolution in the oil. An advantage of $CO_2$ dissolution in oil is that the impact on oil viscosity would be irreversible as long as the pressure of system remains unchanged. Other mechanisms such as extraction of oil components by $CO_2$ are also considered as the benefits of $CO_2$ injection for EHOR. However, a complete understanding of the pore-scale interactions and also the actual mechanisms of heavy oil recovery by $CO_2$ injection are not yet well known. Moreover, the processes by which the additional heavy oil may be recovered by $CO_2$ injection are generally slow in porous media which causes to poor translation of the true potential of $CO_2$ injection. This is further complicated by the fact that many of the investigations reported in the literature have not been conducted under actual reservoir conditions. Given the above, the higher mobility of $CO_2$ compared to heavy oil in porous media is still a huge challenge. The availability of $CO_2$ is also a huge concern in many EOR projects. Therefore, it is essential to facilitate the efficiency of contact between $CO_2$ and heavy oil in porous media.*

## 2.1 Introduction

Petroleum, since the beginning of its modern history (Totten 2004), has made a major turning point in humans' life. However, the impact on every aspect of human life and lifestyle would not begin to register until the invention of the internal combustion engine (Pulkrabek 1997), some decades after the drilling of the first commercial oil well (Owen 1975). Global development and human population growth are indelibly tied together with the increased use of natural resources and energy. The world has relied extensively on the production of oil for many years and continues to be dependent on it as the primary source of energy and transportation fuels.

For several decades, development of easy access (conventional) recourses was the main supply for dampening the world's growing thirst for oil. As the oil production being continued, there is a natural decline in production as the easy access resources are depleted. This obviously is a huge challenge and perhaps the main reason for discovering and development of new oil resources as well as developing techniques to improve the average recovery factor of oil reservoirs.

Until recent years, extensive oil and gas resources have been discovered to be present in tight oil reservoirs which could not be extracted by conventional methods. The development of technologically advanced horizontal drilling and hydraulic fracturing (fracking) has provided the opportunity to access resources from shale rock or other low permeability rock formations. Tight oil formations are heterogeneous and vary widely over relatively short distances. Thus, even in a single horizontal drill hole, the amount of oil recovered may vary, as may recovery within a field or even between adjacent wells. This makes the evaluation of plays and decisions regarding the profitability of wells on a particular lease difficult. Given the above, the recovery performance of these formations declines significantly and the average recovery factor of these reservoirs is below 10% (Sandrea 2012; Zhang, et al., 2015).

Another alternative would be to exploit the abundant energy resources available as heavy oil (including extra-heavy oil) and natural bitumen. The total resources of heavy oil in known accumulations are around 3300 billion barrels and the total natural bitumen resources in known accumulations equals to 5500 billion barrels of oil originally in place. The estimated volume of technically recoverable heavy oil is higher than 400 billion barrels while that is 600 billion barrels for bitumen in known accumulations. The amount of those heavy oil reserves together is almost equal to the remaining conventional oil reserves in the world (Speight, 2011).

Historically, heavy oil was found incidentally during the search for light oil and was produced by conventional methods when economically feasible. However, primary recovery by pressure depletion in heavy oil reservoirs is generally low. Primary recovery techniques rely entirely on natural forces within the reservoir. Heavy oil reservoirs are generally known for their low dissolved gas contents and high oil viscosities and perhaps because of the nature of heavy oil, natural depletion is of minor interest for these reservoirs. Therefore, to sustain commercial production rates, heavy oil production almost always requires measures to reduce oil viscosity. This has mainly been done by introducing energy into the heavy oil reservoirs. When super-heated steam is injected into a reservoir, oil viscosity is reduced and reservoir pressure is increased through

displacement and somewhat partial distillation of the oil (Meyer & Attanasi 2003; Butler & Stephens 1981). However, many heavy oil reservoirs are not suitable for thermal recovery. For instance, thermal techniques would be ineffective and uneconomical in thin and deep heavy oil formations (Butler & Stephens 1981; Farouq Ali & Meldau 1999). Alternative non-thermal recovery methods are, therefore, needed to increase oil recovery from these reservoirs.

Unlike conventional oil, heavy oil is considerably more viscous than water and gas. Thus, displacement of heavy oil by fluid injection normally would lead to unfavourable displacement and viscous fingering which results in the early breakthrough of the injection fluid. This early breakthrough is a signature of poor sweep efficiency which makes the recovery process inefficient and uneconomic. In many conventional oil reservoirs around the world, water has been injected as the main intervention method for improving recovery factor primarily because of its availability and its favourable mobility ratio in those reservoirs. However, the global average recovery factor for waterflood in heavy oil reservoirs is low meaning that significant quantities of oil still remaining in place after waterflood. The low sweep efficiency of waterflood is generally associated with problems such as high water cut production (Jayasekera & Goodyear 2000; Mai & Kantzas 2009).

To overcome to the low sweep efficiency of waterflood, polymer viscosifiers can be added to the injection water and this, therefore, reduces the mobility ratio between water and heavy oil. Although increasing the viscosity of injection water can improve oil recovery, the problems associated with injectivity, retention time of polymer solution and polymer degradation need to be carefully considered before applying it to the reservoir. Moreover, polymer injection generally can improve oil recovery by invading the area untouched by waterflood and hence, it cannot reduce the residual oil saturation in the waterflooded area (Asghari & Nakutnyy 2008; Skauge, et al. 2012; Fabbri, et al. 2013).

Another solution to improve the efficiency of waterflood is to add surfactants to the injection water in order to reduce the interfacial tension (emulsification) between oil and water and hence, the waterflood residual oil saturation. In addition, these chemically surface-active agents can alter the wettability of reservoir rock towards the conditions of more water-wet which results in the displacing of oil from the surface of reservoir rock. Surfactants can also be co-injected or injected in an alternating manner with gas to form foam within the reservoir rock. Foam formation can reduce the mobility of the injection fluids and accordingly, it can improve the sweep efficiency of the process of oil recovery. However, factors such as surfactant adsorption on the reservoir rock, reservoir

temperature, rock type, oil type, adverse mobility ratio, and injectivity should be considered for designing a successful surfactant flooding strategy (Feng, et al. 2012; Angstadt & Tsao 1987; Hirasaki, et al. 2011; Bryan & Kantzas 2009; Emadi, et al. 2011). Gas injection (e.g. $CO_2$, hydrocarbon gases, $N_2$) is another important method for increasing recovery factor from oil reservoirs but suffers from poor sweep efficiency which stems from reservoirs heterogeneity, low density of gas, and low viscosity of gas (Lake 1989). In addition, miscibility between the oil and injected gas is not a target nor achievable at the conditions of most of the heavy oil reservoirs. Therefore, gas injection is usually perceived not to be a viable technology for improving heavy oil recovery. Carbon dioxide, however, has some characteristics which make it a potentially viable choice for enhanced heavy oil recovery. Although it is unlikely to achieve miscibility in heavy oil reservoirs, immiscible $CO_2$ injection can enhance heavy oil recovery by a number of mechanisms including; oil viscosity reduction, oil swelling, interfacial tension reduction, oil extraction, and solution gas drive (Klins 1984; Mumgan 1981; Holm & Josendal 1974; Miller & Jones 1981; Simon, et al. 1978; Campbell & Orr 1985).

Injection strategies such as water alternating gas (WAG) and simultaneous water and gas (SWAG) have been devised to reduce the gas mobility and hence increase the sweep efficiency. In WAG injection, water and gas are injected as separate slugs, whereas in SWAG injection, water and gas are injected simultaneously in the porous media (Caudle & Dyes 1958). Although improved gas handling and oil recovery have been reported in several laboratory studies and field pilots for conventional oil recovery (Christensen, et al. 2001; Sohrabi, et al. 2008; Stephenson, et al. 1993; Berg, et al. 2002; Quale, et al. 2000; Attanucci, et al. 1993), these techniques may not be proper solutions for heavy oil recovery, in particular, when $CO_2$ is injected into the porous media. The process of $CO_2$ dissolution and diffusion in heavy oil in the absence of mechanical mixing is considerably slow (Nguyen & Farouq Ali 1998) and that, therefore, requires actions to facilitate $CO_2$ mixing with heavy oil. In addition, the presence of dissolved gas in the oil further reduces the rate of $CO_2$ diffusion into the oil, in particular, when the oil is fully saturated with hydrocarbon gas (Farzaneh 2015).

## 2.2 Heavy Oil Recovery

Heavy oil is defined as a dense (low API gravity) and viscous oil that is chemically characterised by its content of asphaltenes as well as nitrogen, oxygen, and sulphur compounds and heavy-metal contaminants. Although various definitions of the characteristics of heavy oil can be found in the literature, the most generally acceptable

upper limit is set at 22˚ API gravity and a viscosity of 100 *mPa.s*. The portion of heavy oil having an API gravity of less than 10˚ often is known as extra-heavy oil. Natural bitumen (often called tar sands or oil sands) shares the behaviour of heavy oil but is yet denser and more viscous (higher than 10,000 *mPa.s*) (Meyer & Attanasi 2003).

Heavy oil and bitumen resemble the residuum from the refining of light oil. Most heavy oil resources are found at the margins of geologic basins and are thought to be the residue of formerly light oil that has lost its light-molecular-weight compounds through degradation by bacteria, water-washing, and evaporation (Larter, et al. 2003; Head, et al. 2003).

The understanding of the fluid properties is the key for successful developing of heavy oil reservoirs. The chemical differences between heavy oil and conventional oil affect their physical properties, in particular, the viscosity of oil. Viscosity, in turn, affects every other aspect of the development of a heavy oil resource. Therefore, the technology that has been developed for conventional plays cannot necessarily provide solutions to the challenges involved in heavy oil recovery. Some heavy oil reservoirs have sufficiently high temperature and hence the oil in place is fairly mobile in the porous media which can be recovered by conventional methods when economically feasible. However, most of the heavy oil reservoirs are shallow and likely to have a low temperature which is the main reason for the low mobility of oil in the reservoirs. Additionally, shallow reservoirs tend to have less effective seals which can ease the biodegradation. The less effective seal may also cause the dissolved gas to leave the oil, and hence increasing its viscosity. Another character of heavy oil reservoirs is their relatively high initial water saturation in place. This water saturation can be immobile or mobile under reservoir conditions and it can be displaced by viscous oil into the production wells (Chopra, et al. 2010).

Primary Recovery processes are mostly used to recover conventional oil. Because these methods generally rely on the natural energy of reservoirs, they are not often implemented in heavy oil resources. However, the lithology of heavy oil reservoirs, sandstone deposits with high porosity and permeability, may compensate the elevated viscosity of the oil and hence, the primary recovery from some reservoirs can be economically feasible. Many factors such as reservoir pressure, the permeability of rock, and oil viscosity affect the efficiency of primary recovery which lies between 5 and 15% for the majority of oil reservoirs (Kaczmarczyk, et al. 2013).

The term primary recovery of heavy oil, also known as cold production of heavy oil, refers to the use of operating techniques and specialised pumping equipment to produce oil without applying heat. The recovery factor by this method is generally low and the oil

production can be accompanied by sand production. Sand is allowed to enter the production wells to avoid production decline due to sand accumulation near the wellbore. To obtain economical well production rates, long horizontal wells are drilled and completed through the reservoir. These wells allow achieving large drainage area within the production zone which can improve oil production rate (Deasault 2001).

The main mechanisms of oil displacement into the production wells in the cold production of heavy oil are the expansion of the oil because of the pressure drainage and the liberation of dissolved gas from the oil (solution gas drive). Heavy oil under reservoir conditions has dissolved gas that depressurization of live heavy oil causes nucleation of dissolved gas as bubbles within the oil. The formation of these tiny gas bubbles increases the fluid volume within the reservoir (foamy oil) which displaces oil towards the production wells. These tiny gas bubbles within the oil (foamy oil) are not at equilibrium and the gas bubbles eventually coalesce to form a continuous gas phase at equilibrium with the oil phase. However, in high viscosity oils, the gas bubbles are long-lived and remain distributed throughout the oil phase (Lillico, et al. 2001).

Natural bitumen is significantly viscous that it is practically immobile in the reservoir. Therefore, the conventional recovery methods cannot be applied to these reservoirs. For oil sand deposits less than around 100 *m* deep, bitumen is recovered by mining the sands, then separating the bitumen from the reservoir rock by processing it with hot waters, and finally upgrading the natural bitumen on site to a synthetic crude oil. In deeper oil sand deposits, where the bitumen is commonly less viscous, steam is injected into the reservoir to mobilise the oil for recovery by production wells. The product may be upgraded onsite or mixed with diluent and transported to an upgrading facility.

Significant quantities of oil still remain in place after the cold production of heavy oil and this, therefore, represents a requirement for the development of innovative and efficient oil recovery methods and technologies. This is usually done either by introducing energy into the reservoirs (thermal methods) or by displacing oil by injection fluids (non-thermal methods).

## 2.3 Thermal Heavy Oil Recovery

Thermal recovery techniques are generally applied to the heavy oil reservoirs to alleviate the problem of low mobility of reservoir oil by reducing oil viscosity (Goyal & Kumar 1989). For this purpose, a considerable amount of energy often has to be added to the reservoir to accomplish the objective. It is not normally possible to raise the temperature of the oil in the reservoir without raising the temperature of any water in pore spaces and

the reservoir rock too. The thermal techniques usually include injection of hot fluids (e.g. super-saturated steam) or in-situ combustion of reservoir oil.

The hot fluid injection methods involve several techniques mainly including conventional steam floods where the injectors and producers are drilled in tight spacing patterns, cyclic steam stimulation (CSS) to allow steam to transfer the energy to the reservoir oil and then produce hot oil, and steam assisted gravity drainage (SAGD) where steam is injected into a horizontal well and production is performed from another horizontal well drilled deeper than the injection one (Prats 1982; Butler & McNab 1981; Butler & Stephens 1981). Although the heat from the injection fluid can cause to the partial distillation of oil in the porous media, no considerable chemical reaction occurs between oil and the injection fluid. In most instances, the injection pressure must exceed the reservoir pressure in order to force the steam into the formation and hence the increased reservoir pressure can also improve oil recovery.

As the heat cools off, the steam condenses as well as the evaporated oil fraction. The condensed distilled components of the oil will form a solvent in front of the reduced viscosity oil which can assist the oil recovery. However, this may not be observed in all the steam plants for heavy oil recovery. The formation of this solvent front and its assistance for oil recovery will depend on the properties of oil and also the reservoir conditions. For instance, the distilled fraction is mainly composed of aromatic and naphthenic constituents which are strong solvents of oil. However, the constituents can show paraffinic characteristics which causes to the deposition of asphaltic materials ahead of the oil front. The asphaltene deposition will close the flow pathways and hence it will adversely affect the recovery performance (Al-Murayri, et al. 2011; Ghasemi & Whitson 2015).

Although steam injection is commonly used to enhance heavy oil recovery, some technical drawbacks and disadvantages cause this method to be inefficient and uneconomical for most of the heavy oil reservoirs around the world. Because of heat losses to the around of wellbore as well as the surrounding formations of the reservoir, thermal recovery methods based on steam injection are usually not proper candidates for deep and thin reservoirs (Butler & Stephens 1981). Another drawback of these methods is the negative environmental impacts that place serious limitations on the application of heat (steam) generating plants (Century 2008; Romm 2006).

Another technique of thermal recovery is underground (in-situ) combustion of oil. In this method, either air or oxygen-enriched air is injected into a reservoir to generate heat by burning a portion of the resident oil. In-situ combustion is regarded as a high-risk process

by many, primarily because of the many failures of early field tests. Most of those failures came from the application of a good process to the wrong reservoirs or the poorest prospects. This process is widely attractive for the reservoirs with high pressure, high clay content, and severe wellbore heat losses at which steam injection would be inefficient. In addition, in-situ combustion can be considered for heavy oil recovery in locations where limited water supply is available for steam generation (Sarathi 1999).

In this method, however, a large compression ratio is required to inject air into the formations. Excessive heat losses to the surrounding formations make it uneconomical for thin reservoirs. Poor sweep efficiency is another problem regard to the implementation of this method for heavy oil recovery. Moreover, other factors such as the nature of oil, gravity, and properties of reservoir rock should be considered for designing an efficient strategy. The problems regard to corrosion have also been well-documented in the literature (Thomas 2008).

Some other thermal recovery methods such as hot air or gas injection, a combination of steam and solvent injection have also been devised to improve heavy oil recovery (Romanowski & Thomas 1985; Bracho & Oquendo 1991; Zhao 2007). Given the above, all the above-mentioned methods need to be economically feasible to be applied as an enhanced oil recovery method. An estimate made by Farouq Ali & Meldau (1999) suggested that for various technical and economic reasons, almost around half of the known heavy oil reservoirs are not suitable targets for thermal recovery processes.

## 2.4 Non-thermal Enhanced Heavy Oil Recovery

Various non-thermal techniques have been suggested and sometimes applied to improve average recovery factor for heavy oil reservoirs. These techniques include injection of fluids to displace oil or ease flow of oil towards the production wells. Heavy oil is very viscous and any effort to recover heavy oil generally suffers from the poor mobility of the oil.

In general, the displacement of a fluid by a less viscous one leads to the creation of fingers of low viscosity fluid penetrating the high viscosity fluid (Homsy 1987; Doorwar & Mohanty 2015). Therefore, the early breakthrough of injection fluids and the remaining high saturation of oil (bypassed oil) are common characteristics of any effort for heavy oil recovery. The displacement in heavy oil reservoirs is usually immiscible meaning that it is characterised by a simultaneous flow of multiple phases. A fundamental understanding of immiscible displacement of fluids in oil reservoirs was reported by Buckley and Leverett (1942) in their study of fractional flow. For linear two-phase flow

at the macroscale, the Buckley-Leverett solution provides a saturation profile with a sharp front along the flow direction. It should be mentioned that the solution neglects the effects of capillary pressure and gravity on the flow. Moreover, it is assumed that the fluids are Newtonian and incompressible and the initial saturations are uniform within the system. The impacts of those factors and microscale heterogeneities of porous media on the flow are usually considered by modifying relative permeability functions.

As the flow continues before the breakthrough of the displacing fluid, the saturation of fluids becomes a multiple-valued function of the distance moved by the displacing fluid which can be overcome by material balance considerations. Although the Buckley-Leverett solution ignores capillary pressure, it suggests that the flood front will exist as a stabilised zone of finite length with a saturation gradient. This theory was first confirmed by Terwilliger, et al. (1951) in their study of applying the frontal advance theory to a gravity drainage system. It was reported in that study that the shape of the flood front was constant with respect to time. It was proven by Welge (1952) that the velocity of the stabilised zone is proportional to the slope of the fractional flow curve at the point of the saturation of the displacing fluid at the leading edge of the stabilised zone. This slope is defined by a line drawn tangent to the fractional flow curve from the initial saturation of the displacing fluid. The fractional flow theory predicts that under constant conditions, as the viscosity of the displaced fluid (oil) increases, the slope of the tangent line also increases (Welge 1952). For instance, this implies that the flood front will move at a higher velocity if the oil viscosity is high compared to the case that the oil viscosity is lower. Thus, the frontal advance theory predicts that the injection fluid will have an early breakthrough in more viscous oil systems.

In general, local fluctuations in permeability could trigger frontal instability in porous media. In an analytical solution for two-phase immiscible displacement in 1D composite porous medium, Wu, et al. (1993) extended the Buckley-Leverett theory to flow in a one-dimensional heterogeneous porous medium. The results of that study showed that the displacement could be characterised by discontinuities in saturation profile across the interfaces of adjacent flow domains. Therefore, by extending the Buckley-Leverett theory to flow in heterogeneous systems, it will be possible to capture channelling (or fingering) caused by heterogeneities for immiscible displacements.

In actual systems, the fingering would be initiated by the variations in fluids properties (e.g. viscosity and density) and rock properties. The differences in viscosity or density would accelerate the growth of fingers along the paths previously developed due to permeability variations. In microscale, several small fingers (or branches) are formed

during an unstable displacement along the main fingers. These side branches do not grow as much as the main fingers and the displacing fluid reaches the production outlet by the shortest (least resistance) path (Doorwar & Mohanty 2011).

In high-resolution reservoir simulation studies, this aim is usually achieved by accounting for small heterogeneities in the rock permeability (Fayers, et al. 1994; Garcia & Pruess 2003). However, these simulations are computationally expensive and often field data at high resolutions are not available. Thus, to simulate unstable displacements with conventional simulators, the relative permeability functions need to be modified to account for physics such as fingering.

To overcome the low sweep efficiency in heavy oil reservoirs, either the mobility of oil should be improved or the saturation of oil bypassed by injection fluids should be reduced. Two mechanisms of oil viscosity reduction and reducing the mobility of injection fluids are, therefore, the main processes contributing to oil recovery in any non-thermal heavy oil recovery method. Reducing the mobility of injection fluid as well as the viscosity of oil generally, improve sweep efficiency by increasing contact between the injection fluids and oil. Thus, higher area of the formation can be invaded by the injection fluids and this obviously increases the volumetric sweep efficiency of the EOR technique.

### 2.4.1 Water-based Fluids Injection

In many reservoirs around the world, water has been injected as the first intervention method for improving recovery factor and generally, this aim has been achieved either by maintaining reservoir pressure or by displacing oil by the injection water. In addition, waterflood has sometimes been done to dispose produced brine from reservoirs (Carig 1971; Willhite 1986). The viscosity of water is significantly lower than heavy oil and this would lead to unstable flood front and viscous fingering.

The performance of waterflood for heavy oil recovery is mainly affected by viscous and capillary forces, albeit in varying degrees. Viscous forces are generally important at early times of injection where the pressure gradient is significantly high in porous media. Despite the early breakthrough of water due to unstable nature of adverse mobility ratio conditions, a considerable amount of oil can be recovered after the point of breakthrough which makes the behaviour of waterflood for heavy oil recovery similar to the waterflood in oil-wet systems (Tang & Kovscek 2011). Laboratory investigation of the role of capillary forces on the performance of waterflood for heavy oil recovery by Mai & Kantzas (2009) showed that capillary forces, to a large extent, are responsible for oil production at late times of waterflood.

Waterflood is a relatively inexpensive and easy to control process that can be applied in heavy oil reservoirs. However, most of the field applications for heavy oil recovery have shown poor results (Ahmadloo, et al. 2010; Kumar, et al. 2008). That is, it is important to improve the recovery factor from heavy oil reservoirs by changing the properties of water or by injection of water in a combination with other fluids. Furthermore, the performance of waterflood for heavy oil recovery can be improved if waterflood is applied at optimum pressure.

The properties of injection water can be altered by changing its composition or by adding chemical to the water. Recent investigations have shown that the composition of the brine can affect the performance of oil recovery achieved by waterflooding (Jadhunandan & Morrow 1995; Yildiz & Morrow 1996; Fathi, et al. 2011). However, most of the successful cases reported in the literature are about light oil systems where the viscosity of brine would be fairly sufficient to sweep oil from pore spaces.

The sweep efficiency of waterflood can be improved by adding chemicals to the brine. These chemicals are typically divided into two different groups; polymers and alkaline-surfactants. Polymers are added to the injection water to change and perhaps optimise flow pattern in the reservoirs (to improve sweep efficiency). This purpose is mainly achieved by reducing the mobility (relative permeability) of injection fluid (Skauge, et al. 2014; Fabbri, et al. 2013; Fletcher, et al. 2013). The reduction of water cut and sand cut has also been reported for polymer injection (Zaitoun, et al. 1992; Sydansk & Seright 2007).

Polymers have significantly higher viscosity than water and hence the mobility ratio is improved by polymer injection. However, injection of a fluid of high viscosity means that higher injection pressure is needed to pump the fluid through the injection wells into the porous media. This may not be possible to be applied in all the heavy oil reservoirs. Many heavy oil reservoirs are relatively shallow and can have a maximum formation pressure lower than the design pressure for polymer injection. To compensate this, the volume of polymer pumped into the reservoir should be reduced. Accordingly, oil production rate would be lower and it may not be economically feasible. Although polymer injection is the simplest among chemical EOR processes, it is still complex and hence, care should be taken for designing polymer solutions and applying them to a reservoir.

The success of a polymer oil recovery process hinges on the ability to maintain mobility control from the injection wells towards the production ones. In other words, it is crucial that the injected solution can maintain its quality and physical properties that provide mobility control, not only near the injection wells but also far away through the formation.

A number of factors can affect the properties of a polymer solution during its transport in porous media. First, the adsorption (retention) of polymer on reservoir rock will erode the polymer bank and as a result, effective propagation of polymer is adversely affected. Polymer solutions can mechanically degrade and lose viscosity during flow through rock at high rates. Moreover, polymers can be degraded chemically under reservoir conditions. Polymer rheology in porous media affects both injectivity and sweep efficiency during an EOR process. Polymer solutions are generally non-Newtonian fluids and depending on the type of polymers in the solutions, they can show shear thinning or thickening behaviour at low-to-high fluid velocities in porous media. Therefore, the viscosity of solution would be affected by pore geometry and size distribution. Under certain conditions, polymers can have reactions with salt molecules in the injection solution or the brine in the formation which can affect the viscosity of polymer solutions. To avoid adverse impacts, the phase behaviour of polymer and reservoir fluids should be studied under reservoir conditions. Investigations have shown that (transport) time is also an important parameter to consider for designing polymer solutions. Biodegradation can result in the retardation of polymer solutions in porous media.

Problems associated with retention time (adsorption on rock surface), mechanical and chemical degradation, rheology, phase behaviour (e.g. hydrolysis), biodegradation, and thermal stability have been well discussed and documented in the literature (Huh, et al. 1990; Manichand & Seright 2014; Maerker 1975; Southwick & Manke 1988; Clifford & Sorbie 1985; Seright, et al. 2011; Zaitoun, et al. 1998; Hill, et al. 1974; Zheng, et al. 2000; Li, et al. 2014; Wellington 1983; Samuelson & Constien 1996).

The remaining oil in the waterflooded area is generally trapped by capillary forces and therefore, surfactants are added to injection water to mobilise (wash out) the residual oil in the waterflooded area. Surfactants can enhance microscopic recovery by reducing capillary forces in addition to boosting sweep efficiency. The main underlying mechanisms of oil recovery of surfactant injection are a reduction of oil/water IFT and or wettability alteration (Uren & Fahmy 1927). In addition, surfactants are combined with gas injection to control the mobility of gas in porous media by generating in-situ foam (Emadi, et al. 2011). Another advantage of foam is that it can be utilised at high-temperature reservoirs while polymer degradation is a concern at those reservoirs (Sirvastava & Nguyen 2010).

In addition to the ability to lower the oil/water IFT, a proper surfactant solution must have a good aqueous stability under reservoir conditions. The impacts of the salinity of injection solution and formation brine on the solubility of surfactants should be carefully

investigated to optimise the surfactant concentration in the solution (optimal salinity). Oil composition has a small, but still significant, effect on the optimal salinity of the surfactant solutions. Phase behaviour tests must be repeated with live crude oil to measure the shift in optimal salinity. EOR surfactants are generally poorly soluble in brine (and in oil) and often prefer adsorption at interfaces, either oil/brine or brine/rock interface.

The adsorption of surfactant on reservoir rock surface has crucial impacts on the performance of any surfactant-based EOR. The physical properties of rock such as porosity and permeability affects the adsorption process and hence the amount of surfactant required to enhance oil recovery. The rule of thumb in impacts of physical properties of rock on surfactant adsorption is that higher surfactant concentration is needed in lower permeability rocks. The chemistry of rock surface (e.g. sandstones, carbonates) is another important factor in designing surfactant EOR.

Similar to polymer EOR, surfactant injection is a sensitive and complex process that requires serious attention to various factors and parameters such as solubility, temperature stability, phase behaviour, formation fluids properties, and adsorption (Glover, et al. 1979; Flaaten, et al. 2009; Gupta & Mohanty 2010; Gupta & Trushenski 1979; Hirasaki 1982; Hirasaki, et al. 2011).

A surfactant injection-related concept for improving oil recovery is to generate surfactant in situ by injecting an alkaline solution (Atkinson 1927). According to Jennings (1975), the original concept of alkali flooding was the reduction of oil/water IFT by in-situ generation of soap, which is an anionic surfactant. Moreover, Alkali can alter formation wettability to reach either more water-wet or more oil-wet states. To reduce adsorption of surfactant during displacement through the formation and sequestering divalent ions, alkali is added to surfactant solution. Alkalis are generally added to surfactant solutions as sacrificial agents to reduce the adsorption of more expensive surfactants, most likely anionic surfactants (Nelson, et al. 1984; Hirasaki, et al. 2011). However, some disadvantages associated with the use of alkali in chemical EOR such as reduction of polymer viscosity, emulsification formed by the produced fluids, formation scaling, and corrosion hazards have been addressed in the literature (Wu, et al. 2001; Cao, et al. 2007; Zhang, et al. 2015). Alkali and surfactant can also be injected to recover heavy oil by emulsification and wettability alteration along with displacing the oil as a lower-viscosity, oil-in-water emulsion (Liu, et al. 2006; Bryan, et al. 2008).

Historically, a voidage replacement ratio (VRR) of unity is assumed to be optimal for oil recovery by waterflood regardless of whether production occurs from a conventional oil reservoir or a heavy oil reservoir. In other words, it is assumed that the most oil recovery

occurs when the reservoir pressure is maintained constant. In a reservoir under waterflood, the recovery factor can be improved by maintaining production rates fast enough to cause the reservoir pressure to decline below the bubblepoint. Operating below bubblepoint pressure, some gas evolves from the oil solution which can improve recovery during waterflood compared to operating at or above the bubblepoint (Dyes 1954; Jerauld 1997; Vittoratos, et al. 2011, Delgado, et al. 2013; Kim, et al. 2015). Furthermore, it has been shown that when the pressure of the heavy oil is reduced to some point below the bubblepoint pressure, gas bubbles evolve within the oil emulsifies with water which increases the relative mobility of the oil mixture. However, for the effect to be significant, the oil must lie within a certain ˚API range (Vittoratos & West 2010).

Given the above, many disadvantages are prescribed to dropping the reservoir pressure below the bubblepoint pressure. For instance, the introduction of an additional phase may reduce the relative permeability of the oil. Moreover, as the heavy oil reservoir depletes below the bubblepoint, gas comes out of solution and the oil phase viscosity increases which makes oil less mobile (Firoozabadi 2001). This problem is compounded because gas flows easily in porous media and can be produced rapidly. Thereby, reservoir pressure reduces at a much faster rate compared to depletion above the bubblepoint. Furthermore, problems related to subsidence can occur when the rock compressibility is relatively large (Delgado, et al. 2013).

### 2.4.2 Gas (or Solvent) Injection

Gas injection is the oldest and most utilised EOR strategy around the world. In many conventional oil reservoirs, solvent or enriched hydrocarbon gas (EHG) injection is likely to improve recovery factor by miscible displacement. In heavy oil resources, however, miscibility is not a target nor achievable due to the nature of oil as well as the reservoir conditions (e.g. pressure). Thus, gas injected into heavy oil reservoirs would improve recovery factor by pressure maintenance and displacing oil towards the production wells. In addition, solvents are injected into heavy oil reservoirs to reduce oil viscosity and hence improve the oil mobility. Solvent injection can also be performed for in-situ extraction of light and intermediate fraction of heavy oil.

The main drawback of gas injection is the relatively high mobility of gas in porous media which leads to poor sweep efficiency in the reservoirs. The low density of gas and reservoir heterogeneity are other factors reducing the sweep efficiency (Lake 1989). In heavy oil reservoirs, the poor efficiency of gas injection would be significant because of the high viscosity of the oil and relatively higher permeability of the reservoirs. Therefore,

gas (or solvent) injection is usually combined with a higher viscous fluid (e.g. water) injection to control gas (or solvent) mobility in porous media. Other strategies such as cyclic solvent injection (huff-n-puff) and vapour extraction (VAPEX) have also been investigated for solvent and gas injection for heavy oil recovery.

Cyclic gas (or solvent) injection is a single-well EOR method and it is performed by injecting gas (huff cycle) followed by a period of shut-in and then the well is returned to production (puff cycle). During the shut-in periods, the gas is allowed to interact with the resident oil. The main mechanisms of oil recovery in this process are the oil viscosity reduction, the oil swelling, and the solution gas drive (Sayegh & Maini 1984; Qazvini Firouz & Torabi 2014).

VAPEX is another promising solvent injection process (Butler & Mokrys 1989; Dunn, et al. 1989). VAPEX is a solvent analogue of SAGD in which the oil viscosity is reduced by solvent dissolution instead of heat. A solvent is injected from the upper of two horizontal wells and dissolved in the oil which reduces the oil viscosity and allows it to drain by gravity. Low production rates are an economic barrier to VAPEX as a commercial process because the mobilisation of oil by VAPEX relies on mass diffusion. One advantage of VAPEX highlighted in the literature is the promotion of asphaltene precipitation by the injected solvent which could lead to a higher quality oil recovery (Mokrys & Butler 1993; Das & Butler 1998; Nghiem, et al. 2001). Nonetheless, asphaltene precipitation could lead to formation damage even in high permeability porous media. Thus, VAPEX may not be a viable process because of low rates of oil production despite significant higher quality oil recovery (Haghighat & Maini 2010). The main mechanism of oil production by VAPEX is the oil viscosity reduction which is controlled by the diffusivity of the solvent into the oil and the degree of viscosity reduction. On the other hand, the cost of solvent and the recovery of that are the main problems in VAPEX (Talbi & Maini 2008).

Several studies have also investigated the performance of $CO_2$ as a solvent in VAPEX. The results have shown that $CO_2$ dissolution in heavy oil could cause to a huge reduction in the oil viscosity, in particular at low temperatures and high pressures. Dunn, et al. (1989) compared the performance of pure ethane and $CO_2$ as solvents for VAPEX and reported that $CO_2$ could result in a higher oil recovery. $CO_2$ can also be added to propane or butane to increase the vapour pressure of them. That would maintain the dew point pressure of the injected solvent above the reservoir pressure and hence, the operation costs of the process can be reduced (Badamchizadeh, et al. 2008). $CO_2$ can also be used as a non-condensable gas in VAPEX and it is a better choice than methane because $CO_2$ is

more soluble in heavy oil (Svrcek & Mehrotra 1982). Given the above, a major drawback of the cyclic gas injection and VAPEX process is that the reservoir pressure is usually reduced to low values during the blowdown which would increase the viscosity of the resident oil.

### 2.4.3 Immiscible $CO_2$ Injection

Carbon dioxide is of great interest for enhancing heavy oil recovery because of its characteristics such as high solubility in oil and oil viscosity reduction. The mechanisms that immiscible $CO_2$ injection could enhance oil recovery have been investigated for many years. However, the impact and significance of them have not been well documented in the literature, in particular for heavy oil recovery. For instance, the mechanism of extraction of hydrocarbons by $CO_2$ is generally neglected for heavy oil reservoirs because it is perceived as a slow process. These mechanisms include:

- Oil viscosity reduction
- Oil swelling
- IFT reduction
- Extraction of hydrocarbons
- Asphaltene precipitation

A remarkable decrease in oil viscosity by $CO_2$ dissolution, in particular for viscous oils, has been reported in the literature (Miller & Jones 1981; Klins 1984; Sayegh, et al. 1990). Although heavy oil viscosity reduction by heat is more significant than that by $CO_2$ dissolution, the impact on oil viscosity is reversible by thermal processes because of heat losses to the surrounding formations. Also, oil heated by thermal processes can have a higher viscosity than the original oil because of the distillation of light and intermediate cuts from the oil by heat. However, the oil viscosity reduction by $CO_2$ is relatively irreversible in porous media as long as the pressure of the system remains constant. $CO_2$ dissolution in oil can also result in oil swelling which increases oil volume (saturation) in porous media and hence improves the relative permeability for oil (Li, et al. 2013).

Another benefit of $CO_2$ dissolution in oil is a reduction in interfacial properties of the oil-$CO_2$ system. This phenomenon would contribute to additional oil recovery in light oil systems where the reduction of IFT between the oil and $CO_2$ could induce miscibility. However, in the heavy oil systems, the decrease in the IFT is not as significant as the light oil systems and the contact between the heavy oil and $CO_2$ would remain immiscible (Yang, et al. 2005).

A well-established impact of $CO_2$ injection for oil recovery is the extraction of light and intermediate components of oil by the injected $CO_2$. This process is mainly considered as an active mechanism of recovery when the reservoir oil is a light oil (Hwang, et al. 1995; Al Ghafri, et al. 2014; Wang, et al. 2016). Accordingly, the parameters affecting this process are still missing and the effects of the mechanism of extraction on heavy oil recovery are less pronounced. Moreover, the impacts of this process on oil recovery and flow distribution in porous media have not been fully understood.

One of the major technical challenges in $CO_2$ injection for oil recovery is the possibility of precipitation or deposition of asphaltene and its adverse impacts on the efficiency of oil recovery (Vazquez & Mansoori 2000). Although asphaltene precipitation could cause the production of less viscous oil in comparison with the original oil in a reservoir, asphaltene deposition on the rock surface may lead to wettability alteration and reservoir plugging. Asphaltene precipitation can also cause well damage and plugging of the production pipelines and equipment (Buckley & Jianxin 2002; Idem & Ibrahim 2002). Given the above, many field data have shown that asphaltene precipitation is more likely in the light oil systems because the asphaltene solubility is lower in light oils compared to heavy oils (Behbahani, et al. 2012). In addition, the tendency of asphaltene particles to flocculate and make larger particles is higher by increasing temperature (Zanganeh, et al. 2011).

A huge concern about $CO_2$ injection for heavy oil recovery is the slow dissolution and diffusion of $CO_2$ in heavy oil in porous media. Several factors govern this process such as the area of contact between $CO_2$ and oil, viscosity of oil, density of $CO_2$, temperature, and rock heterogeneity (Unatrakarn, et al. 2011; Ratnakar & Dindoruk 2015). Immiscible $CO_2$ injection for heavy oil recovery is usually carried out through; continuous $CO_2$ injection, $CO_2$ huff-n-puff, injection of slugs of $CO_2$ alternating water ($CO_2$ WAG), and simultaneous water and $CO_2$ injection ($CO_2$ SWAG). To get the advantage of $CO_2$ dissolution in heavy oil and its resultant impacts on oil properties, it is important to facilitate the contact between $CO_2$ and heavy oil in place. Given the above, the impacts of injection strategies on oil recovery should be carefully studied. In addition, it is important to optimise the injection strategies and also devise new techniques to enhance heavy oil recovery by $CO_2$ injection. Another concern about $CO_2$ EOR is the availability of $CO_2$ for injection into the formations. Therefore, $CO_2$ utilisation needs to be evaluated in any injection technique.

Most of the investigations of the performance of $CO_2$ injection for heavy oil recovery have been performed on the dead oil systems in which the oil had no initial dissolved gas

(Sankur & Emanuel 1983; Sayegh & Maini 1984; Nguyen & Farouq Ali 1993; Dong & Huang 2002; Emadi, et al. 2011; Qazvini Firouz & Torabi 2014; Seyyedsar, et al. 2014). However, the oil in actual reservoirs is usually a live crude with dissolved gas in the oil. The presence of dissolved gas in the oil would affect the performance of $CO_2$ injection, in particular when the oil is fully saturated with hydrocarbon gas (Hamouda & Alipour Tabrizy 2013; Farzaneh 2015). Furthermore, several different factors such as oil type, viscosity of oil, and density of $CO_2$-rich phase can affect the process of heavy oil recovery by $CO_2$ injection. Therefore, it is crucial to perform a thorough investigation of the performance of $CO_2$ EHOR and study the parameters that impact the process of heavy oil recovery by $CO_2$ injection and its underlying mechanisms.

The work in this thesis follows a study of the impacts of $CO_2$ on the physical properties of two different heavy crude oils, 'C' and 'J'. Using dead oils, Emadi (2012) performed several micromodel and coreflood experiments to investigate the potential of various $CO_2$ injection scenarios for heavy oil recovery under their reservoir conditions. In that work, it was discussed that the dissolution of $CO_2$ in the oil and the resultant oil viscosity reduction and oil swelling are the main reasons for heavy oil recovery while when the pressure of the system is high, the mechanism of extraction could be dominant at late times of the process. The formation of a new phase in the oil blobs which were not in direct contact with $CO_2$ was also reported. Nevertheless, the potential mechanisms behind this observation were still missing. Using crude 'J', Farzaneh (2015) performed several coreflood experiments under the conditions that $CO_2$ was a liquid. The impact of dissolved gas in the oil on the process of heavy oil recovery by $CO_2$ injection were investigated. It was observed that the performance of heavy oil recovery by $CO_2$ injection is significantly dependent on the presence of light hydrocarbon components in the oil phase. Moreover, the impact of gravity on the efficiency of the displacements was investigated by performing coreflood experiments in vertical and horizontal conditions. Nonetheless, the underlying mechanisms of oil recovery were still unidentified. For instance, it was not clearly known that how the presence of hydrocarbon gas in heavy oil affects the process of oil recovery by $CO_2$ injection. Another major concern was about the efficiency of oil recovery by injection $CO_2$ and that, new injection strategies are needed to reduce the utilisation and recycling of $CO_2$.

In this thesis, the mechanisms of enhanced heavy oil recovery by $CO_2$ injection have been identified and discussed by performing several coreflood and visualisation experiments using fluids under reservoir conditions. In addition, a new injection strategy and its benefits are introduced and discussed.

# CHAPTER 3: PROCEDURES, EXPERIMENTAL FACILITIES AND FLUIDS

*A combination of different instruments has been used in this study to investigate the impact of various parameters and injection strategies on enhancing heavy oil recovery by $CO_2$ injection. A state-of-the-art high-pressure and high-temperature (HPHT) coreflood rig was employed to perform coreflood experiments. In addition, several visualisation experiments were conducted using an HPHT micromodel rig as well as a visual-cell setup to investigate the underlying mechanisms of heavy oil recovery by $CO_2$ injection.*

## 3.1 Procedures

The coreflood experiments and their details were briefly described in Table 1-1. All the experiments were started by saturating the core with brine, Figure 3-1. The dead brine was injected into the core and the permeability of the core was measured. Next, the brine saturated with methane was injected to displace the dead brine from the rock. It should be mentioned that all the fluids injection were performed at the conditions of each experiment and the live fluids were also prepared at those conditions. The live oil injection was performed to establish the initial water and oil saturations in the core. Each experiment was continued by the injection of different combinations of fluids (mainly water and $CO_2$) into the oil-saturated core. The exact combination of fluids and their volumes injected into the core will be described at the beginning of each coreflood experiment in the next chapters. At the end of each experiment, the system was prepared for the next experiment by successive injection of methanol and toluene into the core and connections.

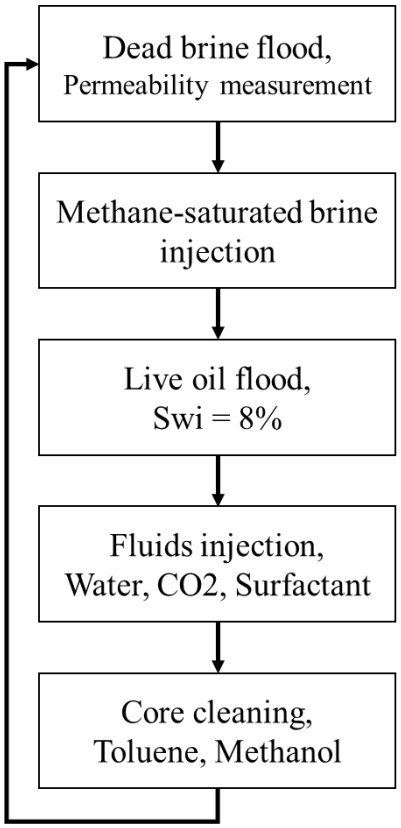


Figure 3-1: A general procedure of the coreflood experiments.

Table 3-1 reports the main objectives of each coreflood experiment and also the measurements performed during or after those experiments. The experiments were performed at three different conditions of pressure and temperature under which $CO_2$ had different physical properties. Unless otherwise stated, all the fluids have been injected at 7 $cm^3/hr$ which equals to the frontal velocity of 1 *ft/day*. A general objective of all the coreflood experiments was to evaluate the performance of different combinations of $CO_2$ and water injection for live extra-heavy oil recovery. Another important objective of those experiments was to investigate and identify the mechanisms of oil recovery by $CO_2$ injection and also to evaluate the contribution of those processes on the efficiency of oil recovery. In addition, the properties of produced oil from the core during and after the experiments were measured. The properties of the core and the fluids are delineated in this chapter. To clearly understand and identify the mechanisms involved in the coreflood experiments, a series of visualisation experiments was performed mainly under the conditions of the coreflood experiments that $CO_2$ was a liquid fluid. The procedures, results, and observations made in these experiments are reported in the next chapter.

Table 3-1 Objectives and measurements for the coreflood experiments.

| # | To Evaluate | Measurements | Properties of Fluids |
|---|---|---|---|
| 1 | $CO_2$ after waterflood for EHOR<br>Impact of extraction of hydrocarbons<br>Impact of dissolved gas in oil | Recovery<br>GOR<br>Composition of produced oil<br>Metal Contents in produced oil | $\mu_{oil} = 12100\ cp$<br>$\mu_{brine} = 0.89\ cp$<br>$\mu_{CO2} = 0.07\ cp$ |
| 2 | Intermittent $CO_2$ injection for EHOR<br>Impact of extraction of hydrocarbons<br>Impact of dissolved gas in oil | Recovery<br>GOR<br>Composition of produced gas<br>Composition of produced oil<br>Metal contents in produced oil | $\mu_{oil} = 12100\ cp$<br>$\mu_{brine} = 0.9\ cp$<br>$\mu_{CO2} = 0.07\ cp$ |
| 3 | Intermittent $CO_2$ injection for EHOR<br>Impact of oil viscosity and $CO_2$ density<br>Impact of extraction of hydrocarbons<br>Impact of dissolved gas in oil | Recovery<br>GOR<br>Composition of produced gas<br>Viscosity of produced oil | $\mu_{oil} = 1600\ cp$<br>$\mu_{brine} = 0.6\ cp$<br>$\mu_{CO2} = 0.03\ cp$ |
| 4 | $CO_2$ after waterflood for EHOR<br>Impact of oil viscosity and $CO_2$ density<br>Impact of extraction of hydrocarbons<br>Impact of dissolved gas in oil | Recovery<br>GOR<br>Composition of produced gas<br>Composition of produced oil<br>Viscosity of produced oil | $\mu_{oil} = 1600\ cp$<br>$\mu_{brine} = 0.56\ cp$<br>$\mu_{CO2} = 0.03\ cp$ |
| 5 | Intermittent VRG injection for EHOR<br>Impact of extraction of hydrocarbons<br>Impact of injection gas composition<br>Impact of dissolved gas in oil | Recovery<br>GOR<br>Composition of produced gas<br>Viscosity of produced oil | $\mu_{oil} = 1600\ cp$<br>$\mu_{brine} = 0.56\ cp$ |
| 6 | Intermittent $CO_2$ injection for EHOR<br>Impact of oil viscosity and $CO_2$ density<br>Impact of extraction of hydrocarbons<br>Impact of dissolved gas in oil | Recovery<br>GOR<br>Composition of produced gas<br>Viscosity of produced oil | $\mu_{oil} = 3500\ cp$<br>$\mu_{CO2} = 0.02\ cp$ |
| 7 | $CO_2$ after waterflood for EHOR<br>Impact of oil viscosity and $CO_2$ density<br>Impact of extraction of hydrocarbons<br>Impact of dissolved gas in oil | Recovery<br>GOR<br>Composition of produced oil<br>Viscosity of produced oil | $\mu_{oil} = 3500\ cp$<br>$\mu_{CO2} = 0.02\ cp$ |
| 8 | Waterflood after $CO_2$ for EHOR<br>Impact of injection rate and time | Recovery<br>GOR<br>Composition of produced oil<br>Viscosity of produced oil | $\mu_{oil} = 3500\ cp$<br>$\mu_{CO2} = 0.02\ cp$ |
| 9 | Water alternating $CO_2$ for EHOR<br>Surfactant and $CO_2$ injection<br>Repeatability of coreflood experiments<br>Impact of injection rate and time | Recovery<br>GOR | $\mu_{oil} = 3500\ cp$<br>$\mu_{CO2} = 0.02\ cp$ |

## 3.2 Coreflood Apparatus

The state-of-the-art coreflood apparatus (rig) which was used for performing fluid characterization and coreflood experiments is shown schematically in Figure 3-2. A temperature-controlled air oven (Carbolite) is used to house the core-holder, storage vessels, back-pressure regulator (BPR), pipelines, and connections (all the components

of the rig other than the pumps) at a constant temperature. The rig consists of five Proserv storage vessels to maintain fluids (e.g. oil, brine, gas, nitrogen, and chemical) under the pressure and temperature of each experiment. The coreflood rig was capable of performing experiments at temperatures as high as 150˚ *C* and pressures up to 10000 *psi*. Given the above, all the required valves could be controlled from the outside of the oven. That, therefore, has ensured that the experiments were performed under constant and well-controlled temperature.

Three pairs of Quizix (Q5000-10 K) pumps are used to deliver the fluids from high-pressure storage vessels into the core and also to apply overburden pressure on the core and supply pressure to the BPR. The core effluent is carried through the BPR where the pressure would drop to atmospheric pressure and hence any dissolved gas would be liberated. Then, the separated liquids are collected in a graduated cylinder while gas production is measured by a Zeal wet-test gas flowmeter. The composition of produced gas would be analysed by an in-line GC instrument (Agilent Micro-GC). The detection limit of GC is less than 10 ppm meaning that it offers accuracy of measurement of +/-0.01% of the mole. The standard conditions at which the effluent volumes were measured in this study were 20˚ *C* and ambient pressure.

The graduated cylinders and the gas flowmeter used in this study had a high accuracy of measurements. For instance, the maximum error of measurements of the liquids by a graduated cylinder in this study was +/-0.2 $cm^3$ whereas the value of measurement of that was 20 $cm^3$ (+/-1% error). Therefore, the maximum error of measurements of oil recovery of the coreflood experiments would have been lower than +/-1% of original oil in place.

The measurement limit of the gas flowmeter was +/-5 $cm^3$ of produced gas at ambient conditions which is significantly lower than the volume of gas during the coreflood experiments. For example, 1 $cm^3$ of liquid $CO_2$ in this study expands to around 450 $cm^3$ at ambient conditions meaning that the measurement error of produced gas would have been +/-1.1%. On the other hand, the pore volume of the core used in the coreflood experiments was large which has ensured that the reported results are reliable. It will be shown in Chapter 6 that the coreflood experiments are also repeatable and their results are reproduced.

A bypass line is used to remove the gas cap of live fluids and to measure the gas content of those fluids. For the experiments reported here, the core orientation was vertical and the fluids were injected from the top of the core. While performing a test, the pressure and temperature at the inlet and outlet of the core-holder are recorded and displayed continuously on a computer monitor, which has a built-in data acquisition system. The

pressure transducers in the coreflood rig offer accuracy of +/-0.01% of reading. This suggests that the maximum error of permeability measurements was +/-0.005 Darcy.

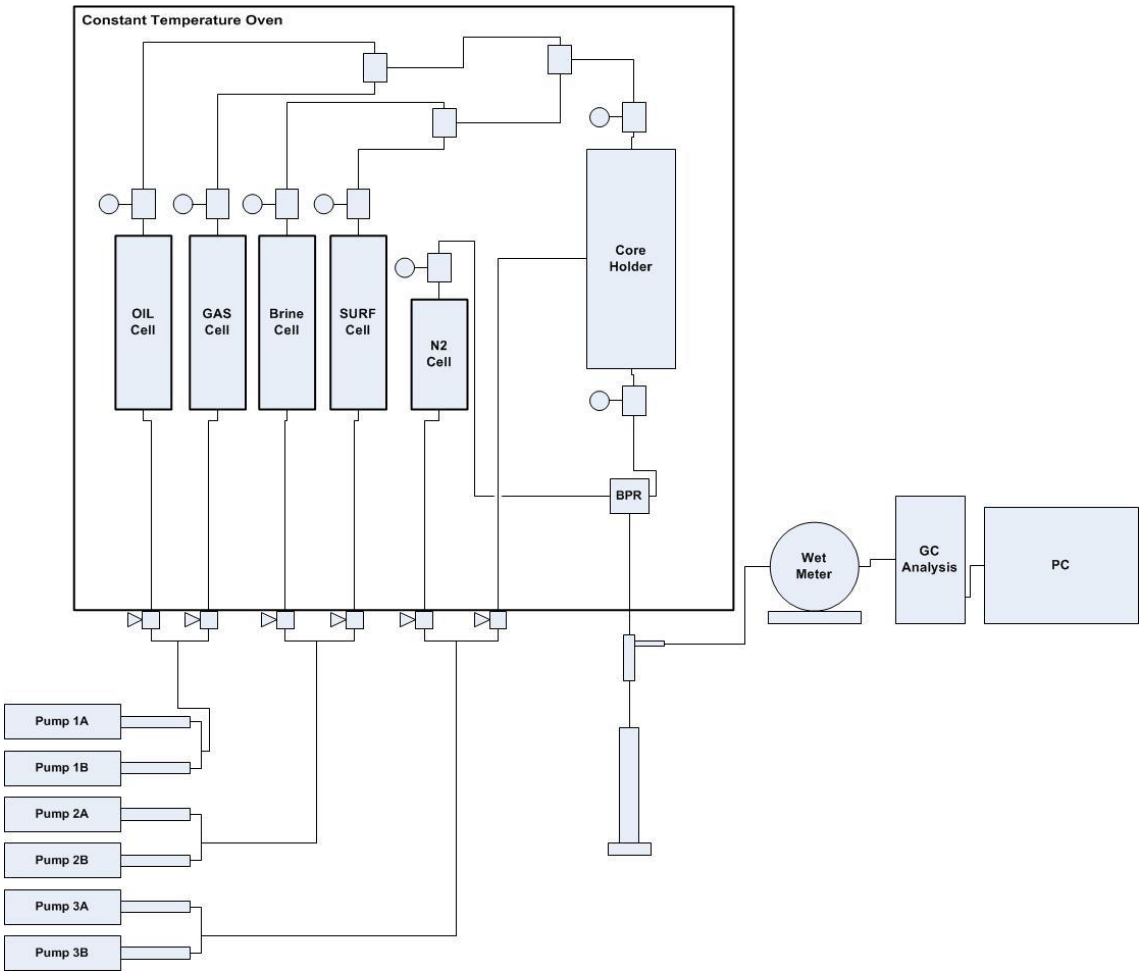


Figure 3-2: A simplified schematic of the coreflood rig.

## 3.3 Micromodel Apparatus

A high-pressure high-temperature micromodel rig was used to investigate pore-scale mechanisms of heavy oil recovery by $CO_2$ injection under reservoir conditions, Figure 3-3. Micromodels are small transparent 1D or 2D porous media which are constructed from two glass plates. The first plate has a pore structure etched onto the surface of the glass plate which is otherwise completely flat. The second glass (the cover plate) plate is then placed over the first, covering the etched pattern and hence creating an enclosed pore space. This second plate has an inlet and outlet hole allowing fluids to be displaced through the network of pores, as shown in Figure 3-4. The visual results of these experiments are invaluable for developing a good understanding of potentially very complex multi-physics phenomena taking place during the process of oil recovery. Because the structure of the micromodel is only pore-deep and the containing walls are all glass, it is possible to observe the fluids as they flow through the pore channels and interact with each other. It would also be possible to observe how the geometry of the

pore network affects the patterns of flow and trapping. Figure 3-5 shows a whole image of the micromodel during displacement of a crude oil (black colour) with brine (colourless) under reservoir conditions.

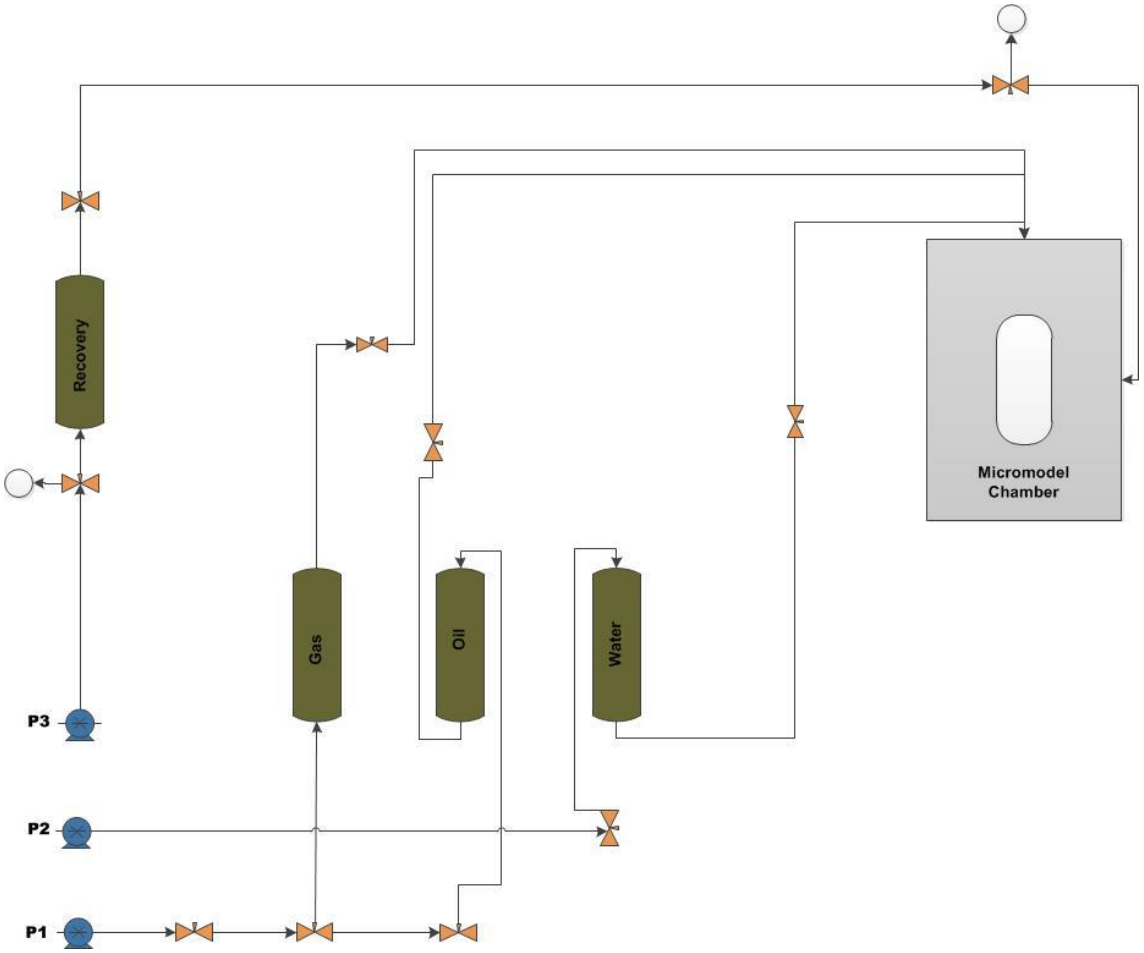


Figure 3-3: A simplified schematic of the micromodel rig.

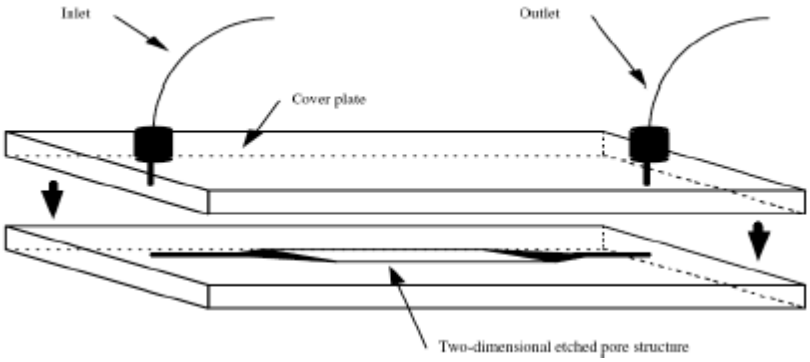


Figure 3-4: A schematic of a glass micromodel.

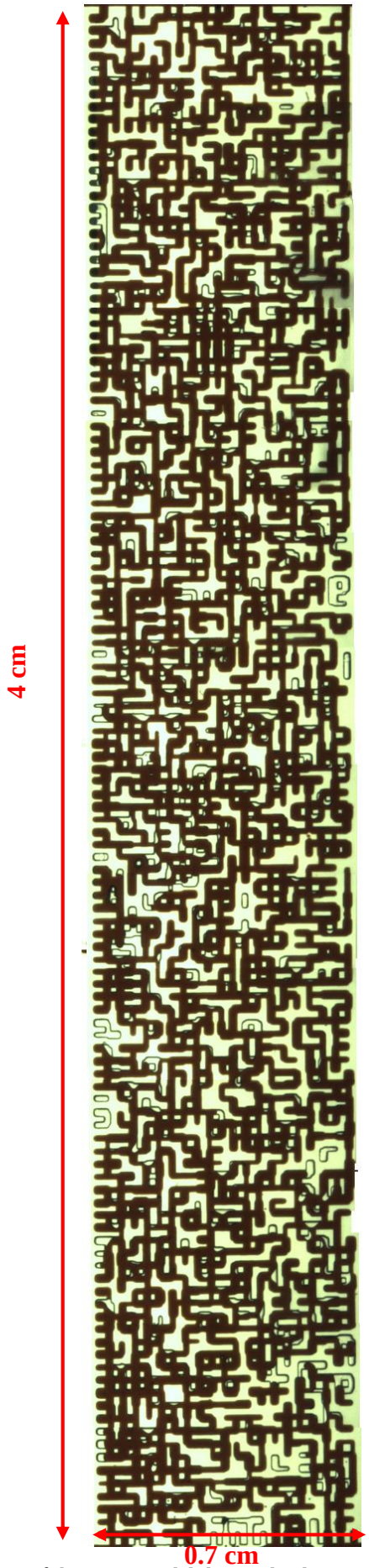


Figure 3-5: A magnified image of the micromodel during displacement of brine (colourless) with crude oil (black colour) under reservoir conditions, refer to Table 3-2 for details and dimensions.

The micromodel with a geometric pore pattern was vertically mounted in the system and all the injections were performed from the bottom of the model to top. The physical properties of the micromodel are given in Table 3-2.

Table 3-2: Physical properties of the micromodel.

| Length (cm) | Width (cm) | Pore Volume ($cm^3$) | Porosity (%) | Permeability (D) | Ave. Pore Depth (µm) | Pore Diameter range (µm) |
|---|---|---|---|---|---|---|
| 4 | 0.7 | 0.01 | 62 | 3 | 50 | 30-500 |

## 3.4 Visual-Cell Setup

A setup was designed and prepared to visually observe the contact of $CO_2$ with heavy oil under reservoir conditions. A simplified schematic of this setup is shown in Figure 3-6. Two pairs of pumps were used to inject fluids into the visual-cell or retract them from the cell. A transducer was connected to the cell to allow us to monitor the pressure of the cell continuously. The cell was covered by a heater jacket to maintain it at a constant temperature during the experiments. A camera and a light source were used to record images of the cell and its fluids during the experiment. The camera was connected to a PC which could record images at predefined intervals of time.

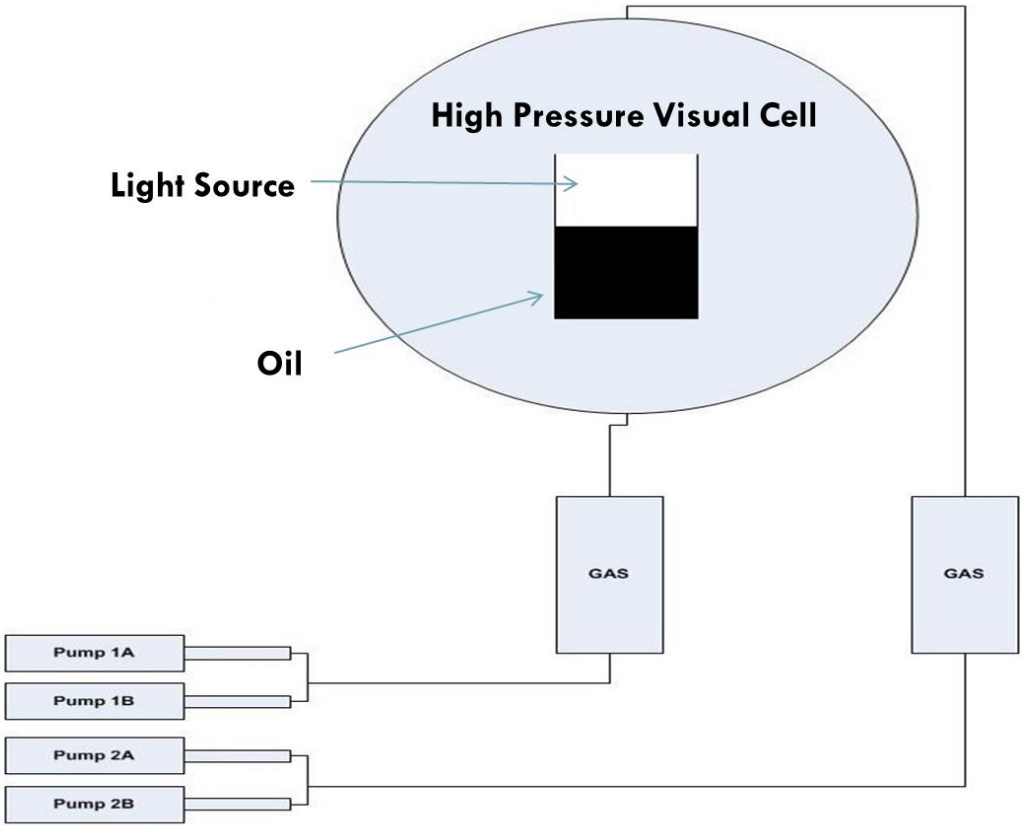


Figure 3-6: A simplified schematic of the visual-cell setup.

Figure 3-7 shows an image of the glass container during depressurizing the visual-cell

after one of the experiments. The oil in the bottom of the container is only accessible from the top side of the container.

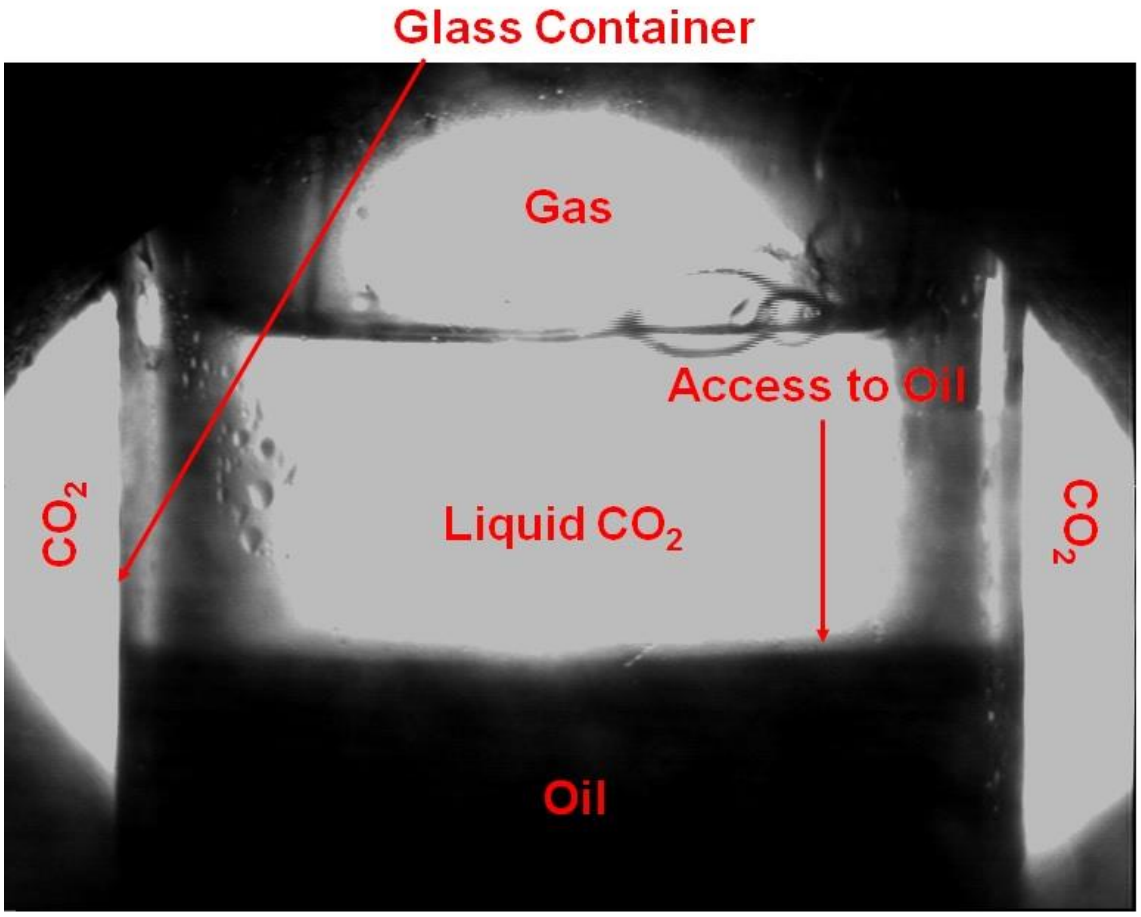


Figure 3-7: An image of the glass container during the depressurizing of the visual-cell.

## 3.5 Viscosity Measurements

A capillary tube viscometer system was designed and installed inside the coreflood rig. In order to eliminate the effect of pressure on viscosity, one short capillary tube (97 *cm*) was used to measure the viscosity of oil samples and one long capillary tube (1524 *cm*) was used for viscosity measurement of brines.

Figure 3-8 shows a simplified schematic of the high-pressure capillary tube viscometer system which was used in this study. Two pairs of pumps were used to flow fluids around the flow system (capillary tube and bypass lines) and apply pressure to the BPR. To measure and record the differential pressure across the core, two very accurate pressure transducers were connected to the inlet and outlet of the capillary tube.

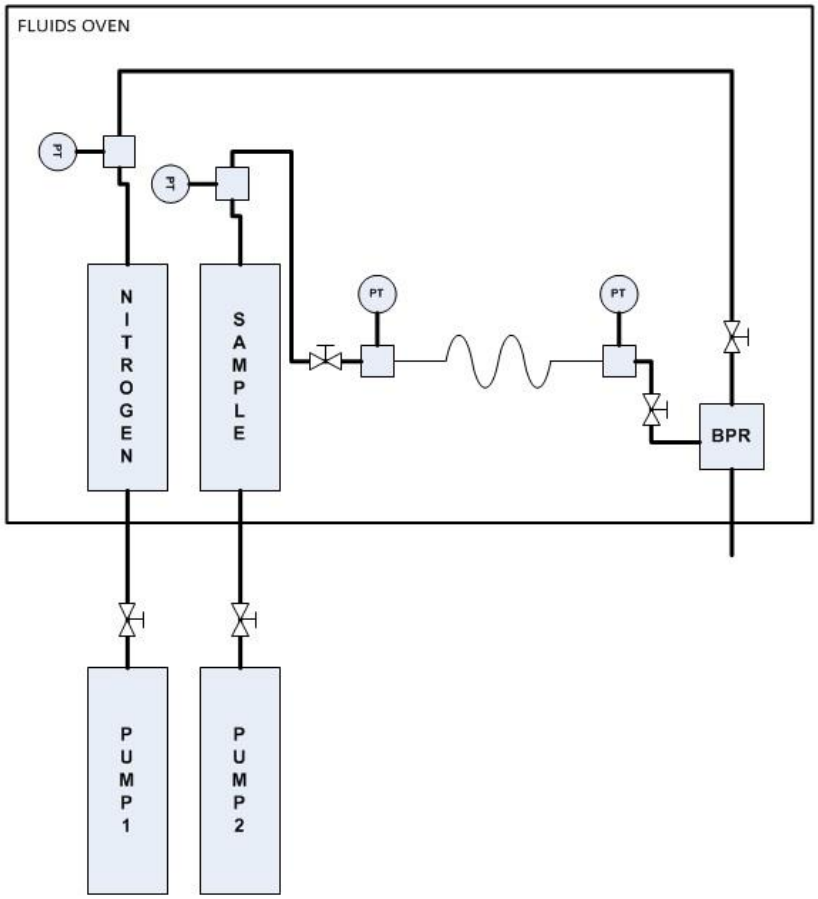


Figure 3-8: A simplified schematic of the capillary tube viscometer.

Before measuring the viscosity of liquid samples, calibration of the capillary tube (diameter) was done to ensure that obtained results are accurate and reliable. To perform calibration, standard fluids with known viscosity at particular temperatures were loaded into the oven. Each fluid was injected with constant rate through the capillary tube at atmospheric pressure. The injection was continued until to reach a constant differential pressure through the tube. The calculated diameter then was used for measuring the viscosity of desired liquids.

## 3.6 Core Sample

The core used in the experiments presented in this study was a sandstone core been taken from a block of Fife silica-sand rock. To minimise laboratory artefacts associated with using small core plugs, and to observe the impacts of adverse viscosity ratio (fingering) on flow and recovery processes, a one-piece large core with a length of 32.1 *cm* and a diameter of 5.1 *cm* was used for the experiments. A thin section of the core was cut from the same block that the core was taken from and was analysed using an environmental scanning electron microscope (ESEM) to identify the mineralogy and pore structure of

the rock. Figure 3-9 and Figure 3-10 present a series of microscale images of the rock sample. The images show that the rock is a high purity, poorly cemented and friable quartz sandstone (Figure 3-9a) with quartz overgrowth on the main quartz grains (Figure 3-9b). As shown in Figure 3-10, there are minor contents of feldspar and clay but open pore structures exist in the absence of cementing materials.

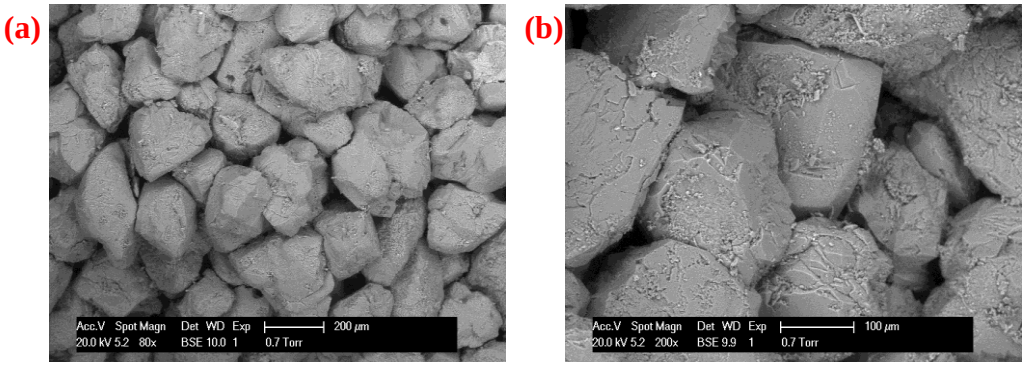


Figure 3-9: Images of the sample taken using ESEM; (a) and (b) two magnified sections of the rock.

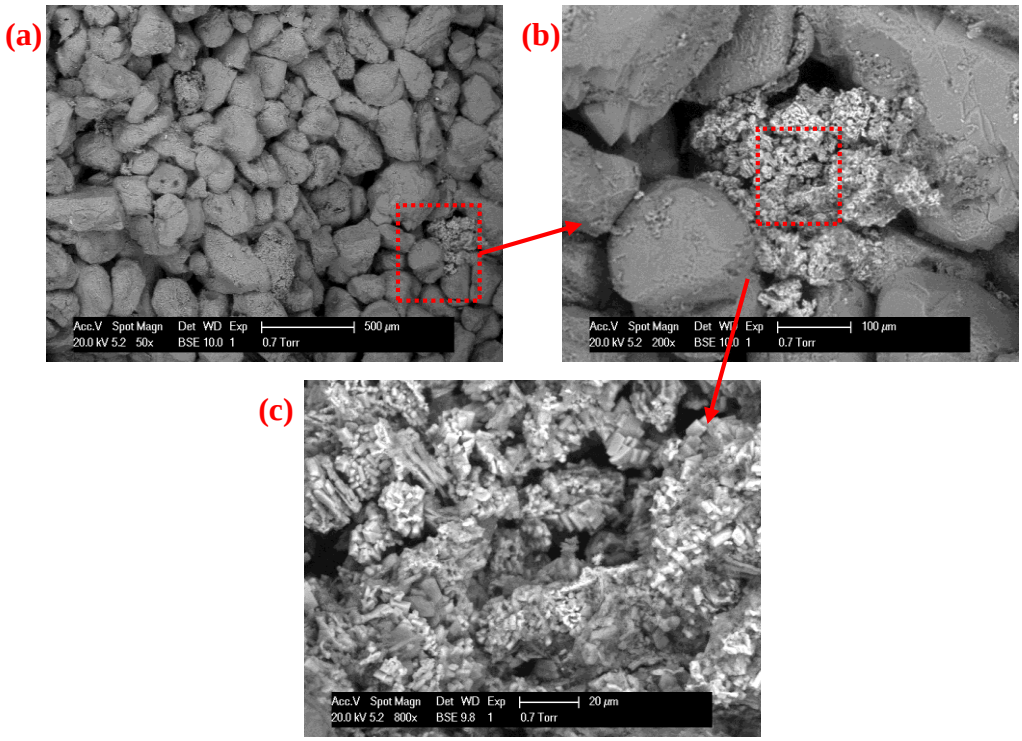


Figure 3-10: Images of the sample taken using ESEM; (a) to (c) clay particles in the rock.

To prepare the experiments, the core was cleaned with methanol and toluene injected in succession before drying. The core was then loaded in the core-holder and the pore volume (PV) of the core was measured using a helium porosity-meter setup. The pore volume of the core was also confirmed with total volume of brine was used to fully saturate the system (core and the connection) minus the dead volumes of the system. The permeability of the core was measured (2.73 Darcy) using brine at the test pressure and temperature. The dimension and properties of the core are given in Table 3-3.

Table 3-3: Physical properties of the core.

| Property | Core |
|---|---|
| Weight, g | 1333.9 |
| Diameter, cm | 5.13 |
| Length, cm | 32.10 |
| Pore volume (PV), $cm^3$ | 151.5 |
| Porosity (Φ), % | 22.84 |
| Permeability to brine (K), D | 2.73 |

## 3.7 Tracer Test (Swept Volume)

Before conducting the coreflood experiments and exposing the rock to oil, a tracer test was performed to evaluate the volumetric sweep efficiency of the core in the direction of injection of fluids in the coreflood experiments which was from the top of the core to the bottom. Generally, the information gained from tracer testing is obtained by observing the breakthrough of the tracer and the chase fluid. To obtain high-quality tracer-response curves that are the basis for the further interpretation, a well-designed sampling program is needed. The ideal tracer would follow the fluid of interest exactly, travelling at the same velocity as the fluid front. But, ideally, it is impractical to attain because adsorption-desorption effects cause the tracer to lag behind the front; these effects, plus diffusion-dispersion effects, cause the tracer front to spread more than the fluid front (Greenkorn 1962; Zemel 1995).

After vacuuming the core, it was saturated with brine and the core pressure was increased to 1500 *psi*. Several pore volumes of brine were injected at 28˚ *C* to ensure that the core is fully saturated with brine. The differential pressure (DP) within the core was also monitored and recorded and a constant DP was observed during the period of brine injection. In this study, lithium was selected as the reference tracer. A small amount (5 *ppm*) of lithium chloride (LiCl) was dissolved in the brine that was injected to saturate the core. The tracer brine was also degassed before injecting that into the core. The injection was performed at 50 $cm^3/hr$ and continued until 2 PVs of injection. Sampling was conducted in short periods of time to have the potential for extraction of more information from the data. Immediately after the tracer flood, brine was injected into the core to remove the tracer brine from the core. The waterflood was also performed at 50 $cm^3/hr$ and it continued for several pore volumes but the sampling was only performed for the first 2 PVs of injection. All the samples were analysed by acquiring an ICP instrument to measure the concentration of lithium in the period of tracer and chase water injection. An advantage of lithium as the tracer agent was that it had a very low detection limit. Figure 3-11 shows the results of the tracer injection and the following waterflood. The vertical axis depicts the normalised concentration of lithium *C* (concentration at time

*t*) divided by $C_0$ (initial concentration).

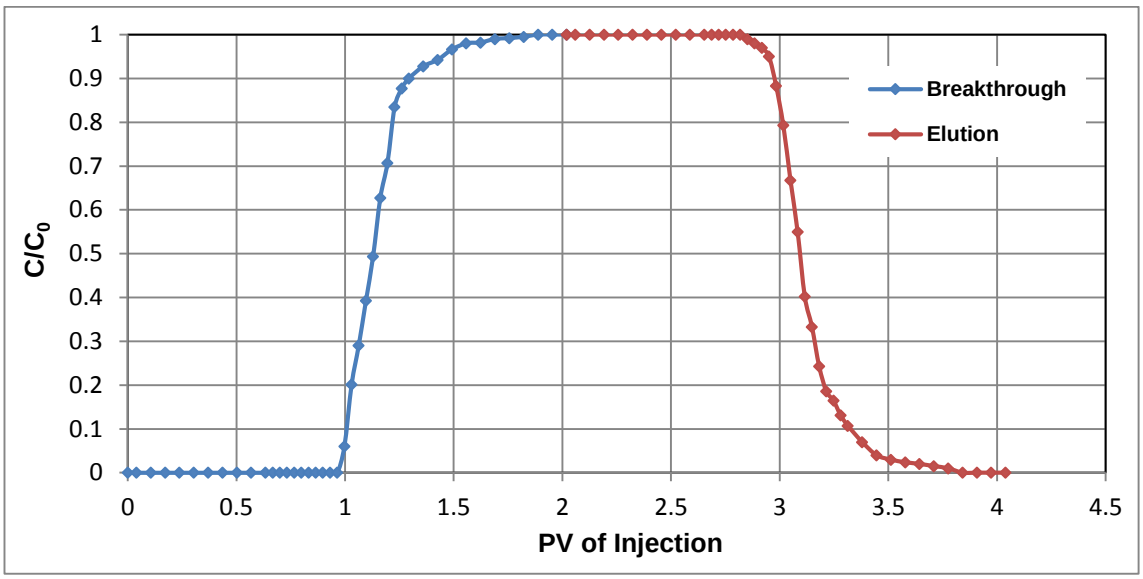


Figure 3-11: Breakthrough-elution curves of the tracer flood.

The addition of 5 *ppm* of lithium chloride to the injection brine would have had an insignificant impact on the physical properties of the brine such as density and viscosity. Thus, it is assumed that the floods were stable and no viscous fingering would have been present in the tracer or the subsequent waterflood. Dispersion of the fluid front is generally caused by heterogeneous fingering, variations in velocity because of variations in pore sizes, and the presence of dead-end pores. Dispersion will cause the breakthrough-elution curves to have an 'S' shape rather than a sharp front (Halevy & Nir 1958).

The breakthrough of lithium at around 1 PV of injection implies that the injected tracer could almost displace all the initial brine in place and no obvious flow impediment or bypassing was present in the core. However, the concentration of lithium after the breakthrough did not rise as sharply as that would have been expected to observe in the case of a passive tracer. Another factor that affects the shape of breakthrough-elution curves is the adsorption of tracer on flow and rock materials.

In this study, the core was a sandstone rock and silica had the highest fraction of the consisting minerals of the rock. Silica group can acquire a different charge depending on the pH of the solution that it is exposed to. At lower pH (i.e. around 2-3), silica acquires positive charges while at higher pH it contains negative surface charge (Sharma, et al. 1987; Appel, et al. 2003; Farooq, et al. 2011). The value of pH of the brine in our experiments is around 6.8. At this pH, the core sample carries a negative surface charge. Therefore, it is likely that a fraction of lithium in the tracer brine has been adsorbed on the surface of the rock. However, this process was reversible and the waterflood after the tracer could remove lithium from the core.

The volume of the core swept by the injected tracer was estimated by Equation (3.1). Estimating volume swept by injected fluids for porous media was first developed by Deans (1978). Asakawa (2005) developed a general derivation of the method to include three-dimensional, heterogeneous reservoirs. The pore volume contacted by injected fluids (i.e. swept volume) is determined from the residence volume of a tracer. For the tracer test performed in this study, the residence volume is calculated from tracer histories at a given production well as follows (Zemel 1995; Shook, et al. 2009)

$$V_s = \frac{m_p}{M_{inj}} \frac{\int_0^\infty qCtdt}{\int_0^\infty Cdt} \tag{3.1}$$

where

$V_s$ is swept pore volume,

$m_p$ is mass of tracer produced at production well,

$M_{inj}$ is mass of tracer injected,

$q$ is flow rate,

$C$ is concentration of tracer,

$t$ is time.

The calculated value of swept volume of the tracer was virtually equal to the value of the volume of the core plus the dead volumes of the system. This observation indicates that the injected tracer could invade the total pore spaces of the core and the core used in this study was a fairly homogeneous rock.

## 3.8 Fluids

### 3.8.1 Gas

Table 3-4 shows the physical properties of $CO_2$ (99.8% purity) and methane (100% purity) under the conditions of the experiments reported here. To understand and also to recognise the impacts of the mechanisms contributing to oil recovery, an enriched hydrocarbon gas experiment was performed to compare its performance with a corresponding $CO_2$ injection experiment. This enriched hydrocarbon gas injection is referred to as viscosity reducing gas (VRG). The composition of VRG used in this study is given in Table 3-5. Pure hydrocarbon components were mixed in the laboratory using a heated 6-litre gas rocking cell to prepare the multi-component gas mixture.

Table 3-4: Physical properties of $CO_2$ and $CH_4$ (NIST 2014).

| Fluid | Temperature (˚C) | Pressure (psi) | Density ($g/cm^3$) | Viscosity (mPa.s) |
|---|---|---|---|---|
| $CO_2$ | 28 | 1500 | 0.798 | 0.070 |
| $CO_2$ | 50 | 1500 | 0.426 | 0.031 |
| $CO_2$ | 50 | 600 | 0.082 | 0.017 |
| $CH_4$ | 28 | 1500 | 0.076 | 0.014 |
| $CH_4$ | 50 | 1500 | 0.069 | 0.014 |
| $CH_4$ | 50 | 600 | 0.026 | 0.013 |

Table 3-5: Composition of VRG.

| Components | Concentration (%mole) |
|---|---|
| Nitrogen | 0.34 |
| $CO_2$ | 1.21 |
| Methane | 78.06 |
| Ethane | 8.93 |
| Propane | 5.88 |
| i-Butane | 1.34 |
| n-Butane | 2.90 |
| i-Pentane | 0.56 |
| n-Pentane | 0.54 |
| n-Hexane | 0.21 |
| n-Heptane | 0.03 |
| n-Octane | 0.01 |

### 3.8.2 Crude Oil

Live oil samples were prepared by using a heated rocking fluid recombination cell. The dead crude oil 'C' sample and hydrocarbon gas (methane) was used to prepare saturated (live) oil at the conditions of each coreflood test. The dead oil was a reservoir stock-tank crude oil sample which had a density of 0.9908 $g.cm^{-3}$ at 25˚ $C$ and ambient pressure. Mixing of the oil and gas performed at a pressure higher than the bubble point, in order to ensure a good mixing of extra-heavy oil with gas. Then the pressure of the cell was slowly decreased down to the experiment pressure. The oil storage vessel inside the coreflood oven was charged with methane before transferring live oil, in order to avoid depressurizing (degassing) of live oil during transferring from the rocking cell. Using a heated line (filled with methane) with the same temperature with the rocking cell, the live oil was transferred with relatively slow rate, to avoid oversaturation of oil, into the oil storage vessel in the rig. Eventually, when the system reached equilibrium, the gas cap on top of the oil vessel was removed.

For the visualisation experiments, the dead crude oil 'J' was used which had significantly lower viscosity than the crude oil 'C'. The dead oil 'J' was also a reservoir stock-tank crude oil which had a density of 0.9548 $g.cm^{-3}$ at 28˚ $C$ and ambient pressure. The above-mentioned procedure for preparing live heavy oil was also followed to prepare live crude 'J' for micromodel experiments. Table 3-6 summarises the main PVT characteristics of the live oil samples. The oil viscosities were calculated by measuring the pressure drop

through an in-line calibrated capillary tube. In order to measure the effect of dissolution of $CO_2$ on the oil viscosity, the viscosity of the oil samples when saturated with $CO_2$ under the conditions of the coreflood experiments were also measured.

Table 3-6: PVT properties of oil samples.

| Oil sample | Temperature (˚C) | Saturation Pressure (psi) | Associated Gas of Oil | GOR ($scm^3/rcm^3$) | Viscosity (mPa.s) | Oil Swelling ($rcm^3/scm^3$) |
|---|---|---|---|---|---|---|
| C | 28 | 1500 | -- | -- | 277000 | -- |
| C | 28 | 1500 | $CH_4$ | 23.75 | 12000 | 1.035 |
| C | 28 | 1500 | $CO_2$ | 66.25 | 717 | 1.070 |
| C | 50 | 1500 | -- | -- | 15000 | -- |
| C | 50 | 1500 | $CH_4$ | 22.10 | 1665 | 1.049 |
| C | 50 | 1500 | $CO_2$ | 56.90 | 219 | 1.053 |
| C | 50 | 1500 | VRG (g:o≡6:1) | 45.00 | 151 | -- |
| C | 50 | 600 | $CH_4$ | 10.60 | 3530 | 1.035 |
| C | 50 | 600 | $CO_2$ | 30.63 | 733 | 1.040 |
| J | 28 | 1500 | -- | -- | 760 | -- |
| J | 28 | 1500 | $CH_4$ | 28.95 | 115 | 1.046 |
| J | 28 | 1500 | $CO_2$ | 83.50 | 17.5 | 1.185 |

### 3.8.3 Brine

A brine solution ('Normal Brine') with a total salinity of 10000 *ppm* was used in the tests reported here. The brine was made of 8000 *ppm* sodium chloride (NaCl) and 2000 *ppm* of calcium chloride ($CaCl_2$) and it was degassed before saturating the core. To avoid diffusion of gas from live oil into the brine in core, methane-saturated (live) brine was injected through the core to displace the dead brine before live oil injection. In addition, $CO_2$-saturated brine was prepared at the conditions of each experiment for injection in the core after the period of $CO_2$ injection. Using another calibrated capillary tube within the setup, the viscosity of the brine samples were measured too. The physical properties of brine samples are shown in Table 3-7.

Table 3-7: PVT properties of brine samples.

| Temperature (˚C) | Saturation Pressure (psi) | Associated Gas of Brine | GWR ($scm^3/rcm^3$) | Viscosity (mPa.s) | Brine Swelling ($rcm^3/scm^3$) |
|---|---|---|---|---|---|
| 28 | 1500 | -- | -- | 0.898 | -- |
| 28 | 1500 | $CH_4$ | 3.43 | 0.890 | -- |
| 28 | 1500 | $CO_2$ | 32.73 | 0.899 | 1.034 |
| 50 | 1500 | -- | -- | 0.560 | -- |
| 50 | 1500 | $CH_4$ | 3.00 | 0.562 | -- |
| 50 | 1500 | $CO_2$ | 26.70 | 0.597 | 1.040 |
| 50 | 600 | $CH_4$ | 1.75 | -- | -- |
| 50 | 600 | $CO_2$ | 15.85 | -- | -- |

### 3.8.4 Surfactant Solutions

PetroStep C1 was used to prepare surfactant solution to inject simultaneously with $CO_2$ in the (chronologically) last coreflood experiment. Table 3-8 shows the basic properties

of surfactant solution.

Table 3-8: Physical properties of surfactant solution.

| Surfactant | Type | Active (Wt. %) | CMC (g/L) | Formula |
|---|---|---|---|---|
| Petrostep C1™ | Anionic | 39 | 0.3 | (C14) Sodium Alpha Olefin Sulfonate |

## 3.9 Compositional Analysis of Heavy Oil

A reservoir oil is generally described by discrete hydrocarbon components up to $C_6$-$C_9$ and the non-hydrocarbon gases, such as nitrogen, $CO_2$, $H_2S$ and hydrocarbon groups for heavier fractions. The hydrocarbon groups are generally determined according to their boiling points by distillation and/or gas chromatography (GC). Whilst an extended oil analysis by distillation takes many days and requires relatively a large volume of sample, GC can identify components in a matter of hours using only a small fluid sample (Danesh 1998).

In a GC instrument, the sample is injected into a heated zone, vaporised, and transported by a carrier gas into a column packed or internally coated with a stationary liquid or solid phase resulting in partitioning of constituents of the injected sample. The eluted compounds are carried into a detector where the component concentration is related to the area under the detector response-time curve (peak area), as evident in Figure 3-12. Individual peaks may be identified by comparing their retention times inside the column with those of known compounds previously analysed at the same GC conditions (Danesh 1998).

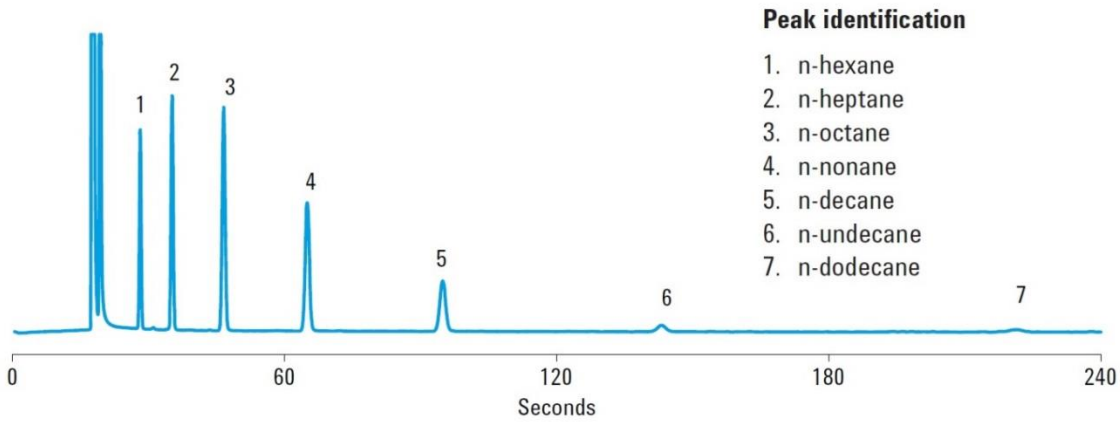


Figure 3-12: Gas chromatogram of a $C_7$-$C_{12}$ hydrocarbon mix on an 8-meter packed column.

The two most commonly used detectors are flame ionisation detector (FID) and the thermal conductivity detector (TCD). The FID response is almost proportional to the mass concentration of the ionised compound. It, however, cannot detect non-hydrocarbons such as nitrogen and $CO_2$. Hence, TCD is often used for analysis of gaseous mixtures that

contain non-hydrocarbon components.

The accuracy of compositional analysis can be improved by calibration of GC. The common method is to analyse a gravimetrically prepared mixture of components with known concentrations, as the standard. Normal alkanes are often used to represent standard carbon numbers (SCN) groups. It is known that the response of detectors to paraffins and aromatics are different. Therefore, the use of typical SCN groups, instead of normal alkanes, in preparing standards appears to be more appropriate.

In this work, a dual channel high-speed Micro-GC was used to analyse gaseous fluids produced during the coreflood experiments. The Micro-GC was equipped with a TCD. The gaseous fluids, after separation from effluent liquids, could be directed into the in-line Micro-GC at any time of the coreflood experiments and hence the composition of the gas stream would have been analysed. Depending on the requirement to target particular components in the produced stream, the Micro-GC was calibrated using pure gas components prior to a test.

In addition, the composition of oil samples produced during coreflood experiments were analysed by employing an FID GC (simulated distillation). All the components detected by GC between the two neighbouring normal paraffins are commonly grouped together and that is measured and reported as an SCN equal to that of the higher normal paraffin. A major drawback of GC analysis is the lack of information, such as the molecular weight and density, on the identified SCN groups. The lack of molecular weight data is quite limiting as the response of FID, used for oil analysis, is proportional to the mass concentration. Thus, molecular weight data are needed to convert the mass fraction to molar basis required for compositional studies. That is, the molecular weight of normal alkanes, as an average, was used to convert the mass fraction of each SCN reported by the GC analysis to molar basis. To improve our understanding, the viscosity of some samples was also measured at the test temperature.

To clearly describe the changes in the composition of produced oil during the experiments, the grouping of the compounds was done and seven groups were selected, as shown in Table 3-9.

Table 3-9: Grouping of GC results of oil samples.

| Group# | SCN |
|---|---|
| 1 | ≤C12 |
| 2 | >C12-≤C16 |
| 3 | >C16-≤C20 |
| 4 | >C20-≤C23 |
| 5 | >C23-≤C29 |
| 6 | >C29-≤C45 |
| 7 | >C45-≤C100 |

# CHAPTER 4: MECHANISMS OF ENHANCED HEAVY OIL RECOVERY BY LIQUID $CO_2$ INJECTION

*The main objective of this chapter was to identify the pore-scale mechanisms responsible for heavy oil recovery by dense (liquid) $CO_2$ injection. Moreover, the impacts of various parameters affecting the process of oil recovery were investigated by performing two coreflood experiments as well as several visualisation experiments. The compositional analysis of the core effluent with the measurements of PVT properties of the fluids led to further understanding of the true potential of $CO_2$ injection for EHOR. Eventually, the observations made in this study and the results of the experiments reported in this chapter were compared and discussed.*

## 4.1 Coreflood#1: Tertiary Liquid $CO_2$ Injection

A tertiary $CO_2$ injection followed secondary waterflood experiment was performed in the vertically mounted core to evaluate the performance of tertiary liquid $CO_2$ injection in heavy oil recovery. The main objective of this experiment was to investigate the effects of oil viscosity on the performance of tertiary $CO_2$ injection and compare the results with the corresponding experiment using a different oil with lower viscosity and higher amount of dissolved gas.

The experiment continued with a period of waterflood after the tertiary $CO_2$ injection to investigate the performance of improved mobility ratio in recovering remaining oil after $CO_2$ injection. A summary of the performance of all the periods of fluid injection in terms of cumulative oil recovery will be shown in Figure 4-24. Table 4-1 shows the pressure and temperature at which the test was carried out as well as the fluids used in the test.

Table 4-1: Fluids and conditions of Coreflood#1.

| **Coreflood#1** | **Experiment 10** (Farzaneh 2015) |
|---|---|
| Crude Oil: Methane-saturated Crude 'C' | Crude Oil: Methane-saturated Crude 'J' |
| Brine: Methane-saturated or $CO_2$-saturated | Brine: Methane-saturated |
| Gas: Liquid $CO_2$ | Gas: Liquid $CO_2$ |
| Temperature: 28° C | Temperature: 28° C |
| Pressure: 1500 psi | Pressure: 1500 psi |
| Injection Rate: 7 $cm^3$/hr | Injection Rate: 7 $cm^3$/hr |
| Core Position: Vertical (top to bottom) | Core Position: Vertical (top to bottom) |

***Procedure***

The following were the main steps to conduct Coreflood#1:

1. **Dead Brine Injection:** Core was saturated with brine and the permeability was measured. The permeability of the core to the brine was unchanged.
2. **Live Brine Injection:** The live brine was injected through the core to avoid gas transfer from following live oil into the brine. The injection was continued until the gas content of the produced brine reached to certain values.
3. **Live Oil Injection:** The core was flooded with live crude 'C' and an irreducible water saturation of 8% was achieved.
4. **1st (Secondary) Waterflood:** 2 PVs of methane-saturated brine were injected into the core.
5. **1st (Tertiary) $CO_2$ Injection:** 6 PVs of $CO_2$ were injected into the core after the first waterflood.
6. **2nd Waterflood:** Around 1 PV of $CO_2$-saturated brine was injected through the core after $CO_2$ injection.
7. **Core Cleaning:** The core was cleaned by several cycles of toluene and methanol injection.

***Results and Discussion***

### 4.1.1 1st (Secondary) Waterflood

This run involves injecting water into the oil-flooded core until 2 pore volumes of water are injected. In a gas-free conventional oil porous medium, most of the oil is produced until breakthrough. After this point, as water is injected, very little extra oil is recovered and virtually all the water injected is produced. This happens because the oil trapped in the porous medium at the end of the waterflood is due to capillary forces (Carig 1971; Anderson 1987).

However, the behaviour of heavy oil waterfloods is distinctively different. Despite conventional oil, heavy oil is considerably more viscous than water. Therefore injection of fluid with high mobility to recover heavy oil leads to unfavourable displacement and viscous fingering. This results in early water breakthrough and reduces the efficiency of the waterflood. Figure 4-1 shows the profiles of oil recovery and differential pressure across the core during the period of secondary waterflood. Breakthrough of water occurred at 0.11 PV of injection, as evidenced by the rapidly rising water cut at early times in Figure 4-2.

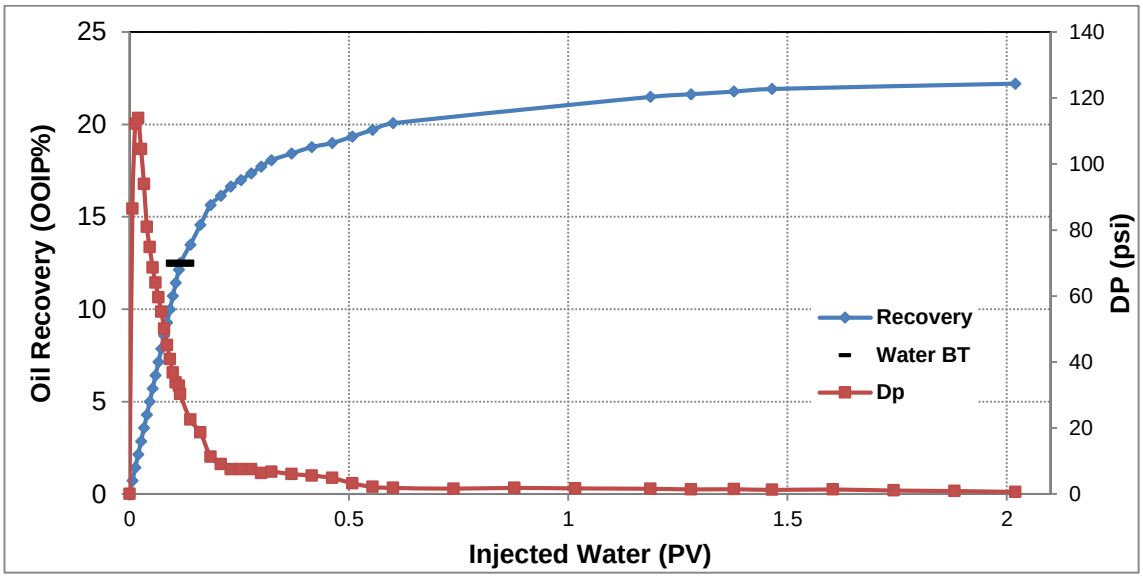


Figure 4-1: Oil recovery and differential pressure across the core during the period of 1st (secondary) waterflood.

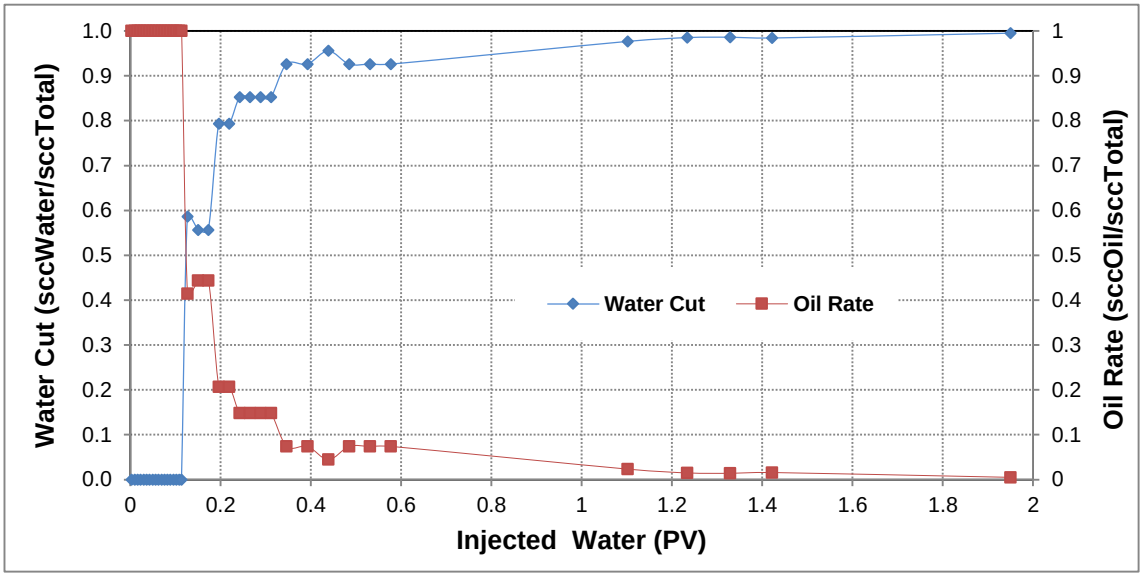


Figure 4-2: Oil rate and water cut during the period of 1st (secondary) waterflood.

It is significant that after the breakthrough a considerable fraction of oil, around 10% of original oil in place (OOIP), was still produced at high water cuts. At first glance, the recovery profile is similar to waterflooding of conventional oil in an oil-wet system. However, the rock used in this experiment is clean sandstone, and during the preparation of the experiment, the rock was always exposed to brine before oil. These factors should have ensured that the core remained water-wet. Additionally, the pressure profile does not match that of a waterflood in an oil-wet core. At early times, pressure builds up upon constant rate water injection, but after the breakthrough, pressure decreases down to very low values. After the breakthrough, water has found continuous pathways from the inlet to the outlet and further injection has followed these paths of least resistance. Water continued to contact oil along its paths and, thus, improved recovery. In the experiments

performed in this work, although the floods were performed vertically, the density of oil and water were almost equal and therefore gravitational mechanism for oil recovery was negligible. At the low-velocity flow rate utilised in this experiment, inertial (shear) forces would have been negligible, too. Therefore, after the breakthrough, the two competing mechanisms were viscous and capillary forces.

### 4.1.2 Effect of Oil Viscosity on Performance of Secondary Waterflood

Figure 4-3 compares the recovery profiles of secondary waterflood performed in the core saturated with live crude 'J' (Farzaneh 2015) and secondary waterflood performed in the core saturated with live crude 'C'. Although the breakthrough has occurred later and the ultimate recovery is significantly higher for the waterflood experiment in the case of lower viscous oil, the results show that secondary waterfloods followed a similar trend for both oils. Lower viscosity of live crude 'J' causes lower instabilities at the flood front and hence a large fraction of the oil has recovered before the breakthrough. Macroscopically, a significant area of the porous medium in both experiments was unswept due to severe bypassing. Therefore, a large fraction of the remaining oil is still continuous and can still be produced after water breakthrough.

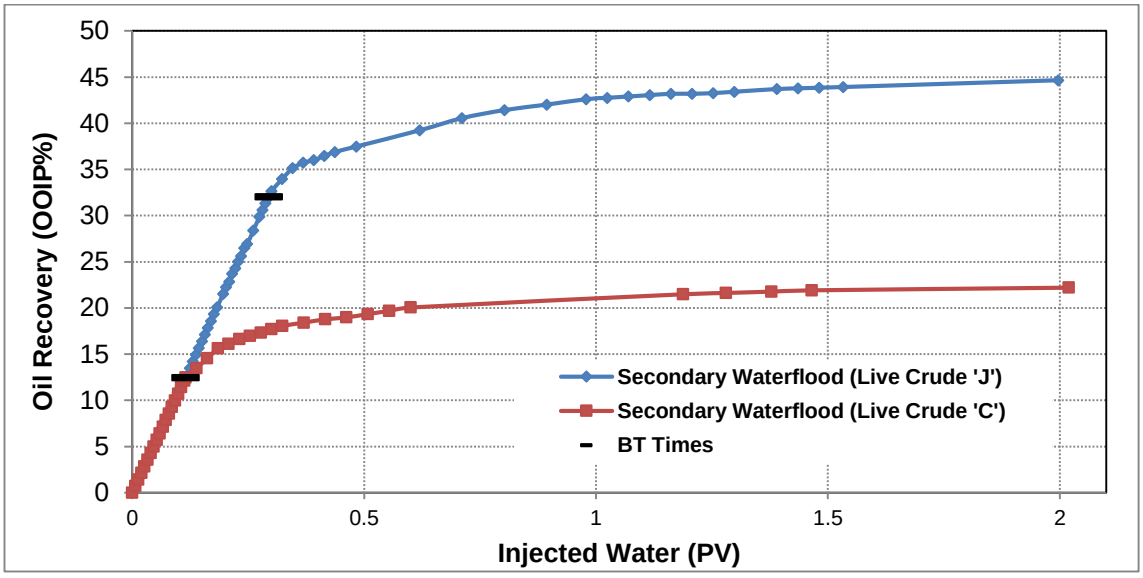


Figure 4-3: Comparison of oil recovery profiles of secondary waterflood live crude 'J' (Farzaneh 2015) and secondary waterflood live crude 'C'.

### 4.1.3 1st (Tertiary) $CO_2$ Injection

Water was produced from the core as the injection of $CO_2$ started. Water production continued at high water cuts until $CO_2$ breakthrough and a small fraction of oil was also recovered in this period as a result of water and oil contact. The $CO_2$ breakthrough happened at 0.15 PV of injection, as shown in Figure 4-4. Most of the water in the core was produced until the breakthrough of $CO_2$. However, water production continued until

around 0.35 PV of injection at low water cuts. Lower the water saturation in the core, higher the surface area between $CO_2$ and oil would have been.

Oil was produced with relatively constant rate after around 0.5 PV of injection, where the pressure gradient within the core was also constant until the end of the run, indicating that the effect of viscous flow on oil recovery was decreased. The main recovery mechanisms of oil recovery were the dissolution of $CO_2$ in oil and the resultant oil viscosity reduction, oil swelling, extraction of light and intermediate components of the oil, gravity drainage, and capillary hysteresis due to the nature of multi-phase flow in porous media. These mechanisms and their underlying phenomena will be discussed later. Around 23% of the remaining oil after the waterflood was recovered by $CO_2$ injection.

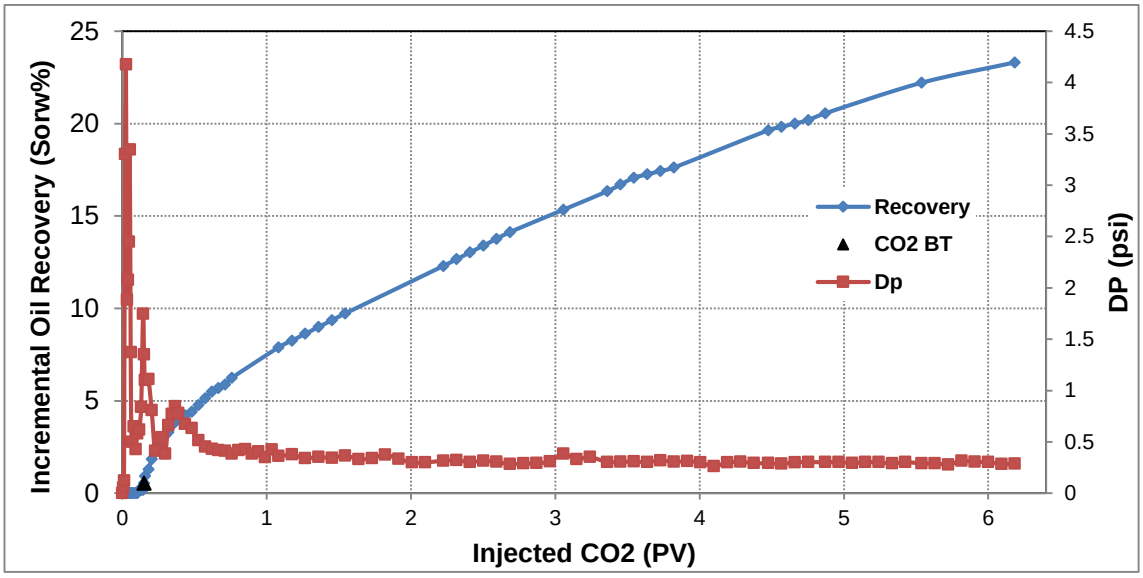


Figure 4-4: Incremental oil recovery (relative to the remaining oil saturation after waterflood, Sorw) and differential pressure across the core during the period of tertiary $CO_2$ injection.

### 4.1.4 Effects of Oil Composition and Viscosity on Performance of Tertiary $CO_2$ Injection

Figure 4-5 compares the incremental recovery of the waterflooded remaining oil obtained during tertiary $CO_2$ injection into the core saturated initially with live crude 'J' (Farzaneh 2015) and into the core saturated initially with live crude 'C'. A Higher fraction of oil was recovered by $CO_2$ injection into the core with crude 'J' in place mainly because of the significantly lower viscosity of the oil. The lower viscosity of crude 'J' compared to crude 'C' would have enhanced the rate of $CO_2$ dissolution and diffusion into the oil as well as the contribution of gravity drainage to oil production. In addition, crude 'C' has a lower fraction of light and intermediate cuts which adversely affects the process of $CO_2$ dissolution in the oil. The higher capacity of crude 'J' to uptake $CO_2$ would have resulted in relatively higher oil swelling. Because of the higher number of fingers and branches generated by waterflood in the core saturated with lower viscosity oil, a higher contact

area between the injected $CO_2$ and the remaining oil may have been present in pore spaces which could cause to a higher rate of $CO_2$ dissolution in the oil.

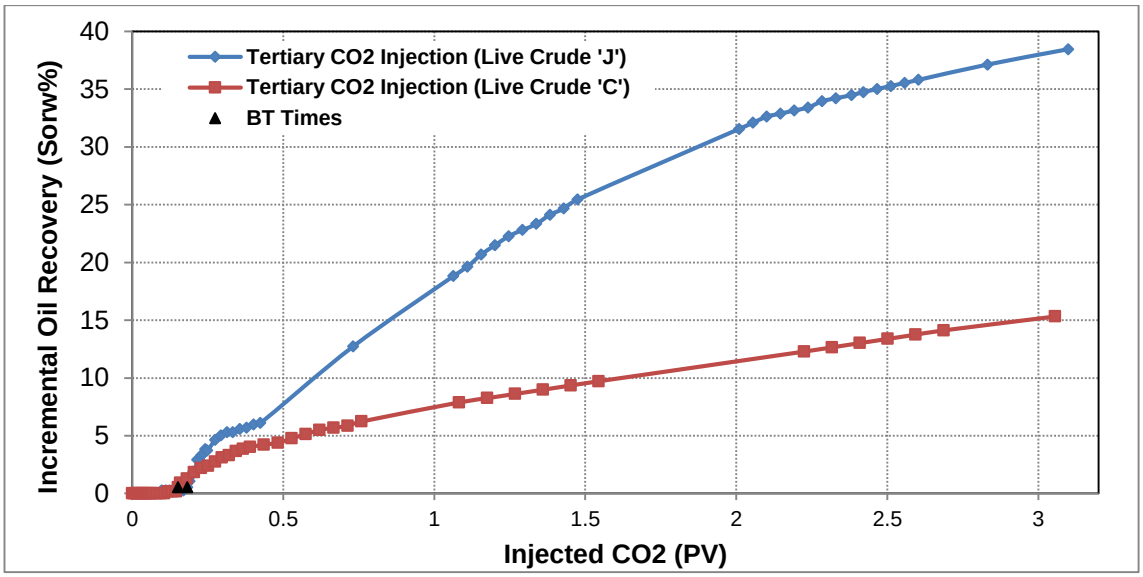


Figure 4-5: Comparison of incremental oil recovery profiles of tertiary $CO_2$ injection live crude 'J' (Farzaneh 2015) and tertiary $CO_2$ injection live crude 'C'.

### 4.1.5 2nd Waterflood

$CO_2$-saturated brine was injected through the core immediately after the period of tertiary $CO_2$ injection. By the beginning of waterflood, gas production started and continued until the breakthrough. As shown in Figure 4-6, oil production started with water breakthrough and continued almost until the end of the run. It is significant that a considerable fraction of 14% of the remaining oil after the period of $CO_2$ injection was recovered by waterflood.

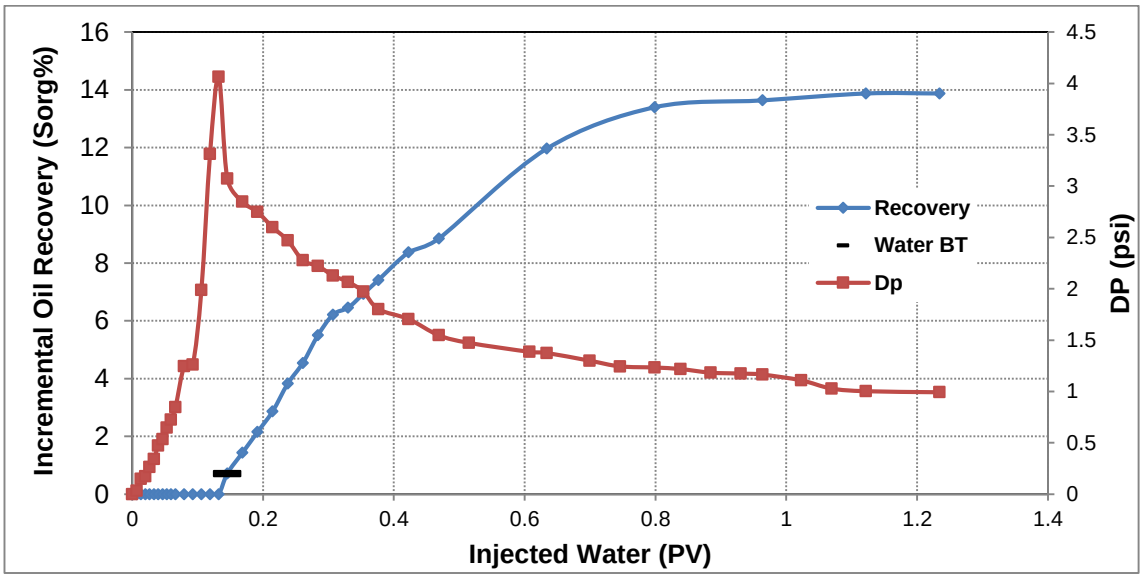


Figure 4-6: Incremental oil recovery (relative to the remaining oil saturation after $CO_2$ injection, Sorg) and differential pressure across the core during the period of 2nd waterflood.

### 4.1.6 Compositional Analysis of Oil Recovered by Liquid $CO_2$ Injection

The composition of produced oil during different periods of Coreflood#1 was analysed

and reported in Table 4-2 and Figure 4-7. It was assumed that waterflood would not have a significant impact on the composition and the physical properties of oil and hence the composition of oil produced at late times of secondary waterflood is considered as the composition of the original oil in the core.

Table 4-2: Composition of recovered oil during different periods of Coreflood#1.

| Sample | PV of Injection | ≤C12 (%mole) | >C12-≤C16 (%mole) | >C16-≤C20 (%mole) | >C20-≤C23 (%mole) | >C23-≤C29 (%mole) | >C29-≤C45 (%mole) | >C45-≤C100 (%mole) |
|---|---|---|---|---|---|---|---|---|
| 1#1WF#1 | 0.6-1.2 | 21.2 | 21.9 | 16.6 | 5.2 | 10.2 | 16.1 | 8.8 |
| 1#1GF#1 | 0.2-0.3 | 31.1 | 26.0 | 14.1 | 4.2 | 7.3 | 11.4 | 5.9 |
| 1#1GF#2 | 0.3-0.4 | 29.7 | 27.2 | 14.4 | 4.2 | 7.5 | 11.1 | 5.8 |
| 1#1GF#3 | 0.4-1.1 | 32.8 | 31.4 | 16.6 | 5.3 | 5.9 | 5.7 | 2.2 |
| 1#1GF#4 | 1.1-1.5 | 30.0 | 32.1 | 18.9 | 5.6 | 5.2 | 5.9 | 2.4 |
| 1#1GF#5 | 1.5-2.2 | 28.7 | 31.6 | 18.1 | 5.9 | 6.7 | 6.3 | 2.7 |
| 1#1GF#6 | 2.2-2.7 | 28.2 | 30.7 | 19.1 | 5.9 | 6.8 | 6.5 | 2.7 |
| 1#1GF#7 | 2.7-3.4 | 28.1 | 31.5 | 19.3 | 5.5 | 6.8 | 6.2 | 2.6 |
| 1#1GF#8 | 3.4-3.8 | 27.7 | 31.7 | 19.9 | 6.0 | 6.5 | 5.9 | 2.2 |
| 1#1GF#9 | 3.8-4.5 | 27.2 | 31.0 | 20.0 | 6.1 | 6.9 | 6.4 | 2.5 |
| 1#1GF#10 | 4.5-4.9 | 27.4 | 31.2 | 20.1 | 6.3 | 7.2 | 6.0 | 1.9 |
| 1#1GF#11 | 4.9-5.5 | 28.4 | 31.6 | 18.9 | 6.1 | 7.2 | 6.0 | 1.9 |
| 1#1GF#12 | 5.5-6.2 | 28.3 | 30.0 | 19.0 | 6.1 | 7.4 | 6.7 | 2.5 |
| 1#2WF#1 | 0.2-0.24 | 26.0 | 16.6 | 16.6 | 7.2 | 11.6 | 14.6 | 7.4 |
| 1#2WF#2 | 0.24-0.28 | 26.6 | 16.2 | 16.7 | 7.0 | 11.2 | 15.2 | 7.1 |

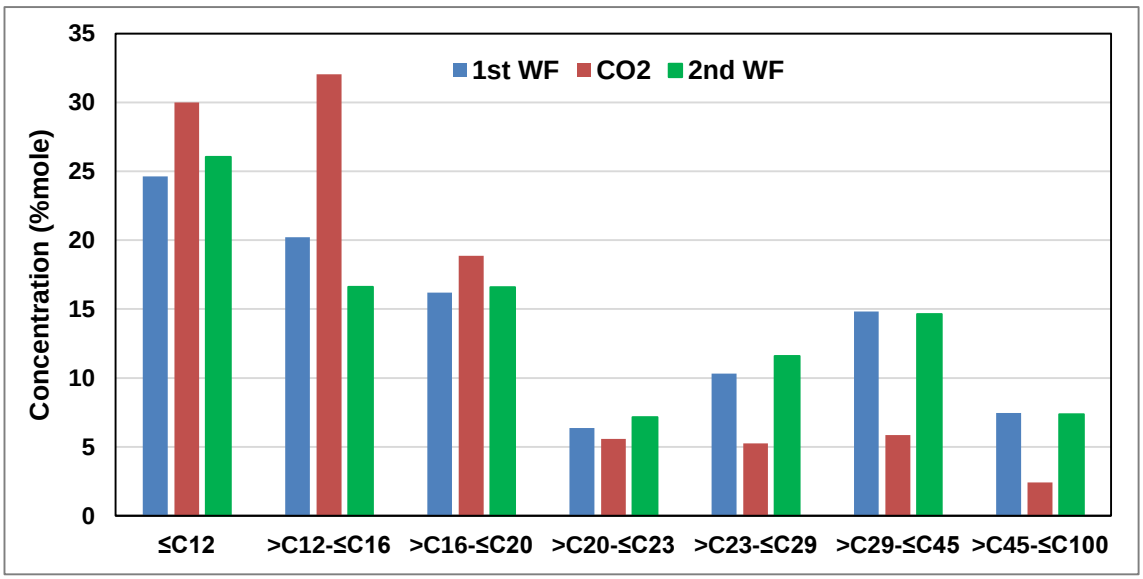


Figure 4-7: Composition of recovered oil during three periods of fluid injection.

It is seen that the composition of produced oil during various stages of the period of tertiary $CO_2$ injection is clearly different from the composition of the original oil in place (1#1WF#1), albeit in varying degrees. This observation indicates the ability of $CO_2$ to

(in-situ) improve the composition of heavy oil in porous media. The changes in the composition of the oil would also affect other physical properties of the oil such as its viscosity.

### 4.1.7 Direct Visualisation Study of Mechanisms of Heavy Oil Recovery by Dense $CO_2$ Injection

An important characteristic of $CO_2$ is its ability to extract or vaporise hydrocarbons from a crude oil. That is, it is believed that the process of extraction occurs under certain conditions of temperature and pressure and it is, fundamentally, dependent on the density of $CO_2$-rich phase. Another crucial factor controlling the strength of extraction by $CO_2$ is the ratio of the volume of $CO_2$ to the volume of oil. Investigations, under similar and constant conditions, have shown that decreasing the ratio of $CO_2$ to oil to a smaller ratio (but still above that required to saturate the oil) reduces the amount of oil extracted. However, the pressure at which the extraction begins remains unchanged indicating that the density of $CO_2$ is the dominant factor determining the extraction behaviour of it (Menzie & Nielsen 1963; Holm & Josendal 1974). Given the above, the oil used in previous investigations had usually the characteristics of a conventional (light) oil. It recurs in the literature that small hydrocarbon molecules are extracted more efficiently into a $CO_2$-rich phase than are large ones. For example, Orr & Silva (1987) measured compositions of $CO_2$-rich and oil-rich phases. Their data confirm that small molecules partition preferentially over large molecules into a $CO_2$-rich phase.

However, the oil, crude 'C', that was used in the Coreflood#1 is a stock-tank oil sample and is characterised as an extra-heavy oil. Therefore, to understand the interactions between $CO_2$ and crude 'C' under the conditions of the experiment, it is important to investigate the extraction behaviour of $CO_2$-rich phase and heavy oil under similar conditions. A setup was designed and prepared to visually observe the contact of $CO_2$ with heavy oil under reservoir conditions. A simplified schematic of this setup was presented in the previous chapter.

Around 0.4 $cm^3$ of the crude 'J' was poured into the container using a syringe. Care was taken to ensure that no air was trapped within the oil and also to have a flat level of oil in the container. Then, the container was vertically mounted inside the visual-cell. After isolating the cell, the heater was switched on and set at 28˚ *C*. Later, methane was introduced to the system firstly at low pressure and then the pressure was gradually and at a controlled rate increased to the test pressure. The oil in the container was only accessible from the top end of the container. It was observed that the level of oil started rising after having contact with methane as a result of dissolution and diffusion of

methane into the dead oil. This swelling of the oil was relatively rapid at early times of contact of methane with oil and the speed of rising of the level of oil decreased later on. The images were taken during this process clearly show the swelling of the oil. Figure 4-8 depicts the level of oil in the container before the contact with methane (left) and after the equilibrium between the oil and methane (right).

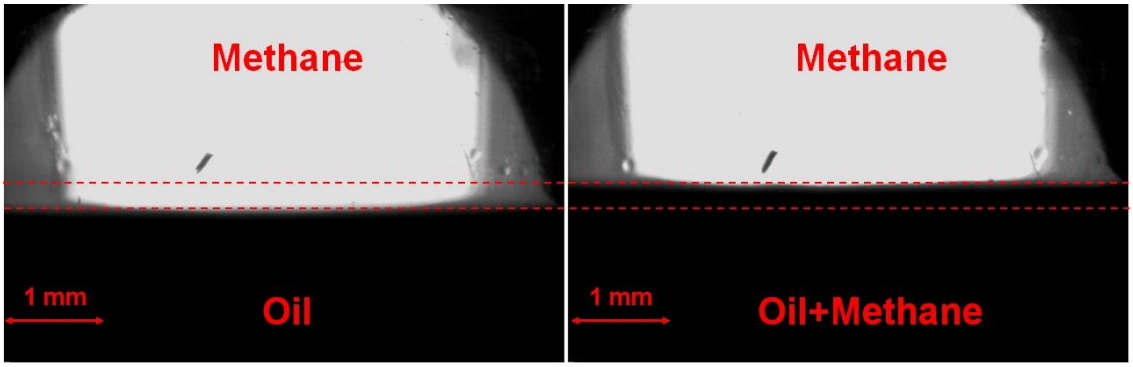


Figure 4-8: Level of oil in the container before the contact with methane (left) and after equilibrium with methane (right).

When the oil in the container was eventually fully saturated with methane, $CO_2$ was introduced to the system from the bottom of the visual-cell and methane was removed from the top of the cell at constant pressure. The procedure was performed at a slow and controlled rate to ensure complete displacement of methane by $CO_2$ and to ensure that the pressure of the system remained constant during this displacement. This was continued until the time that the volume of injected $CO_2$ in the visual-cell reached to slightly higher than the volume of the visual-cell. Then, the top valve was isolated and the visual-cell was kept connected to the $CO_2$ cell until the end of the run. This process was aimed to visually observe the interactions between heavy oil and $CO_2$. The difference in the density of $CO_2$ and methane are significantly high under the conditions of this experiment which were T=28˚ *C* & P=1500 psi. Therefore, the injection of $CO_2$ from the bottom of the cell and removing methane from the top of the cell would completely remove the methane from the system.

It was observed that once $CO_2$ contacted the oil in the container, the extraction of hydrocarbons, mostly methane at the beginning, from the oil started instantly, as evidenced in Figure 4-9. The contact between $CO_2$ and the oil in container caused to the extraction of light and intermediate components of the oil from the interface. It was seen that this phenomenon initially led to a sudden swelling of the oil mainly due to the liberation of dissolved methane from the oil. The liberation of methane and other hydrocarbon components from the oil was continued as time went on which indicates that $CO_2$ had also affected the oil below the surface. The process of extraction of hydrocarbon

continued although the speed of it decreased dramatically after a complete liberation of the light components of the oil such as methane.

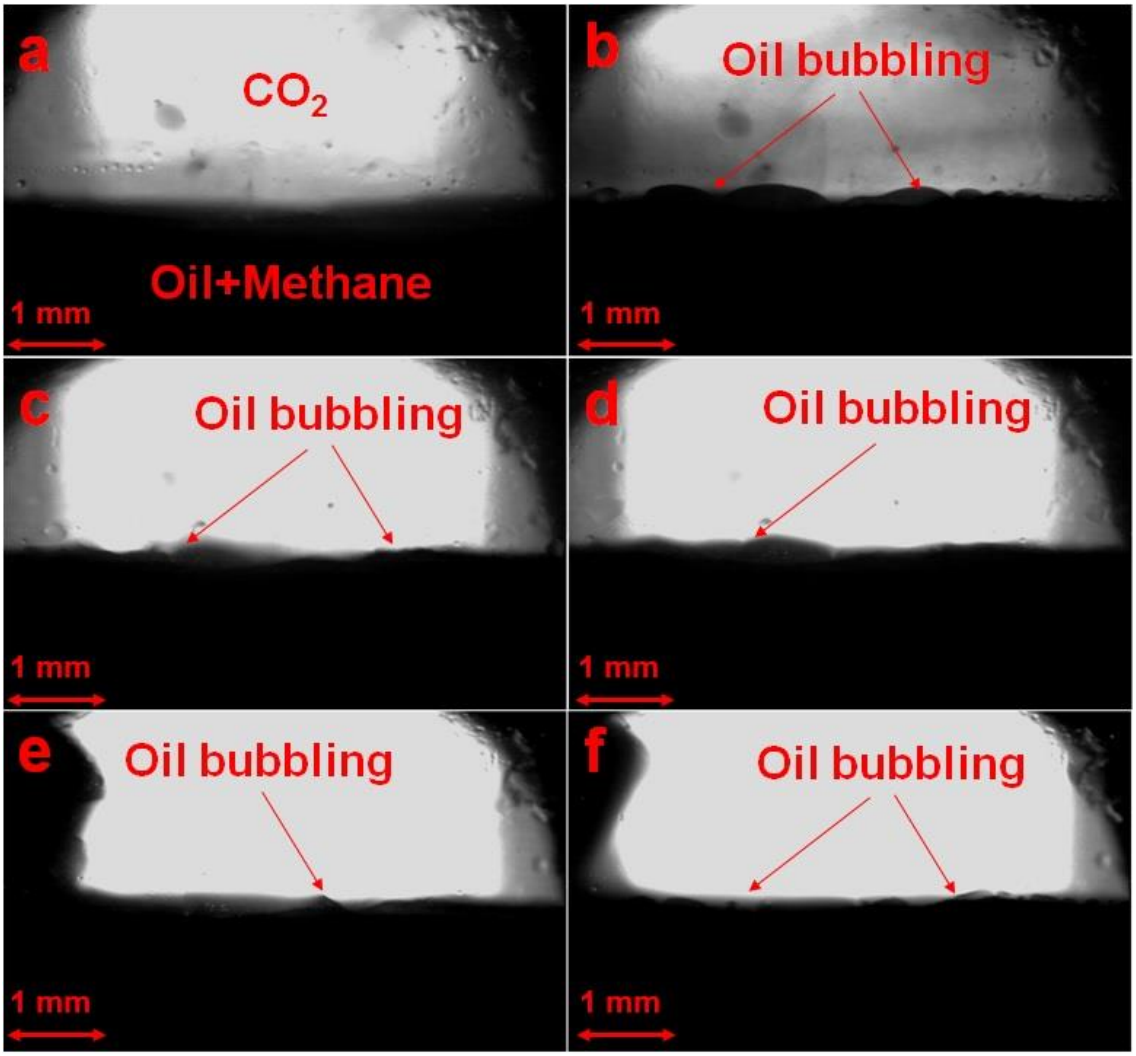


Figure 4-9: Extraction of oil components by $CO_2$ (a) first contact, (b) 1 minute, (c) 4 minutes, (d) 10 minutes, (e) 20 minutes, (f) 100 minutes after the first contact.

Eventually, more hydrocarbon components were extracted from the oil by $CO_2$ and the level of the oil went below the original level of the oil before the contact with $CO_2$ started. Figure 4-10 shows that the volume of oil in the container has decreased significantly after around 10 days of the contact between the oil and $CO_2$. At this stage, to be able to record the level of oil in the container, the height of camera was lowered.

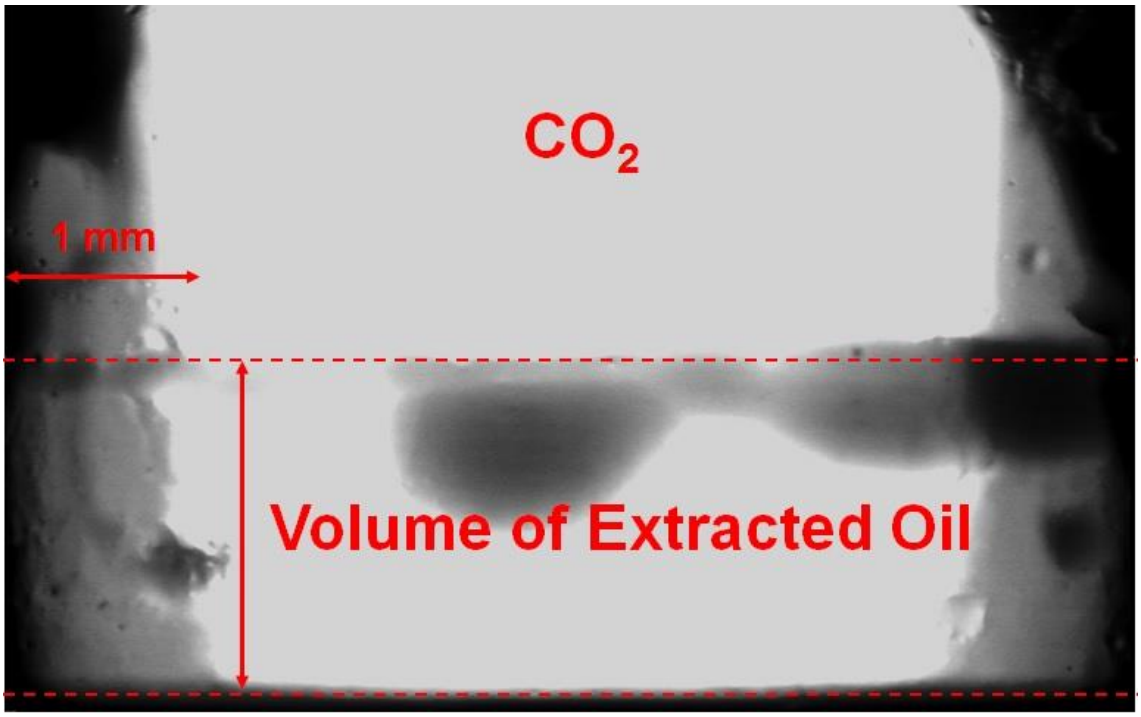


Figure 4-10: Shrinkage of oil volume because of the extraction of light to intermediate components by $CO_2$, after 10 days.

A behaviour similar to what was described above was also observed when the oil was dead (no dissolved hydrocarbon gas) albeit to a lesser extent, in particular at the beginning of the contact between $CO_2$ and the dead oil, since the oil did not have solution gas (methane). In the dead oil again it was observed that the extraction of oil components continued and a significant volume of the oil was gone into the $CO_2$-rich phase. After completing each test, the pressure of the system was decreased slightly at constant temperature and it was observed that the volume of oil was slightly decreased due to the liberation of dissolved $CO_2$ from the oil. Moreover, it was observed that a small amount of colourless greasy-nature liquid was left at the bottom of the visual-cell after decreasing the pressure to the ambient conditions which is believed to be the extracted hydrocarbons in the $CO_2$-rich phase which were condensed to liquid at atmospheric pressure.

The composition of the remaining oil after the extended contact of oil and $CO_2$ was analysed and compared to the composition of the original dead oil, Figure 4-11. It should be mentioned that a fraction of heavy cuts of both oil samples could not be recovered by the compositional analysis (simulated distillation) which accounted for around 10% and 14% of the mass of the crude 'J' and the remaining oil in the visual-cell, respectively. As shown, all the components up to $C_{10}$ have been completely extracted from the original oil by $CO_2$. Moreover, the concentration of the intermediate components up to $C_{23}$ has been reduced significantly in the remaining oil whereas the amount of the heavier components remained unchanged or changed little. It should be mentioned that the concentrations of

components of carbon numbers of 25 and 26 have also decreased slightly. The changes in the composition of the oil because of the extraction accounts for a decrease around 29% of the mass of the original oil but it was seen that that is even higher in terms of volume of oil under reservoir conditions.

In a porous medium, the components extracted by the $CO_2$-rich phase could be easily displaced and recovered at the production outlet because of the high mobility of the carrying phase. The remaining oil that has lost a significant fraction of its light and intermediate compounds is a heavier oil than it was before the contact with $CO_2$ and hence, it would have higher viscosity and density than the original oil. However, it appears that $CO_2$ dissolution in the remaining oil would reduce its viscosity and density and the oil can also be displaced towards the production outlet by the displacing fluid.

The process of extraction is generally slow and hence, it is more likely to take place near the injection wells where the volume (amount) of $CO_2$ compared to the saturation of oil in place and the time that the injected $CO_2$ and the reservoir oil are in contact would be significant. Thus, the amount of oil extracted by $CO_2$ would be facilitated. In addition, fluids are usually pumped into a formation at pressures higher than the reservoir pressure and this obviously improves the strength of extraction by $CO_2$. Therefore, the mechanism of extraction of hydrocarbon components by $CO_2$ appears to lead to the recovery of a significant fraction of higher quality oil than the original oil in heavy oil reservoirs.

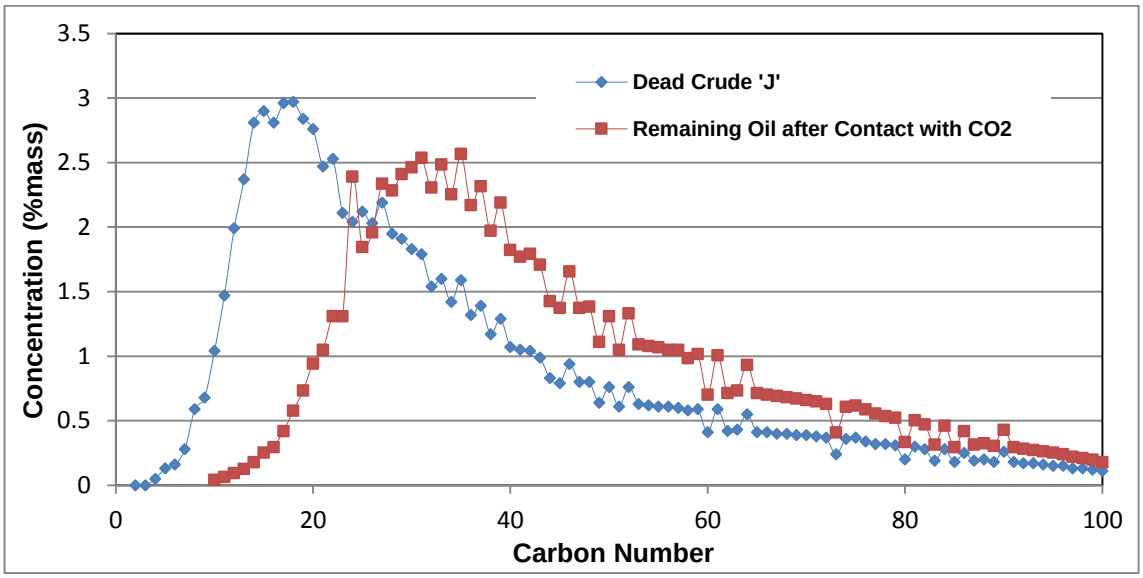


Figure 4-11: Compassion of compositional analysis of crude 'J' and the remaining oil after contact with (liquid) $CO_2$.

It is believed that density of $CO_2$ is the dominant factor in determining the size of extracted components (Menzie & Nielsen 1963; Holm & Josendal,1974). The $CO_2$-rich phase at T=28˚ *C* & P=1500 *psi* is a liquid and hence, it has a high density of around 0.8 $g/cm^3$ and could extract some hydrocarbon components with a density ranging from the

lowest (methane) up to as high as the density of $CO_2$ phase. However, it is seen that the effect of extraction by $CO_2$ was not uniformly distributed for components with different carbon numbers. For instance, the concentration of components with a carbon number of 24 has increased whereas it has decreased for carbon numbers of 25 and 26. This shows that $CO_2$ perhaps had a higher ability to extract some components with certain chemical structure than the other molecules with the same carbon number.

Another compositional analysis, mass spectrometry (MS) 19x19 matrix analyses, was performed on the dead crude 'J' and the remaining oil after the contact with $CO_2$ to investigate the effects of molecular structure on the mechanism of extraction of hydrocarbon components by $CO_2$. This run was performed using a mass spectrometer operating at high mass resolution. This method is applicable for the determination of hydrocarbon types in petroleum distillates boiling in the range 350 to 510˚ *C*. Samples were introduced into the mass spectrometer using a water-cooled, heated probe, operating over a temperature programme of 40° *C* (1 min hold) to 600° *C* (10 min hold), at 12.5° *C/min*. Given the above, the results shown in Table 4-3 are not representative of the whole samples and should be treated, therefore, as indicative only.

Table 4-3: 19x19 matrix analysis of crude 'J' and the remaining oil after contact with (liquid) $CO_2$.

| **Hydrocarbon Type** | **Crude 'J' (%wt)** | **Remaining Oil after Contact with $CO_2$ (%wt)** |
|---|---|---|
| Paraffins, CnH2n+2 | 1.8 | 7.0 |
| Monocycloparaffins, CnH2n | 14.9 | 15.5 |
| Dicycloparaffins, CnH2n-2 | 4.4 | 2.9 |
| Tricycloparaffins, CnH2n-4 | 1.8 | 0.8 |
| Tetracycloparaffins, CnH2n-6 | 0.7 | 0.9 |
| Pentacycloparaffins, CnH2n-8 | 0.7 | 0.9 |
| Hexacycloparaffins, CnH2n-10 | 0.5 | 1.1 |
| Alkyl Benzenes, CnH2n-6 | 7.4 | 6.0 |
| Benzocycloparaffins, CnH2n-8 | 8.0 | 3.3 |
| Benzodicycloparaffins, CnH2n-10 | 9.0 | 1.0 |
| Naphthalenes, CnH2n-12 | 3.5 | 3.3 |
| Acenaphthenes, CnH2n-14 | 5.0 | 4.8 |
| Fluorenes, CnH2n-16 | 13.2 | 13.1 |
| Phenanthrenes/Anthracenes, CnH2n-18 | 16.2 | 22.1 |
| Pyrenes, CnH2n-22 | 5.0 | 7.5 |
| Chrysenes, CnH2n-24 | 0.1 | 2.3 |
| Benzothiophenes, CnH2n-10S | 2.6 | 0.6 |
| Dibenzothiophenes, CnH2n-16S | 4.9 | 5.6 |
| Naphthobenzothiophenes, CnH2n-22S | 0.5 | 1.4 |

Around 36% and 37% of the mass of the original (dead) crude 'J' and the remaining oil in the visual-cell were within the scope range of 19x19 MS analysis. Having said that, the values should be treated as indicative only because a fraction of oil in the visual-cell had been extracted by $CO_2$. Compared to the original oil, it is seen that the concentration of some of the components has decreased in the remaining oil after contact with liquid $CO_2$. In an experimental investigation using a mass spectrometer, Hagedorn & Orr (1994) showed that K-values for cyclic compounds is lower compared to that of similarly eluting alkanes. Multi-ring aromatic compounds have also lower K-values than similarly eluting normal alkanes. Therefore, it was concluded that multi-ring aromatic components in crude oils are extracted less efficiently by dense $CO_2$ than other hydrocarbons compounds of similar size or similar GC elution time can be extracted. However, the results of 19x19 matrix analysis on our samples reflect that some of the cyclic and multi-ring components have shown significant extraction behaviour. This, therefore, requires further investigations to understand the importance of different factors on the phase behaviour of $CO_2$ and crude oil. However, that is not the main objective of this study.

The compositional analysis of the samples of produced oil during the coreflood#1 (Table 4-2) showed that the concentration of intermediate components in the oil produced by $CO_2$ injection is higher than that of the original oil. The main mechanisms of oil recovery during the period of $CO_2$ injection were viscous flow, $CO_2$ dissolution in the oil and the resultant oil viscosity reduction and oil swelling, gravity drainage, and the extraction of hydrocarbons by $CO_2$-rich phase.

At first glance, the increase in the concentration of light and intermediate components in the samples of recovered oil during the period of $CO_2$ injection is attributed to the presence of the mechanism of extraction by $CO_2$ in the core. It was visually observed that the contact of dense (liquid) $CO_2$ with heavy oil under reservoir conditions leads to the extraction of light and intermediate components from the oil. Therefore, the improvement in the composition of oil recovered by $CO_2$ appears to be related to the impact of the mechanism of extraction in the core where the extracted hydrocarbons were carried out to the production outlet by the $CO_2$-rich phase.

However, it is significant that from the early times of the period of $CO_2$ injection into the core, higher quality oil in terms of composition was recovered. It was shown that the speed of the mechanism of extraction decreases significantly after the sudden extraction of relatively light components (mainly methane) from the oil at early times of the process, albeit it is a continuous process. The speed of this process would be further decreased in porous media due to the presence of water in pore spaces between oil and $CO_2$ (water-

shielding) and heterogeneity of rock. Moreover, other parameters such as oil composition and oil viscosity can affect the process of extraction of hydrocarbons by $CO_2$. The oil used in the coreflood experiments (crude 'C') had significantly higher viscosity than the oil used in the visual-cell experiments (crude 'J'). Also, crude 'C' has a lower concentration of light and intermediate components than crude 'J'. These factors, therefore, would have decreased the speed of the extraction of hydrocarbon compounds by $CO_2$ in the coreflood experiment.

An indication of oils recovered due to the extraction in fluid flow processes is their lighter colour compared with that of the original oil (Holm & Josendal 1974). Therefore, if the extraction mechanism was stronger in the coreflood experiment, it could have been expected to observe two different types of oils (in terms of colour, viscosity, etc.) in the production outlet but that was not the case in this experiment. The produced oil in the coreflood tests was a relatively homogeneous black oil and no obvious interface was observed among the production liquid, except for water and oil. Moreover, no considerable condensate accumulation was observed in the wet-gas-meter systems during the coreflood test. The same dead crude oil, that was used to prepare live oil for the coreflood tests, was used to prepare $CO_2$-saturated oil for viscosity measurements. Whilst the volume of $CO_2$ in the rocking cell was significant compared to the volume of oil, no considerable condensate (oil) production was also observed during removing the gas cap from the $CO_2$-saturated oil.

Overall, these observations indicate that for the viscous oil that was used in the coreflood experiments, the extraction process may not have been the only reason for the improvement of the composition of produced oil from the core. The other active mechanism during the period of $CO_2$ injection which could potentially alter the composition of recovered oil was $CO_2$ dissolution and diffusion in the oil. It was shown that the dissolution of $CO_2$ in heavy oil results in oil swelling as well as significant reduction in the oil viscosity, Table 3-6. Consequently, the oil saturated with $CO_2$ will have higher mobility than the original oil and it will also travel faster in porous media. Thus, it is believed that the dissolution of $CO_2$ in heavy oil causes the light and intermediate fraction of heavy oil to move faster than the rest of the oil. In other words, although $CO_2$ dissolution in heavy oil reduces the viscosity of the whole oil, these results suggest that its impact may not be uniformly distributed for compounds with different carbon numbers. This behaviour of $CO_2$ is somehow similar to the process of solvent injection for oil recovery which usually results in the formation of a lighter and less viscous oil phase.

To evaluate these phenomena and also to understand the impacts of them on the process of oil recovery, direct visualisation of flow of $CO_2$ and heavy oil using a transparent micromodel was performed under the similar conditions of the coreflood experiment. Initially, the micromodel was fully saturated with brine and then dead crude oil 'J' was injected through the micromodel to establish initial water and oil distributions. Figure 4-12 shows a magnified section of the micromodel at the end of the period of oil injection.

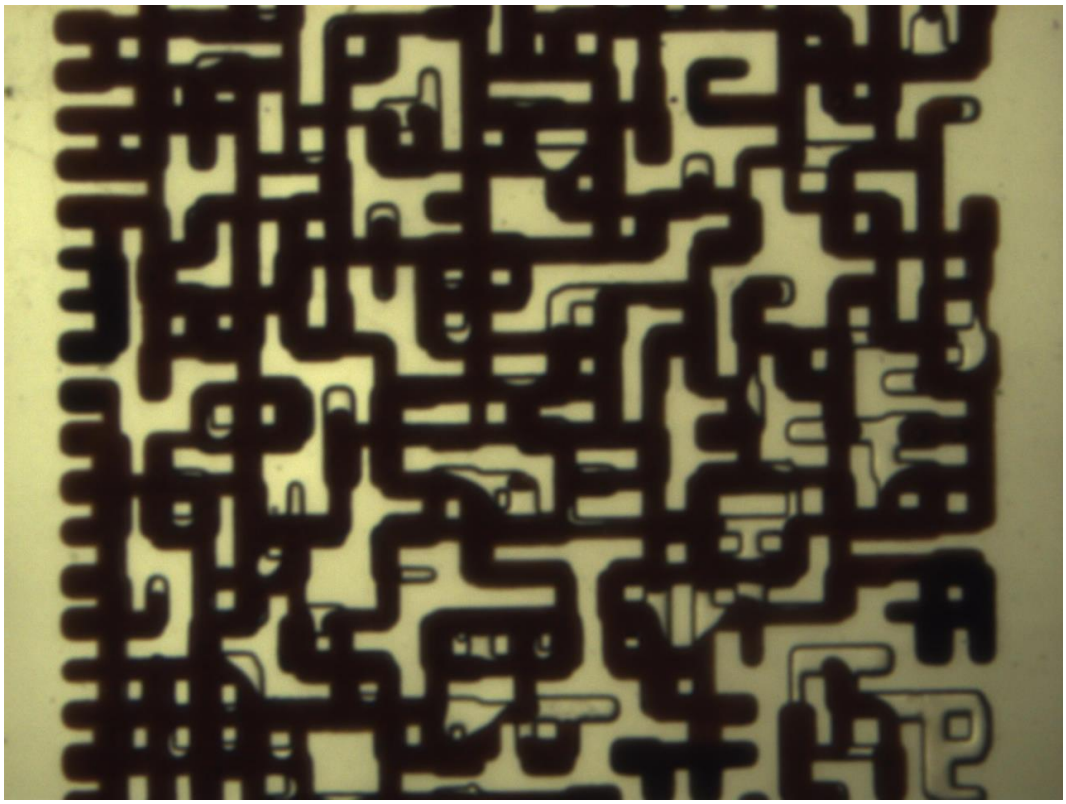

Figure 4-12: A magnified section of the micromodel at the end of the period of oil injection.

Having established the initial water and oil distributions, $CO_2$ was injected at 0.01 $cm^3/hr$ through the micromodel from the bottom end of the model. Figure 4-13 shows a section of micromodel before the breakthrough of $CO_2$. It is seen that because of the adverse viscosity ratio between oil and $CO_2$, the sweep efficiency of $CO_2$ is relatively poor and viscous fingering dominates the flow. Although several branches can be seen around the stream of $CO_2$, only one main finger was generated in the model. This can also be related to the topology of the porous medium. Moreover, it was observed that parts of the oil which were in direct contact with $CO_2$ became lighter in colour due to the dissolution of $CO_2$ in the oil.

After the breakthrough, oil production continued with relatively low rates mainly because of viscous forces and the dissolution of $CO_2$ in the oil and the resultant oil swelling and oil viscosity reduction. As shown in Figure 4-14, the flow of a new phase with a light

colour in the $CO_2$-rich stream was observed. Although this new phase could not travel in the porous medium as fast the stream of $CO_2$, it was seen that this phase is significantly mobile. At first glance, this can be related to the mechanism of extraction of oil compounds by $CO_2$. However, the extracted compounds are essentially miscible with $CO_2$ and the extraction generally occurs in all parts of the interface between oil and $CO_2$. Thus, the obvious colour difference in the stream of $CO_2$ cannot be explained by the mechanism of extraction. In addition, it was observed that this new phase was formed as a result of $CO_2$ and oil contact in the flow path of $CO_2$. It is, therefore, believed that this new phase is a fraction of the oil in contact with $CO_2$ which has significantly low viscosity and probably it is rich in light and intermediate components of the oil which can explain the high mobility of this phase in the porous medium.

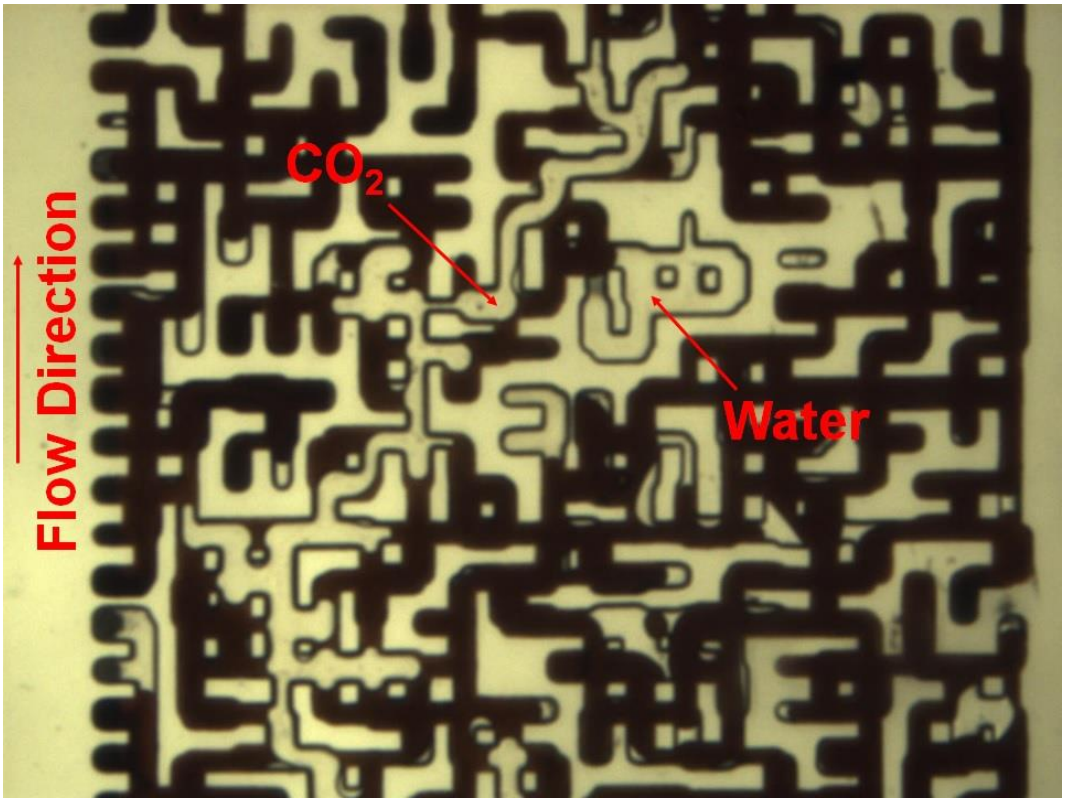


Figure 4-13: A magnified section of the micromodel before the breakthrough of $CO_2$.

It was shown that dense (liquid) $CO_2$ can extract heavy oil components. As soon as $CO_2$ becomes in contact with the oil in micromodel, light and intermediate compounds of the oil are attracted by $CO_2$-rich phase. Therefore, an accumulation of these components would be expected to take place in the oil phase, near the interface of oil and $CO_2$. That is, it is assumed that the similar process occurred during the period of $CO_2$ injection in the micromodel and hence, the displaced oil due to the flow of $CO_2$ had a higher concentration of the light and intermediate components than the original oil in place. Oil Swelling due to the dissolution of $CO_2$ would have also had a contribution in this process

by limiting the flow path of $CO_2$.

In general, it is considered that when dense $CO_2$ is injected into an oil reservoir, three hydrocarbon phases may exist at high $CO_2$ concentrations (Hamouda & Alipour Tabrizy 2013; Pan, et al. 2014). These three phases include a vapour phase, an oil-rich phase, and a $CO_2$-rich phase. The results of our coreflood experiment and visual-cell experiments also confirmed that at least three phases could appear in pore spaces when dense $CO_2$ contacts oil, including a vapour phase (mainly methane in our experiments), an oil-rich phase, and a $CO_2$-rich phase. Here, it was shown that a second oil-rich phase also forms in porous media during injection of dense $CO_2$ for heavy oil recovery which contributes to additional oil recovery as well as higher quality oil production.

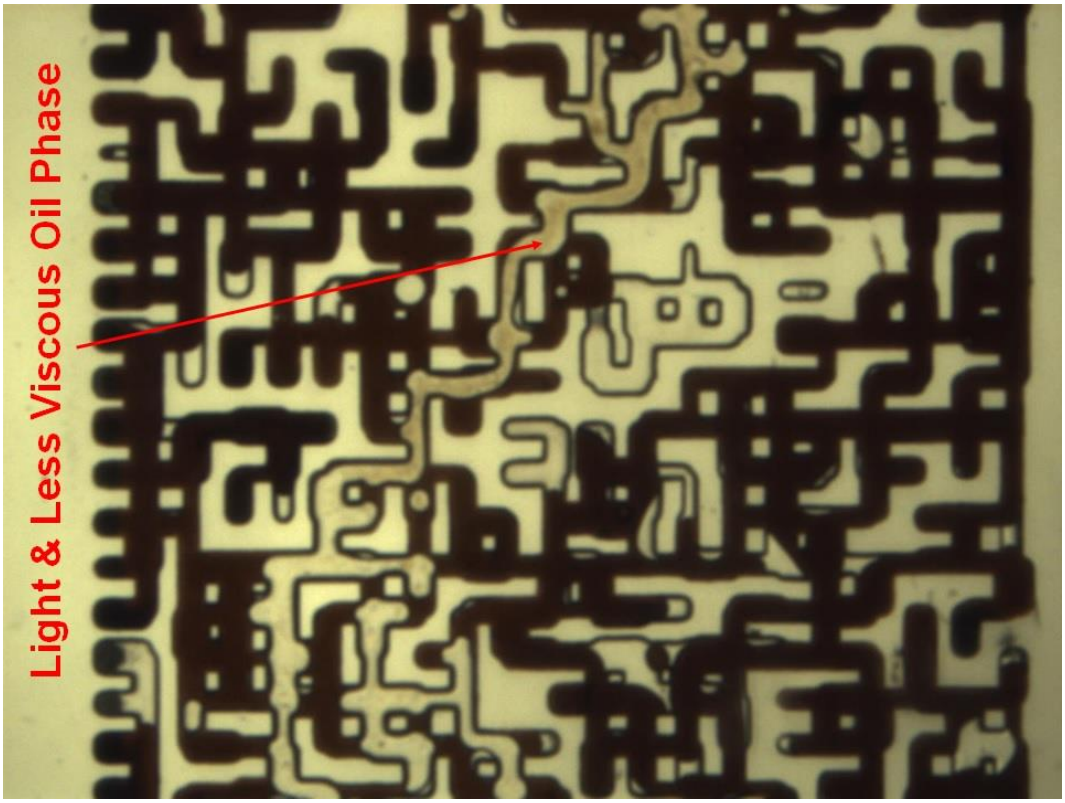


Figure 4-14: The same magnified section of the micromodel after a short time after the breakthrough.

Figure 4-15 depicts a sequence of images showing the formation of the light and less viscous oil phase as a result of the contact between the oil and $CO_2$. A small layer of the surface of the oil is removed and displaced by the flow of $CO_2$ (Figure 4-15a). That part of the oil has a higher concentration of the light and intermediate components than the original oil in the micromodel due to the extraction strength of dense $CO_2$. Hence, the light and less viscous oil phase has a high mobility and it is displaced fast (Figure 4-15b-f). Figure 4-15g-h shows that this process takes place at various locations in the porous system. However, the fact that the light and less viscous oil phase is formed in a part of the main path of $CO_2$ confirms that the contact between the oil and $CO_2$ contributes to

this process.

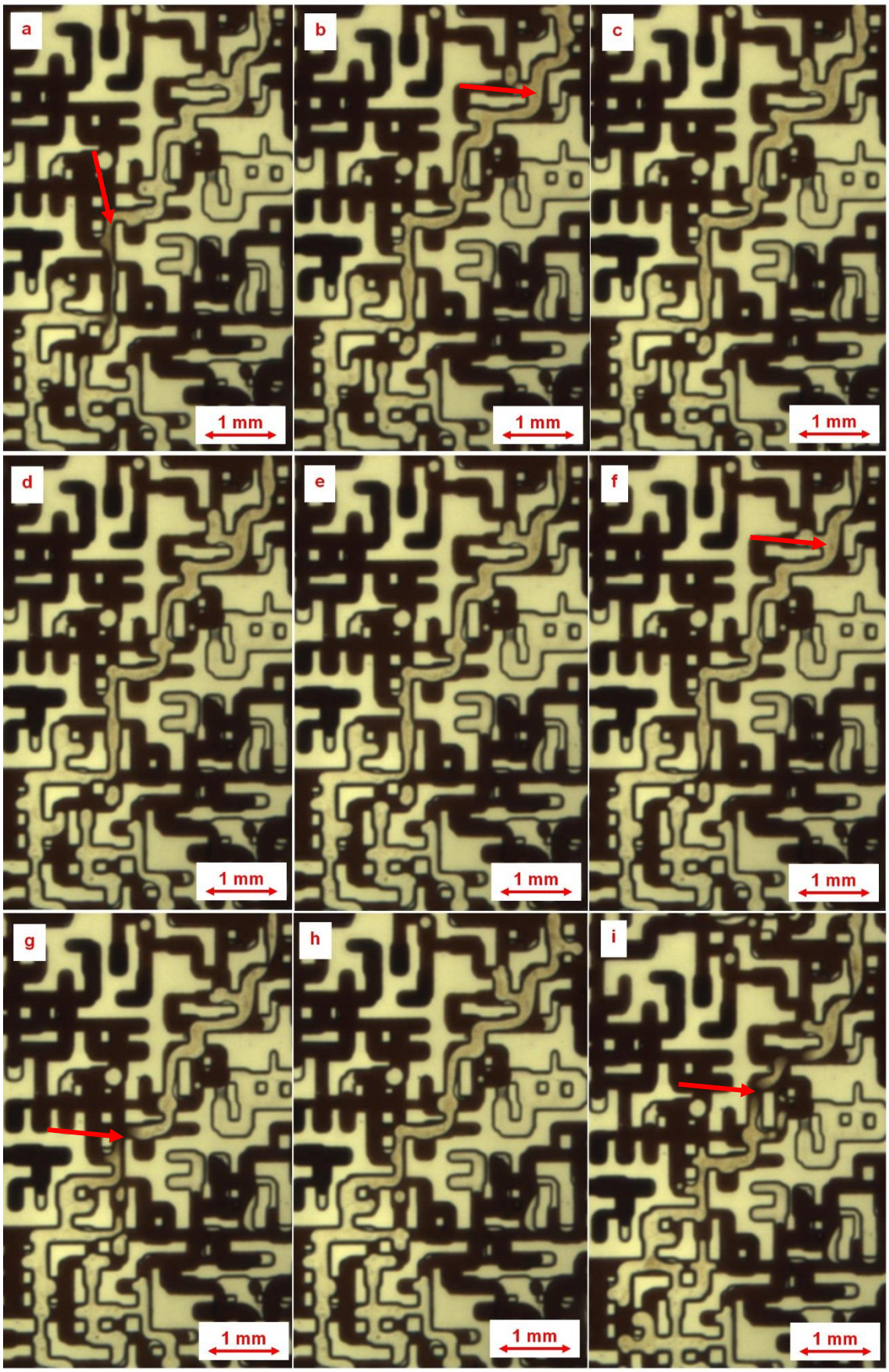


Figure 4-15: A sequence of images taken every 2 minutes from the same magnified section of the micromodel after the breakthrough. The formation of a light colour oil phase in the $CO_2$-rich stream is happening due to the contact and flow of $CO_2$ and the oil (arrows indicate points of interest).

For a relatively short time after the breakthrough, it was observed that the dissolution and diffusion of $CO_2$ in the oil were still dominant and a larger fraction of the oil near the stream of $CO_2$ became lighter in colour. However, as the injection of $CO_2$ continued, Figure 4-16, it was noticed that parts of the oil close to the $CO_2$-rich stream became darker in colour which indicates that light and intermediate components of the oil have left the oil.

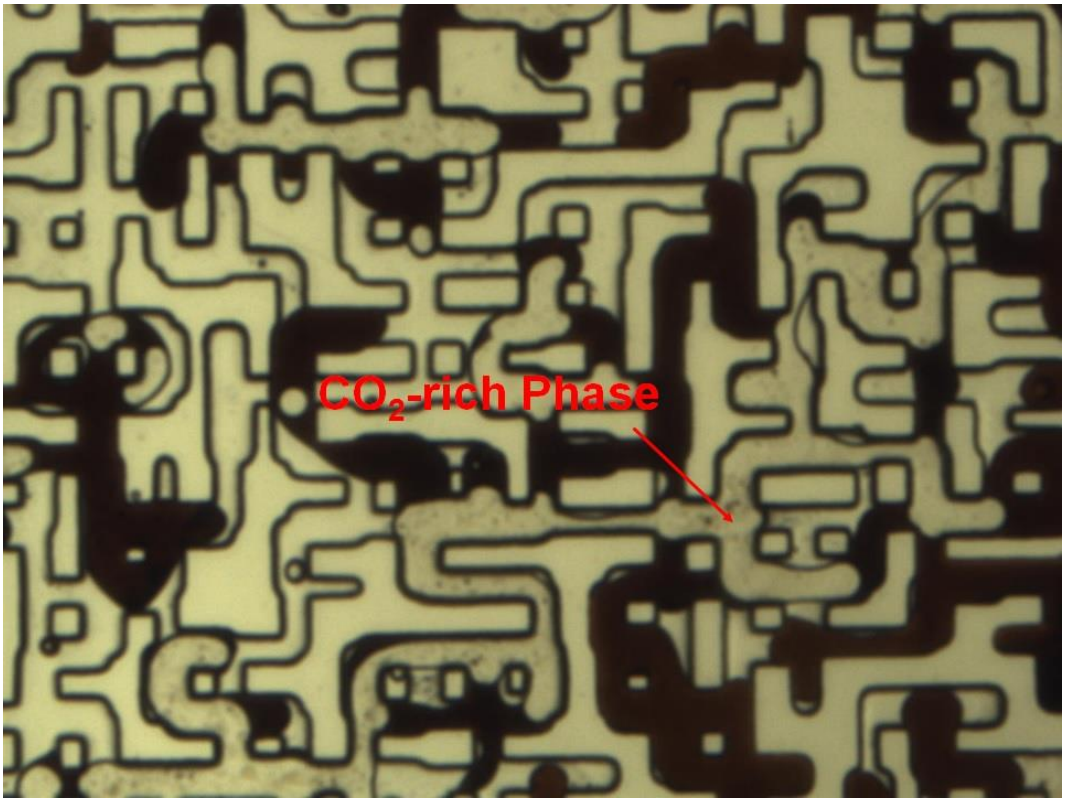


Figure 4-16: A magnified section of the micromodel after a long time after the breakthrough.

After the period of $CO_2$ injection, water (methane-saturated) was injected through the micromodel. Figure 4-17 depicts a magnified section of the micromodel during the period of tertiary waterflood. The injected water initially had no dissolved $CO_2$ and hence it had a tendency to uptake $CO_2$ in the micromodel; either as a free phase or as dissolved $CO_2$ in the oil. It should be mentioned that this is different from the direct displacement of $CO_2$ in the place by the injected water. Figure 4-18 shows the same section of the micromodel during the period of waterflood. It is seen that the injected water could remove a saturation of $CO_2$ in the model by diffusion of $CO_2$ into the water. Water could also take $CO_2$ from the oil saturated with $CO_2$ and that caused to the shrinkage and redistribution of the oil.

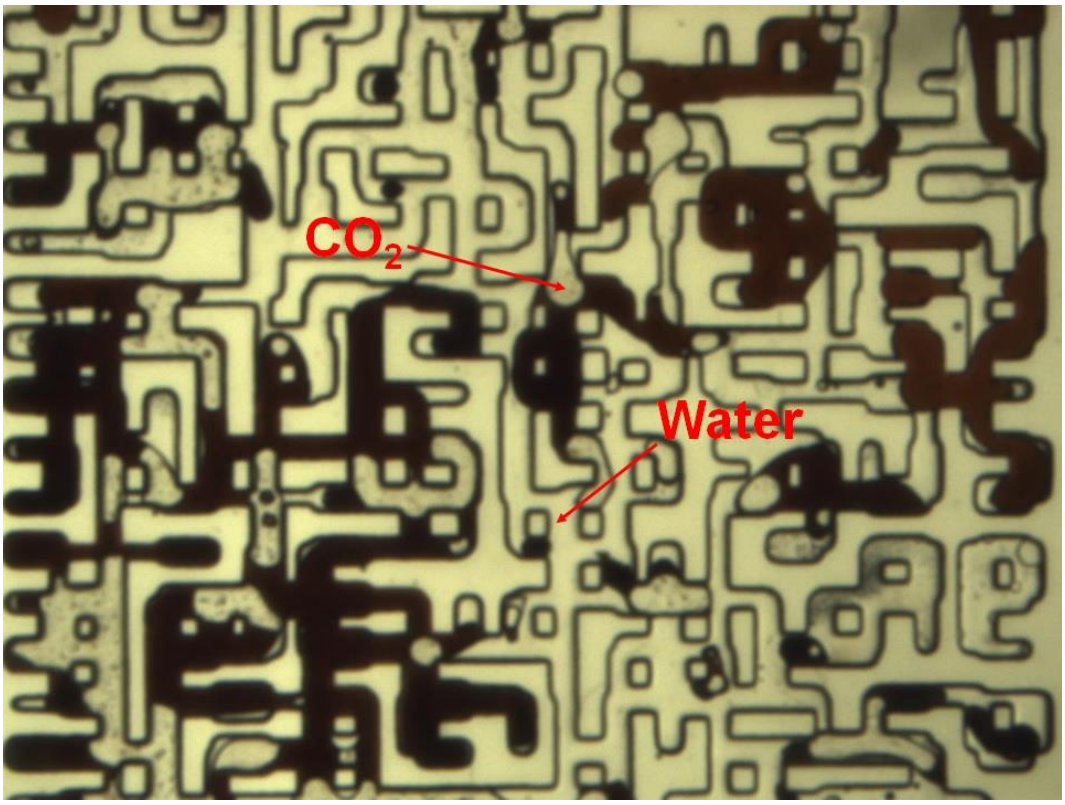


Figure 4-17: A magnified section of the micromodel during the period of tertiary waterflood.

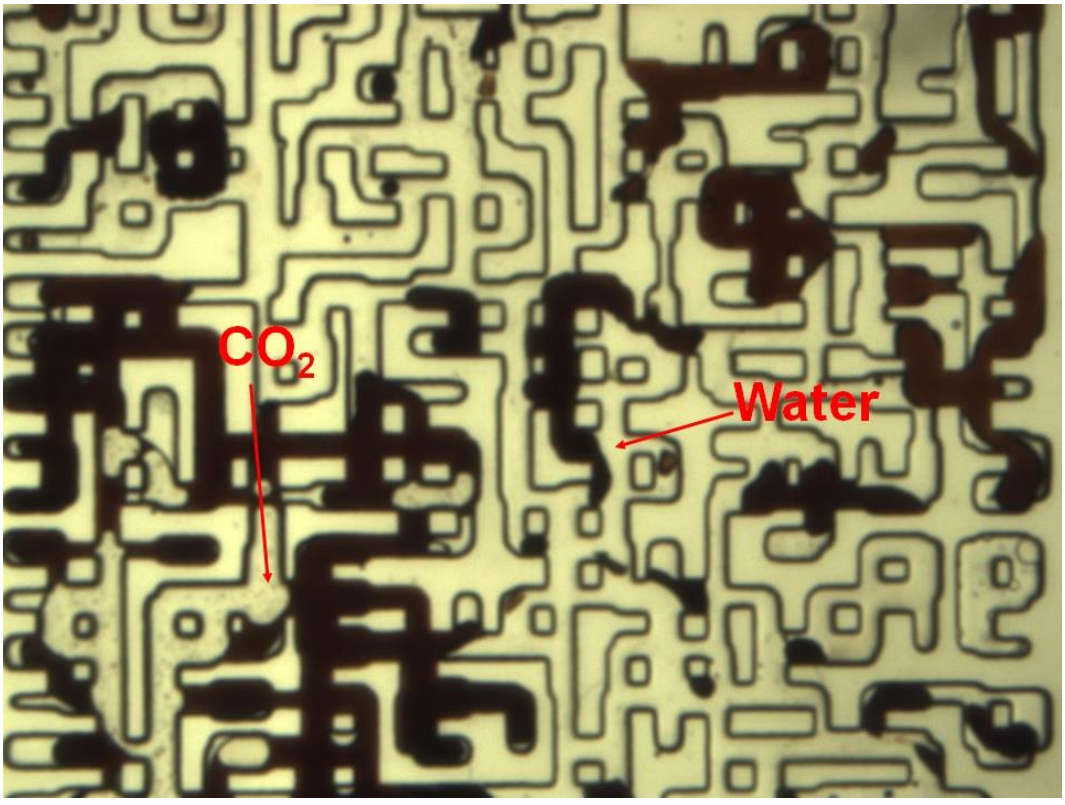


Figure 4-18: The same magnified section of the micromodel during the period of tertiary waterflood.

In another experiment, $CO_2$ was injected into the micromodel after the extended period of tertiary waterflood. The tertiary waterflood was continued until there was virtually no free $CO_2$ in porous media, Figure 4-19. Three different types of oil in term of colour can

be seen in the image; first, the dark colour oil which was the oil in direct contact with the injected $CO_2$ and water. The extraction of components of the oil during the period of $CO_2$ injection as well as the diffusion of $CO_2$ from the oil into the injected water led to a darker colour of the oil in the micromodel. Second, the light colour oil is the fraction of oil which was not in direct contact with the flowing stream of secondary $CO_2$. Thus, the extraction of hydrocarbon compounds by $CO_2$ was not as significant as the extraction of the oil components from the fraction of oil in contact with the flow of $CO_2$. In addition, the injected water could not directly invade this area and water and oil contact happened because of the diffusion of free $CO_2$ into the water. The third oil type is the light and less viscous oil phase which was trapped due to the topology of the micromodel.

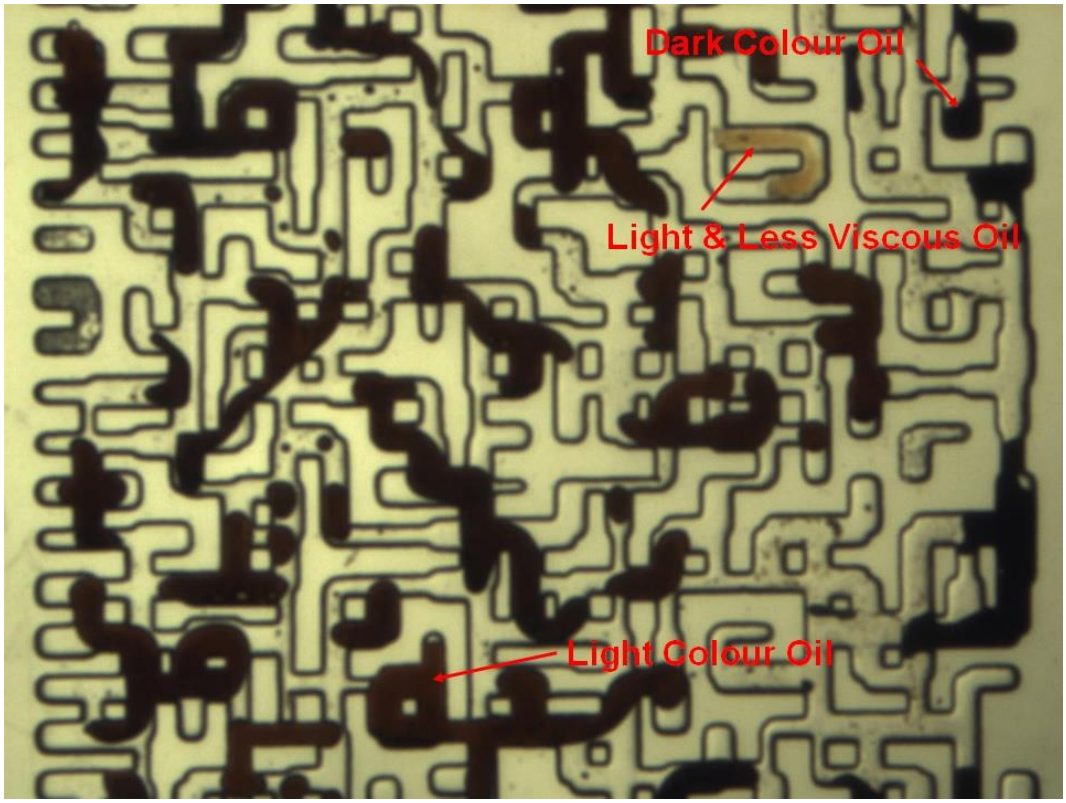


Figure 4-19: A magnified section of the micromodel after the extended period of tertiary waterflood.

After the period of tertiary waterflood, $CO_2$ was injected through the micromodel. The main observation during this period of $CO_2$ injection was the changes in the colour of the trapped oil in the right-hand side of the path of $CO_2$ which has been indicated in Figure 4-20 as 'light colour oil'. This saturation of oil had been trapped by water and it did not have any direct contact with the injected $CO_2$. However, $CO_2$ could diffuse into the water surrounded the oil and partially saturate the water. The higher tendency of the oil to absorb $CO_2$ and the fact that oil had lost its dissolved $CO_2$ during the period of waterflood caused to the extraction of $CO_2$ from the surrounded water by oil. Therefore, there was a continuous transfer of $CO_2$ into the oil through the water around it. This

process led to the swelling of oil as well as the changes in its colour. Another observation during this period of $CO_2$ injection was the formation and displacement of a light and less viscous oil phase through the flowing path of $CO_2$ which was an important reason for the production of higher quality oil during the period of $CO_2$ injection.

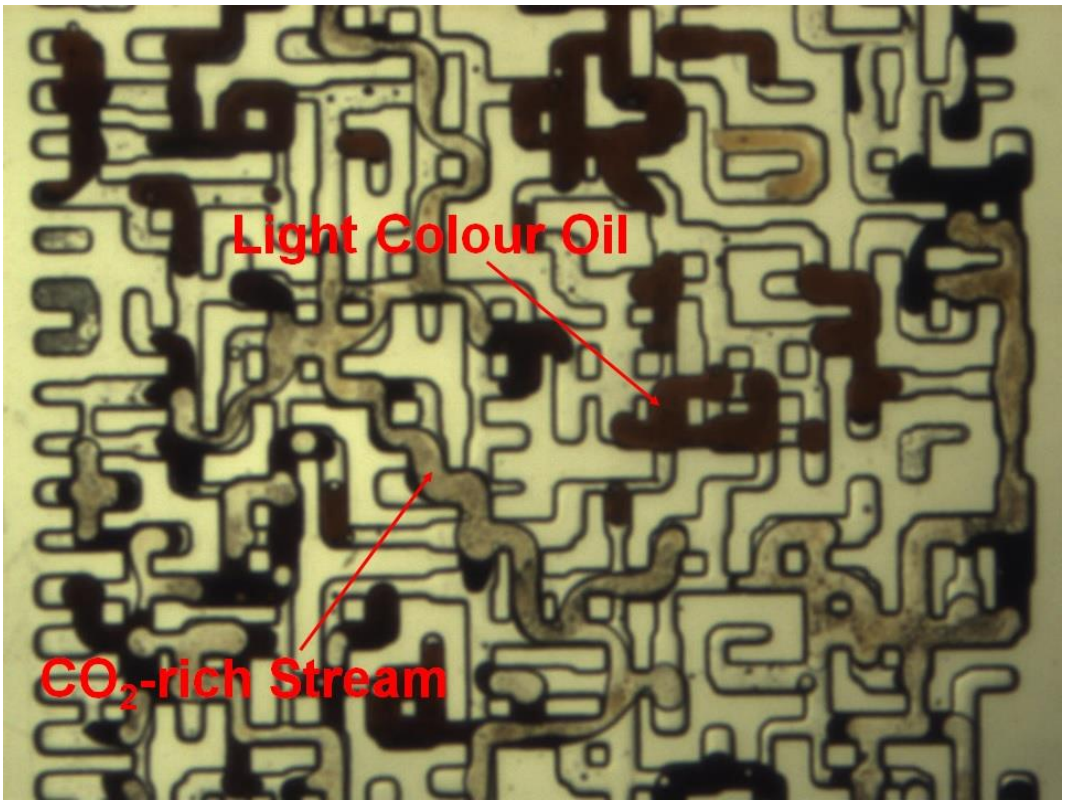


Figure 4-20: A magnified section of the micromodel at the early time of the period of 2nd $CO_2$ injection.

As the injection of $CO_2$ continued, the oil surrounded by water became partially saturated with $CO_2$ and hence the rate of $CO_2$ dissolution and diffusion in the oil would have decreased. At a certain time, as shown in Figure 4-21, the rate of extraction of $CO_2$ from the water by the oil would have exceeded the rate of $CO_2$ diffusion into the oil and that caused to the nucleation of $CO_2$ among the oil. The nucleation of dense $CO_2$ within the crude oil led to the extraction of light and intermediate components of the oil by $CO_2$ and as a result, the volume of $CO_2$-rich phase increased.

Using a transparent micromodel system, Sohrabi & Emadi (2012) visually observed these phenomena when tertiary injection of high pressure (dense) $CO_2$ in crude oil was performed. They considered three factors as the required conditions of the formation of this new phase; first, the oil should be a real crude oil. They did not observe the formation of this new phase when a synthetic fluid (decane) was used instead of crude oil in the experiments. Second, the injection of $CO_2$ should be performed after a period of waterflood. In other words, the presence of water between oil and $CO_2$ which acts as a membrane for transport of $CO_2$ is necessary. Thus, they did not observe the formation of

the new phase when $CO_2$ was injected in the secondary mode. Third, $CO_2$ should be in either liquid or supercritical states and not in the form of vapour. The rate of diffusion of $CO_2$ depends on the density of $CO_2$ and hence $CO_2$ in vapour state would have a significantly lower rate of diffusion (Laidler & Meiser 1982). In addition, the extraction performance of $CO_2$ is affected by the density of $CO_2$ and vapour $CO_2$ cannot extract hydrocarbon components as much as a liquid or supercritical $CO_2$ would extract. Therefore, larger time is required for vapour $CO_2$ to saturate oil surrounded by water and perhaps the proper time has not been given to $CO_2$ during the experiments performed by Sohrabi & Emadi (2012).

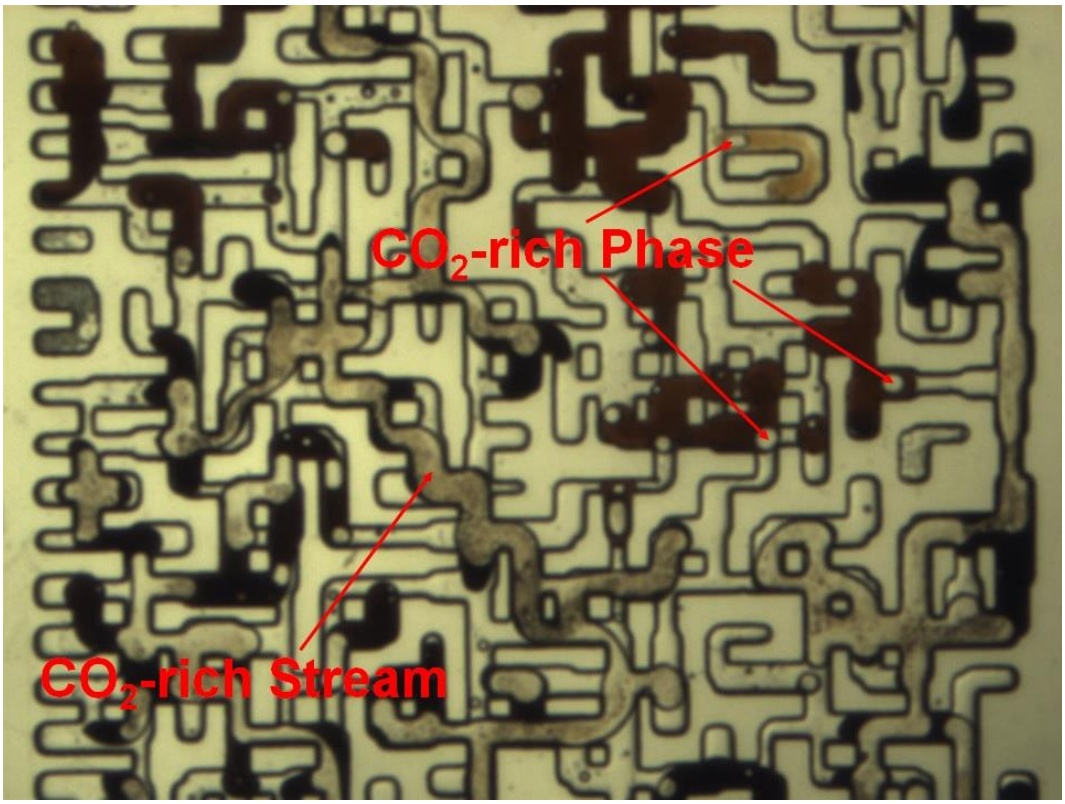


Figure 4-21: The same magnified section of the micromodel after the early time of the period of 2nd $CO_2$ injection.

By continuing $CO_2$ injection, the growth of the $CO_2$-rich phase resulted in enlargement of the isolated oil ganglia. This process contributed to additional oil recovery through reconnection of trapped oil and or by changing the flow path by blocking the main flow paths. However, the impact may not be always favourable. For instance, the growth of the $CO_2$-rich phase within the light and less viscous oil phase, Figure 4-22, caused to the extraction of the light and intermediate components from the oil and consequently, the volume of oil decreased.

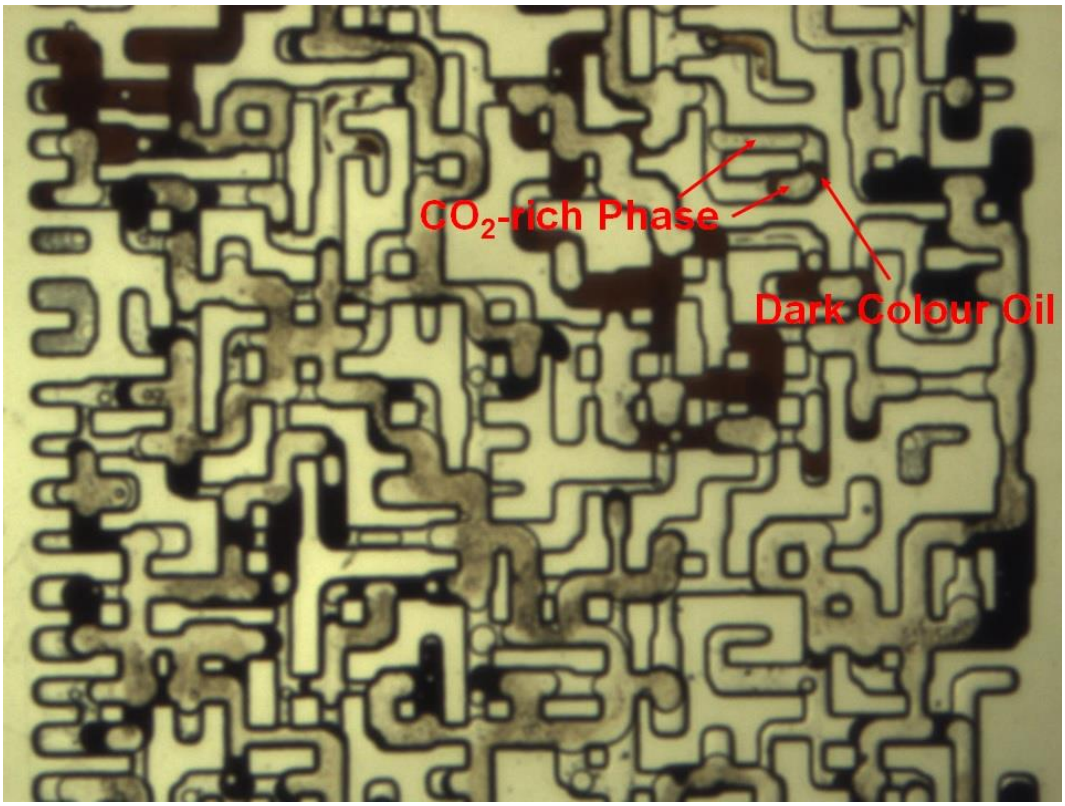


Figure 4-22: The same magnified section of the micromodel at the late time of the period of 2nd $CO_2$ injection.

It was shown that the two mechanisms of extraction of hydrocarbon compounds and dissolution of $CO_2$ in oil are mainly responsible for the recovery of higher quality oil during the period of liquid $CO_2$ injection for heavy oil recovery. Another reason of the alteration of the properties of oil during the period of $CO_2$ injection could be due to the in-situ precipitation and deposition of the asphaltene fraction of the oil. Asphaltenes are high-molecular-weight hydrocarbons and consist of nitrogen, oxygen, and sulphur. They are also known for their high metal content such as nickel, iron, and vanadium. Asphaltenes are generally soluble in light aromatics such as benzene and toluene but are insoluble in lighter paraffins. Thus, they are normally classified by the particular paraffin used to precipitate them from crude oil (Mitchell & Speight 1973; Speight, et al. 1984). The asphaltene content of crude 'C', which was used in the coreflood experiments, was measured gravimetrically after fractionation with heptane and toluene. The asphaltene fraction was defined as the heptane insoluble fraction that was soluble in toluene, which was calculated to be around 11.6% *w/w*. Furthermore, the isolated asphaltene fraction was analysed by inductively coupled plasma (ICP) for the required elements (i.e. iron, nickel, and vanadium). The similar ICP analysis was also performed for the original crude 'C' and the recovered oil during the coreflood experiment. The amounts of iron, nickel, and vanadium in the original crude 'C', the asphaltene fraction of the oil, and the samples of

recovered oil during the coreflood experiment were measured and compared in Table 4-4 and Figure 4-23.

Table 4-4: Metal content analysis of crude 'C' and its asphaltene fraction.

| Sample | Fe (mg/kg) | Ni (mg/kg) | V (mg/kg) |
|---|---|---|---|
| Crude 'C' | 3.1 | 72 | 341 |
| Asphaltene fraction | 15.5 | 155 | 750 |
| Asphaltene-free crude oil - calculated | 1.3 | 54 | 254 |
| Mixture of (1#1GF#3, 1#1GF#4, 1#1GF#5) | 3.4 | 68 | 271 |
| Mixture of (1#1GF#6, 1#1GF#7, 1#1GF#8) | 1.8 | 42 | 199 |
| Mixture of (1#1GF#9, 1#1GF#10, 1#1GF#11) | 1.3 | 41 | 181 |

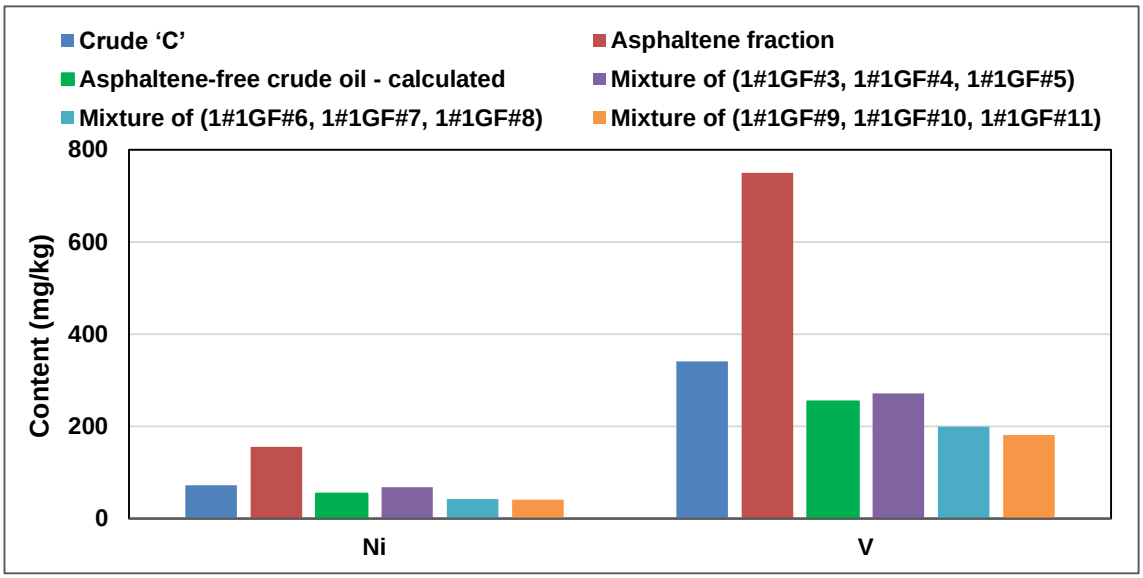


Figure 4-23: Metal content analysis of crude 'C' and its asphaltene fraction.

If, therefore, the alteration in the composition of the produced oil during the period of $CO_2$ injection was considered as a result of precipitation and deposition of the asphaltene fraction of the oil in porous medium, the metal content of the recovered oil during the coreflood experiment would be expected to be equal or higher than that of the asphaltene-free fraction of the oil. However, it was noted that the produced oil during the period of tertiary $CO_2$ injection in the core had even lower metal content than the asphaltene-free fraction of the oil. This observation indicates that not only the asphaltene fraction of the oil remains in pore spaces, but also the heavier and viscous parts of the asphaltene-free fraction of the oil remains in the core by $CO_2$ injection. In addition, no notable inconsistent change in the differential pressure in the core was observed during the period of tertiary $CO_2$ injection. Therefore, it is concluded that the precipitation and deposition of asphaltene, as they have been cited in the literature for some scenarios of gas or solvent injection (Srivastava, et al. 1999; Yin & Yen 2000), were probably not the main reason

for the improved quality of the produced oil in the coreflood experiment reported here.

The results of the metal content analysis in Table 4-4 are clearly showing the benefit of $CO_2$ injection in reducing the amount of those elements in the recovered heavy oil. The presence of these metal elements in the crude oil reduces the processing capacity in the refineries and it also causes to additional processing costs because of technical problems such as catalyst poisoning and environmental impacts (Koliander & Kunar-Schreferl 2000).

The viscosity of heavy oil is generally sensitive to the asphaltene content of the oil as well as the amount of heavy hydrocarbon cuts in the oil (Luo & Gu 2005). Accordingly, if it is assumed that the metal elements are mainly found attached to heavy hydrocarbon cuts and asphaltene fractions of heavy oil, the viscosity of oil decreases by reducing the metal content of the oil. This, therefore, suggests that the recovered oil from the core during the period of $CO_2$ injection had a lower viscosity than the original oil in the core. On the surface point of view, a huge drawback of heavy oil recovery is the technical problems associated with the separation and the transportation of the oil because of the high gravity and viscosity of the oil. To mitigate those concerns, heavy oil is usually heated or upgraded by mixing it with a lighter oil or solvents (Urquhart 1986; Martinez-Palou, et al. 2011). But such solutions can be expensive and detrimental to the economics of projects. This, however, highlights the advantages of $CO_2$ injection for heavy oil recovery which can result in higher quality oil recovery in addition to enhancing the recovery factor.

***Summary***

Figure 4-24 illustrates the cumulative oil recovery during different periods of the Coreflood#1. The presence of instability in the flood front due to adverse viscosity ratio between oil and water dominated the flow and caused to early breakthrough of secondary waterflood. After the breakthrough, the production of oil continued at high water cuts and virtually no considerable amount of oil was recovered after around 1 PV of waterflood. As a result of severe bypassing, a significant area of the core remained unswept and around 70% of the pore volume of the core was still saturated with oil at the end of secondary waterflood. However, a significant fraction of water in the core was displaced by $CO_2$ injection and this assisted oil recovery by increasing the contact between $CO_2$ and oil. The quality of recovered oil after around 0.4 PV of $CO_2$ injection was more improved which shows that the effect of viscous flow was reduced. Oil production was continued by $CO_2$ injection mainly because of $CO_2$ dissolution in the oil and the resultant oil

swelling and viscosity reduction, extraction of hydrocarbon components, gravity drainage, and perhaps capillary mixing. Eventually, 20% of the initial oil in the core was recovered after 6 PVs of $CO_2$ injection.

The ($2^{nd}$) Waterflood after the period of $CO_2$ injection led to the additional recovery of around 8% of the initial oil in place. The production of this amount of oil by the second waterflood indicates that $CO_2$ could invade the area that was bypassed by the secondary waterflood. Thus, more pore space was accessible to the second waterflood and water could contact the oil and displace a fraction of that to the production outlet. In addition, the mechanisms involved during the period of $CO_2$ injection would have increased the mobility of the remaining oil in the core and water due to its higher viscosity than $CO_2$ could enhance the sweep efficiency and hence improved the recovery factor. The compositional analysis of the recovered oil during the period of $2^{nd}$ waterflood is clearly showing that the accessible oil for the injected water had been in contact with $CO_2$ and its composition is different compared to the composition of the original oil in the core.

The results of cumulative oil production show that the application of $CO_2$, when no further oil recovery was possible by waterflood, could lead to the additional recovery of extra heavy and viscous oil. Moreover, the recovered oil by $CO_2$ was a higher quality oil than the oil recovered by the prior waterflood.

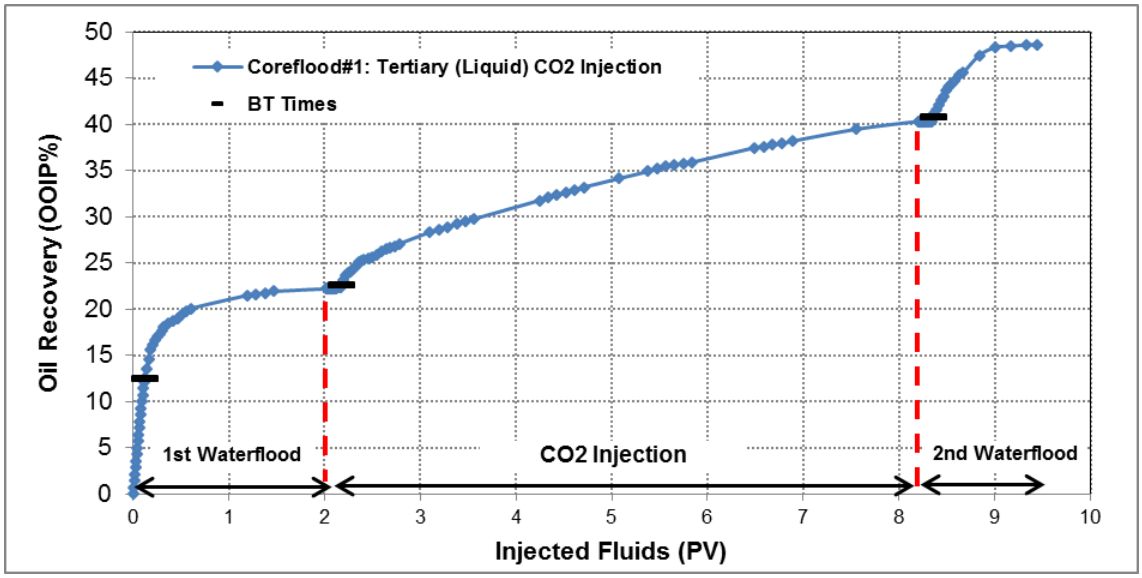


Figure 4-24: Cumulative oil recovery during different periods of Coreflood#1.

## 4.2 Coreflood#2: Intermittent Liquid $CO_2$ Injection

A secondary continuous $CO_2$ injection followed by several periods of shut-in (soak period) and $CO_2$ injection was performed to evaluate the effects of soaking on the performance of $CO_2$ injection in extra-heavy oil recovery. Another objective of this experiment was to the impacts of heavy oil viscosity on the performance of secondary $CO_2$ injection and compare the results with the corresponding experiment using a different oil with lower viscosity and higher amount of dissolved gas. The experiment was continued with several periods of water and $CO_2$ injection. Moreover, the gas chromatography (GC) analysis was performed on produced gas from the core to observe how $CO_2$ interacts with methane-saturated oil in a porous medium. A summary of the performance of all the periods of fluid injection in terms of cumulative oil recovery will be shown in Figure 4-34. Table 4-5 shows the fluids and conditions of the test.

Table 4-5: Fluids and conditions of Coreflood#2.

| **Coreflood#2** | **Experiment 7** (Farzaneh 2015) |
|---|---|
| Crude Oil: Methane-saturated Crude 'C' | Crude Oil: Methane-saturated Crude 'J' |
| Brine: $CO_2$-saturated | Brine: Methane-saturated |
| Gas: Liquid $CO_2$ | Gas: Liquid $CO_2$ |
| Temperature: 28° C | Temperature: 28° C |
| Pressure: 1500 psi | Pressure: 1500 psi |
| Injection Rate: 7 $cm^3$/hr | Injection Rate: 7 $cm^3$/hr |
| Core Position: Vertical (top to bottom) | Core Position: Vertical (top to bottom) |

***Procedure***

The main steps of the coreflood experiment are as follows:

1. **Dead Brine Injection:** Core was saturated with brine and the permeability was re-measured. The permeability of the core was measured to be 2.73 *D* to the brine.
2. **Live Brine Injection:** The live brine was injected through the core to avoid gas transfer from following live oil into the brine. The injection was continued until the gas content of the produced brine reached to certain values.
3. **Live Oil Injection:** The core was flooded with live crude 'C' and an irreducible water saturation of 8% was achieved.
4. **1st Continuous (Secondary) $CO_2$ Injection:** 1.3 PVs of $CO_2$ were injected into the core.
5. **Intermittent $CO_2$ Injection:** 4 cycles of shut-in and injection were performed.
6. **1st (Tertiary) Waterflood:** Around 1 PV of $CO_2$-saturated brine was injected

through the core after $CO_2$ injection.

7. **Water alternating $CO_2$:** Pre-defined shut-in periods and injection of water alternating $CO_2$ slugs were performed.
8. **Core Cleaning:** The core was cleaned by injection of several cycles of toluene and methanol into the core.

***Results and Discussion***

### 4.2.1 1st Continuous (Secondary) $CO_2$ Injection

Following the above-mentioned procedure, 1.3 PVs of $CO_2$ was injected through the oil-saturated core. Figure 4-25 shows the recovery profile and differential pressure across the core during the period of continuous $CO_2$ injection. It was observed that as $CO_2$ was injected, heavy oil with limited mobility could not be produced as fast as the injection rate. Hence, the pressure gradient across the core increased. After around 0.09 PV of injection, $CO_2$ has fingered through the oil and reached the production outlet. The breakthrough of $CO_2$ is also indicated in Figure 4-26 when $CO_2$ was detected in the produced gas stream and thereby the concentration of methane decreased.

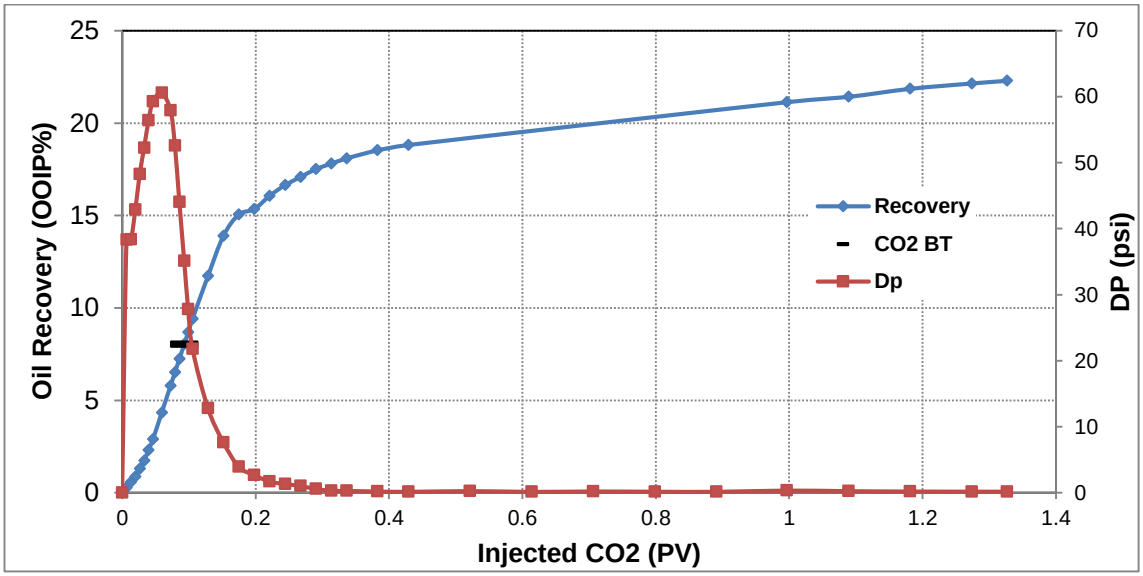


Figure 4-25: Oil recovery and differential pressure across the core during the period of continuous (secondary) $CO_2$ injection.

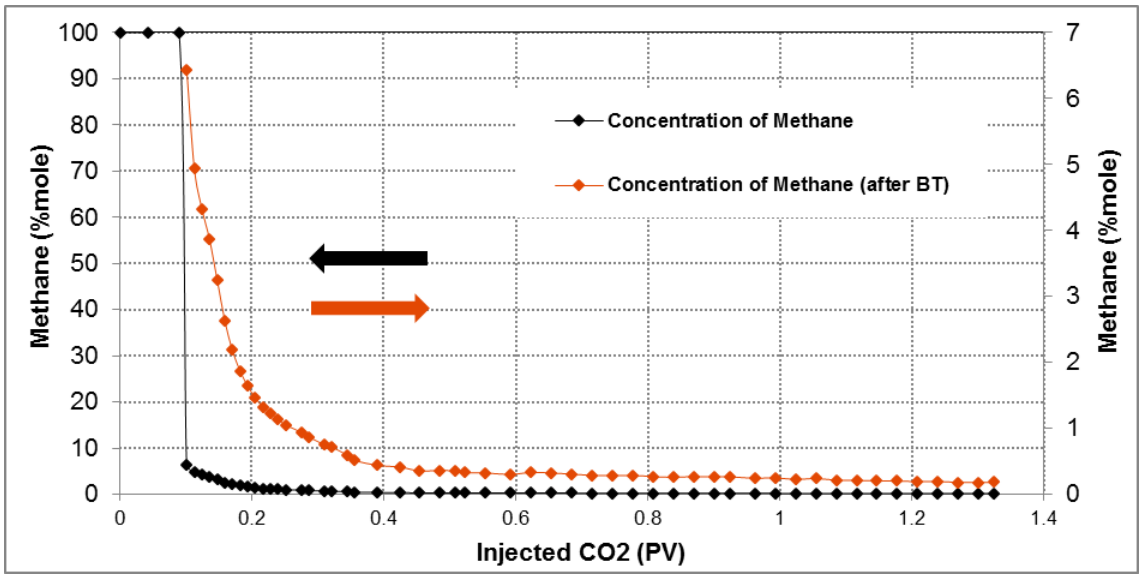


Figure 4-26: Compositional analysis of produced gas during the period of continuous (secondary) $CO_2$ injection.

Oil produced before the breakthrough was essentially the oil which was flooded to displace the initial water in the core. However, production of oil with foamy nature and liberation of gas from produced oil was observed after $CO_2$ breakthrough. Foamy oil can be characterised as a colloidal dispersion of gas bubbles in a continuous liquid phase (Lillico, et al. 2001; Firoozabadi 2001; Alshmakhy & Maini 2012). The production of foamy oil happened for two reasons; first, it was observed that liquid $CO_2$ can cause to the liberation of the methane in heavy oil as tiny bubbles within the oil phase. Second, the higher differential pressure has led to a higher amount of $CO_2$ dissolution in the oil (super-saturation). The relatively slow reduction of the methane content of the produced gas after the breakthrough is also an indication of methane liberation by $CO_2$ and foamy oil production. The oil rate was relatively high until around 0.3 PV of injection mainly because of a large pressure gradient (viscous flow) in the core. This is also reflected from the compositional analysis of the oil recovered during the period of continuous $CO_2$ injection, as evidence in Table 4-6. It is seen the changes in the quality of produced oil until the time that oil rate was relatively high was not as significant as it became later.

Table 4-6: Composition of oil recovered during the period of continuous (secondary) $CO_2$ injection.

| Sample | PV of Injection | ≤C12 (%mole) | >C12-≤C16 (%mole) | >C16-≤C20 (%mole) | >C20-≤C23 (%mole) | >C23-≤C29 (%mole) | >C29-≤C45 (%mole) | >C45-≤C100 (%mole) |
|---|---|---|---|---|---|---|---|---|
| 2#1GF#1 | 0.0-0.08 | 20.0 | 24.4 | 15.9 | 4.8 | 10.2 | 16.5 | 8.2 |
| 2#1GF#2 | 0.08-0.1 | 20.9 | 23.9 | 15.4 | 5.1 | 10.0 | 16.7 | 8.1 |
| 2#1GF#3 | 0.1-0.15 | 25.5 | 21.0 | 16.2 | 5.5 | 9.9 | 14.3 | 7.6 |
| 2#1GF#4 | 0.15-0.4 | 30.5 | 23.5 | 14.9 | 5.0 | 8.2 | 12.1 | 5.9 |
| 2#1GF#5 | 0.4-1.3 | 34.7 | 31.6 | 16.0 | 4.3 | 5.6 | 5.3 | 2.5 |

Despite continuous oil production, a further decline in oil rate and rapid increase in the produced GOR was noted after 0.3 pore volume of $CO_2$ injection. This reduction in oil production is related to the low residence time of $CO_2$ in the core. The lower $CO_2$ residence time in porous medium results to lower time for $CO_2$ to contact the oil and, thus, this reduces the rate of $CO_2$ dissolution in the oil.

### 4.2.2 Effects of Oil Composition and Viscosity on Performance of Secondary $CO_2$ Injection

Figure 4-27 compares the oil recovery profiles of secondary $CO_2$ injection into the core saturated with live crude 'J' (Farzaneh 2015) and into the core saturated with live crude 'C'. Although the displacement was more unstable in the case of more viscous oil, the limited mobility of crude 'C' caused a delay in the breakthrough of $CO_2$. The impact of solution gas drive was more pronounced in the core saturated with crude 'C' because of the higher pressure gradient in the core before the breakthrough. However, the recovery factor was significantly higher in the case of crude 'J' mainly due to its lower viscosity and relatively lighter composition.

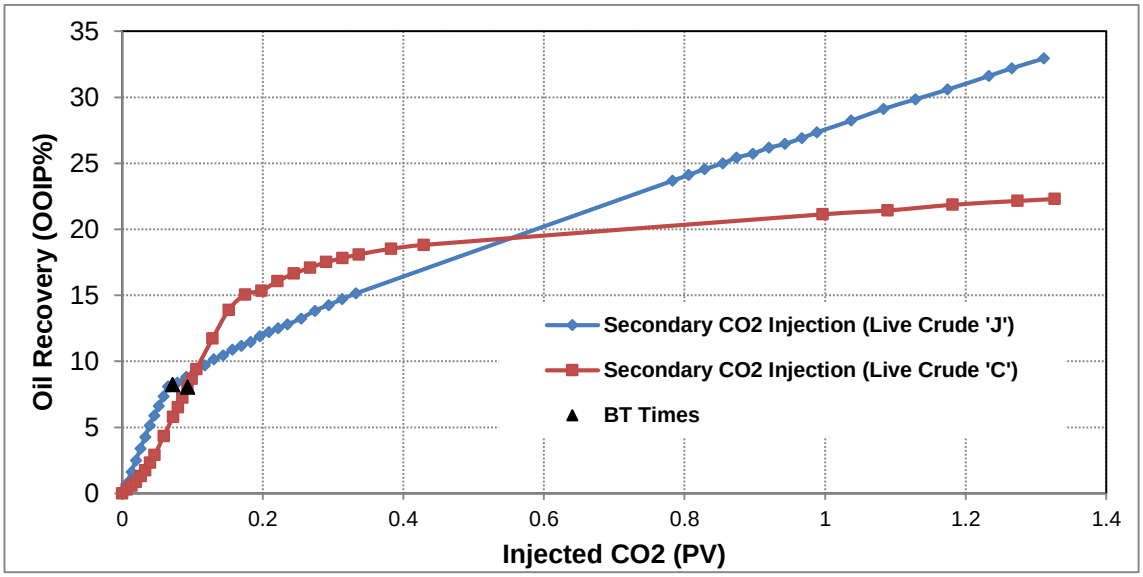


Figure 4-27: Comparison of oil recovery profiles of secondary $CO_2$ injection live crude 'J' (Farzaneh 2015) and secondary $CO_2$ injection live crude 'C'.

### 4.2.3 Intermittent $CO_2$ Injection

After continuous $CO_2$ injection, the core was shut-in for a period of 24 hours (soaking period) and the core pressure was monitored and recorded during this period. Then, 0.3 PV of $CO_2$ was injected into the core to displace the oil in contact with $CO_2$ towards the outlet of the core. This intermittent injection of $CO_2$ was repeated 4 times. Figure 4-28 illustrates the changes of core pressure during the shut-in periods. The increase in the pressure during each of the shut-in periods is an indication of the extraction of

hydrocarbon compounds of the oil, mainly methane, by $CO_2$. The volume of the fluid in the core was increased by the liberation of hydrocarbon components and because the total volume of the core was constant (no flow condition), the core pressure has increased. Oil swelling as a result of $CO_2$ dissolution in the oil may also have had a contribution to the increase of core pressure. This behaviour of $CO_2$ and live heavy oil is somehow similar to the concept of solution gas drive as well as optimal VRR for improving heavy oil recovery. The contact between $CO_2$ and heavy oil causes to the liberation of methane from the oil. Methane in the oil would nucleate as tiny bubbles in the oil phase and hence the volume of oil would increase. Other advantages of this process are that $CO_2$ dissolution in the oil reduces the viscosity of the oil and the core pressure is maintained constant or can be increased whilst in the process of solution gas drive oil viscosity increases because of the evolution of gas from the solution. In addition, the pressure of the system declines during the process of solution gas drive. Injection of a higher viscous fluid after the period of $CO_2$ injection would improve recovery factor.

The strength of the liberation of hydrocarbon components is a function of time as it can be seen that the ultimate increase of core pressure in the 4$^{th}$ period of soaking is lower than the previous periods. This implies that the rate of $CO_2$ diffusion into heavy and viscous oil is essentially slow in porous media. The aforementioned observation is also in agreement with the lower concentration of methane in the produced stream of the 4$^{th}$ cycle of injection, as shown in Figure 4-29.

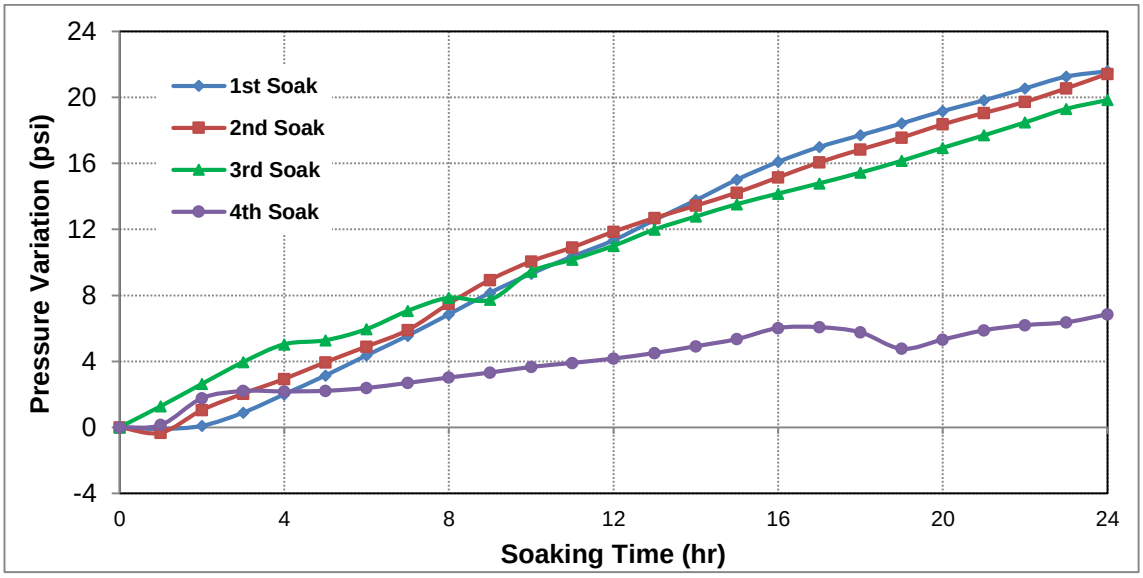


Figure 4-28: Pressure variation of the core during the shut-in periods.

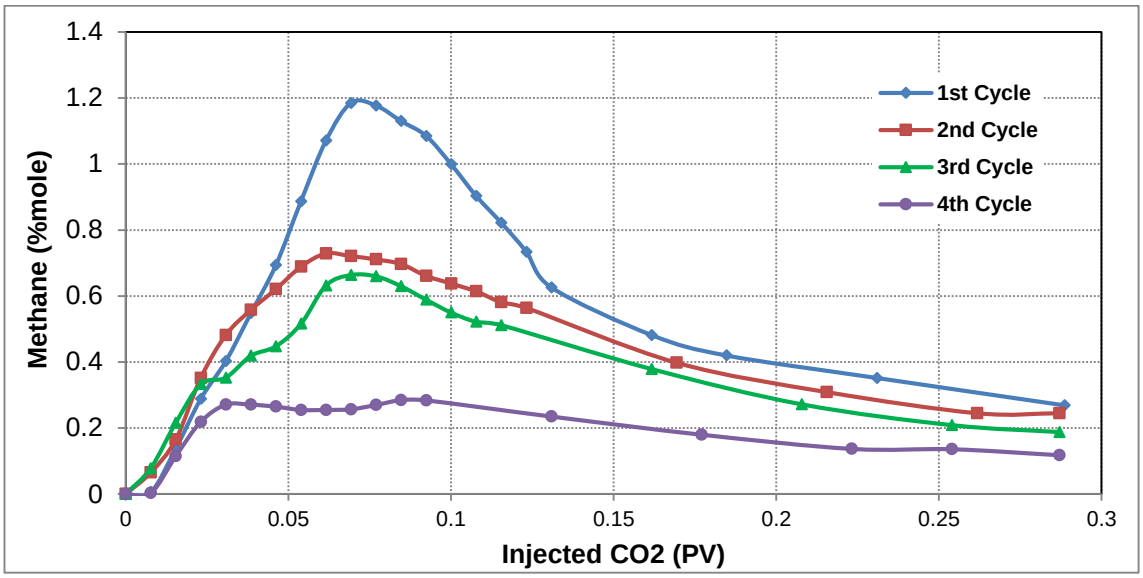


Figure 4-29: Compositional Analysis of produced gas during each cycle of intermittent injection.

Cuthiell, et al. (2006) conducted a visual test in sandpack to investigate the roles of different mechanisms in VAPEX. In particular, the work was focused on capillary effects. It was observed that for the sand of typical heavy oil reservoir permeability, capillary mixing occurred significantly between gas and oil and as time went on, a drainage zone developed and oil began to collect at the bottom of the pack that was initially dry. Because of the high contrast between $CO_2$ density and the oil density, gravity would have assisted oil drainage to the bottom of the core. Figure 4-30 summarises the mechanisms which were active during the shut-in periods in the contact areas between $CO_2$ and the oil.

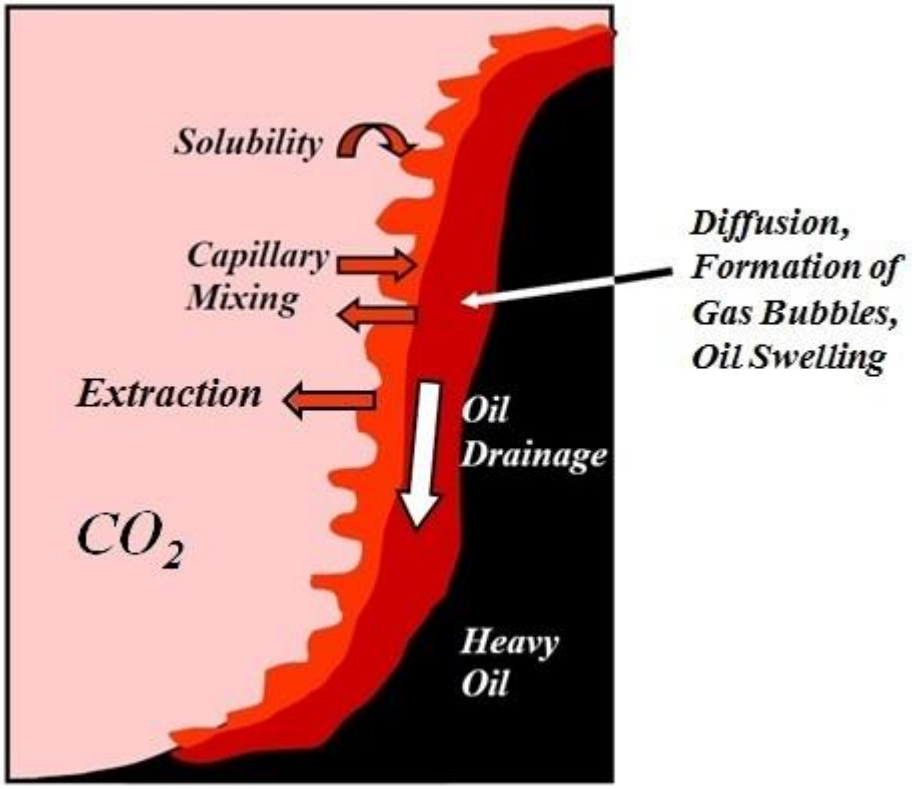


Figure 4-30: The mechanisms between $CO_2$ and heavy oil, adapted from Cuthiell, et al. (2006).

The composition of oil recovered during each cycle of intermittent injection was analysed and compared to the composition of oil produced before the beginning of this injection scenario in Table 4-7. The results are clearly showing the impact of gravity drainage during halt periods on the quality of recovered oil. The produced oil from the core during the cycles of intermittent injection has lower quality than the oil recovered before changing the injection scenario from the continuous injection to the scheme of halt and injection. The metal content analysis of oil, Table 4-8 and Figure 4-31, recovered by continuous and intermittent injection of $CO_2$ also highlights the impact of gravity drainage during the shut-in periods. It is shown that amount of metal elements increased in the oil produced after each shut-in which reflects that the mobility of heavier cuts of the oil was increased due to higher $CO_2$ dissolution in the oil. However, the recovered oil by intermittent $CO_2$ injection has still higher quality than the original oil in the core. Moreover, the composition of produced oil relatively improves by the continuation of intermittent $CO_2$ injection which shows that the effect of $CO_2$ dissolution on oil recovery is reducing perhaps because of the presence of heavier cuts of the oil between $CO_2$ and oil in the core. Respectively, around 5.2%, 3.5%, 5.1%, and 3.2% of the remaining oil before each intermittent injection cycle was recovered by 0.3 PV of injection.

Table 4-7: Composition of oil recovered during each period of intermittent $CO_2$ injection.

| Sample | PV of Injection | ≤C12 (%mole) | >C12-≤C16 (%mole) | >C16-≤C20 (%mole) | >C20-≤C23 (%mole) | >C23-≤C29 (%mole) | >C29-≤C45 (%mole) | >C45-≤C100 (%mole) |
|---|---|---|---|---|---|---|---|---|
| 2#1GF#5 | 0.4-1.3 | 34.7 | 31.6 | 16.0 | 4.3 | 5.6 | 5.3 | 2.5 |
| 2#2GF#1 | 1.3-1.6 | 29.1 | 24.0 | 16.6 | 5.6 | 8.3 | 11.0 | 5.4 |
| 2#3GF#1 | 1.6-1.9 | 30.7 | 25.7 | 16.1 | 5.2 | 7.5 | 10.0 | 4.9 |
| 2#4GF#1 | 1.9-2.2 | 30.0 | 24.6 | 16.3 | 5.2 | 7.9 | 10.8 | 5.3 |
| 2#5GF#1 | 2.2-2.5 | 31.4 | 27.6 | 16.2 | 5.0 | 7.0 | 8.7 | 4.1 |

Table 4-8: Metal content analysis of oil recovered by continuous and intermittent injection of $CO_2$.

| Sample | Fe (mg/kg) | Ni (mg/kg) | V (mg/kg) |
|---|---|---|---|
| Crude 'C' | 3.1 | 72 | 341 |
| Mixture of (2#1GF#4, 2#1GF#5) | 5.5 | 47 | 199 |
| 2#2GF#1 | 7.4 | 77 | 366 |
| 2#3GF#1 | 3.3 | 73 | 347 |
| 2#4GF#1 | 2.3 | 76 | 355 |
| 2#5GF#1 | 1.8 | 70 | 344 |

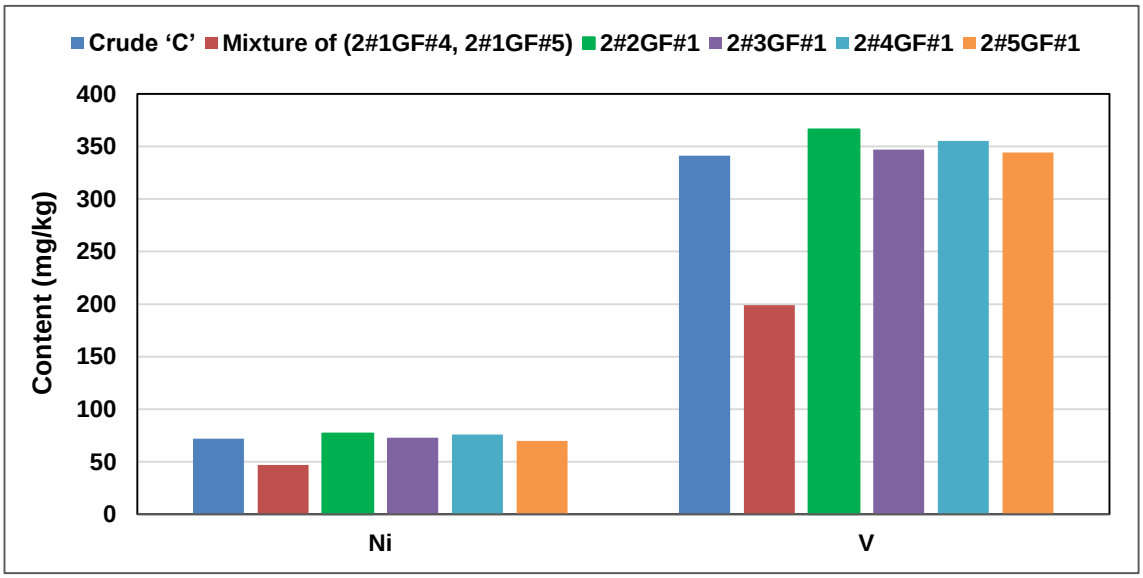


Figure 4-31: Metal content analysis of oil recovered by continuous and intermittent injection of $CO_2$.

Figure 4-32 shows the cumulative oil recovery performance of intermittent injection following secondary continuous $CO_2$ injection. The intermittent injection of $CO_2$ led to additional oil recovery of 13% of initial oil place. This performance resulted in around 10% of additional oil recovery if the continuous $CO_2$ injection would have been continued.

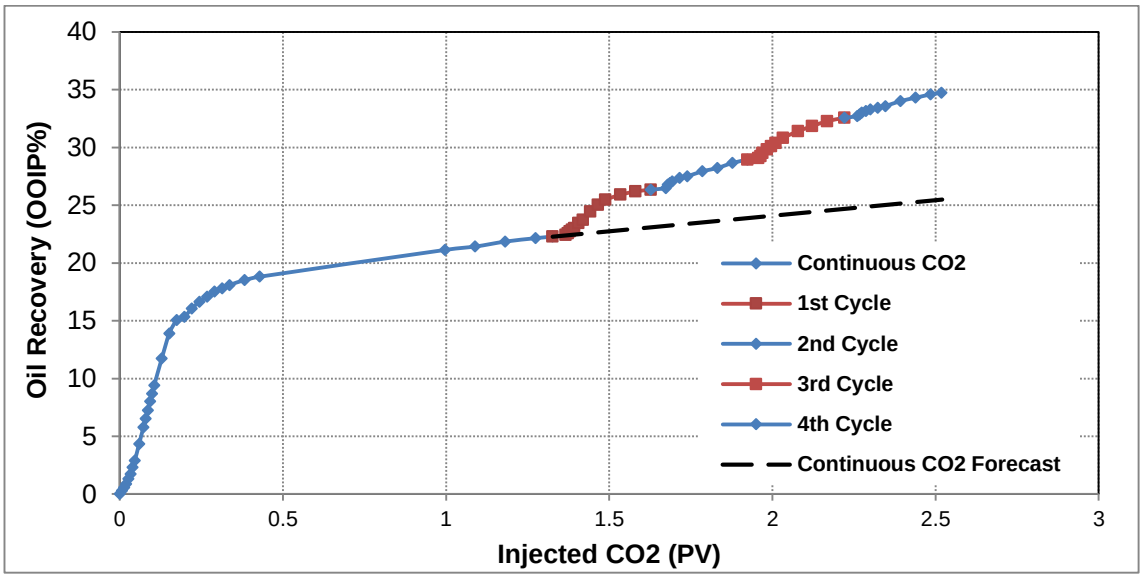


Figure 4-32: Cumulative oil recovery during the periods of continuous and intermittent $CO_2$ injection.

### 4.2.4 1st (Tertiary) Waterflood

After the 4th cycle of intermittent $CO_2$ injection, the core was shut-in for another period of 24 hours and then 1 PV of $CO_2$-saturated brine was injected through the core. The core pressure increased around 3 psi at the end of the shut-in period. The injected water followed the less resistance path of gas within the core and displaced gas to the production outlet. Oil production began with relatively low rate after 0.1 PV of injection as a result of the formation of an oil bank in front of injected water, as evidenced in Figure 4-33. After the breakthrough, oil production rate declined but oil was still produced at high rates until around 0.5 PV of waterflood.

Free gas production stopped after water breakthrough and the produced gas after this point was the dissolved gas in either produced water or oil. The compositional analysis of produced oil during the period of waterflood is shown in Table 4-9. It can be seen that the composition of oil recovered by waterflood is notably similar to the composition of the original oil. This indicates that water could displace a significant fraction of the remaining oil in the core which was relatively rich in heavier hydrocarbon cuts than the original oil.

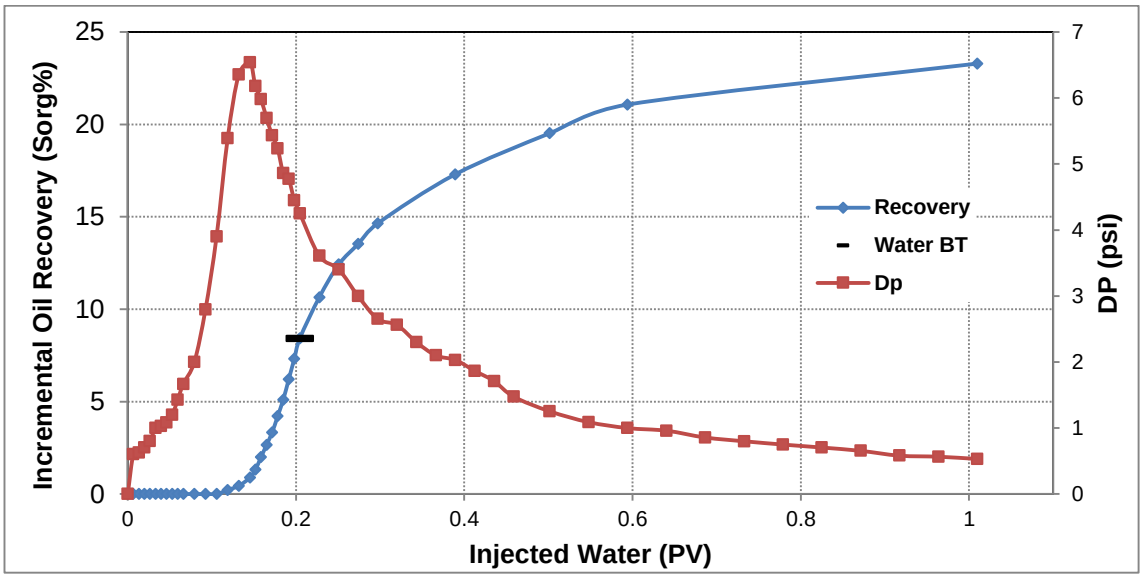


Figure 4-33: Incremental oil recovery and differential pressure across core during the period of 1st (tertiary) waterflood.

Table 4-9: Composition of oil recovered during the period of 1st (tertiary) waterflood.

| Sample | PV of Injection | ≤C12 (%mole) | >C12-≤C16 (%mole) | >C16-≤C20 (%mole) | >C20-≤C23 (%mole) | >C23-≤C29 (%mole) | >C29-≤C45 (%mole) | >C45-≤C100 (%mole) |
|---|---|---|---|---|---|---|---|---|
| 2#1WF#1 | 2.5-2.7 | 24.3 | 20.9 | 16.1 | 6.0 | 9.9 | 15.2 | 7.6 |
| 2#1WF#2 | 2.7-2.75 | 22.1 | 18.5 | 17.2 | 6.9 | 10.7 | 16.1 | 8.4 |
| 2#1WF#3 | 2.75-2.8 | 22.4 | 20.2 | 16.0 | 6.8 | 10.6 | 15.8 | 8.1 |
| 2#1WF#4 | 2.8-2.9 | 23.5 | 18.2 | 17.2 | 6.6 | 10.6 | 15.8 | 8.1 |
| 2#1WF#5 | 2.9-3.1 | 21.6 | 18.8 | 17.4 | 6.8 | 11.3 | 15.9 | 8.3 |
| 2#1WF#6 | 3.1-3.5 | 23.7 | 18.4 | 16.2 | 6.5 | 10.7 | 16.4 | 8.0 |

After the period of 1st waterflood, a slug of 0.3 PV of $CO_2$ was injected through the core which resulted in the recovery of 4.5% of the remaining oil in the core. Then, the core was shut-in for 24 hours and the pressure of core ultimately decreased around 1 psi. Subsequently, water and $CO_2$ were injected into the core. The compositional analysis of produced oil, as shown in Table 4-10, revealed that $CO_2$ could improve the quality of produced oil after the waterflood.

Table 4-10: Composition of oil recovered during the period of 1st (tertiary) waterflood.

| Sample | PV of Injection | ≤C12 (%mole) | >C12-≤C16 (%mole) | >C16-≤C20 (%mole) | >C20-≤C23 (%mole) | >C23-≤C29 (%mole) | >C29-≤C45 (%mole) | >C45-≤C100 (%mole) |
|---|---|---|---|---|---|---|---|---|
| 2#6GF#1 | 3.5-3.8 | 24.0 | 26.3 | 15.2 | 4.6 | 9.0 | 14.1 | 6.7 |
| 2#7GF#1 | 4.1-4.4 | 28.5 | 26.0 | 17.0 | 5.7 | 7.8 | 10.2 | 4.8 |

***Summary***

Figure 4-34 shows the cumulative oil recovery during different periods of the Coreflood#2. The adverse viscosity ratio between oil and $CO_2$ dominated the flow and

led to the early breakthrough of secondary $CO_2$ injection. The elevated pressure of $CO_2$ before the breakthrough improved oil recovery by a period of foamy oil production after the breakthrough. However, GOR increased rapidly because of the low oil rate as well as the low residence time of $CO_2$ in the core. To mitigate these issues, the intermittent $CO_2$ injection was employed to facilitate the contact between $CO_2$ and oil in porous media. As could be expected, it was understood that the liberation of oil components was present in the core and that phenomenon increased the pressure of core during the shut-in periods. The dissolution of $CO_2$ in the oil during the soaking periods enhanced the impact of gravity drainage on oil recovery. The intermittent $CO_2$ injection resulted in additional oil recovery than if the continuous $CO_2$ injection would have been continued. Waterflood after the intermittent injection improved the sweep efficiency and considerable amount of oil was displaced to the production outlet. It is significant that oil could still be recovered by $CO_2$ injection after the periods of waterflood.

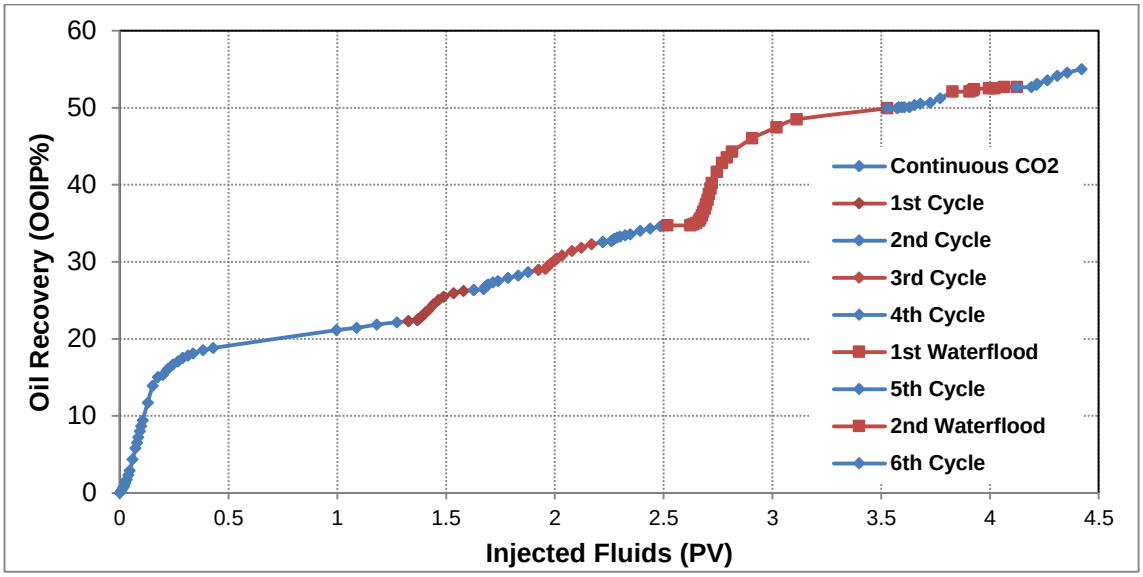


Figure 4-34: Cumulative oil recovery during different periods of Coreflood#2.

## 4.3 Conclusions

Two coreflood experiments were conducted to investigate the performance of different water and $CO_2$ injection scenarios in the recovery of heavy oil. In addition, the mechanisms involved in these experiments and the impacts of those processes on the performance of oil recovery were carefully investigated by performing several visualisation experiments. The compositional analysis of the effluent (e.g. oil, gas) of both coreflood experiments was performed at various periods of the tests. Furthermore, some PVT properties of the fluids were measured or calculated to improve our understanding of the impacts of the parameters affecting the process of heavy oil recovery by $CO_2$ injection. Based on the results of the experiments presented in this chapter, the following conclusions are drawn:

- The earlier the breakthrough of injection fluids occurs if the contrast in the viscosity of heavy oil and displacing fluids is higher.
- Viscous forces are observed to be much important at early times of waterflood where the differential pressure within the core is still significant.
- After the period of high differential pressure (viscous forces) in the core, oil is produced at high water cuts and further water injection would not result in notable oil recovery.
- Despite its lower viscosity than water, $CO_2$ injection into the core saturated with live viscous oil can recover more oil than waterflood by the mechanisms linked to the interactions between $CO_2$ and live oil.
- Because of lower viscosity of $CO_2$ than water, higher injectivity is another advantage of $CO_2$ injection instead of waterflood.
- Intermittent injection of $CO_2$ in heavy oil reservoirs improves oil recovery while $CO_2$ utilisation is significantly reduced. The improvement is due to the increase in $CO_2$ residence time in porous media.
- Mechanisms of solution gas drive (foamy oil) and gravity drainage can significantly improve the performance of heavy oil recovery by $CO_2$ injection.
- Waterflood after an extended period of $CO_2$ injection improves sweep efficiency and a considerable amount of heavy oil can be recovered.
- A higher quality oil (e.g. lower density, lower viscosity) than the original heavy oil in porous media can be recovered by liquid $CO_2$ injection.
- As soon as dense (liquid) $CO_2$ contacts heavy oil, extraction of hydrocarbons from the oil starts.

- The extraction of hydrocarbons to the $CO_2$-rich phase happened from the interface of the oil and $CO_2$. However, it was noted that methane in the oil was liberated within the oil far from the interface with $CO_2$.
- The liberation of methane of heavy oil and the extraction of other hydrocarbons by $CO_2$ leads to a sudden swelling of the oil which was also noted by the increase of core pressure during the shut-in period of intermittent injection.
- The liberation of methane of heavy oil by $CO_2$ is somehow similar to the concept of solution gas drive (foamy oil) and VRR for optimal heavy oil recovery. An indication would be the difference in the behaviour of oil recovery of waterflood after intermittent $CO_2$ injection that of waterflood after continuous $CO_2$ injection.
- Although the speed of extraction decreases after complete liberation of methane from heavy oil, extraction is a continuous process and eventually the volume of oil decreases as more light and intermediate hydrocarbon components are extracted.
- The density of $CO_2$-rich phase is a dominant factor in determining the size of extracted components.
- The effect of hydrocarbon extraction by $CO_2$ is not uniformly distributed over components with different carbon numbers.
- In porous media, the components extracted by $CO_2$-rich phase can be more easily displaced compared to oil-rich phase.
- The process of extraction is considerably slow and its impacts on the process of oil recovery are likely to be significant near the injection wells.
- Extraction of hydrocarbon components is an important reason for higher quality oil recovery by $CO_2$ injection.
- Formation of a new phase in the $CO_2$-rich stream was observed. This oil-rich has a relatively lighter colour than the oil in contact with $CO_2$ and it is significantly mobile in porous media but not as fast as the $CO_2$-rich phase.
- The above-mentioned new phase is formed as a result of $CO_2$ and oil contact in the flow paths of $CO_2$.
- Because of the extraction strength of liquid $CO_2$, an accumulation of light and intermediate components of heavy oil takes place in the oil phase, near the interface of oil and $CO_2$. $CO_2$ dissolution in the oil and the resultant oil viscosity reduction and oil swelling facilitates this process.
- The light colour oil in the stream of $CO_2$ is an oil-rich phase which has a higher concentration of light and intermediate components as well as lower viscosity than

the original oil in pore spaces.

- $CO_2$ can reach to the oil surrounded by water (either initial water or remaining water after a period of waterflood) by dissolving in the water and diffusing from it into the trapped oil.
- The transfer of $CO_2$ into oil by the water surrounding the oil is a continuous process and the oil encompassed by water becomes relatively saturated with $CO_2$. Therefore, at a certain time, the rate of extraction of $CO_2$ from the water by the oil exceeds the rate of $CO_2$ dissolution in the oil which results in the nucleation of $CO_2$ among the oil.
- The nucleation of dense $CO_2$ within the oil (surrounded by water) leads to the extraction of oil components by $CO_2$ and the volume of $CO_2$-rich phase increases.
- The growth of $CO_2$-rich phase within the oil surrounded by water results in enlargement of the isolated oil ganglia. This process contributes to additional oil recovery through reconnection of trapped oil and/or by changing the flow path by blocking the main flow paths of $CO_2$.
- The nucleated $CO_2$-rich phase within oil phase surrounded by water is significantly mobile in porous media and it can contribute to additional higher quality oil recovery.
- No notable sign of asphaltene precipitation and deposition was not observed in the coreflood experiments reported here.
- Heavy oil recovered by $CO_2$ can have a lower amount of metal elements such as nickel and vanadium than the original oil in rock.
- The extent of in-situ improvement of the quality of recovered oil is a function of the injection strategy of $CO_2$.
- A properly designed and executed $CO_2$ injection can recover a significant amount of heavy oil at reservoir conditions.

# CHAPTER 5: MECHANISMS OF ENHANCED HEAVY OIL RECOVERY BY SUPERCRITICAL $CO_2$ INJECTION

*The primary objective of this chapter was to investigate the impacts of oil viscosity and density of $CO_2$ on the process of heavy oil recovery by $CO_2$ injection. Two different gas compositions were used in the coreflood experiments to evaluate the significance of the underlying mechanisms of heavy oil recovery by gas injection. In addition to three coreflood experiments, the visualisation contact of heavy oil and $CO_2$ was conducted to truly understand the pore-scale mechanisms of heavy oil displacement by $CO_2$ as a supercritical fluid. The compositional analysis of the core effluent and the measurements of PVT properties of fluids were also performed.*

## 5.1 Coreflood#3: Intermittent Supercritical $CO_2$ Injection

A secondary continuous injection followed by several periods of shut-in and $CO_2$ injection was performed to evaluate the effect of soaking on the performance of dense (supercritical) $CO_2$ injection in heavy oil recovery. Other objectives of this experiment were to evaluate the effects of oil viscosity and physical state of $CO_2$ on oil recovery and also to investigate the performance of tertiary waterflood in heavy oil recovery after $CO_2$ injection. In addition, the in-line GC analysis was performed on produced gas from the core to observe how $CO_2$ interacts with methane-saturated oil in porous media. A summary of the performance of all the periods of fluid injection in terms of cumulative oil recovery will be shown in Figure 5-12. Table 5-1 shows the fluids and conditions of Coreflood#3.

Table 5-1: Fluids and conditions of Coreflood#3.

| **Coreflood#3** | **Coreflood#2** |
|---|---|
| Crude Oil: Methane-saturated Crude 'C' | Crude Oil: Methane-saturated Crude 'C' |
| Brine: $CO_2$-saturated | Brine: $CO_2$-saturated |
| Gas: Supercritical $CO_2$ | Gas: Liquid $CO_2$ |
| Temperature: 50° C | Temperature: 28° C |
| Pressure: 1500 psi | Pressure: 1500 psi |
| Injection Rate: 7 $cm^3$/hr | Injection Rate: 7 $cm^3$/hr |
| Core Position: Vertical (top to bottom) | Core Position: Vertical (top to bottom) |

***Procedure***

The following were the main steps to conduct Coreflood#3:

1. **Dead Brine Injection:** Core was saturated with brine and the permeability was re-measured and it remained unchanged compared to the original permeability of the core.
2. **Live Brine Injection:** The live brine was injected through the core to avoid gas transfer from following live oil into the brine. The injection was continued until the gas content of the produced brine reached to certain values.
3. **Live Oil Injection:** The core was flooded with live crude 'C' and an irreducible water saturation of 8% was achieved.
4. **1st Continuous (Secondary) $CO_2$ Injection:** 1.3 PVs of $CO_2$ were injected into the core.
5. **Intermittent $CO_2$ Injection:** 9 cycles of shut-in and injection were performed.
6. **1st (Tertiary) Waterflood:** Around 1 PV of $CO_2$-saturated brine was injected through the core after $CO_2$ injection.
7. **$CO_2$ Slug:** A slug of 0.3 PV of $CO_2$ was injected into the core.
8. **Core Cleaning:** The core was cleaned by injection of several cycles of toluene and methanol into it.

***Results and Discussion***

### 5.1.1 1st Continuous (Secondary) $CO_2$ Injection

Following the above-mentioned procedure, continuous $CO_2$ injection through the core saturated with live oil was started. The primary objective of this run was to evaluate the performance of continuous supercritical $CO_2$ injection in displacing methane-saturated crude 'C'. Another objective was to compare the results of this experiment with the performance of liquid $CO_2$ injection of the corresponding experiment (Coreflood#2). Figure 5-1 illustrates the recovery profile and differential pressure across the core during the period of continuous injection. After around 0.12 PV of injection, when $CO_2$ reached to the production outlet, the GOR rose sharply. The breakthrough is also indicated in Figure 5-2 when $CO_2$ was detected in the produced gas stream.

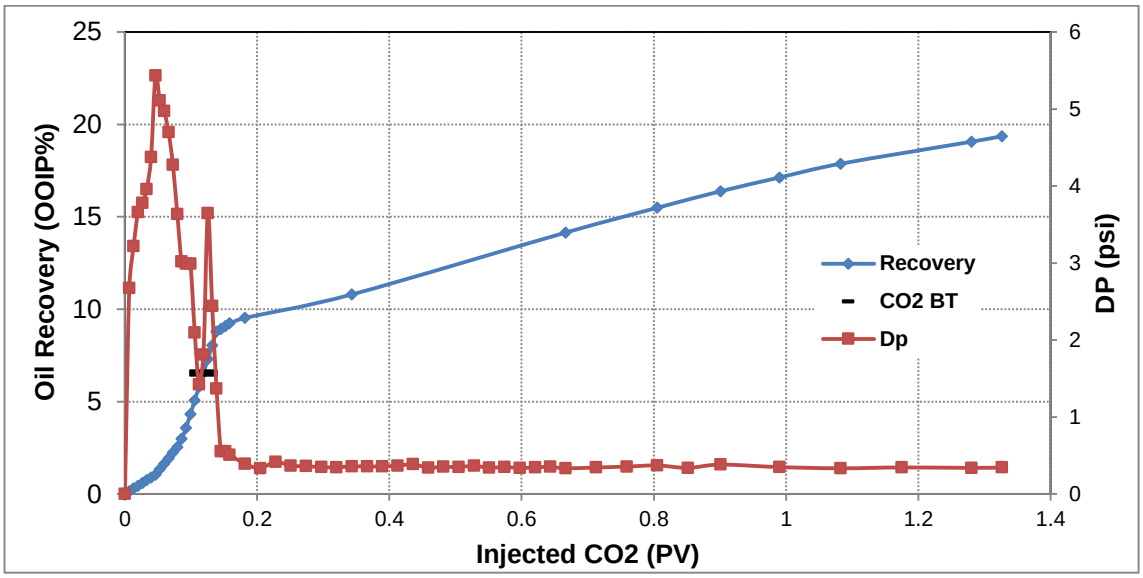


Figure 5-1: Oil recovery and differential pressure across the core during the period of continuous (secondary) $CO_2$ injection.

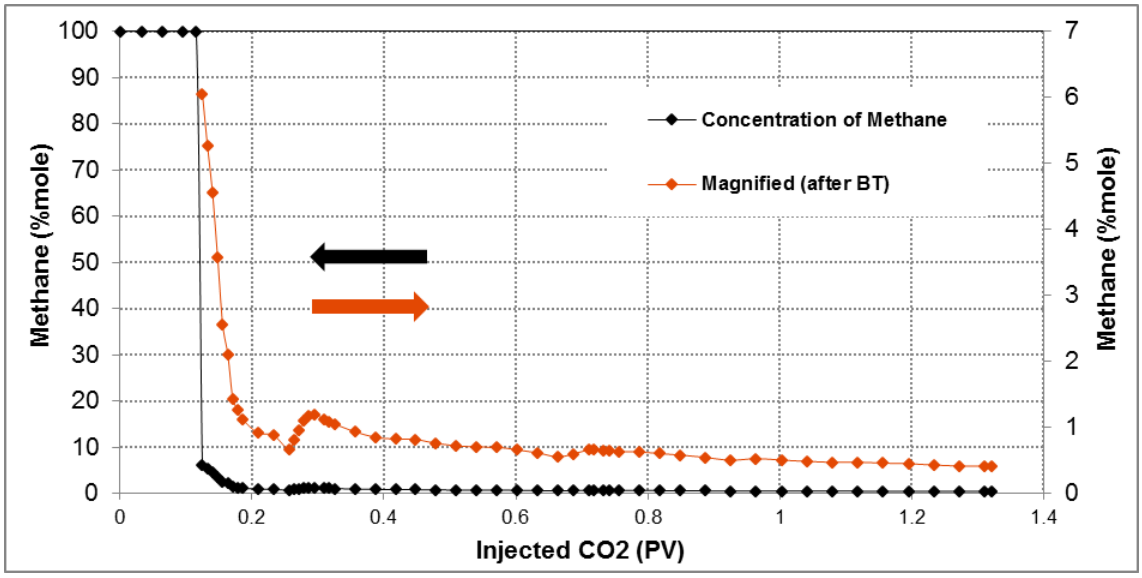


Figure 5-2: Compositional analysis of produced gas during the period of continuous (secondary) $CO_2$ injection.

The oil recovered before the breakthrough was essentially the oil which was flooded to displace the initial water in the core. A relatively short period of foamy oil production was observed after the breakthrough. Table 5-2 compares the viscosity of oil recovered, after complete separation of gas from oil, at different stages of this coreflood experiment with the viscosity of the original crude 'C' at 50˚ *C*. It is shown that the contact between $CO_2$ and heavy oil in the core has improved the quality of produced oil and significantly lower viscosity oil was recovered by $CO_2$ injection. These results would also imply that $CO_2$ has been a dense supercritical fluid in the core during different periods of the experiment.

Table 5-2: Viscosity of oil recovered during different periods of Coreflood#3.

| Sample | PV of Injection | Viscosity Ratio, (%) |
|---|---|---|
| Dead Crude 'C' | -- | 100 |
| 3#1GF#1 | 0.0-0.14 | 69 |
| 3#1GF#2 | 0.14-0.67 | 60 |
| 3#1GF#3 | 0.67-1.3 | 65 |
| 3#3GF#1 | 1.6-1.9 | 77 |
| 3#8GF#1 | 3.1-3.4 | 73 |

### 5.1.2 Effects of Oil Viscosity and State of $CO_2$ on Performance of Continuous $CO_2$ Injection

Figure 5-3 compares the oil recovery profiles of secondary liquid $CO_2$ injection and secondary supercritical $CO_2$ injection. The core in both experiments was flooded with crude 'C' saturated with methane under the initial conditions of both experiments. It is notable that relatively late breakthrough of supercritical $CO_2$ did not result in a higher amount of oil recovery in this run. Under the conditions of the coreflood experiments reported here, $CO_2$ in the supercritical state is around 20 times more compressible than the liquid $CO_2$. Because of the limited mobility of crude 'C', more supercritical $CO_2$ was required to be compressed to provide driving force (pressure gradient) in the core. In addition, the higher pressure gradient in the core caused by the higher viscosity of oil in the core in the case of liquid $CO_2$ injection led to a higher amount of $CO_2$ dissolution in the oil and the resultant oil swelling. That is, it is assumed that the effect of gravity (density of $CO_2$) was negligible in both experiments due to severe fingering.

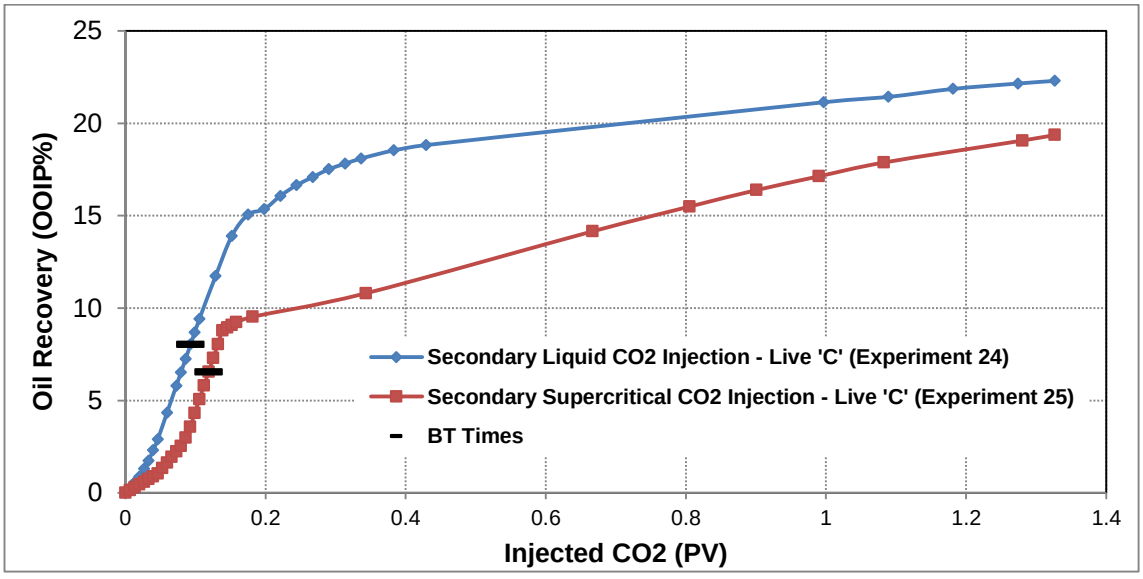


Figure 5-3: Comparison of oil recovery profiles of continuous liquid $CO_2$ injection and continuous supercritical $CO_2$ injection.

To improve our understanding, the same procedure (visual-cell), which was conducted

for the contact of liquid $CO_2$ and live heavy oil, was followed for a test under the conditions of supercritical $CO_2$. Similar behaviour was observed during early times of the contact of $CO_2$ and oil. However, the test was terminated early. The consistency of the behaviour of $CO_2$ and oil in both tests shows that the extraction power of $CO_2$ does not depend directly on temperature or whether the $CO_2$-rich phase is a liquid or supercritical fluid. It is, therefore, concluded that similar mechanisms were active in both experiments, albeit in varying degrees because of the different properties of oil and $CO_2$.

The GC results after the $CO_2$ breakthrough in both experiments, Figure 5-4, show that after 0.3 PV of injection, the concentration of methane in the produced stream is higher when $CO_2$ was a supercritical fluid. At first glance, this can be attributed to the relatively higher oil rate in that run. Additionally, the composition of produced gas has been analysed at a pressure lower than the pressures of the coreflood experiments, Chapter3. When $CO_2$ reaches the GC analyser, it expands at the ambient conditions compared to its volume in the core. Therefore, 1 $cm^3$ of liquid $CO_2$ in the core expands to double the volume that 1 $cm^3$ of in-core supercritical $CO_2$ would reach. Accordingly, the higher fraction of methane in the produced gas in the second experiment can be related to the ratio of volumes of the produced methane and $CO_2$. However, as shown in Figure 5-5, after 0.3 PV of injection, methane rate is almost equal in both experiments despite the relatively higher oil rate in the run that initial oil viscosity was lower. This observation implies that the oil recovered by supercritical $CO_2$ had lower methane content than the oil recovered by liquid $CO_2$.

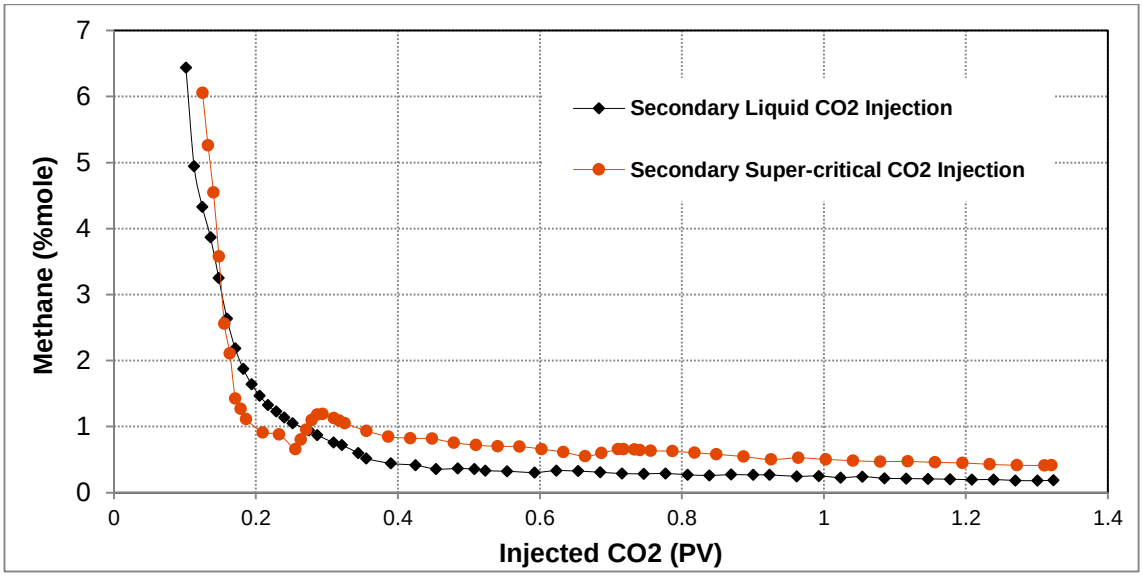


Figure 5-4: Comparison of GC analysis of produced gas during continuous liquid $CO_2$ injection and continuous supercritical $CO_2$ injection.

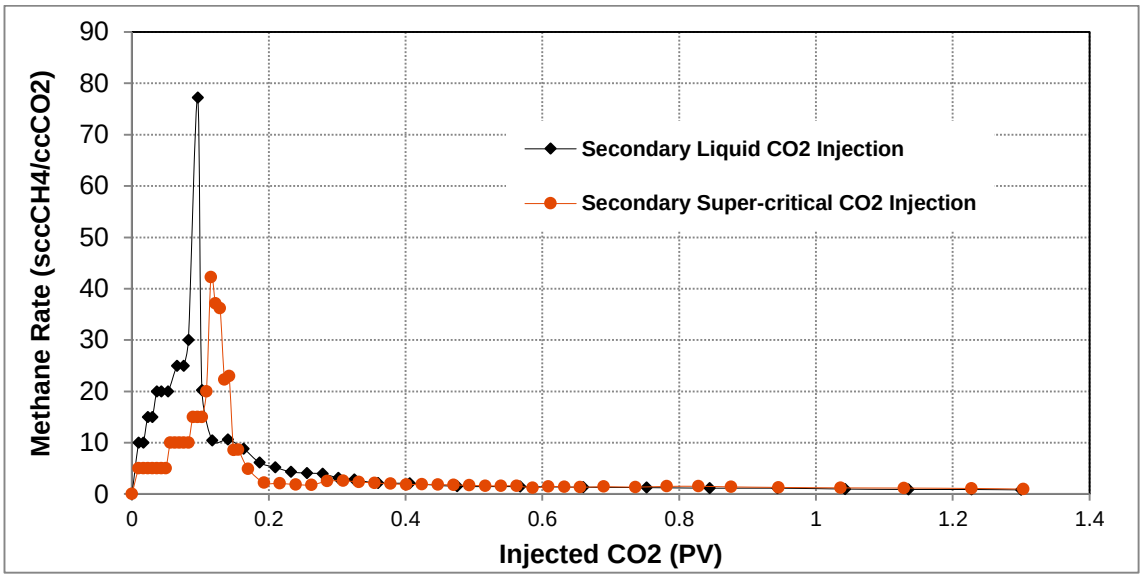


Figure 5-5: Methane rate during continuous liquid $CO_2$ injection and continuous supercritical $CO_2$ injection.

The aforementioned observations depict that the relatively lower oil viscosity and the higher temperature in Coreflood#3 increased the rate of methane liberation from the heavy oil probably because of the higher rate of $CO_2$ diffusion in that experiment. The diffusivity of a fluid into liquid depends on several parameters such as temperature and the liquid viscosity and it is generally given by Stokes-Einstein equation in which diffusion coefficients in liquid systems are inversely proportional to viscosity (Vignes 1966; Riazi & Whitson 1993). Stokes-Einstein equation predicts that

$$\frac{D_{T_1}}{D_{T_2}} = \frac{T_1}{T_2}\frac{\mu_{T_2}}{\mu_{T_1}} \tag{5.1}$$

where,

$T_1$ and $T_2$ denote temperatures 1 and 2, respectively.

$D$ is the diffusion coefficient ($cm^2/s$),

$T$ is the absolute temperature ($K$),

$\mu$ is the dynamic viscosity of the liquid ($Pa.s$).

It should be mentioned that although the Stokes-Einstein describes the diffusivity qualitatively, it may not be quantitatively accurate for complex hydrocarbon systems. The humps in the methane rate curves after the breakthrough in both experiments also demonstrate that methane liberation from the oil was present during early times of $CO_2$ injection.

### 5.1.3 Intermittent $CO_2$ Injection

The core was shut-in for a period of 24 hours after the period of continuous injection. Then, 0.3 PV of $CO_2$ was injected into the core to displace the oil in contact with $CO_2$ toward the production end. This process was repeated for 9 cycles to evaluate the

performance of oil recovery at different cycles. The core pressure was monitored and recorded during each period of shut-in. Similar to the test at the conditions of liquid $CO_2$, it was observed that the core pressure was increased by the start of each halt period. Figure 5-6 shows the ultimate core pressure at the end of each shut-in period. The risen pressure of the core would have assisted $CO_2$ dissolution in oil and this has caused to further viscosity reduction and swelling of the oil.

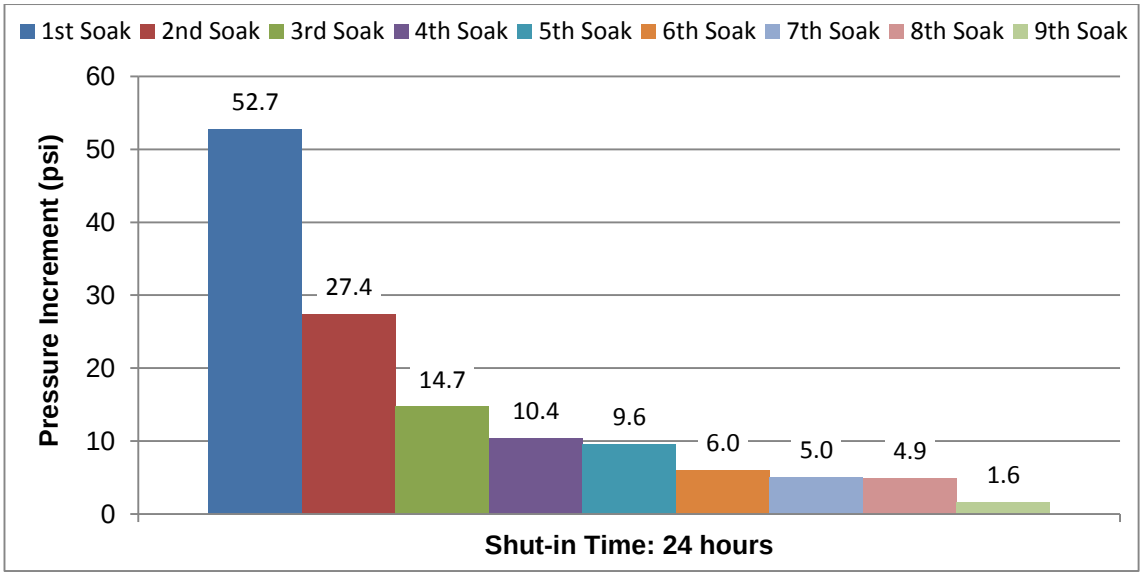


Figure 5-6: Ultimate increase of core pressure at the end of each shut-in period.

The increase of core pressure, however, was not equal in all of the shut-in periods and the amount of this increment is decreasing in successive cycles. As discussed previously, the main reason of pressure rising during the no-flow periods is the liberation of methane of the oil. Thus, the core pressure increment is notably high in the first periods of shut-in. 0.3 pore volume of $CO_2$ was injected into the core after each shut-in period. Figure 5-7 compares the incremental oil recovery of each cycle of the period of intermittent injection. In the first two periods of injection, oil produced with relatively highs rates from the beginning of injection whereas no oil production was observed at the beginning of other periods of $CO_2$ injection. The results of oil recovery highlight the impact of $CO_2$ dissolution in oil and the resultant oil viscosity reduction which, on the other hand, enhances the impact of gravity drainage on the performance of oil recovery. These observations are also confirmed by the results of the viscosity of oil recovered during the cycles of intermittent injection.

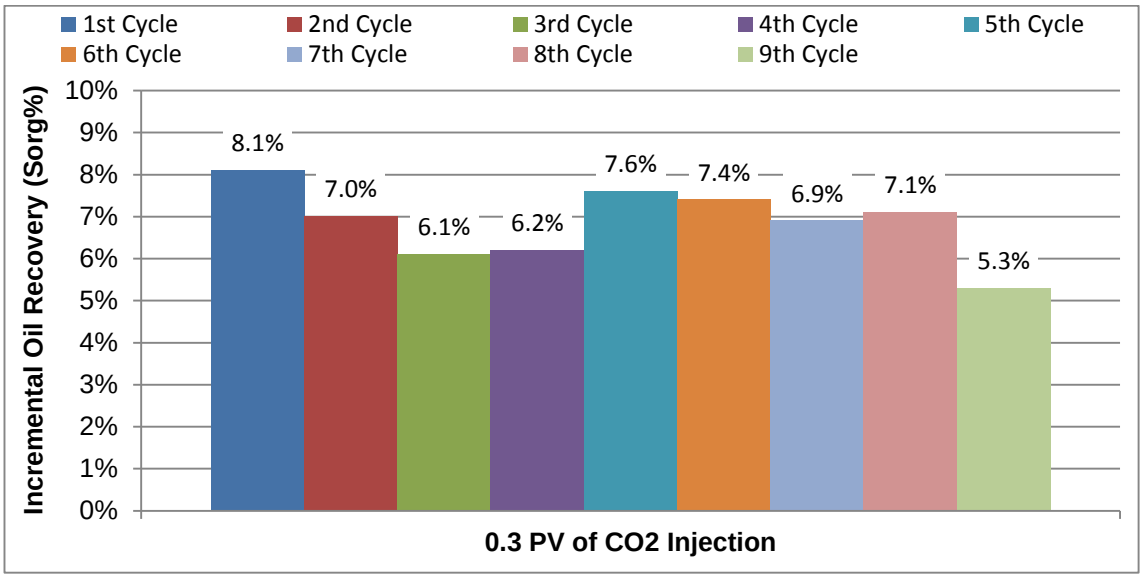


Figure 5-7: Incremental oil recovery of each cycle of intermittent $CO_2$ injection.

The oil recovery forecast of continuous $CO_2$ injection is illustrated in Figure 5-8 with this assumption that the oil production would have continued equal to the last oil rate. The results show that 9 cycles of intermittent $CO_2$ injection have improved oil recovery around 20% of the original oil in core.

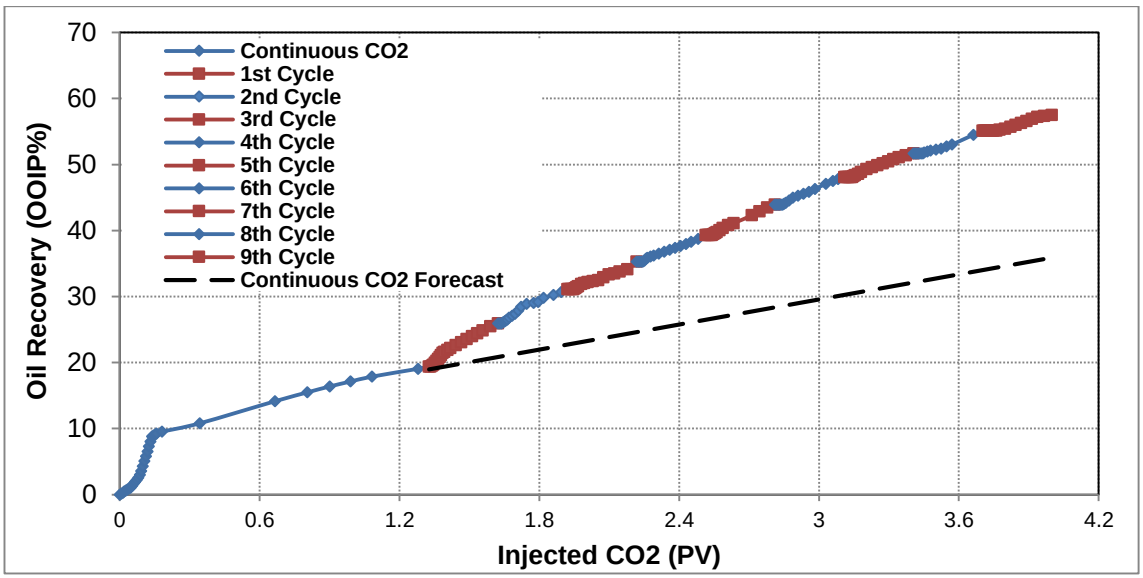


Figure 5-8: Cumulative oil recovery during the periods of continuous and intermittent CO2 injection.

### 5.1.4 Effects of Oil Viscosity and State of $CO_2$ on Performance of Intermittent $CO_2$ Injection

Figure 5-9 shows the oil recovery profiles of intermittent injection when $CO_2$ was a liquid or supercritical fluid. It was demonstrated that the same mechanisms were active in both experiments, albeit in varying extent. The higher amount of oil recovery at the conditions that $CO_2$ was a supercritical fluid (its density was half of the density of liquid $CO_2$) is mainly attributed to the initial lower oil viscosity (around 7 times) in place. The lower oil

viscosity is also an important reason for the higher increase of core pressure in the first period of shut-in. In both experiments, the saturation of the remaining oil in the core after continuous $CO_2$ injection is almost equal and thus, the effects of oil saturation on the performance of intermittent injection would be eliminated. Nonetheless, this does not necessarily imply that the area of contact between $CO_2$ and the remaining oil was similar in these experiments.

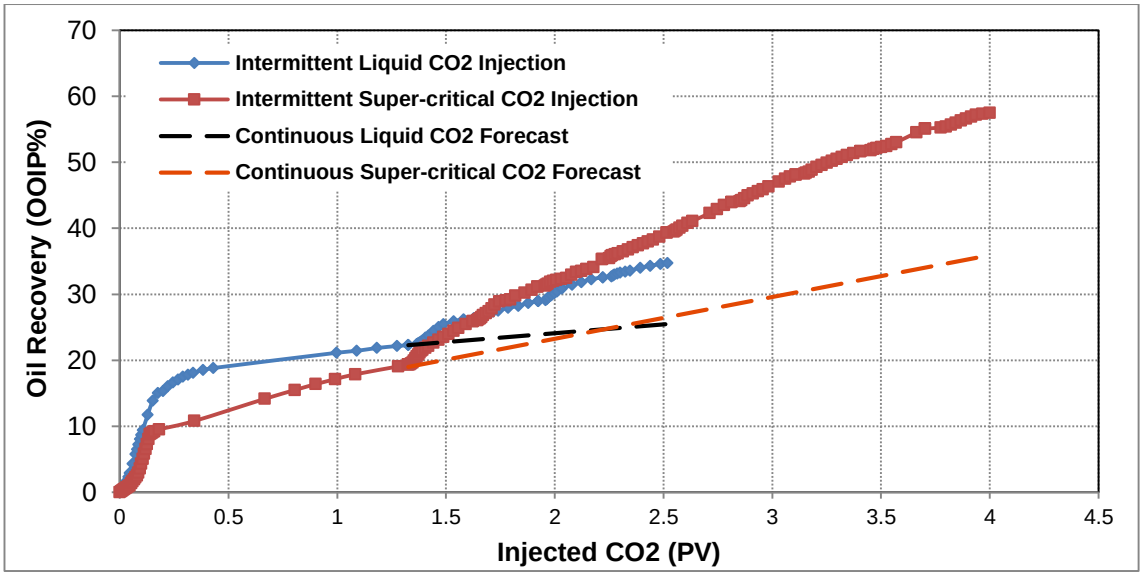


Figure 5-9: Comparison of oil recovery profiles of intermittent liquid $CO_2$ injection and intermittent supercritical $CO_2$ injection.

Although the capacity of oil to uptake $CO_2$ reduces with an increase in temperature, Table 3-6, a higher temperature can increase the rate of $CO_2$ diffusion into the oil. This is another reason of higher pressure rising in the first shut-in period of the intermittent supercritical $CO_2$ injection. This is also reflected by the significant drop in the pressure increment after the first cycle of intermittent injection. Figure 5-10 shows the results of in-line analysis of the composition of produced gas during injection slugs of intermittent injection. A direct relationship between the extent of core pressure increment in each period of shut-in and the concentration of methane in gas produced from the core in the subsequent injection period is understood. This observation can also be extended to the behaviour of the core pressure during corresponding soaking periods in both experiments.

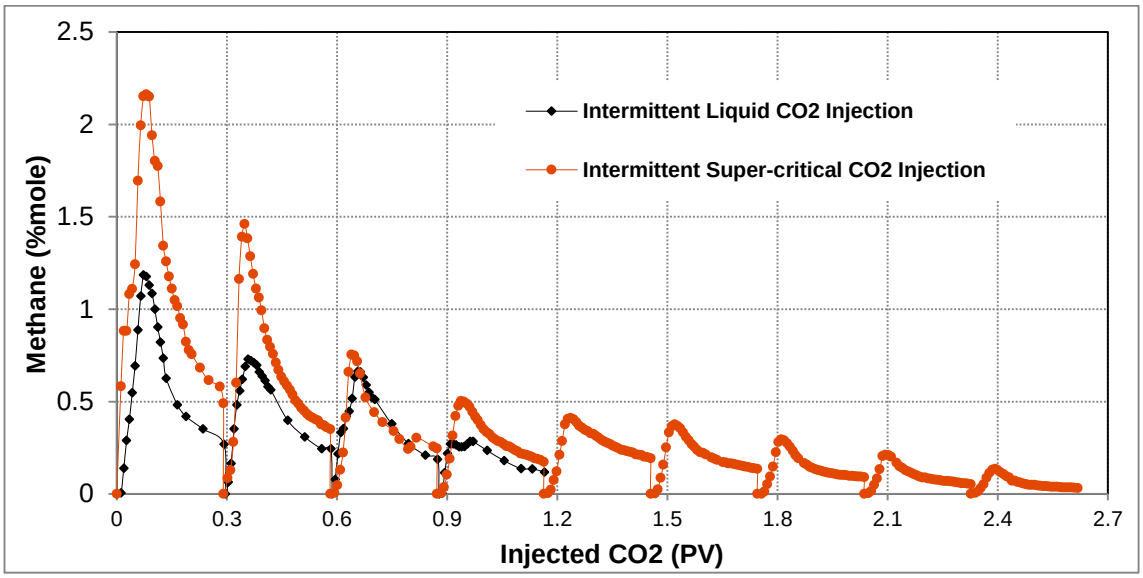


Figure 5-10: Compositional analysis of produced gas during cycles of intermittent liquid $CO_2$ injection and intermittent supercritical $CO_2$ injection.

Table 5-3 shows some of the physical properties of the fluids under two different conditions; liquid $CO_2$ and supercritical $CO_2$. Here it is assumed that $CO_2$ in contact with the original oil in the core is able to extract all the dissolved methane from the oil and $CO_2$ is also dissolved in the oil to the maximum extent. For instance, under the conditions that $CO_2$ is in the supercritical state, 0.212 $cm^3$ of methane is nucleated from the live oil and becomes a gas phase while 0.244 $cm^3$ of $CO_2$ can be dissolved in the oil without any dissolved methane (dead oil). This process results in a decrease in the volume of the system and hence that cannot explain the increase in core pressure during the shut-in periods of Coreflood#3. The fact that the pressure of the core increased in shut-in periods indicates that $CO_2$ in contact with the oil could trigger methane liberation from the oil without the need for $CO_2$ to become dissolved completely in the oil. This is also consistent with the observation made during the contact of $CO_2$ and live oil in the visual-cell experiments. The sharp swelling of the oil at the early time of contact with $CO_2$ is an indication of sudden nucleation of methane of the oil. It should be mentioned that the changes in total volumes due to the swelling or the shrinkage of oil is negligible.

Table 5-3: PVT properties of fluids under the conditions of Coreflood#2 and Coreflood#3.

| Temperature (˚C) | Pressure (psi) | Volume of Methane ($cm^3$/mole) | Volume of $CO_2$ ($cm^3$/mole) | Volume of methane in oil ($cm^3/cm^3$Oil) | Volume of $CO_2$ in oil ($cm^3/cm^3$Oil) |
|---|---|---|---|---|---|
| 28 | 1500 | 206.87 | 55.18 | 0.203 | 0.152 |
| 50 | 1500 | 232.29 | 103.29 | 0.212 | 0.244 |

The liberation of methane from the oil leads to an increase in the viscosity of the oil. This

increase would be significant for heavy oil systems. However, the dissolution of $CO_2$ in the oil would compensate this viscosity increment. Experimental investigations have shown that the $CO_2$ content of heavy oil does not have a linear relationship with the ratio of reduction of heavy oil viscosity. In the other words, a huge fraction of the oil viscosity can be reduced only by a small fraction of $CO_2$ in the oil (Mumgan 1981; Miller & Jones 1981; Emadi 2012).

### 5.1.5 1st (Tertiary) Waterflood

One PV of $CO_2$-saturated brine was injected through the core immediately after the 9th cycle of intermittent $CO_2$ injection. As water entered into the core, gas production was started and it continued until the breakthrough of water which occurred at 0.29 PV of injection, as evidenced in Figure 5-11. Similar to the waterflood after intermittent liquid $CO_2$ injection, production of an oil bank before the breakthrough was observed. Oil production continued at high water cuts until the end of the period of waterflood and around 14% of the remaining oil in the core was recovered. The production of this relatively large fraction of oil is attributed to the improved viscosity of displacing fluid and also the lowered viscosity of displaced fluid.

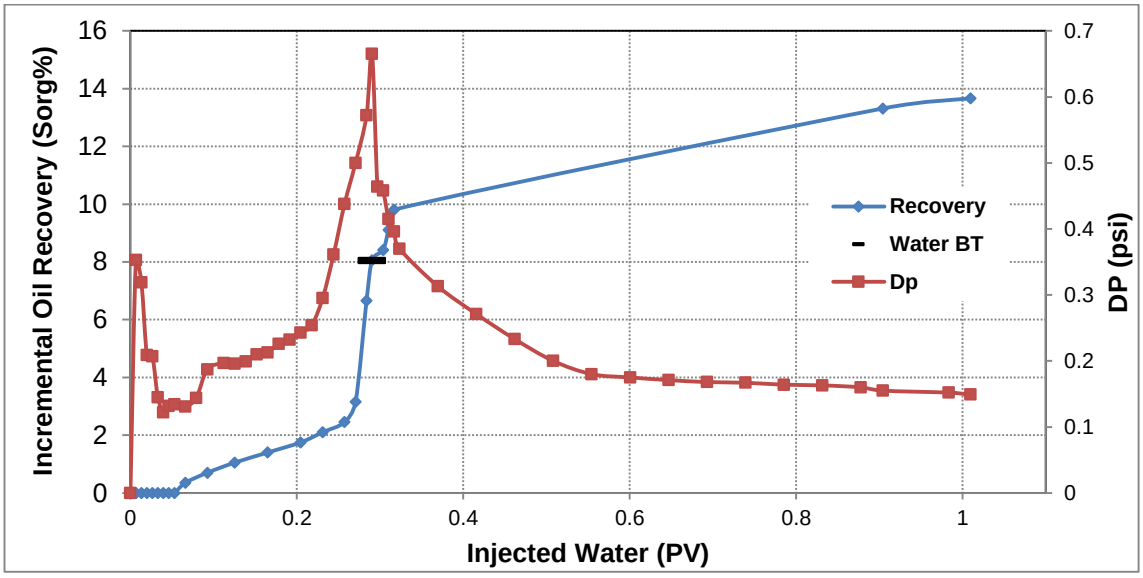


Figure 5-11: Incremental oil recovery and differential pressure across the core during the period of tertiary waterflood.

A small slug of $CO_2$ (0.3 PV) was injected into the core after the period of tertiary waterflood. Water was produced before the breakthrough of $CO_2$. After the breakthrough, oil recovery started and continued with water and gas production. Eventually, around 4.5% of the remaining oil of tertiary waterflood was recovered at the end of the slug of $CO_2$ injection.

***Summary***

Figure 5-12 illustrates the cumulative oil recovery during different stages of Coreflood#3. The sweep efficiency of continuous (secondary) $CO_2$ injection was relatively poor because of the nature of the flow in porous media saturated with viscous oil. However, $CO_2$ is able to enhance recovery of heavy oil by a number of mechanisms associated with the advantage of gravity. To further improve the recovery factor, the residence time of $CO_2$ in the core was increased and that significantly improved oil recovery. A waterflood after the period of intermittent $CO_2$ injection also improved the sweep efficiency. Despite the relatively low saturation of oil in the core after the period of tertiary waterflood, it is significant that $CO_2$ could recover a considerable fraction of the remaining oil. Similar to the experiments at the conditions that $CO_2$ was a liquid fluid, it was observed that $CO_2$ in the supercritical state can also alter the physical properties of heavy oil in porous media and a higher quality oil can be recovered by the application of supercritical $CO_2$.

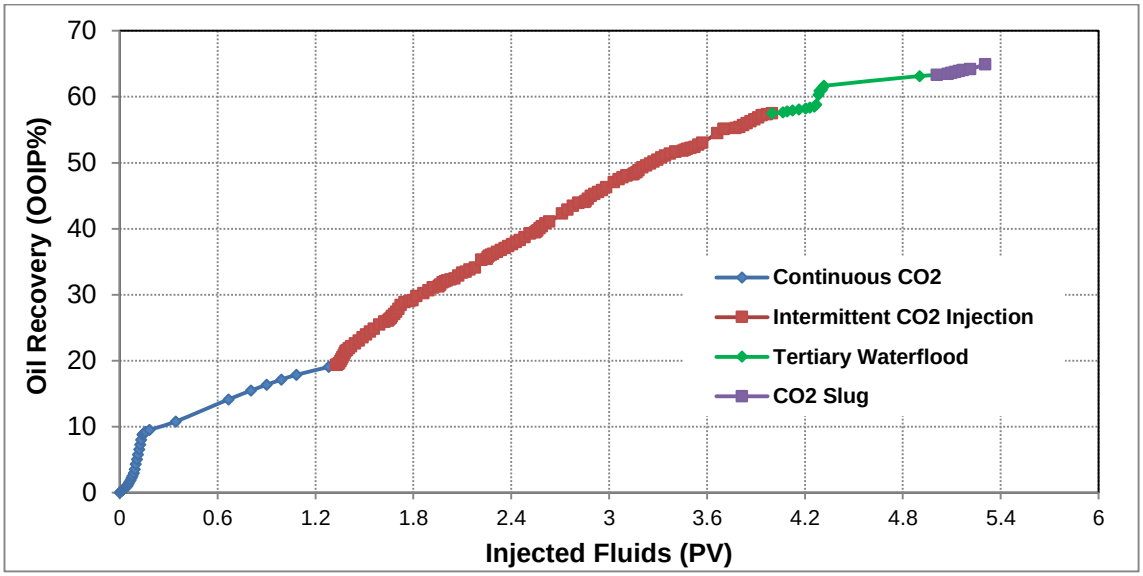


Figure 5-12: Cumulative oil recovery during different periods of Coreflood#3.

## 5.2 Coreflood#4: Tertiary Supercritical $CO_2$ Injection

A tertiary $CO_2$ injection following a secondary waterflood experiment was performed to evaluate the performance of tertiary supercritical $CO_2$ injection in heavy oil recovery. The main objective of this experiment was to investigate the effects of oil viscosity and state of $CO_2$ on the performance of tertiary $CO_2$ injection. The experiment was followed by a period of waterflood after the tertiary $CO_2$ injection in order to evaluate the performance of improved mobility ratio in enhancing oil recovery. A summary of the performance of all the periods of fluid injection in terms of cumulative oil recovery will be shown in Figure 5-18. Table 5-4 gives the conditions at which the test was performed as well as the fluids in this experiment.

Table 5-4: Fluids and conditions of Coreflood#4.

| **Coreflood#4** | **Coreflood#1** |
|---|---|
| Crude Oil: Methane-saturated Crude 'C' | Crude Oil: Methane-saturated Crude 'C' |
| Brine: Methane-saturated or $CO_2$-saturated | Brine: Methane-saturated or $CO_2$-saturated |
| Gas: Supercritical $CO_2$ | Gas: Liquid $CO_2$ |
| Temperature: 50° C | Temperature: 28° C |
| Pressure: 1500 psi | Pressure: 1500 psi |
| Injection Rate: 7 $cm^3$/hr | Injection Rate: 7 $cm^3$/hr |
| Core Position: Vertical (top to bottom) | Core Position: Vertical (top to bottom) |

***Procedure***

The following were the main steps to conduct Coreflood#4:

1. **Dead Brine Injection:** Core was saturated with brine and the permeability was re-measured and it was unchanged.
2. **Live Brine Injection:** The live brine was injected through the core to avoid gas transfer from following live oil into the brine. The injection was continued until the gas content of the produced brine reached to certain values.
3. **Live Oil Injection:** The core was flooded with live crude 'C' and an irreducible water saturation of 8% was achieved.
4. **1st (Secondary) Waterflood:** 1.1 PVs of methane-saturated brine were injected into the core.
5. **1st (Tertiary) $CO_2$ Injection:** 3 PVs of $CO_2$ were injected into the core after the first waterflood.
6. **2nd Waterflood:** Around 1 PV of $CO_2$-saturated brine was injected through the core after $CO_2$ injection.

7. **2nd $CO_2$ Injection:** Continuous $CO_2$ was injected into the core immediately after the 2nd waterflood.
8. **Core Cleaning:** Several cycles of toluene and methanol were injected into the core.

***Results and Discussion***

### 5.2.1 1st (Secondary) Waterflood

After establishing the initial water and oil distributions in the core, methane-saturated brine was injected through the core. Figure 5-13 shows the recovery profile and differential pressure across the core during the period of injection. The recovery profile is similar to waterflooding of heavy oil reservoirs and a considerable fraction of oil was still produced at high water cuts after the water breakthrough. Ultimate oil recovery of around 24% of the initial oil in the core was obtained at the end of waterflood.

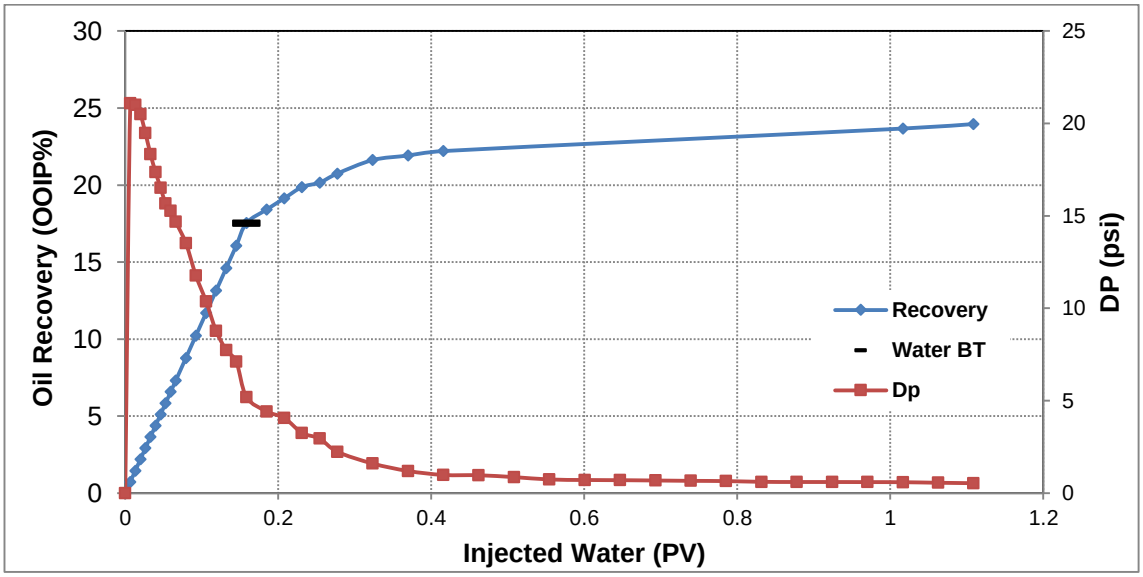


Figure 5-13: Oil recovery and differential pressure across the core during the period of 1st (secondary) waterflood.

Similar to the previous secondary waterflood at a lower temperature, a significant area of the core was bypassed and remained unswept. The viscosity of the oil in this experiment was considerably lower than the viscosity of the same oil at a lower temperature but the instability in the flood front and viscous fingering still dominated the flow of water in the core. The composition of oil recovered during different stages of Coreflood#4 was analysed and reported in Table 5-5. Oil produced before the breakthrough was only in contact with the core and the irreducible water in the core and therefore it is considered as the original oil in the core. It can be seen that the composition of oil recovered before and after the breakthrough of water is unchanged. To confirm this observation, the

viscosity of both samples was measured at the temperature of the experiment and the results are reported in Table 5-6. No change in the viscosity of the recovered oil was caused by the waterflood.

Table 5-5: Composition of oil recovered during different stages of Coreflood#4.

| Sample | PV of Injection | ≤C12 (%mole) | >C12-≤C16 (%mole) | >C16-≤C20 (%mole) | >C20-≤C23 (%mole) | >C23-≤C29 (%mole) | >C29-≤C45 (%mole) | >C45-≤C100 (%mole) |
|---|---|---|---|---|---|---|---|---|
| 4#1WF#1 | 0.0-0.07 | 14.9 | 23.4 | 27.0 | 12.8 | 12.0 | 8.1 | 1.7 |
| 4#1WF#2 | 0.18-0.37 | 15.0 | 22.7 | 27.1 | 13.1 | 12.4 | 8.3 | 1.5 |
| 4#1GF#1 | 0.8-0.2 | 13.9 | 19.0 | 28.3 | 13.9 | 13.2 | 9.4 | 2.3 |
| 4#1GF#2 | 0.2-1.0 | 18.9 | 23.3 | 24.6 | 12.1 | 11.3 | 8.1 | 1.7 |
| 4#1GF#3 | 1.0-2.1 | 24.5 | 21.8 | 25.2 | 10.9 | 10.2 | 6.4 | 0.9 |
| 4#1GF#4 | 2.1-3.1 | 19.1 | 26.0 | 26.1 | 11.0 | 10.2 | 6.5 | 1.1 |
| 4#2WF#1 | 0.0-0.24 | 14.8 | 23.3 | 27.0 | 13.0 | 12.2 | 8.2 | 1.6 |
| 4#2WF#2 | 0.58-1.1 | 11.8 | 22.6 | 27.5 | 14.0 | 13.2 | 9.3 | 1.7 |
| 4#2GF#1 | -- | 20.2 | 24.9 | 24.9 | 11.5 | 10.6 | 6.9 | 1.0 |
| 4#2GF#2 | -- | 25.4 | 31.3 | 22.9 | 8.4 | 7.0 | 4.4 | 0.6 |

Table 5-6: Viscosity of oil recovered during different periods of Coreflood#4.

| Sample | PV of Injection | Viscosity Ratio, (%) |
|---|---|---|
| 4#1WF#1 | 0.0-0.07 | 100 |
| 4#1WF#2 | 0.18-0.37 | 100 |
| 4#1GF#4 | 2.1-3.1 | 46 |

### 5.2.2 1st (Tertiary) $CO_2$ Injection

After the period of secondary waterflood, $CO_2$ was injected into the core to evaluate the performance of tertiary injection of $CO_2$ under the conditions that $CO_2$ was a supercritical fluid. Before the breakthrough, water was mainly recovered from the core but a small fraction of oil was also produced as a result of water and oil contact. The highest oil rate was obtained after the breakthrough of $CO_2$ as a result of the production of an oil bank. Oil was then recovered with a relatively constant rate until the end of the injection of $CO_2$. Figure 5-14 shows the profiles of oil recovery and differential pressure across the core during the period of tertiary $CO_2$ injection.

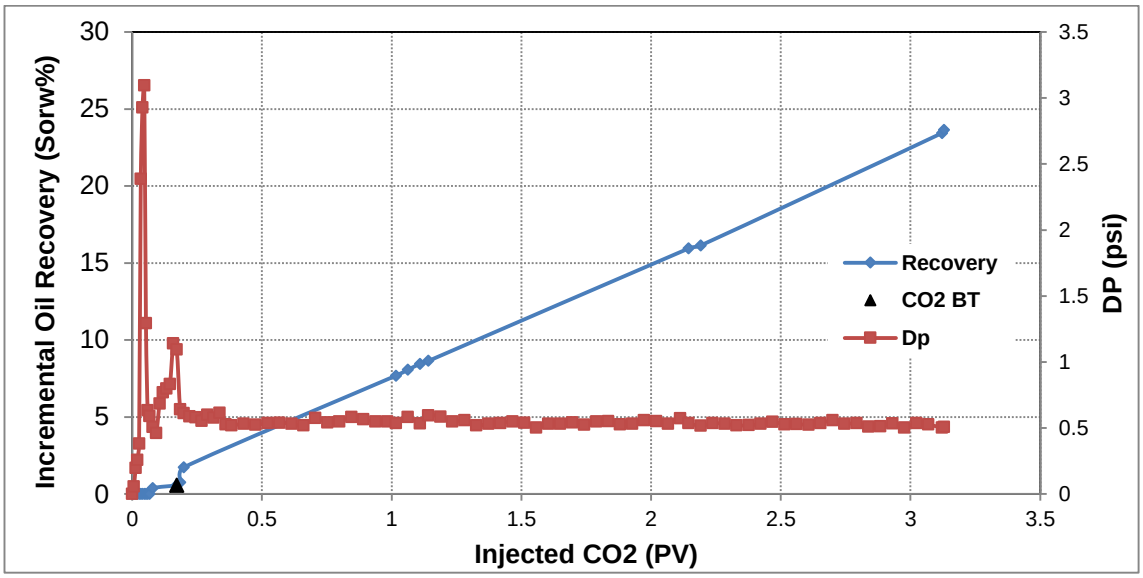


Figure 5-14: Incremental oil recovery and differential pressure across the core during the period of tertiary $CO_2$ injection.

Water production continued after the breakthrough although at low cuts. Viscous forces were responsible for oil recovery at early times of injection of $CO_2$. However, their impact reduced when the pressure gradient within the core decreased. Note that the composition of oil recovered at this stage (4#1GF#1) is somehow similar to that of the original oil in the core. The relatively lower concentration of light and intermediate compounds in the oil recovered mainly by viscous forces is attributed to the effect of extraction of hydrocarbons by dense (supercritical) $CO_2$. Later, the impacts of other mechanisms such as $CO_2$ dissolution in the oil and the resultant viscosity reduction and oil swelling, the liberation of methane of the oil as well as extraction of hydrocarbon components by $CO_2$, and gravity drainage increased on oil recovery. An important indication of these processes is the changes in the properties (i.e. composition, viscosity) of oil recovered after the breakthrough.

Figure 5-15 depicts the results of GC analysis of produced gas during the period of tertiary $CO_2$ injection. The fraction of methane was significant after the breakthrough due to high oil rate production as well as the production of methane that was liberated from the oil in the core by $CO_2$. Despite constant oil rate until the end of the period of $CO_2$ injection, the concentration of methane notably decreased. This implies that the amount of methane dissolved in the recovered oil was lower than the initial content of methane of the oil. In addition, some factors such as gravity segregation and trapping could be responsible for the lower fraction of methane in the effluent of the core.

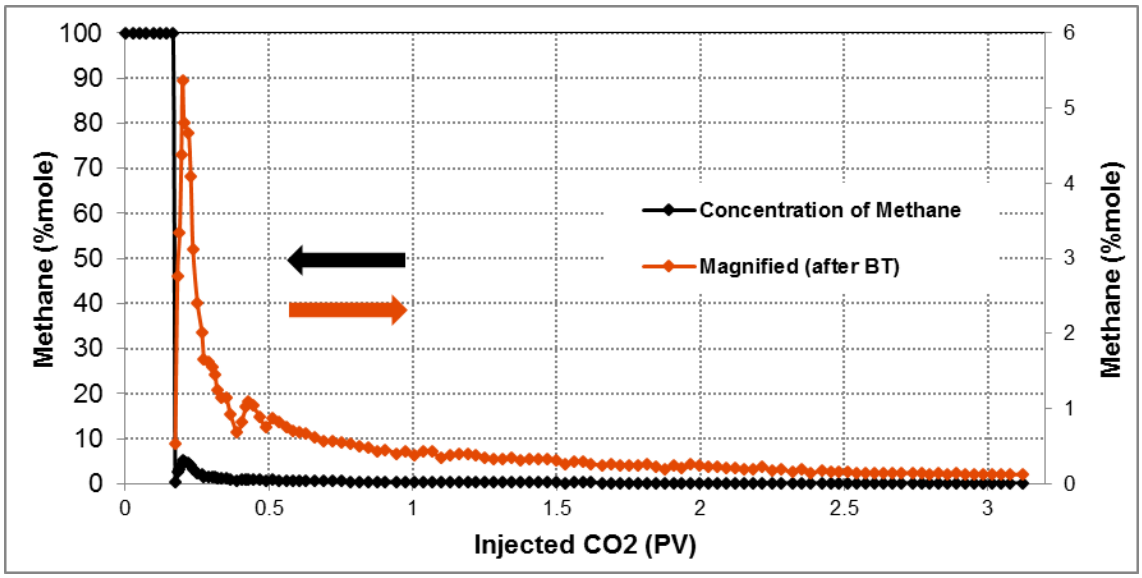


Figure 5-15: Compositional analysis of produced gas during the period of tertiary $CO_2$ injection.

### 5.2.3 Effects of Oil Viscosity and State of $CO_2$ on Performance of Tertiary $CO_2$ Injection

Figure 5-16 compares the profiles of oil recovery of tertiary $CO_2$ injection at two different temperatures under which $CO_2$ was either a liquid or a supercritical fluid. Additionally, the viscosity of the fluids was higher in the test at the lower temperature. The remaining oil in the core after the period of secondary waterflood in both experiments was almost equal. Thus, the effects of oil saturation on the performance of $CO_2$ injection would be eliminated. It was observed that similar mechanisms, albeit in varying impacts, were active in the both runs. However, a significantly lower amount of $CO_2$ in the supercritical state was utilised to recover the same amount of oil in the experiment that $CO_2$ was in the liquid state. This is mainly attributed to the lower viscosity of the initial oil in the test at the higher temperature. The lower viscosity of the oil could have enhanced the effects of $CO_2$ dissolution in oil and gravity drainage on the process of oil recovery.

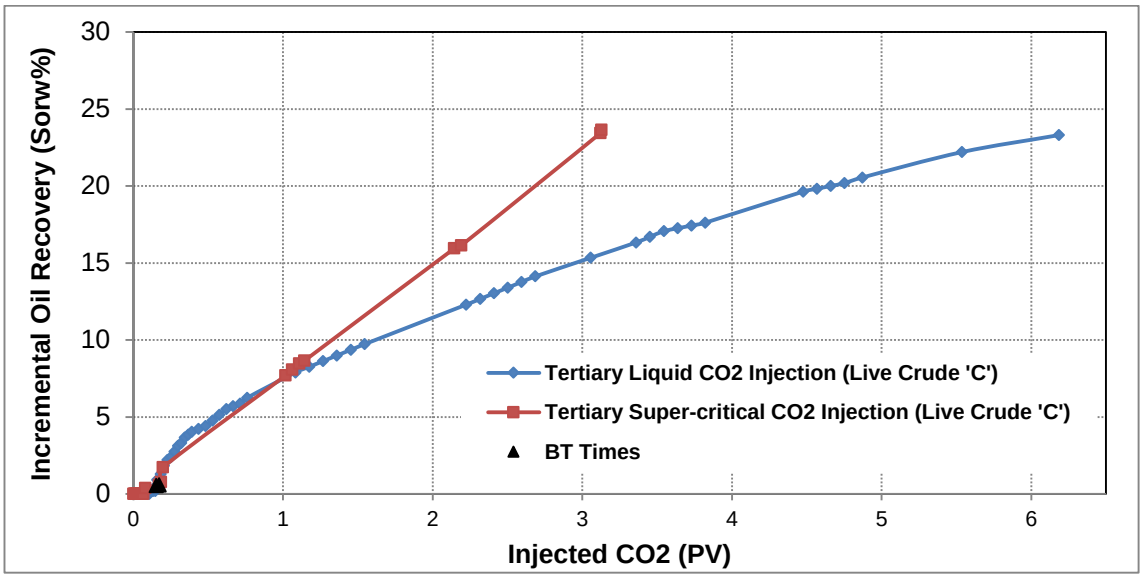


Figure 5-16: Comparison of incremental oil recovery profiles of tertiary liquid $CO_2$ injection (Figure 4-4) and tertiary supercritical $CO_2$ injection.

Another important observation was the higher impact of $CO_2$ in the liquid state on the quality of produced oil. Because of the higher density of $CO_2$, the composition (quality) of oil was more improved in the test at the lower temperature. This also confirms the previously reported observation that the density of $CO_2$ is the dominant factor in determining the size of extracted components from oil.

### 5.2.4 2nd Waterflood

After the period of tertiary $CO_2$ injection, around 1 PV of $CO_2$-saturated brine was injected through the core. Before the breakthrough, the injected water displaced the free gas in the core toward the production outlet. A small fraction of oil was also recovered during this period. The oil rate was increased sharply after the breakthrough of water and it continued until around 0.3 PV of injection. A considerable fraction of the remaining oil was also produced at high water cuts until the end of the waterflood. It is less likely that the injected water could invade the area of the core that had been bypassed by the previous water and $CO_2$ injection. Although its composition is similar to the composition of original oil in the core, the oil recovered during the period of 2nd waterflood would have been the oil in contact with $CO_2$. It is observed from the results of the compositional analysis that the concentration of light and intermediate components in the produced oil during the period of 2nd waterflood is relatively lower than that of the original oil in place.

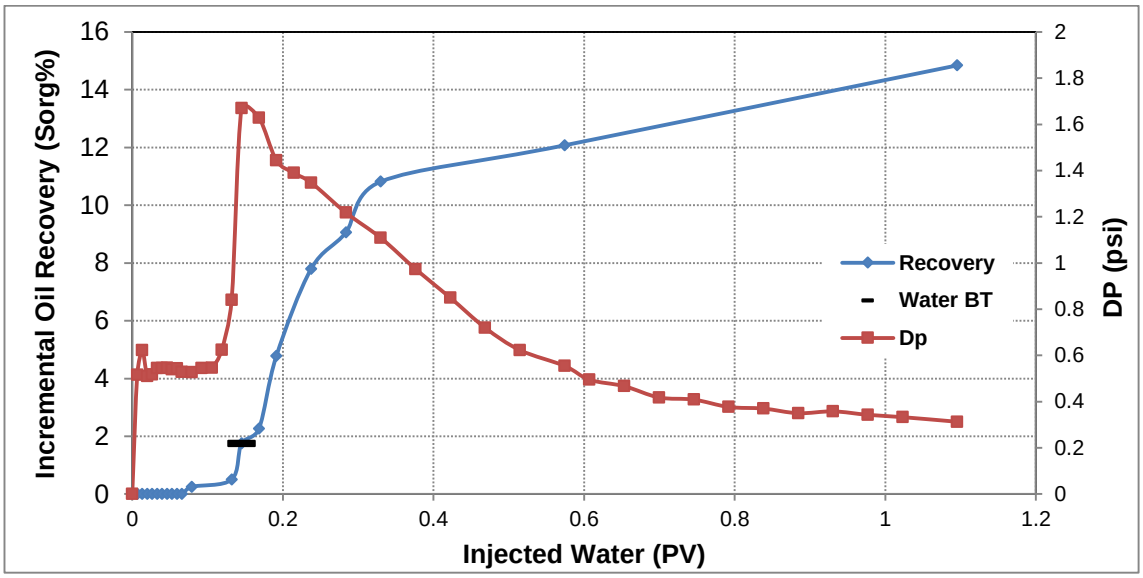


Figure 5-17: Incremental oil recovery and differential pressure across the core during the period of 2nd waterflood.

After the period of 2nd waterflood, $CO_2$ was injected through the core to further evaluate the impact of $CO_2$ injection on the quality of recovered oil. In the micromodel experiments, it was observed that $CO_2$ after the period of tertiary or second waterflood can still enhance oil recovery, mainly by the mechanisms attributed to the extraction of hydrocarbons and dissolution of $CO_2$. The saturation of oil in porous media becomes significantly low after repeated slugs of water and $CO_2$ injection. At this stage, oil trapped in potential flow paths is not a continuous phase within the system and it is generally surrounded by water after a period of waterflood. Therefore, oil would be fairly immobile in porous media and this is, of course, more evident in the case of heavy oil systems because of the higher viscosity of heavy oils. However, dense $CO_2$ would still improve recovery factor by extraction of hydrocarbons and the mechanism of the formation of light and less viscous phase as it was observed during the micromodel tests in Chapter 4. The compositional analysis of the oil recovered during the period of 2nd $CO_2$ injection reveals that the concentration of light and intermediate components is chronologically increasing, meaning that $CO_2$ as a supercritical fluid is highly capable of (in-situ) improving the quality of recovered heavy oil. Two main reasons that the impact on the quality of recovered oil was not as significant as it was in the case of the experiment that $CO_2$ was a liquid fluid are the differences in density of $CO_2$ and viscosity of the original oil in place. The lower viscosity of the oil has caused that higher amount of the original oil or the oil that much of its light and intermediate components has been stripped by $CO_2$ could be displaced by gravity toward the production end of the core.

***Summary***

Figure 5-18 illustrates the cumulative oil recovery during different periods of Coreflood#4. An early breakthrough as a result of instability in the front of the flood is a signature of waterflood for heavy oil recovery. However, oil production continues at high water cuts after the breakthrough. $CO_2$ was continuously injected into the core after the waterflood and a significant fraction of the water in the core was displaced until the breakthrough of $CO_2$. Three PVs of $CO_2$ injection led to the recovery of around 20% of the initial oil in the core. A period of waterflood after the period of tertiary $CO_2$ injection could also improve the recovery factor by around 10% of the initial oil in the core. The recovery of oil by the period of 2$^{nd}$ waterflood shows that $CO_2$ either generated new paths within the core or changed the physical properties of the remaining oil in the core. Thus, waterflood after the period of $CO_2$ injection could enhance oil recovery. The results of compositional analysis of oil produced during different stages of the experiment revealed that $CO_2$ in a supercritical state can alter the physical properties of the heavy oil. This in-situ process resulted in the recovery of higher quality oil during the period of $CO_2$ injection.

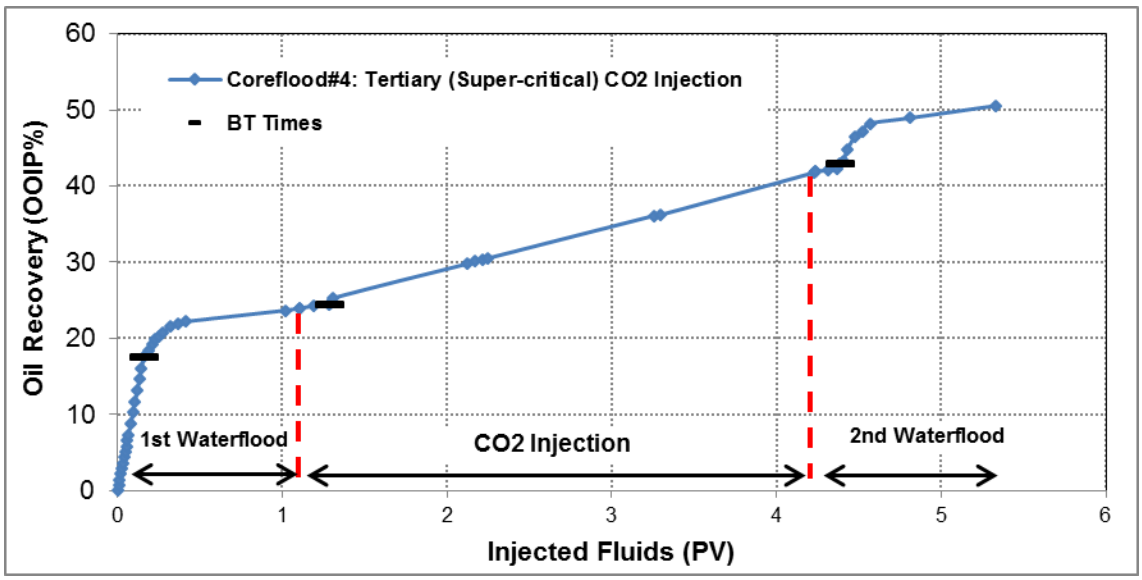


Figure 5-18: Cumulative oil recovery during different periods of Coreflood#4.

## 5.3 Coreflood#5: Intermittent Viscosity Reducing Gas (VRG) Injection

To evaluate the impacts of the mechanisms linked to dense $CO_2$ injection on the performance of oil recovery, an enriched hydrocarbon gas was injected into the core saturated with live crude 'C'. The dissolution of this multi-component gas in crude 'C' can significantly reduce the viscosity of the oil while no significant extraction of hydrocarbons of oil would take place. A secondary continuous viscosity-reducing gas (VRG) injection followed by several periods of shut-in and injection was performed to also evaluate the performance of VRG injection in heavy oil recovery. A summary of the performance of all the periods of fluid injection in terms of cumulative oil recovery will be shown in Figure 5-27. Table 5-7 shows the fluids and conditions of Coreflood#5.

Table 5-7: Fluids and conditions of Coreflood#5.

| **Coreflood#5** | **Coreflood#3** |
|---|---|
| Crude Oil: Methane-saturated Crude 'C' | Crude Oil: Methane-saturated Crude 'C' |
| Brine: Methane-saturated | Brine: $CO_2$-saturated |
| Gas: VRG | Gas: Supercritical $CO_2$ |
| Temperature: 50° C | Temperature: 50° C |
| Pressure: 1500 psi | Pressure: 1500 psi |
| Injection Rate: 7 $cm^3$/hr | Injection Rate: 7 $cm^3$/hr |
| Core Position: Vertical (top to bottom) | Core Position: Vertical (top to bottom) |

***Procedure***

The following were the main steps to conduct Coreflood#5:

1. **Dead Brine Injection:** Core was saturated with brine and its permeability was re-measured. The permeability of the core was equal to the initial permeability of it.
2. **Live Brine Injection:** The live brine was injected through the core to avoid gas transfer from following live oil into the brine. The injection was continued until the gas content of the produced brine reached to certain values.
3. **Live Oil Injection:** The core was flooded with live crude 'C' and an irreducible water saturation of 8% was achieved.
4. **1st Continuous (Secondary) VRG Injection:** 1.3 PVs of VRG were injected through the core.
5. **Intermittent VRG Injection:** 5 cycles of shut-in and injection were performed.
6. **2nd Continuous VRG Injection:** Around 2 PVs of VRG were injected through the core after the period of intermittent injection.
7. **1st (Tertiary) Waterflood:** Around 1 PV of methane-saturated brine was injected

through the core.

8. **Core Cleaning:** The core was cleaned by the injection of several cycles of toluene and methanol.

***Concept of VRG***

Viscous oils have generally poor waterflood recoveries and should be good targets for thermal or miscible gas EOR processes. However, many heavy oil reservoirs are not suitable for thermal recovery. For instance, thermal techniques would be ineffective and uneconomical in thin and deep heavy oil formations. High well costs and large well spacing also make thermal methods impractical. In miscible gas displacements, miscibility between the injectant and reservoir oil is usually achieved by mixing lean gas with expensive NGL (natural gas liquid) or by pressurising the reservoir by waterflood. In heavy oil reservoirs, large amounts of NGL are required, and it is often both impractical and uneconomic to achieve miscibility.

Viscosity reducing gas was first applied in the Kuparuk reservoir of the Milne Point Unit to replace the miscible gas EOR project, which used purchased NGL. In Kuparuk reservoir, the process of VRG injection reduced oil viscosity by 45% and improved oil recovery by about 6% OOIP. It should be mentioned that the reservoir pressure was 3500 *psi* while bubble point pressure was 1800 *psi*. For viscous oil reservoirs that are at or near their bubble point pressure, heavy components in the produced gas can be stripped out and mixed with produced lean gas to manufacture VRG. Alternatively, lean gas can be blended with small volumes of NGL to make VRG. Viscosity reduction of as much as 90% is practical (McGuire, et al. 2005). The composition of the multi-component gas used in this experiment is given in Table 3-5.

***Results and Discussion***

### 5.3.1 1st Continuous (Secondary) VRG Injection

Following the above-mentioned procedure, continuous VRG injection through the core saturated with live crude ‘C’ was started. Figure 5-19 shows the profiles of oil recovery and differential pressure across the core during the period of continuous VRG injection. The early breakthrough of gas is an indication of the presence of instability in the flood front because of the low viscosity of the injection gas. The oil rate was decreased significantly after the breakthrough but oil continued to flow with a relatively constant rate until the end of gas injection. The oil in the coreflood experiment is a stock-tank oil saturated with methane under the conditions of each test. Thus, the injected fluid can

dissolve in the oil and it affects the properties of oil in two ways; first, it reduces the viscosity of the oil as the amount of gas dissolved in the oil increases. Secondly, it causes the oil to swell which increases the oil saturation in the core. The mechanisms of extraction of hydrocarbons and other mechanisms associated with that would have been less pronounced in this run mainly because of the composition of the VRG.

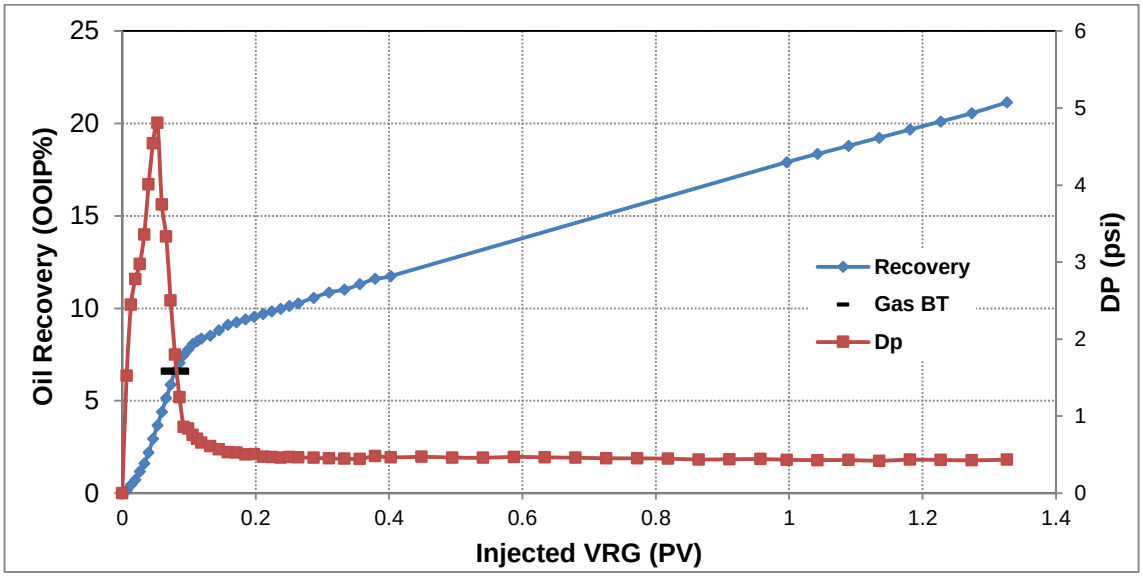


Figure 5-19: Oil recovery and differential pressure across the core during the period of continuous (secondary) VRG injection.

Table 5-8 compares the viscosity of some of the samples of recovered oil, after complete separation of gas from oil, during different stages of the experiment with the viscosity of the original crude 'C' as well as the VRG-saturated crude 'C'. All the measurements were performed at 50˚ *C* and ambient pressure. It is shown that the dissolution of VRG in the oil has reduced the viscosity of the original oil in the core. Although the oil in the coreflood experiments is saturated with methane which is more likely representative of heavy oil reservoirs, it is not completely similar to an actual reservoir oil. It lacks the crucial light hydrocarbon components which can significantly affect the performance of gas injection. The presence of the light components in the oil would lower the dissolution of those components of the gas in the oil and hence it would reduce the impacts of VRG on oil viscosity as well as oil recovery.

Table 5-8: Viscosity of oil recovered during different periods of Coreflood#5.

| Sample | PV of Injection | Viscosity Ratio, (%) |
|---|---|---|
| 5#1GF#1 | 0.0-0.08 | 100 |
| 5#1GF#3 | 0.27-1.0 | 66 |
| 5#4GF#1 | 1.9-2.2 | 47 |
| 5#6GF#2 | 2.8-3.2 | 60 |
| 5#6GF#4 | 3.6-4.4 | 62 |
| VRG-saturated Crude 'C' (g:o≡6:1) | -- | 38 |

### 5.3.2 Effects of Composition of Injection Gas on Heavy Oil Recovery

Figure 5-20 compares the recovery profiles of secondary supercritical $CO_2$ injection and secondary VRG injection, both carried out in the core saturated with live crude 'C'. Although the breakthrough of the injection fluids varies notably in both runs, an equal amount of oil was produced in both experiments at the breakthrough of injection fluids. This may be due to the higher rate of $CO_2$ dissolution in the oil than the rate of dissolution of VRG.

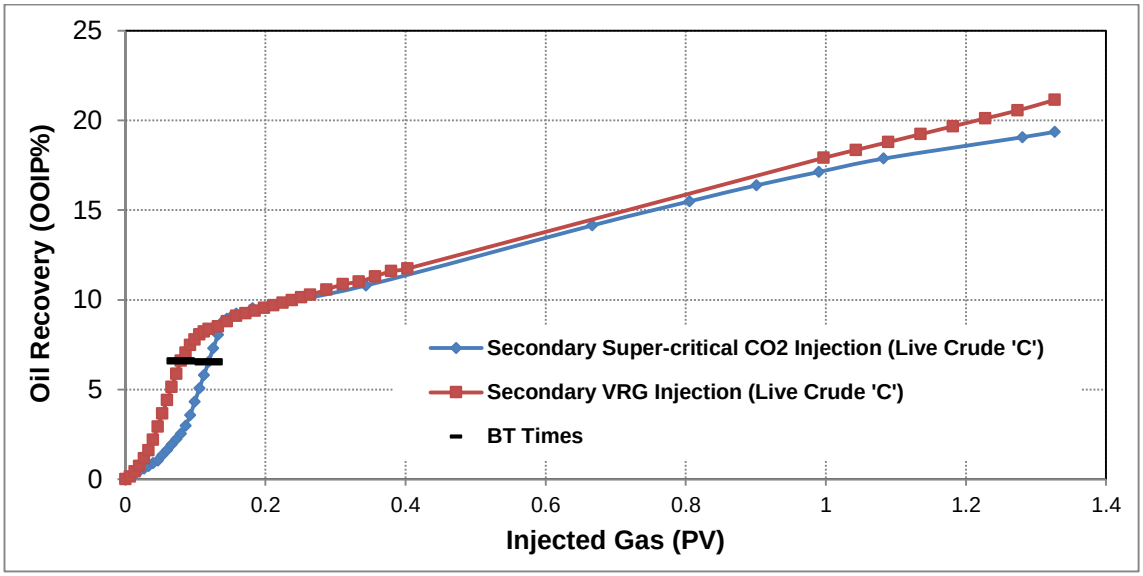


Figure 5-20: Comparison of oil recovery profiles of continuous supercritical $CO_2$ injection and continuous VRG injection.

After the breakthrough, the main mechanisms of oil recovery in case of $CO_2$ injection were the dissolution of $CO_2$ in the oil and the extraction of oil components by $CO_2$. The impact of the dissolution of gas in the oil would have been higher when the injection fluid was VRG, Table 3-6. In addition, the oil recovered in our experiments is collected at atmospheric pressure and hence it will be a mixture with no associated (dissolved) gas. However, in the case of VRG injection, some of the compounds of the gas dissolved in the oil would have remained in the oil and therefore, it has been considered as oil recovery. Due to the composition of injection gas, it is believed that the mechanisms of

extraction during VRG injection was not as significant as it was when the injected gas was $CO_2$.

### 5.3.3 Intermittent VRG Injection

The core was shut-in for a period of 24 hours after the period of continuous injection. Then, 0.3 PV of VRG was injected into the core to displace the remaining oil in the core toward the production outlet. This process was repeated for 5 cycles to evaluate the performance of oil recovery at different cycles. Another objective of this test was to compare the behaviour of VRG and $CO_2$ during shut-in periods. Thus, the core pressure was monitored and recorded during the periods of shut-in. Figure 5-21 illustrates the changes of core pressure during the shut-in periods. It is shown that the pressure of the core at the end of each shut-in period was higher than that at the beginning of each period of shut-in. This observation is attributed to the interactions between the components of VRG and the original (live) oil in the core. The original oil in the core was initially saturated with methane under the conditions of the test. Although the major fraction of VRG was methane, a significant amount of this gas could be dissolved in the live crude 'C'. The dissolution of gas in oil in a close system will lead to pressure reduction. However, the pressure of core slightly increased in the periods of shut-in which implies that some of the original methane of the oil has been extracted perhaps by $CO_2$ and other intermediate components of VRG.

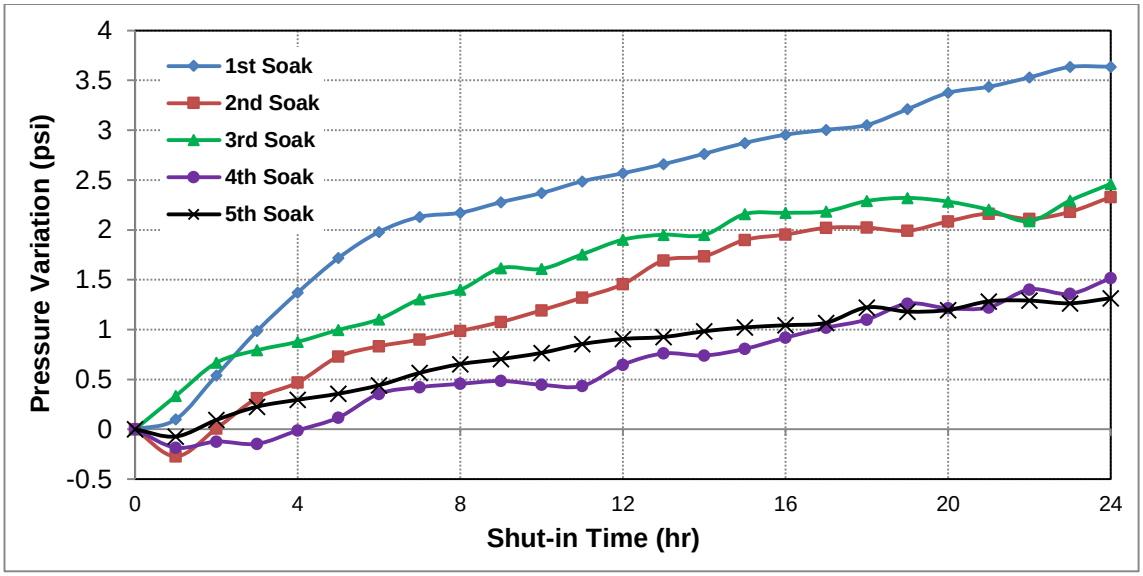


Figure 5-21: Pressure variation of the core during the shut-in periods.

Figure 5-22 shows the incremental oil recovery of each injection period of intermittent enriched hydrocarbon gas injection. The performance of oil recovery of each cycle of intermittent injection is relatively equal which indicates that the gas dissolution in the oil

and the resultant oil swelling and viscosity reduction were the main mechanisms of oil recovery in successive cycles of shut-in and injection. The partial compositional analysis of the produced gas during the injection period of the 1st cycle of intermittent injection is shown in Figure 5-23. It is observed that the concentration of the light hydrocarbon components and $CO_2$ is low during the early times of injection which shows that these components have been dissolved in the oil in the core. Later, the composition of these components increases which indicates that the injected VRG has reached to the outlet of the core.

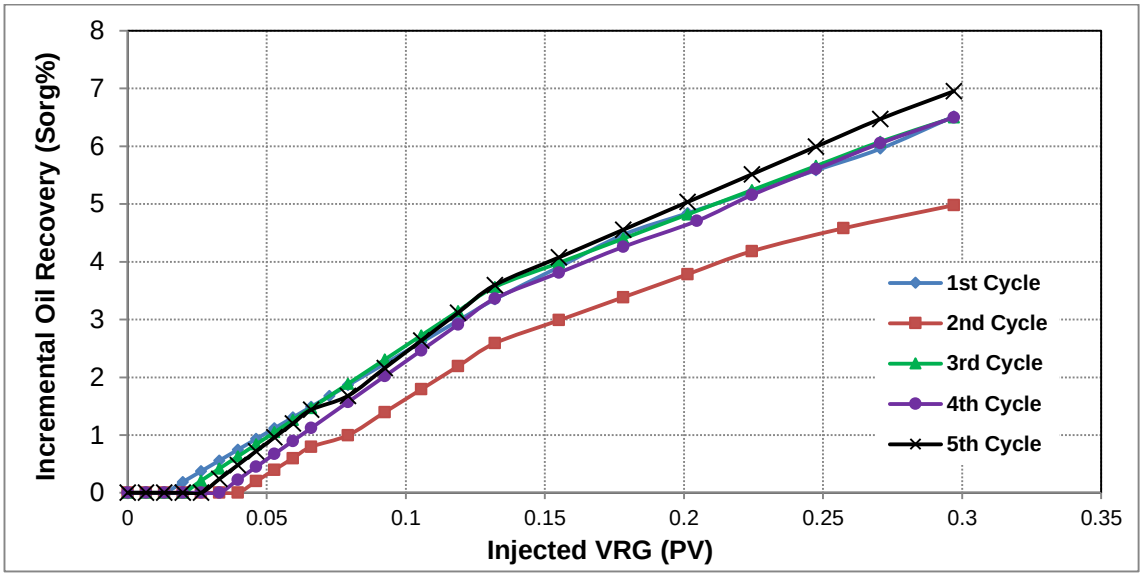


Figure 5-22: Incremental oil recovery of each cycle of intermittent VRG injection.

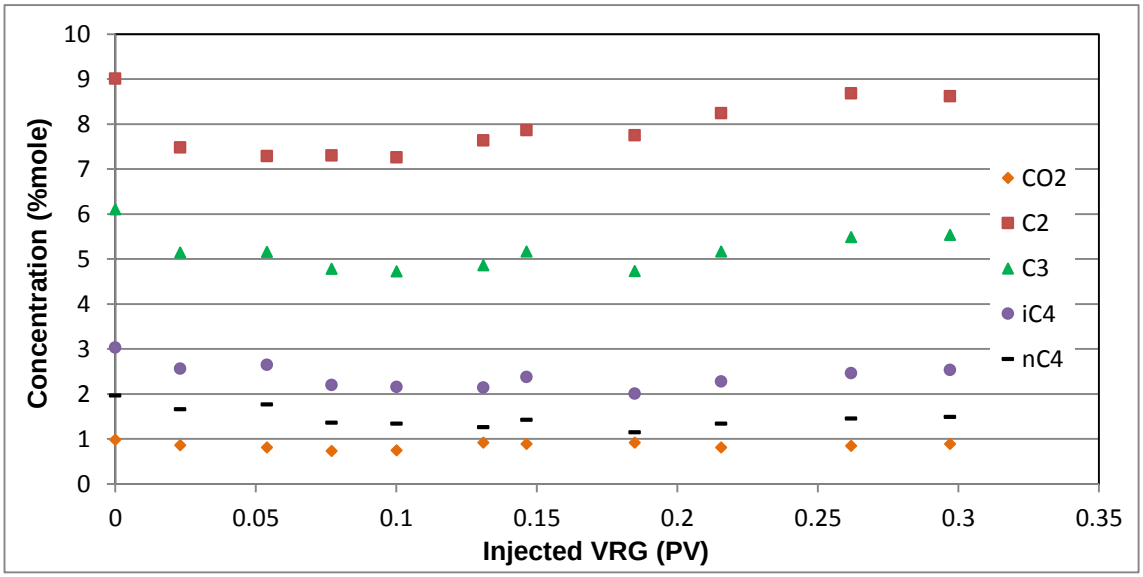


Figure 5-23: Compositional analysis of produced gas during each cycle of intermittent injection.

After the 5th cycle of intermittent injection, the gas injection was continued and around 2 PVs of VRG was injected into the core. This period of continuous injection led to additional oil recovery of around 17% of the initial oil in the core. The oil recovery

extrapolation for the 1st continuous VRG injection is illustrated in Figure 5-24 with this assumption that the oil production rate would have continued equal to the last oil rate. The results show that 5 cycles of intermittent injection have improved oil recovery by around 6% of the initial oil in place. It also implies that the shut-in periods has enhanced the impact of gravity drainage on oil recovery. The results of viscosity measurements of oil recovered during the periods of intermittent and 2nd continuous injection are clearly showing the significance of the dissolution of the compounds of VRG in the oil.

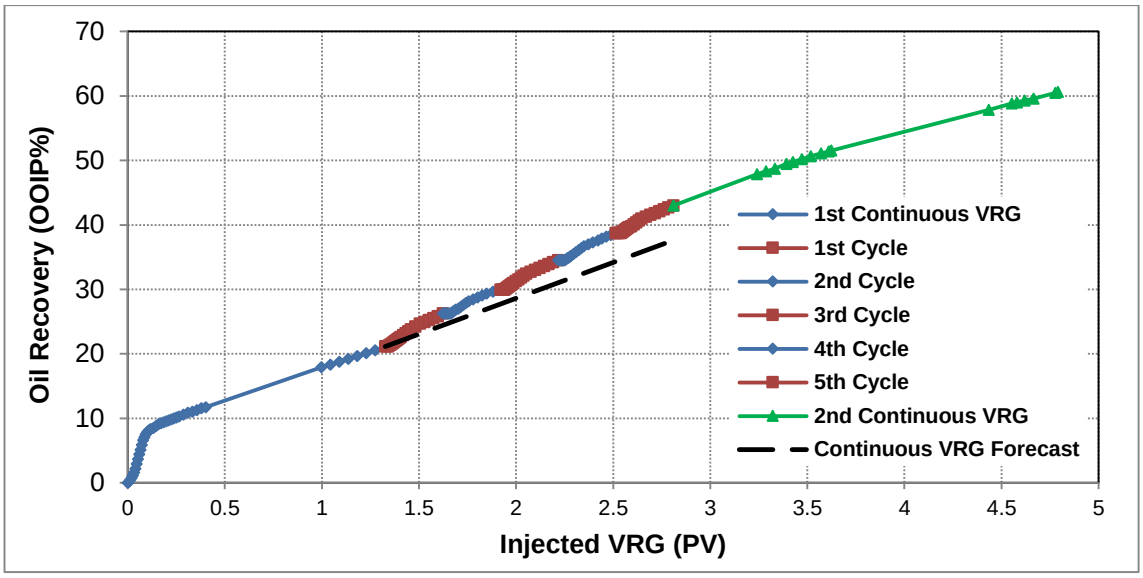


Figure 5-24: Cumulative oil recovery during the periods of continuous and intermittent VRG injection.

### 5.3.4 Effects of Composition of Injection Gas on Performance of Intermittent Injection

Figure 5-25 compares the profiles of oil recovery of intermittent supercritical $CO_2$ injection and intermittent VRG injection. The amount of remaining oil in the core is almost equal in both experiments after the period of secondary continuous injection. The viscosity of crude 'C' saturated with $CO_2$ is around 1.5 times higher than the viscosity of that crude saturated with VRG with the gas to oil ratio 6:1.

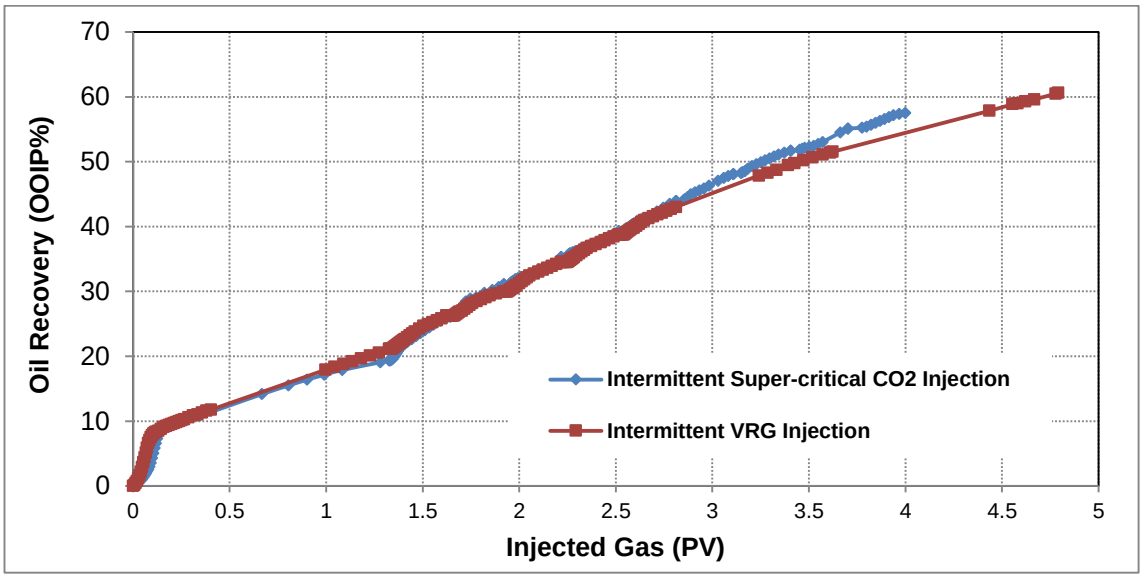


Figure 5-25: Comparison of oil recovery profiles of intermittent Supercritical $CO_2$ injection and intermittent VRG injection.

At first glance, it seems that both types of injection gas have equal ability to improve oil recovery from the core. However, significant differences in the factors contributing to oil recovery exist in these individual experiments. It was mentioned that the oil in the coreflood experiments is not completely similar to an actual reservoir oil. The presence of the crucial light components in the oil would reduce the performance of VRG injection whilst that can increase the dissolution of $CO_2$ in the oil which would lead to additional oil recovery (Luo, et al. 2012). The reason why the performance of VRG in a real live reservoir oil would be lowered is that the rate and amount of the gas that can be dissolved in the oil would decrease in the presence of light hydrocarbons and the reservoir oil would have a lower capacity to uptake those components. Another important difference is the ability of $CO_2$ to extract light and intermediate components of oil which would have led to higher oil recovery. The contribution of this mechanism to oil recovery and its impacts on the properties of recovered oil was shown in previous sections. The notably different pressure increment in the VRG injection compared to the $CO_2$ injection experiment also confirms that the significance of the mechanisms responsible for oil recovery was different.

In addition, $CO_2$ has the advantage of contacting oil in the presence of water in the rock but water-shielding would further reduce the performance of immiscible hydrocarbon gas after waterflood (Bijeljic, et al. 2002). Unlike intermittent $CO_2$ injection, the quality of oil is much improved during the shut-in periods of intermittent VRG injection. The reason for this is the higher amount of dissolution of the components of the gas in the oil.

### 5.3.5 1st (Tertiary) Waterflood

One PV of methane-saturated brine was injected through the core immediately after the period of VRG injection. The results of tertiary waterflood performed after the period of intermittent $CO_2$ injection showed that sweep efficiency is significantly improved because of the higher viscosity of water than the injection gas. With the injection of water, gas production from the core began and continued until the breakthrough of water which occurred at 0.22 PV of injection, as evidenced in Figure 5-26.

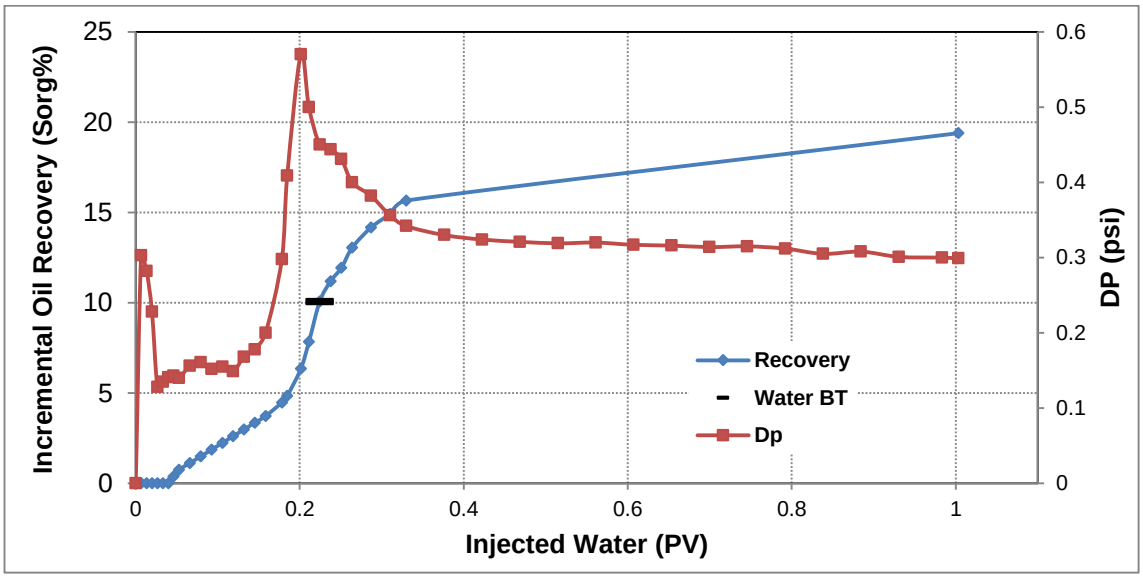


Figure 5-26: Incremental oil recovery and differential pressure during the period of tertiary waterflood.

The behaviour of this period of waterflood is similar to the performance of tertiary waterflood in the experiments that $CO_2$ was injected in an intermittent fashion. The production of free gas phase in the core was continued until the breakthrough of water and after this point, the produced gas was the dissolved gas in either oil or water. As a result of the formation of an oil bank, a significant fraction of the remaining oil was recovered before the breakthrough. Oil production continued at high water cuts until the end of waterflood.

***Summary***

Figure 5-27 shows the cumulative oil recovery during different stages of Coreflood#5. The behaviour of oil recovery by VRG injection was somehow similar to the performance of supercritical $CO_2$ injection although different mechanisms with different strength were dominant in each run. The technique of intermittent injection could improve oil recovery compared to continuous VRG injection. Moreover, the dissolution of the components of VRG in the oil improved the quality (e.g. density, viscosity) of the recovered oil. However, the performance of an enriched hydrocarbon gas (i.e. VRG) should be

evaluated under fully reservoir conditions, meaning that the oil should have the original light and intermediate components. The presence of the light and intermediate components in the oil would assist to have a higher resolution image of the performance of VRG in an actual reservoir.

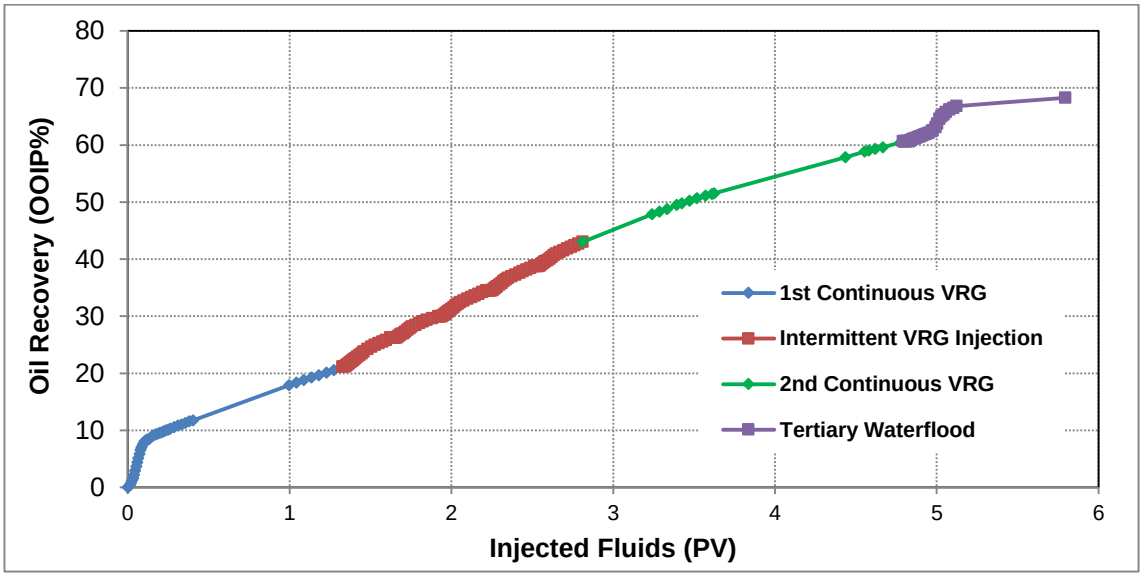


Figure 5-27: Cumulative oil recovery during different periods of Coreflood#5.

## 5.4 Conclusions

Three coreflood experiments were conducted to investigate the performance of different water and gas injection scenarios in the recovery of heavy oil. Two different gas composition were used in these experiments; pure $CO_2$, and an enriched hydrocarbon gas (VRG). Under the conditions of the experiments reported in this chapter, $CO_2$ was a relatively dense fluid and it was in a supercritical state. The underlying mechanisms of heavy oil recovery by those different gas types were discussed. The mechanisms of oil recovery by supercritical $CO_2$ were also compared with the behaviour of oil recovery of $CO_2$ as a liquid fluid. The compositional analysis and the measurement of physical properties of the effluent (e.g. oil, gas) of the coreflood experiments were performed at various stages of the tests. Based on the results of the experiments presented in this chapter, the following conclusions are drawn:

- Early breakthrough is a signature of water or gas injection for heavy oil recovery even in a relatively homogeneous porous system.
- The density of $CO_2$ and the viscosity of original oil in porous media are two crucial factors determining the performance of heavy oil recovery by $CO_2$ injection.
- Higher injectivity is an advantage of gas injection compared to waterflood for heavy oil recovery.
- Mechanism of gravity drainage can significantly enhance oil recovery during gas injection scenarios.
- A higher quality oil than the original heavy oil in porous media can be recovered by supercritical $CO_2$ and VRG injection while waterflood on its own cannot enhance the physical properties of the oil.
- As soon as dense (supercritical) $CO_2$ contacts heavy oil, extraction of hydrocarbon from the oil starts.
- The mechanism of solution gas drive has a significant impact on the performance of heavy oil recovery by $CO_2$ injection.
- The contact of $CO_2$ with live heavy oil triggers the liberation of methane from the oil without the requirement for $CO_2$ to dissolve completely in the oil.
- The rate of $CO_2$ diffusion into the oil is a significant function of oil viscosity and reservoir temperature.
- The speed of dissolution of $CO_2$ in heavy oil is higher than that of hydrocarbon gas.
- Intermittent injection of $CO_2$ or VRG enhances heavy oil recovery by allowing that

higher amount of gas to dissolve and diffuse into the oil.

- It was observed that the similar mechanisms involved during the periods of liquid $CO_2$ injection for live heavy oil recovery were also active during supercritical $CO_2$ injection for live heavy oil recovery, albeit in varying degrees.
- A relatively enriched hydrocarbon gas (i.e. VRG) can enhance heavy oil recovery by mechanisms associated with the dissolution of gas in the oil.
- Waterflood after an extended period of supercritical $CO_2$ or VRG can enhance the sweep efficiency and a considerable amount of oil is recovered.
- To truly evaluate the performance of VRG in heavy oil recovery, the oil in the experiments should be an actual reservoir oil.
- The density of $CO_2$-rich phase is a dominant factor in determining the size of extracted components.
- The extent of in-situ alteration of the quality of recovered oil is a function of injection strategy and it is affected by parameters such as gravity.
- Under similar conditions, VRG has higher potential than $CO_2$ or equal to that to reduce the viscosity of heavy oil.
- A properly designed and executed $CO_2$ or VRG injection can recover a significant amount of heavy oil at reservoir conditions.

# CHAPTER 6: MECHANISMS OF ENHANCED HEAVY OIL RECOVERY BY LOW-DENSITY (VAPOUR) $CO_2$ INJECTION

*The main objective of the experiments reported in this chapter was to evaluate the feasibility of low-density $CO_2$ injection for oil recovery, in particular, heavy oil recovery. Four coreflood experiments were performed at different schemes of fluids injection. The observations made in this chapter were compared to the results and observations of the experiments using dense $CO_2$ which led to a true understanding of the impacts of different parameters on the process of heavy oil recovery. The compositional analysis of the core effluent and the measurements of PVT properties of fluids were performed to identify underlying mechanisms of the process of oil recovery. It was also discussed that whether the results and observations of core-scale experiments reported in this study could be translated to actual reservoir conditions. Furthermore, the repeatability of the experiments reported in this study was shown in this chapter.*

## 6.1 Coreflood#6: Intermittent Vapour $CO_2$ Injection

The mechanisms involved during injection of $CO_2$ in either liquid state or supercritical state for heavy oil recovery were investigated and discussed in the previous chapters. Furthermore, the performance of oil recovery at those conditions was evaluated. It was observed that $CO_2$ is capable of enhancing recovery factor for heavy oil reservoirs. However, $CO_2$ was a dense fluid under the conditions of those experiments and it was discussed that density of $CO_2$ is a crucial factor in the performance of oil recovery. Not only the density of $CO_2$ affects the rate of dissolution and diffusion of $CO_2$ in heavy oil, it also determines the impact and strength of extraction on the process of oil recovery. However, it was discussed how the lack of mechanisms linked to the extraction of hydrocarbons affected the performance of VRG injection.

Many conventional or heavy oil reservoirs have high temperatures. Moreover, the pressure of reservoirs decreases because of natural depletion. Under the conditions of those reservoirs, $CO_2$ would have a low density. Therefore, it is crucial to investigate the performance of oil recovery by low-density $CO_2$ injection. To accomplish this task, the same core and fluids (e.g. oil, brine, $CO_2$) used in previous experiments were used in the experiments reported in this chapter to be able to compare the behaviour of oil recovery at different conditions. Thus, to achieve a condition that under which $CO_2$ could have a low density and also minimise the effects of variables on the observations, the

temperature of the experiments was maintained at 50˚ *C* (temperature of the experiments with supercritical $CO_2$) and the pressure was set at 600 *psi*. Under these conditions, $CO_2$ was a vapour gas and it had a density of around 0.0822 $g/cm^3$. A summary of the performance of all the periods of fluid injection in terms of cumulative oil recovery will be shown in Figure 6-10. Table 6-1 shows the fluids and conditions of Coreflood#6.

Table 6-1: Fluids and conditions of Coreflood#6.

| **Coreflood#6** | **Coreflood#3** | **Coreflood#2** |
|---|---|---|
| Crude Oil: Methane-saturated Crude 'C' | Crude Oil: Methane-saturated Crude 'C' | Crude Oil: Methane-saturated Crude 'C' |
| Brine: $CO_2$-saturated | Brine: $CO_2$-saturated | Brine: $CO_2$-saturated |
| Gas: Vapour $CO_2$ | Gas: Supercritical $CO_2$ | Gas: Liquid $CO_2$ |
| Temperature: 50° C | Temperature: 50° C | Temperature: 28° C |
| Pressure: 600 psi | Pressure: 1500 psi | Pressure: 1500 psi |
| Injection Rate: 7 $cm^3$/hr | Injection Rate: 7 $cm^3$/hr | Injection Rate: 7 $cm^3$/hr |
| Core Position: Vertical (top to bottom) | Core Position: Vertical (top to bottom) | Core Position: Vertical (top to bottom) |

***Procedure***

The following were the main steps to conduct Coreflood#6:

1. **Dead Brine Injection:** Core was saturated with brine and the permeability was re-measured. The permeability to brine was 2.73 *D*.
2. **Live Brine Injection:** The live brine was injected through the core to avoid gas transfer from following live oil into the brine. The injection was continued until the gas content of the produced brine reached to certain values.
3. **Live Oil Injection:** The core was flooded with live crude 'C' and an irreducible water saturation of 8% was achieved.
4. **1st Continuous (Secondary) $CO_2$ Injection:** 1.3 PVs of $CO_2$ were injected into the core.
5. **Intermittent $CO_2$ Injection: 7** cycles of shut-in and injection were performed.
6. **1st (Tertiary) Waterflood:** Around 1 PV of $CO_2$-saturated brine was injected through the core after $CO_2$ injection.
7. **Core Cleaning:** The core was cleaned by the injection of several cycles of toluene and methanol.

***Results and Discussion***

### 6.1.1 1st Continuous (Secondary) $CO_2$ Injection

Having established the initial water and oil distributions in the core, continuous $CO_2$ injection was started. The primary objective of this run was to evaluate the performance of continuous vapour $CO_2$ injection in displacing heavy oil toward the production outlet. Another objective was to compare the results of this run with the performance of oil recovery of injection of $CO_2$ as a liquid fluid and as a supercritical fluid. Figure 6-1 shows the recovery profile and differential pressure across the core during the period of continuous injection. By the start of $CO_2$ injection, it was observed that heavy oil in the core could not be produced as fast as the injection rate. However, the oil production rate increased gradually until the breakthrough. At 0.14 PV of injection, $CO_2$ had reached the production end, resulted in oil recovery of 6.5% of the original oil in place.

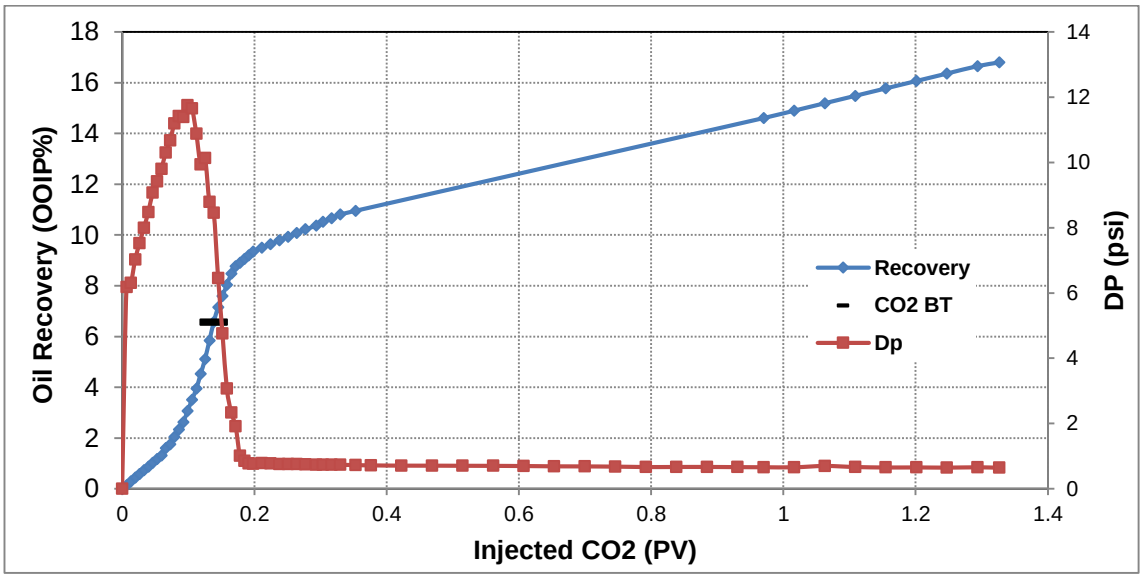


Figure 6-1: Oil recovery and differential pressure across the core during the period of continuous (secondary) $CO_2$ injection.

In an immiscible displacement, due to the significantly higher mobility of gas than heavy oil in porous media, a dramatic drop in the oil rate would be expected to happen after the breakthrough of the gas (Emadi 2012; Farzaneh 2015). However, that was not the case in this experiment and it was noted that the oil rate reduction was relatively slow. The main reason for this observation probably was the impact of the mechanism of solution gas drive as a result of $CO_2$ dissolution in oil until the breakthrough. It was mentioned in previous chapters that the speed of nucleation of dissolved gas of heavy oil has an inverse relationship with the viscosity of the oil and also the gas bubbles evolved throughout the oil phase are generally long-lived in high viscosity oils. After 0.3 PV of injection, oil was recovered at a relatively constant rate until the end of continuous injection. Figure 6-2

reveals the concentration of methane in the produced gas during various stages of the period of continuous $CO_2$ injection. As can be seen, the concentration of methane in the produced gas was relatively high after the breakthrough due to relatively high oil rates. However, the fraction of methane reduced as the oil rate decreased. Further reduction of the fraction of methane is attributed to the presence (dissolution) of $CO_2$ in the produced oil and perhaps the liberation of methane of oil in the core.

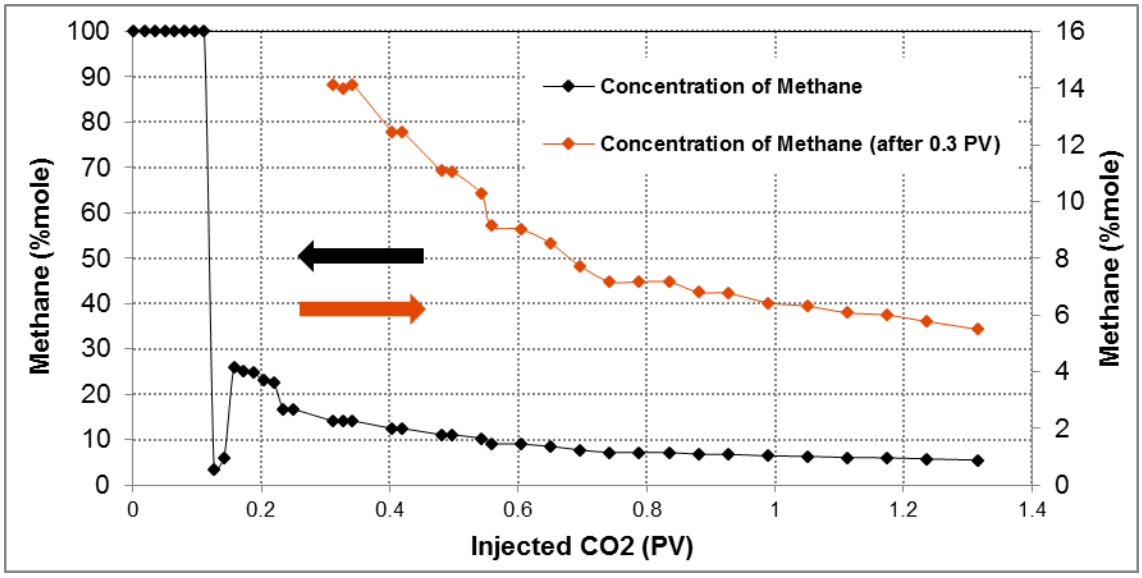


Figure 6-2: Compositional analysis of produced gas during the period of continuous (secondary) $CO_2$ injection.

The viscosity of oil recovered during the periods of $CO_2$ injection, after complete separation of gas from oil, was measured at 50˚ *C* and the results were compared with the viscosity of the original crude 'C', Table 6-2. It is shown that oil recovered after the breakthrough of $CO_2$ had a notable lower viscosity than the original oil in the core. In this experiment, the density of $CO_2$ was relatively low and hence the impacts of extraction of hydrocarbons by $CO_2$ could not be as significant as it was when $CO_2$ was either a liquid fluid or a supercritical fluid. Thus, the dissolution of $CO_2$ in the oil and the mechanisms associated with that would have been the main reason for the alteration of the viscosity of oil recovered after the breakthrough of $CO_2$. In addition, it is understood that the changes caused by $CO_2$ on the viscosity of heavy oil were not as significant as it was when $CO_2$ was a much more dense fluid (i.e. supercritical $CO_2$).

Table 6-2: Viscosity of oil recovered during different periods of Coreflood#6.

| Sample | PV of Injection | Viscosity Ratio, (%) |
|---|---|---|
| Dead Crude 'C' | -- | 100 |
| 6#1GF#1 | 0.35-0.97 | 86 |
| Mixture of (6#2GF#1, 6#4GF#1, 6#6GF#1, 6#7GF#1) | (1.3-1.6, 1.9-2.2, 2.5-3.1) | 79 |

### 6.1.2 Effect of Density of $CO_2$ on Performance of Continuous $CO_2$ Injection

After establishing the irreducible water saturation by flooding the core with live crude 'C', $CO_2$ was injected into the core, Figure 6-3. This process was repeated in three experiments at different conditions. Under the conditions of these experiments, the density of $CO_2$ was varied from a dense liquid fluid to a vapour gas. Although the breakthrough of an injection fluid during immiscible displacement of heavy oil in porous media is generally controlled by the ratio of the viscosity of both fluids, other factors such as density of the injectant can affect the breakthrough, in particular, when the injection fluid is $CO_2$. The equal amount of oil recovery at breakthrough, despite higher viscosity ratio between oil and $CO_2$ in the experiment that $CO_2$ was a vapour gas than the experiment that $CO_2$ was in the supercritical state, is a clear example of the above-mentioned statement. The mechanisms of extraction of oil components, as well as the liberation of methane of oil, were dominant when $CO_2$ was a more dense fluid. However, these mechanisms were not significant in the case that $CO_2$ was a vapour gas. The liberation of methane from the oil in porous media results in a sharp increase in the viscosity of crude oil which can lead to an early breakthrough of $CO_2$.

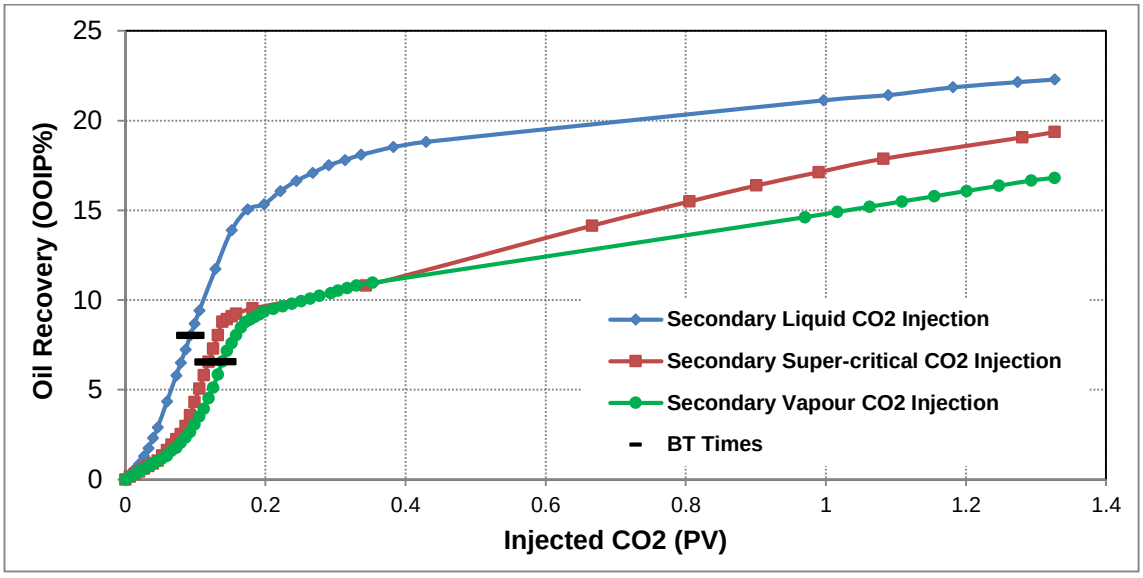


Figure 6-3: Comparison of profiles of oil recovery of continuous dense $CO_2$ injection and continuous vapour $CO_2$ injection.

The profiles of differential pressure across the core of three runs of continuous (secondary) $CO_2$ injection are compared in Figure 6-4. The extent of pressure rising before the breakthrough was mainly a function of the viscosity of the oil in place and the physical properties of $CO_2$ such as its density. In the experiment in which the density of $CO_2$ was the lowest in this study, the main recovery mechanism before the breakthrough is believed to be viscous flow as $CO_2$ displaces oil toward the outlet of the core. In

addition, $CO_2$ dissolution in the oil and the resultant reduction of oil viscosity would have contributed to oil production. It is significant that vapour $CO_2$ injection and supercritical $CO_2$ injection have shown equal performance during the early times of both runs despite the difference in viscosity of the oil in place. This is somehow related to the magnitude of the mechanism of extraction of hydrocarbons by supercritical $CO_2$ as well as the impact of the mechanism of solution gas drive in the case of higher viscosity oil (higher differential pressure before breakthrough). However, the notable difference can be seen in the performance of oil recovery of those two runs after around 0.5 PV of injection. This highlights that the rate of diffusion of $CO_2$ into heavy oil is a significant function of the pressure of the system. Pressure, on the other hand, affects the properties of $CO_2$ such as its density.

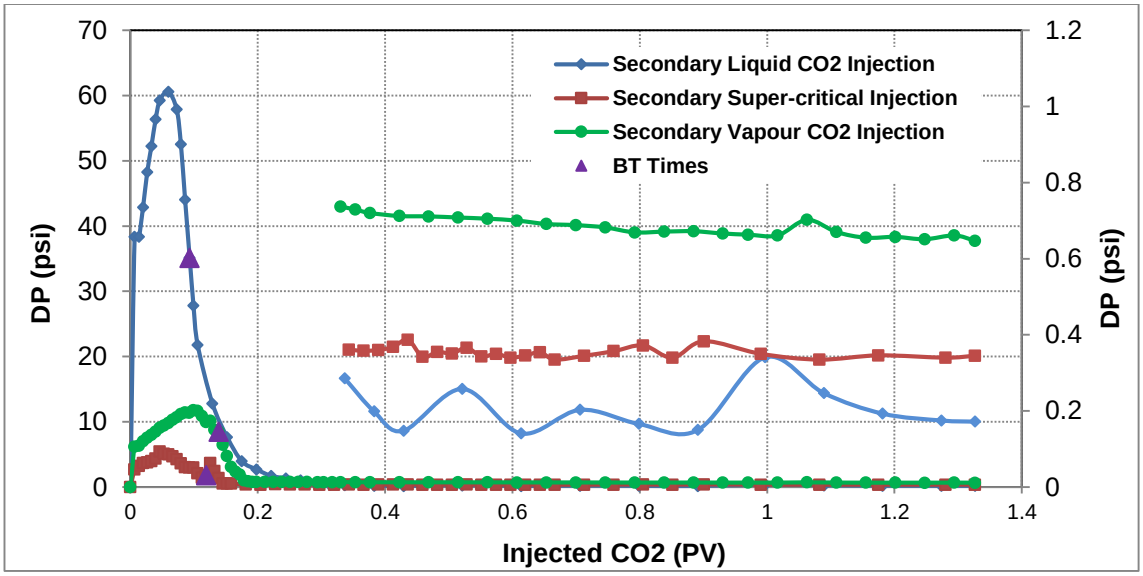


Figure 6-4: Comparison of profiles of differential pressure across the core of continuous dense $CO_2$ injection and continuous vapour $CO_2$ injection.

The DP across the core after 0.3 PV of injection was magnified in Figure 6-4. The DP was higher in the case of vapour $CO_2$ injection although the oil rate in this test was lower than or equal to the oil rate of the other two experiments. It was shown that significantly lower viscosity oil can be recovered by dense $CO_2$ due to the mechanisms associated with the extraction of oil compounds and dissolution of $CO_2$ in oil. These processes, however, were less pronounced in the case of low-density (vapour) $CO_2$ injection.

### 6.1.3 Intermittent $CO_2$ Injection

The main objective of this run was to investigate the impacts of the density of $CO_2$ on the mechanisms of heavy oil recovery. Another objective was to evaluate the effect of intermittent injection in the performance of oil recovery of low-density $CO_2$ injection. After the period of continuous injection, the core was shut-in for a period of 24 hours.

Then, 0.3 PV of $CO_2$ was injected into the core to improve recovery factor. This process of halt/injection was repeated for 7 cycles. The pressure of core was monitored during the shut-in periods and it was observed that the core pressure decreased during each of the shut-in periods, Figure 6-5. This observation is in contrast with the observations made during the halt periods of the experiments where $CO_2$ was a more dense fluid and also to some extent with the case of VRG injection. The reduction of pressure during the shut-in periods is an indication of dissolution of $CO_2$ in the oil and as the oil in contact with $CO_2$ became relatively saturated with that, the rate of pressure reduction decreased notably in successive cycles.

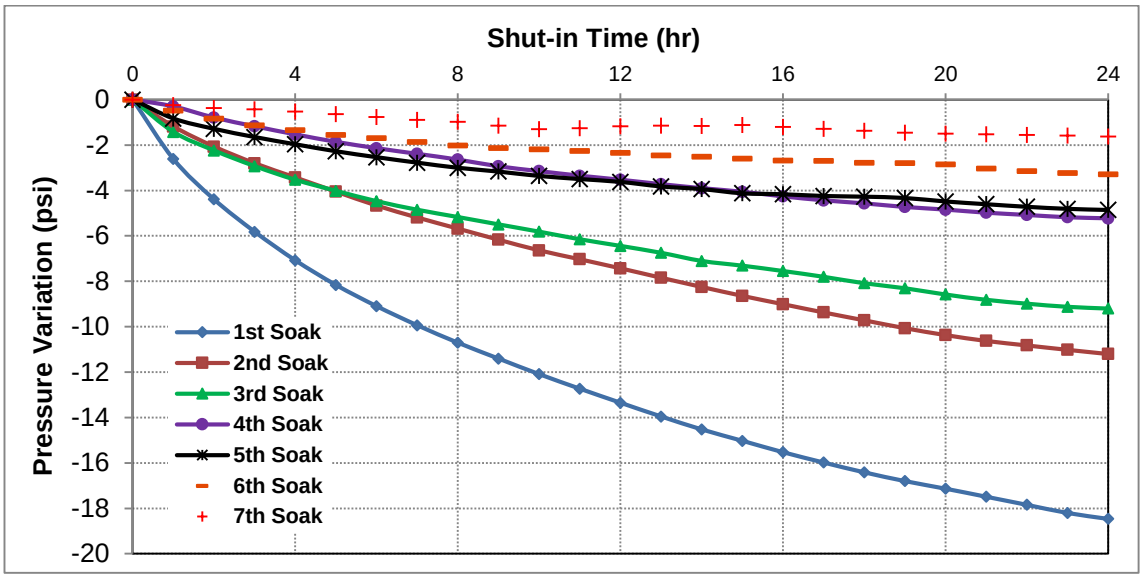


Figure 6-5: Pressure variation of the core during the shut-in periods.

The profiles of incremental oil recovery of each slug of $CO_2$ injection of intermittent injection are shown in Figure 6-6. Before the beginning of injection, the core pressure was increased up until the flowing pressure of the system. No oil production happened at early times of injection periods. Although $CO_2$ dissolution in oil was dominant during halt periods, the viscosity difference between $CO_2$ and oil in contact would have been significant. The main mechanisms of oil recovery were oil viscosity reduction as a result of the dissolution of $CO_2$ in the oil, gravity drainage, and, of course, viscous forces.

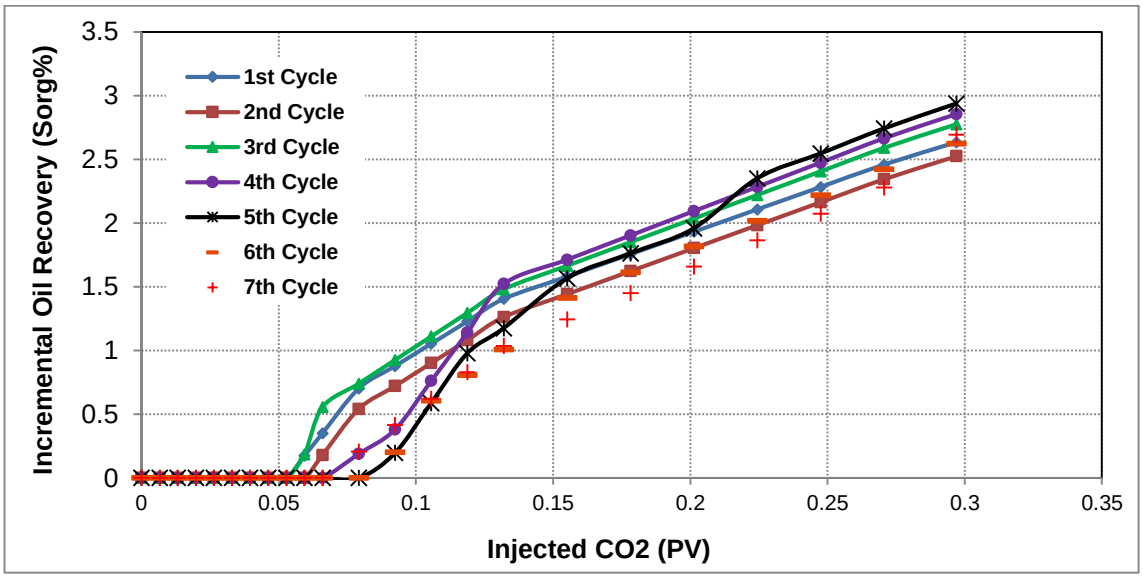


Figure 6-6: Incremental oil recovery of each cycle of intermittent $CO_2$ injection.

Despite the relatively low amount of oil recovery in each cycle of intermittent injection, Figure 6-7 clearly shows that the changing of injection scheme has improved oil recovery. This significant additional oil recovery was achieved mainly due to increasing the residence time of $CO_2$ in a porous medium which facilitated the dissolution of $CO_2$ in oil. The viscosity of a mixture of oil produced during some cycles of the period of intermittent injection was measured and compared to the viscosity of the original oil. Lower viscosity oil was recovered by intermittent $CO_2$ injection. Additionally, unlike the experiments that $CO_2$ was a dense fluid, the viscosity of oil recovered by intermittent injection of low-density oil was even lower than the viscosity of oil recovered during the period of continuous (secondary) $CO_2$ injection. These observations imply that dissolution of $CO_2$ in oil in porous media alters the physical properties of oil and probably the composition of the oil is also altered by $CO_2$ injection.

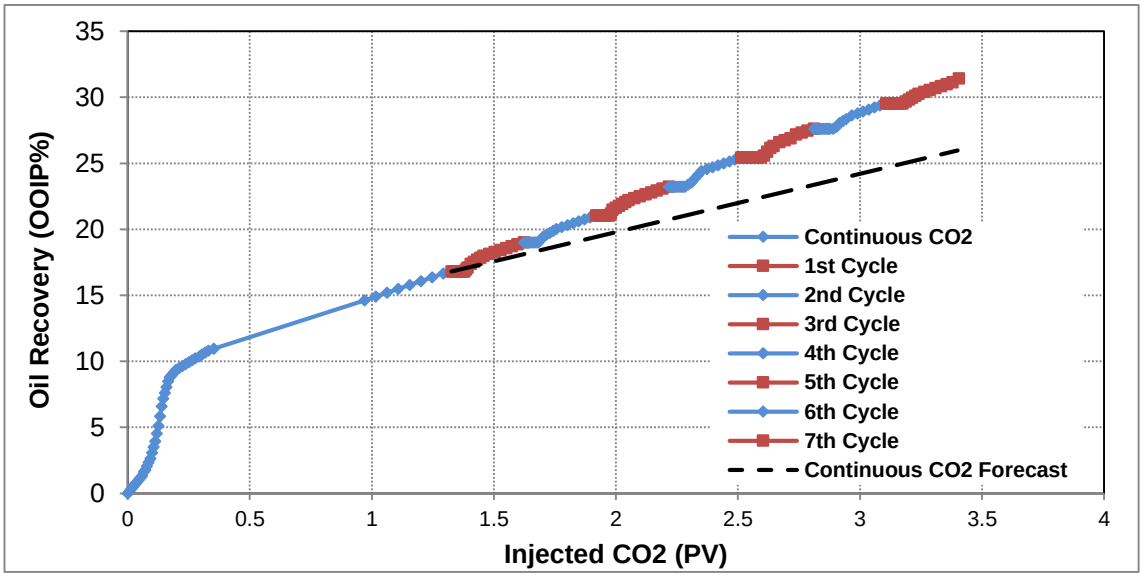

Figure 6-7: Cumulative oil recovery during the periods of continuous and intermittent $CO_2$ injection.

### 6.1.4 Effect of Density of $CO_2$ on Performance of Intermittent $CO_2$ Injection

Figure 6-8 compares the performance of oil recovery of intermittent injection of dense and low-density $CO_2$. It is observed that the mechanism of $CO_2$ dissolution in oil and the resultant reduction of oil viscosity is the main mechanism of oil recovery by $CO_2$ injection. $CO_2$ can also alter the physical properties of the produced oil. However, this impact is much significant when the density of $CO_2$ is relatively high due to the mechanisms associated with the extraction of hydrocarbons. Overall, the results indicate that the mass transfer between oil and $CO_2$ dominates the recovery of heavy oil by $CO_2$ injection which is a time dependent process. The rate of dissolution and diffusion of $CO_2$ in heavy oil is a significant function of the viscosity of oil, pressure, and temperature (density of $CO_2$). Moreover, the presence of dissolved gas in heavy oil considerably affects the process of oil recovery. It is, therefore, important to evaluate the performance of any process of EHOR of by gas injection under the actual conditions of the reservoirs.

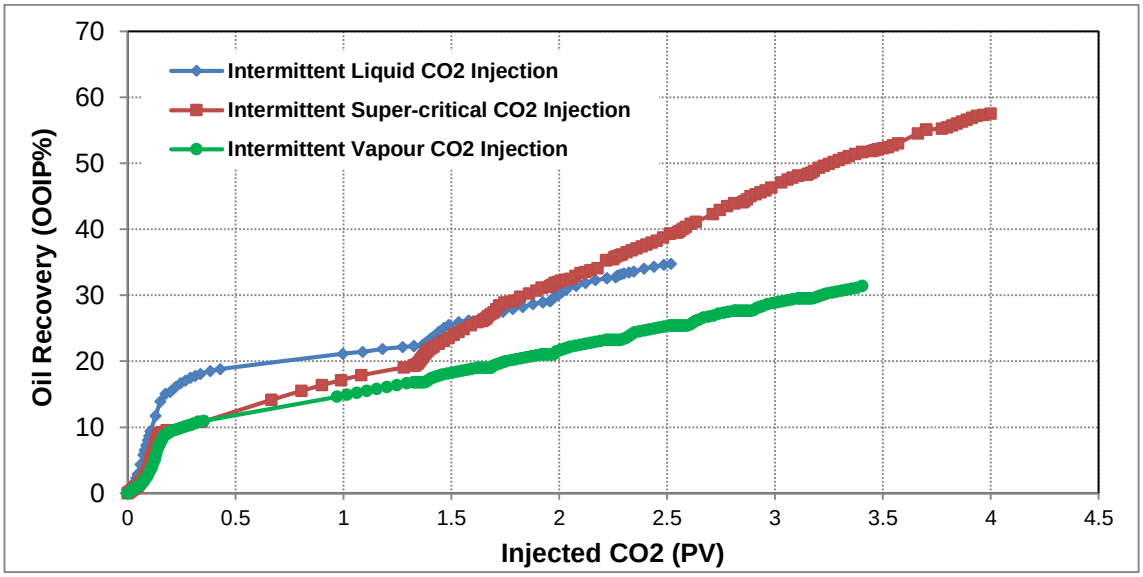


Figure 6-8: Comparison of oil recovery profiles of intermittent dense $CO_2$ injection and intermittent vapour $CO_2$ injection.

### 6.1.5 1st (Tertiary) Waterflood

One PV of $CO_2$-saturated brine was injected through the core after the 7th cycle of intermittent $CO_2$ injection. Similar to the previous waterfloods after intermittent injection of $CO_2$, water followed the least resistance path of gas in the core. Water advancement in the core resulted in the displacement and accumulation of oil ahead of the water front and an oil bank was formed. The oil bank then reached the outlet of the core and led to a considerable amount of oil recovery, Figure 6-9. At a certain point, water reached to the production outlet but the oil recovery continued at high water cuts after the breakthrough.

Moreover, gas production decreased sharply when the oil bank reached to the production outlet.

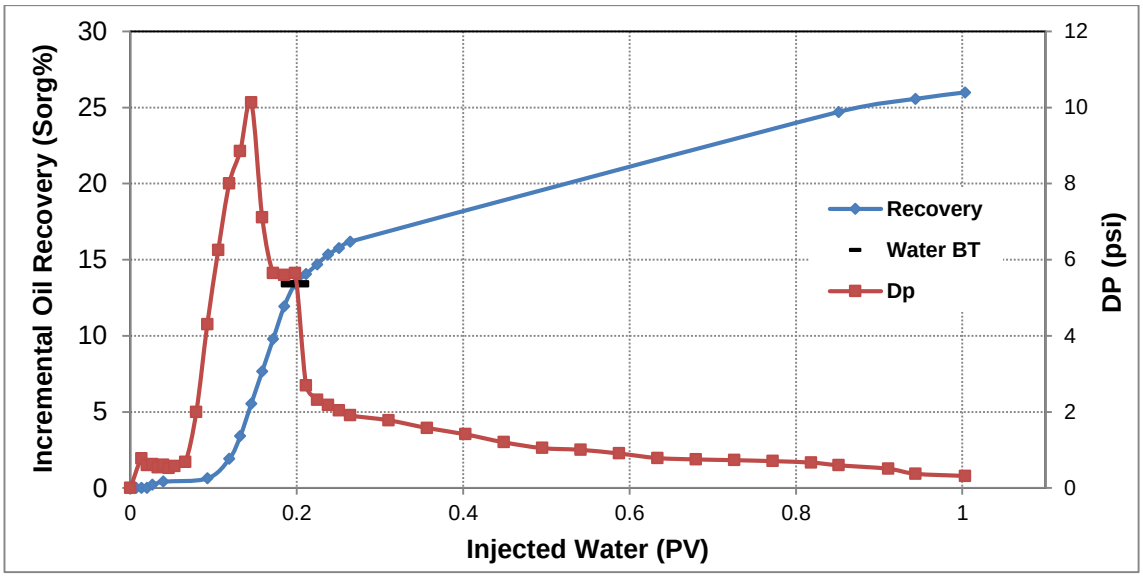


Figure 6-9: Incremental oil recovery and differential pressure across the core during the period of tertiary waterflood.

***Summary***

Figure 6-11 illustrates the cumulative oil recovery during different stages of Coreflood#6. The $CO_2$ dissolution in the oil and the resultant effects of that on the physical properties of oil enhanced the efficiency of oil recovery. The increasing of the residence time of $CO_2$ in porous media facilitated the contact between $CO_2$ and oil while the utilisation of gas was significantly reduced. In addition, a lower viscosity oil could be recovered as a result of the injection of $CO_2$. It was observed that improving the viscosity of displacing fluid led to the recovery of a significant fraction of oil that has been in contact with $CO_2$.

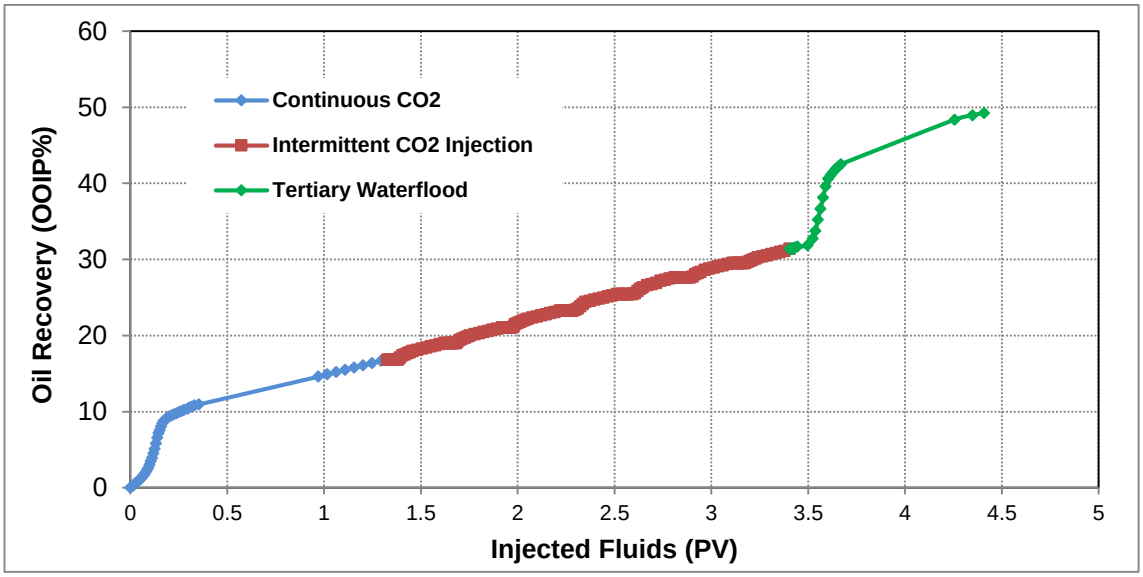


Figure 6-10: Cumulative oil recovery during different periods of Coreflood#6.

Figure 6-11 compares the cumulative oil recovery during three different intermittent $CO_2$

injection experiments. The main contrast between those experiments is that the viscosity of the original oil in place and the density of $CO_2$ were different. The results indicate that the rate of oil production is a significant function of the pressure of the system.

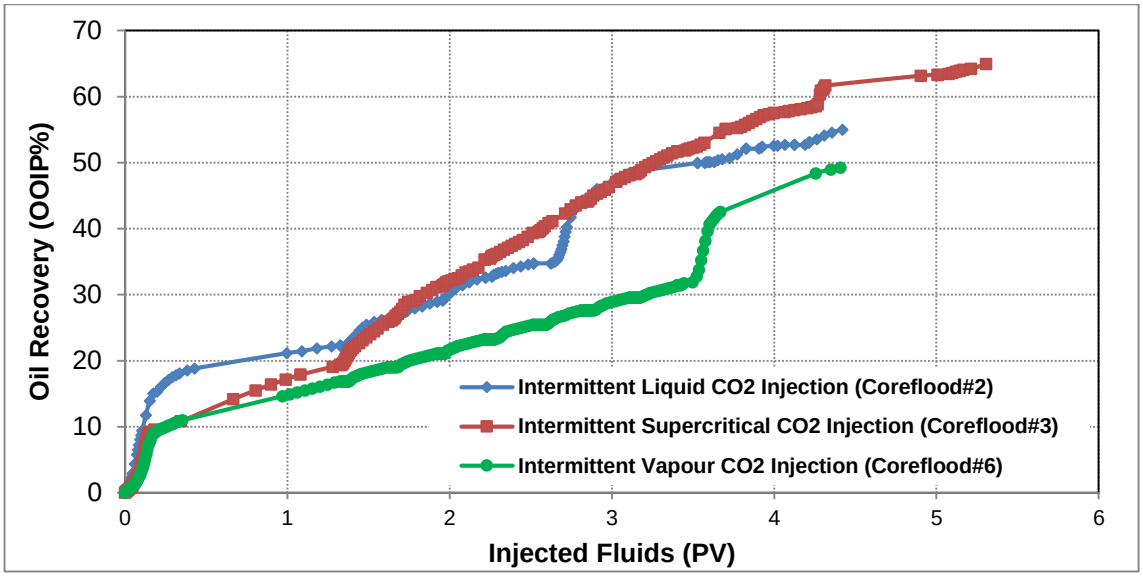


Figure 6-11: Cumulative oil recovery during different coreflood experiments of intermittent $CO_2$ injection.

## 6.2 Coreflood#7: Tertiary Vapour $CO_2$ Injection

A tertiary $CO_2$ injection following a secondary waterflood experiment was performed to evaluate the performance of tertiary low-density (vapour) $CO_2$ injection in heavy oil recovery. The main objective of this experiment was to investigate the impact of density of $CO_2$ on the performance of tertiary $CO_2$ injection. Tertiary injection of $CO_2$ was followed by a period of waterflood in order to evaluate the effect of $CO_2$ dissolution in the oil on improving recovery factor. The composition of produced oil at different stages of the test was also analysed to investigate the effects of low-density $CO_2$ on the physical properties of the heavy oil. A summary of the performance of all the periods of fluid injection in terms of cumulative oil recovery will be shown in Figure 6-17. Table 6-3 presents the conditions and fluids of Coreflood#7.

Table 6-3: Fluids and conditions of Coreflood#7.

| **Coreflood#7** | **Coreflood#4** | **Coreflood#1** |
|---|---|---|
| Crude Oil: Methane-saturated Crude 'C' | Crude Oil: Methane-saturated Crude 'C' | Crude Oil: Methane-saturated Crude 'C' |
| Brine: Methane-saturated or $CO_2$-saturated | Brine: Methane-saturated or $CO_2$-saturated | Brine: Methane-saturated or $CO_2$-saturated |
| Gas: Vapour $CO_2$ | Gas: Supercritical $CO_2$ | Gas: Liquid $CO_2$ |
| Temperature: 50° C | Temperature: 50° C | Temperature: 28° C |
| Pressure: 600 psi | Pressure: 1500 psi | Pressure: 1500 psi |
| Injection Rate: 7 $cm^3$/hr | Injection Rate: 7 $cm^3$/hr | Injection Rate: 7 $cm^3$/hr |
| Core Position: Vertical (top to bottom) | Core Position: Vertical (top to bottom) | Core Position: Vertical (top to bottom) |

***Procedure***

The following were the main steps to conduct Coreflood#7:

1. **Dead Brine Injection:** Core was saturated with brine and the permeability was re-measured. No change was observed in the permeability of the core.
2. **Live Brine Injection:** The live brine was injected through the core to avoid gas transfer from following live oil into the brine. The injection was continued until the gas content of the produced brine reached to certain values.
3. **Live Oil Injection:** The core was flooded with live crude 'C' and an irreducible water saturation of 8% was achieved.
4. **1st (Secondary) Waterflood:** Around 1 PV of methane-saturated brine was injected through the core.
5. **1st (Tertiary) $CO_2$ Injection:** 6 PVs of $CO_2$ was injected into the core.

6. **2nd Waterflood:** 1 PV of $CO_2$-saturated brine was injected through the core after $CO_2$ injection.
7. **Core Cleaning:** Several cycles of toluene and methanol were injected into the core.

***Results and Discussion***

### 6.2.1 1st (Secondary) Waterflood

Following the above-mentioned procedure, methane-saturated brine was injected through the core. Figure 6-12 shows the profile of oil recovery and differential pressure within the core during the period of secondary waterflood. The recovery profile is similar to waterflooding of heavy oil systems. An early breakthrough and production of a considerable fraction of oil at high water cuts are the main characteristics of those systems. Thus, a significant volume of the core remained unswept and continuing waterflood could not target the remaining oil.

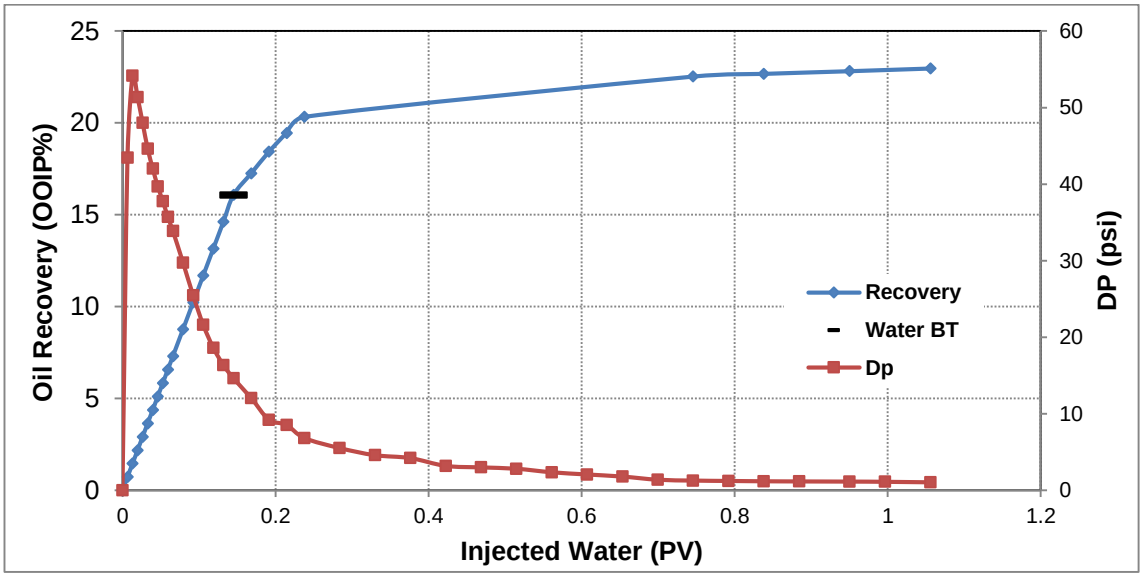


Figure 6-12: Oil recovery and differential pressure across the core during the period of 1st (secondary) waterflood.

### 6.2.2 1st (Tertiary) $CO_2$ Injection

After the period of secondary waterflood, $CO_2$ was injected through the core to evaluate the performance of tertiary injection of low-density $CO_2$. Unlike the experiments performed with dense $CO_2$, water could not be displaced as fast as the injection rate probably due to the dissolution of low-density (vapour) $CO_2$ in the fluids (either water or oil) in the core. However, a significant fraction of water in the core was displaced during the period of $CO_2$ injection, mainly up to the breakthrough. The dissolution of $CO_2$ in the oil, either by direct contact or by diffusing from the water around oil, has resulted in oil viscosity reduction as well as the swelling of oil. Consequently, oil was recovered at a

relatively constant rate until the end of the period of $CO_2$ injection. Despite the production of oil at a constant rate, the DP is decreasing continuously (Figure 6-13) which means that the viscosity of fluids contributing to flow (mainly oil) is continuously decreasing. Other mechanisms such as gravity drainage would have also contributed to oil recovery.

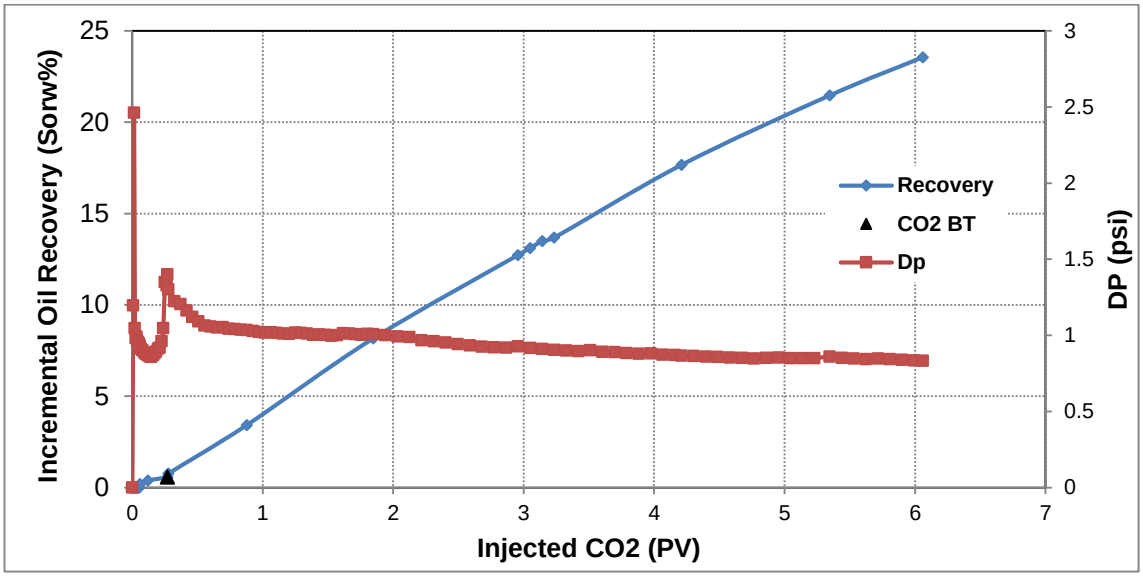


Figure 6-13: Incremental oil recovery and differential pressure across the core during the period of tertiary $CO_2$ injection.

The composition of oil recovered during different stages of Coreflodd#7 was analysed and reported in Table 6-4. Additionally, the viscosity of oil recovered by tertiary $CO_2$ injection was measured at the temperature of the experiment. The results were compared with the viscosity of original crude 'C' in Table 6-5. It is shown that the physical properties of oil have been altered by injection of $CO_2$ into the core, albeit to a small extent. These observations are mainly attributed to the mechanisms which were also active during the injection of dense $CO_2$ for heavy oil recovery. The lower density of $CO_2$ in the vapour state is believed to be the main reason for the small extent of the in-situ changes of the properties of the heavy oil. Another reason could be due to the impact of gravity drainage which was more significant on oil recovery in this experiment.

Table 6-4: Composition of oil recovered during different periods of Coreflood#7.

| Sample | PV of Injection | ≤C12 (%mole) | >C12-≤C16 (%mole) | >C16-≤C20 (%mole) | >C20-≤C23 (%mole) | >C23-≤C29 (%mole) | >C29-≤C45 (%mole) | >C45-≤C100 (%mole) |
|---|---|---|---|---|---|---|---|---|
| 7#1WF#1 | 0.0-0.07 | 12.8 | 22.9 | 28.9 | 12.2 | 12.7 | 8.5 | 2.0 |
| 7#1GF#2 | 3.0-4.2 | 15.9 | 21.8 | 28.6 | 11.7 | 11.9 | 8.0 | 2.0 |
| 7#2WF#1 | 0.24-0.28 | 9.4 | 24.1 | 26.0 | 12.0 | 13.5 | 11.5 | 3.4 |

Table 6-5: Viscosity of oil recovered during the period of tertiary $CO_2$ injection.

| Sample | PV of Injection | Viscosity Ratio, (%) |
|---|---|---|
| Dead Crude 'C' | -- | 100 |
| 7#1GF#1 | 1.8-3.0 | 81 |
| 7#1GF#2 | 3.0-4.2 | 83 |

### 6.2.3 Effect of Density of $CO_2$ on Performance of Tertiary $CO_2$ Injection

Figure 6-14 compares the profiles of incremental oil recovery of tertiary dense $CO_2$ injection with tertiary low-density $CO_2$ injection. The saturation of oil after the period of secondary waterflood was almost equal in all the experiments. However, the breakthrough of vapour $CO_2$ occurred later than dense $CO_2$ mainly due to the higher compressibility $CO_2$ under the conditions of that experiment.

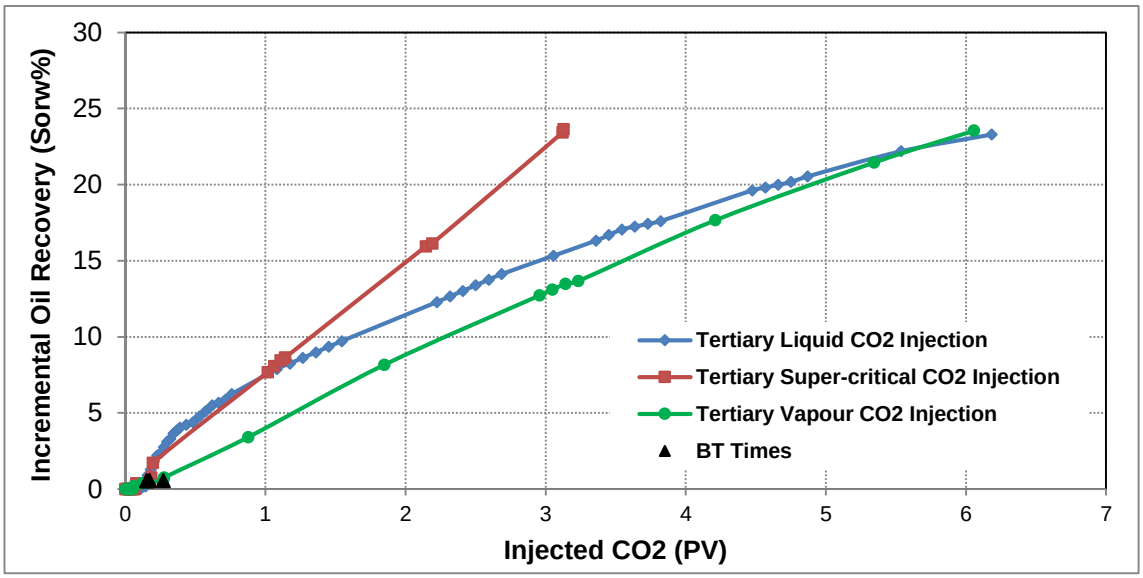


Figure 6-14: Comparison of profiles of incremental oil recovery of tertiary dense $CO_2$ injection and tertiary vapour $CO_2$ injection.

Initially, oil was recovered with relatively high rates in the experiments that $CO_2$ was a dense fluid, highlighting the importance of the mechanisms of $CO_2$ dissolution in oil and extraction of oil components in the process of oil recovery. This is also noticed from the comparison of the DP within the core during the periods of tertiary $CO_2$ injection, Figure 6-15. For instance, the DP in the experiment of vapour $CO_2$ injection was notably higher than the other runs, stemming from the higher viscosity of flowing fluids (mainly oil) in a porous medium. That is, the oil rate was also lower in the experiment at the condition of vapour $CO_2$.

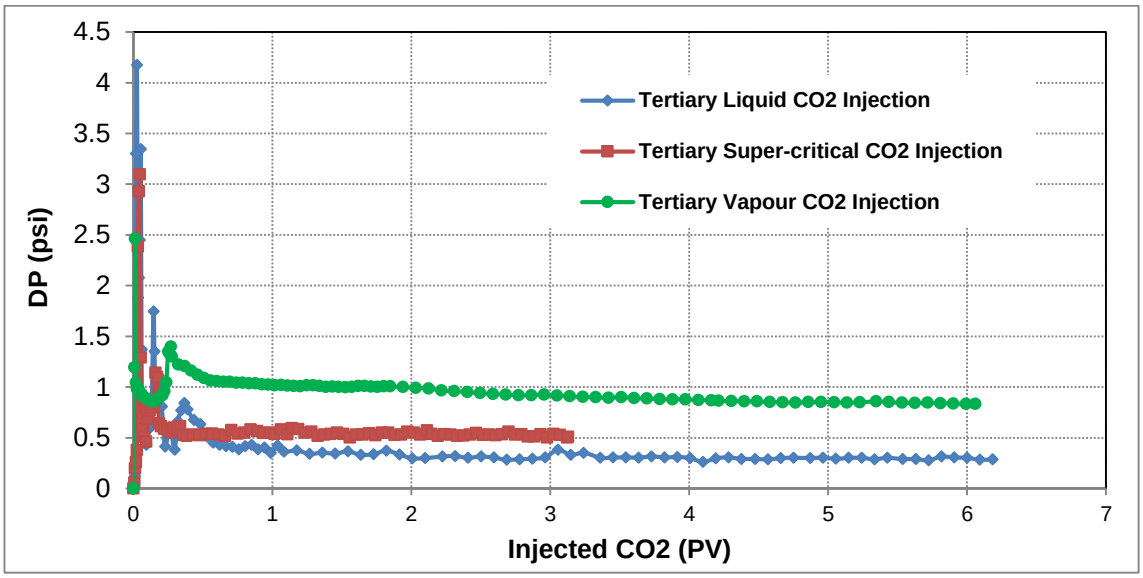


Figure 6-15: Comparison of profiles of differential pressure across the core during tertiary dense $CO_2$ injection and tertiary vapour $CO_2$ injection.

### 6.2.4 2nd Waterflood

Around 1 PV of $CO_2$-saturated brine was injected through the core after the period of tertiary $CO_2$ injection. The injected water followed the least resistance paths of gas in the core and then reached to the production outlet. A small fraction of oil was recovered before the breakthrough, Figure 6-16. However, the oil rate increased sharply after the breakthrough and oil production continued until the end of waterflood. The compositional analysis of the oil displaced by water confirms that the injected water contacted the oil which was in contact with $CO_2$.

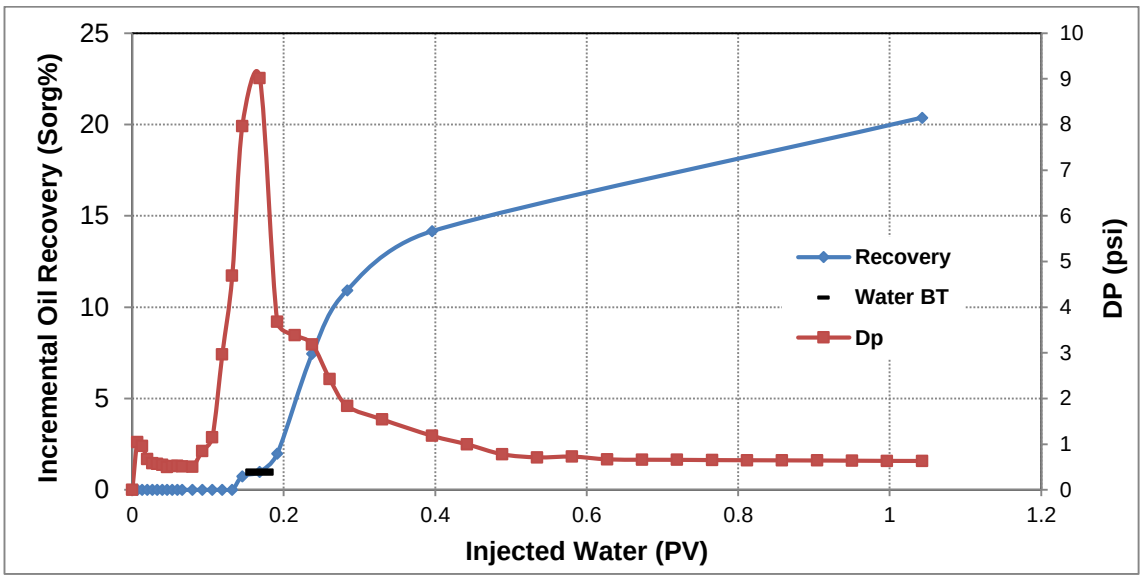


Figure 6-16: Incremental oil recovery and differential pressure across the core during the period of 2nd waterflood.

The results of coreflood experiments in this study show that the behaviour of waterflood after an extended period of $CO_2$ injection probably depends on to the scheme of recovery

prior to that waterflood. For example, a distinct difference is the production of a considerable fraction of oil before the breakthrough by waterflood after the period of intermittent injection while an insignificant amount of oil is recovered before the breakthrough during waterflood after tertiary injection of $CO_2$. One reason for this observation may be due to the higher saturation of water in the main flowing paths in the core as a result of secondary waterflood. In our experiments, the mobility of water is significantly higher than the mobility of oil and the presence of water, although immobile, could speed up the flow of injected water and cause to an early breakthrough. Another reason of the above-mentioned observation would be related to the injection scenario of $CO_2$ before the waterflood. $CO_2$ during the shut-in periods could invade a higher area of the core and therefore the potential pore volume for water to invade would have been higher after intermittent injection of $CO_2$.

***Summary***

Figure 6-17 shows the cumulative oil recovery during different periods of Coreflood#7. The performance of waterflood for heavy oil recovery is a function of viscosity ratio of oil and water in porous media. Thus, the sweep efficiency of waterflood is generally poor for viscous oil recovery. The injection of low-density $CO_2$ after waterflood can still enhance heavy oil recovery mainly by mechanisms associated with the dissolution of $CO_2$ in the oil. It was known that the dissolution and diffusion of $CO_2$ is a slow process, particularly, in low-pressure systems. Therefore, time is an important factor determining the efficiency of enhanced heavy oil recovery by $CO_2$ injection. The physical properties of oil can be altered by $CO_2$ even at low pressures. This alteration is more dominant in viscosity of produced oil. The injection of a fluid with lower mobility than $CO_2$ can improve the sweep efficiency significantly. This is further facilitated by the lower viscosity of the oil in porous media because of the dissolution of $CO_2$ in the oil.

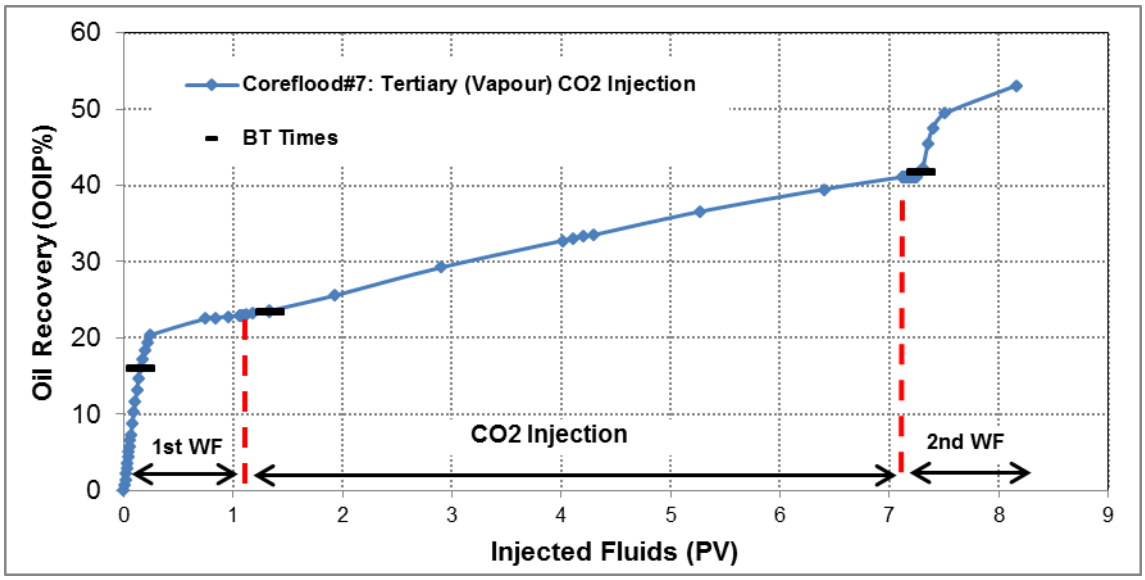


Figure 6-17: Cumulative oil recovery during different periods of Coreflood#7.

## 6.3 Coreflood#8: Secondary Vapour $CO_2$ Injection

An important purpose of a coreflood experiment is to understand or predict the behaviour of fluids and rocks during a variety of field processes such as production or injection schemes, of course, on a small scale. Although a test with a core cannot completely mimic the complexity of processes in an actual reservoir, the information obtained from that can be used to predict the behaviour of a reservoir. Among those advantages, however, one critical disadvantage of a coreflood experiment is that the trace of reservoir time cannot be seen in a coreflood run and, thus, in processes in which time-dependent phenomena take place (e.g. diffusion), that could lead to incorrect translation of the coreflood results. The practice of $CO_2$ injection for enhancing heavy oil recovery is one of the processes in which time plays a crucial role in the performance of oil recovery. It was shown that the altering the continuous injection of $CO_2$ to the intermittent fashion improved heavy oil recovery. In the intermittent injection, $CO_2$ is allowed to diffuse into the oil in the core and hence the recovery factor is improved.

A secondary injection of $CO_2$ followed by a period of waterflood was performed to evaluate the potential of low-density $CO_2$ injection for heavy oil recovery. Here, using the state-of-the-art coreflood rig, the injection rate of $CO_2$ was set at 1 $cm^3/hr$ to evaluate the effects of time and rate of injection on the process of oil recovery. The composition of oil recovered during different stages of the experiment was analysed in order to investigate the impact of low-density $CO_2$ on the physical properties of the heavy oil. A summary of the performance of all the periods of fluid injection in terms of cumulative oil recovery will be shown in Figure 6-23. The conditions at which the coreflood experiments was performed and also the fluids used in this experiment are given in Table 6-6.

Table 6-6: Fluids and conditions of Coreflood#8.

| **Coreflood#8** | **Coreflood#6** |
|---|---|
| Crude Oil: Methane-saturated Crude 'C' | Crude Oil: Methane-saturated Crude 'C' |
| Brine: $CO_2$-saturated | Brine: $CO_2$-saturated |
| Gas: Vapour $CO_2$ | Gas: Vapour $CO_2$ |
| Temperature: 50° C | Temperature: 50° C |
| Pressure: 600 psi | Pressure: 600 psi |
| Injection Rate: 1 or 7 $cm^3$/hr | Injection Rate: 7 $cm^3$/hr |
| Core Position: Vertical (top to bottom) | Core Position: Vertical (top to bottom) |

***Procedure***

The following were the main steps to conduct Coreflood#8:

1. **Dead Brine Injection:** Core was saturated with brine and the permeability was re-measured. No change was observed in the permeability of the core.
2. **Live Brine Injection:** The live brine was injected through the core to avoid gas transfer from following live oil into the brine. The injection was continued until the gas content of the produced brine reached to certain values.
3. **Live Oil Injection:** The core was flooded with live crude 'C' and an irreducible water saturation of 8% was achieved.
4. **1st Continuous (Secondary) $CO_2$ Injection:** 4.3 PVs of $CO_2$ were injected into the core. The rate of injection of $CO_2$ was 1 $cm^3/hr$.
5. **1st (Tertiary) Waterflood:** 1 PV of $CO_2$-saturated brine was injected through the core after the period of $CO_2$ injection.
6. **Core Cleaning:** Several cycles of toluene and methanol were injected into the core.

***Results and Discussion***

### 6.3.1 1st Continuous (Secondary) $CO_2$ Injection

Following the above-mentioned procedure, continuous injection of $CO_2$ through the core was started. The primary objective of this run was to compare its results with the performance of the intermittent $CO_2$ injection at similar conditions. Figure 6-18 shows the profiles of oil recovery and DP across the core during the period of secondary injection of $CO_2$. It was observed that the oil in the core could not be produced as fast as the injection rate. The relatively low rate of injection of $CO_2$ would have assisted the low oil rate before the breakthrough by reducing the impact of viscous forces. Nonetheless, for a short period of time before the breakthrough, oil was produced at high rates. The early breakthrough of $CO_2$ demonstrates that the rate of injection does not have a significant impact on the sweep efficiency and the instability in the flood front dominates the flow in the systems of adverse viscosity ratio.

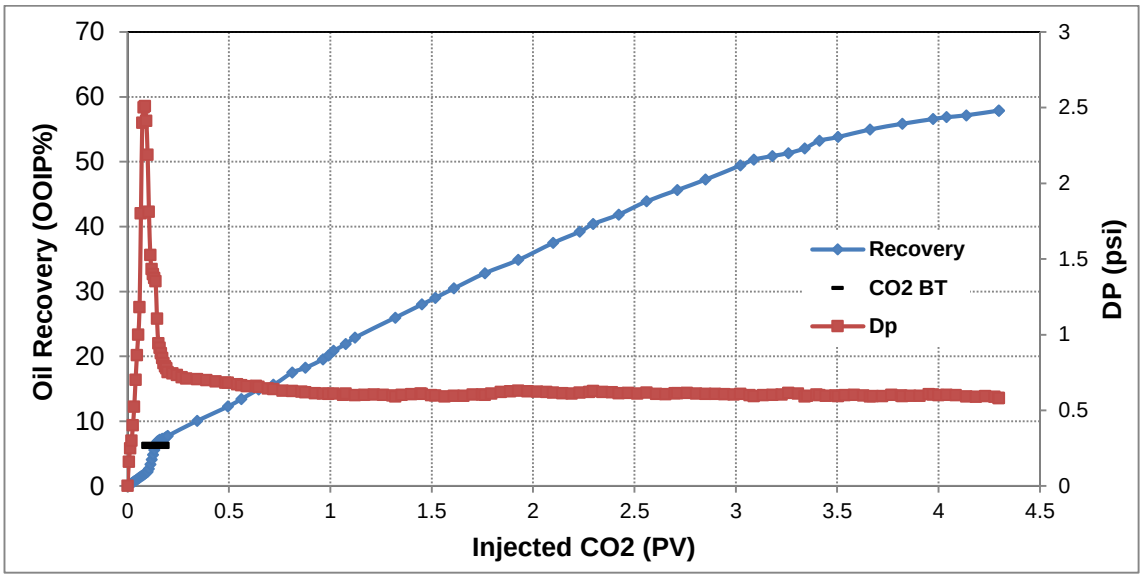


Figure 6-18: Oil recovery and differential pressure across the core during the period of secondary (continuous) $CO_2$ injection.

After the breakthrough, oil production continued at relatively constant and low rate until around 3 PVs of injection. The main mechanism of oil recovery was the dissolution of $CO_2$ in the oil and the resultant oil viscosity reduction. After 3 PVs of injection, the oil rate was further decreased which was noticed by the rising GOR until the end of the injection of $CO_2$, Figure 6-19. The reduction of oil rate during late times of the run was perhaps due to the lower saturation of oil in the core as well as the reduction of the rate of diffusion of $CO_2$ in the oil. It should be mentioned that the impact of gravity drainage would have been significant on oil recovery, mainly because of the significant time of the contact of oil and $CO_2$ in the core.

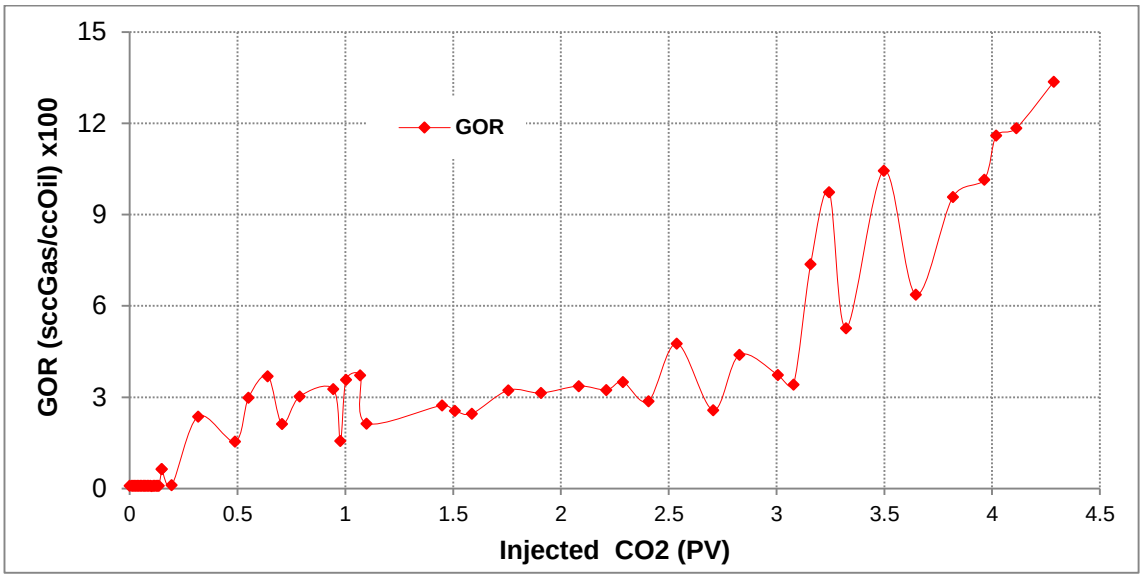


Figure 6-19: GOR during the period of secondary (continuous) $CO_2$ injection, the variations are thought to be genuine as the error of measurements is small.

The compositional analysis of oil recovered during different stages of Coreflood#8 is

reported in Table 6-7. After the breakthrough, the composition of oil recovered by $CO_2$ injection was remained relatively unchanged at different times of this run. This implies that the impacts of $CO_2$ dissolution and gravity drainage were significant during the period of $CO_2$ injection. However, this is not necessarily meaning that $CO_2$ could not alter the physical properties of the initial oil in the core. The composition of oil recovered by waterflood changed slightly, reflecting that the remaining oil in the core was relatively heavier than the oil recovered during the previous period of $CO_2$ injection. In addition, the viscosity of oil recovered during the period of $CO_2$ injection was measured and the results, given in Table 6-8, confirmed that a higher quality oil has been recovered by $CO_2$ injection. All the viscosity measurements were performed at the temperature that the coreflood experiment was conducted.

Table 6-7: Composition of oil recovered during different periods of Coreflood#8.

| Sample | PV of Injection | ≤C12 (%mole) | >C12-≤C16 (%mole) | >C16-≤C20 (%mole) | >C20-≤C23 (%mole) | >C23-≤C29 (%mole) | >C29-≤C45 (%mole) | >C45-≤C100 (%mole) |
|---|---|---|---|---|---|---|---|---|
| 8#1GF#1 | 0.15-0.34 | 13.3 | 24.2 | 29.1 | 11.8 | 12.1 | 7.9 | 1.6 |
| 8#1GF#2 | 1.1-1.3 | 13.1 | 24.5 | 29.2 | 11.6 | 12.0 | 7.9 | 1.7 |
| 8#1GF#5 | 2.9-3.3 | 13.9 | 24.1 | 29.5 | 11.9 | 12.1 | 7.5 | 1.0 |
| 8#1WF#1 | 0.26-0.37 | 12.0 | 23.2 | 28.9 | 12.7 | 12.8 | 8.4 | 2.1 |

Table 6-8: Viscosity of oil recovered during the period of secondary $CO_2$ injection.

| Sample | PV of Injection | Viscosity Ratio, (%) |
|---|---|---|
| Dead Crude 'C' | -- | 100 |
| 8#1GF#3 | 1.6-1.9 | 90 |
| 8#1GF#4 | 2.4-2.9 | 88 |

### 6.3.2 Effect of Rate of Injection (Time) on Performance of Secondary $CO_2$ Injection

After establishing the irreducible water saturation by flooding the core with live crude 'C', $CO_2$ was injected into the core, Figure 6-20. However, the rate of injection of $CO_2$ was 7 times lower in Coreflood#8. In the other words, $CO_2$ had almost sevenfold more time in contact with the oil in that experiment than Coreflood#6. The instability in the flood front, regardless of the rate of injection, dominated the flow in both experiments. Thus, the rate of injection of $CO_2$ did not have a notable impact on the amount of oil produced before the breakthrough. But, for a short period after the breakthrough, oil was recovered with a lower rate in the experiment that the rate of injection was also lower. This observation highlights the impact of solution gas drive on oil recovery as a result of pressure rising before the breakthrough. The higher pressure of injection fluid until the

breakthrough would have resulted in a higher amount of $CO_2$ dissolution in the oil. The higher pressure gradient would also enhance the effects of viscous forces on the process of oil recovery.

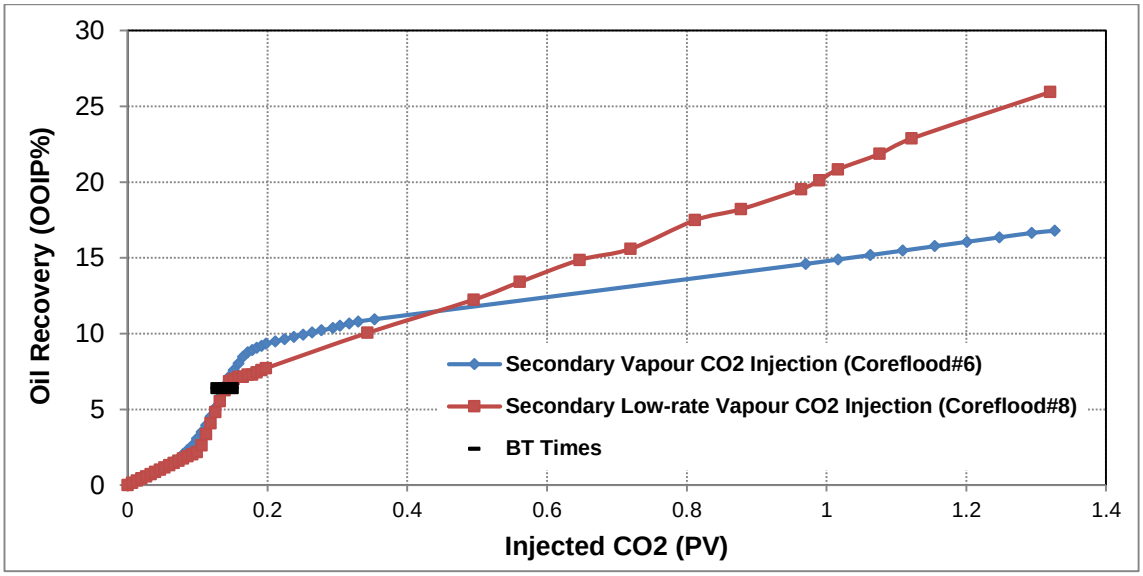


Figure 6-20: Comparison of profiles of oil recovery of secondary vapour $CO_2$ injection and secondary low-rate vapour $CO_2$ injection.

Since the main mechanism of oil recovery was the dissolution of $CO_2$ in oil and this process is time dependent, the amount of oil recovered by $CO_2$ injection in the test that the rate of injection was lower, eventually, exceeds that in the other experiment. Figure 6-21 compares the performance of oil recovery of intermittent $CO_2$ injection with secondary (continuous) $CO_2$ injection. The periods of shut-in of intermittent injection are shown as periods of no oil production. The impact of viscous forces on oil recovery is obvious during early times of the experiment of intermittent injection. In core scale, $CO_2$ utilisation was notably reduced by decreasing the rate of injection of $CO_2$. For instance, 3.4 PVs of $CO_2$ was utilised in the experiment of intermittent injection to recover the equal amount of oil by injecting 1.6 PVs of continuous but low-rate injection of $CO_2$. However, the distance that $CO_2$ would transfer in an actual reservoir would be significantly longer. This implies that the time of contact of $CO_2$ and oil in the reservoir, which is a key factor for dissolution of $CO_2$ in the oil (Riazi & Whitson 1993), would become higher. In addition, the amount of $CO_2$ available for injection is a huge challenge in any field pilots (Moffitt, et al. 2015). Thus, intermittent injection of $CO_2$ offers several benefits compared to continuous injection. For example, the dissolution of $CO_2$ in oil is facilitated during the periods of shut-in, in particular, after the breakthrough of $CO_2$. Moreover, the recovery factor can be improved by increasing the rate of injection while the utilisation of $CO_2$ is lowered. Injection of any fluid into a reservoir is generally accompanied by a pressure increase in the system. The elevated pressure as a result of

increasing the rate of injection would lead to the higher amount of dissolution of $CO_2$. That can also enhance oil recovery by increasing the density of $CO_2$ in porous media.

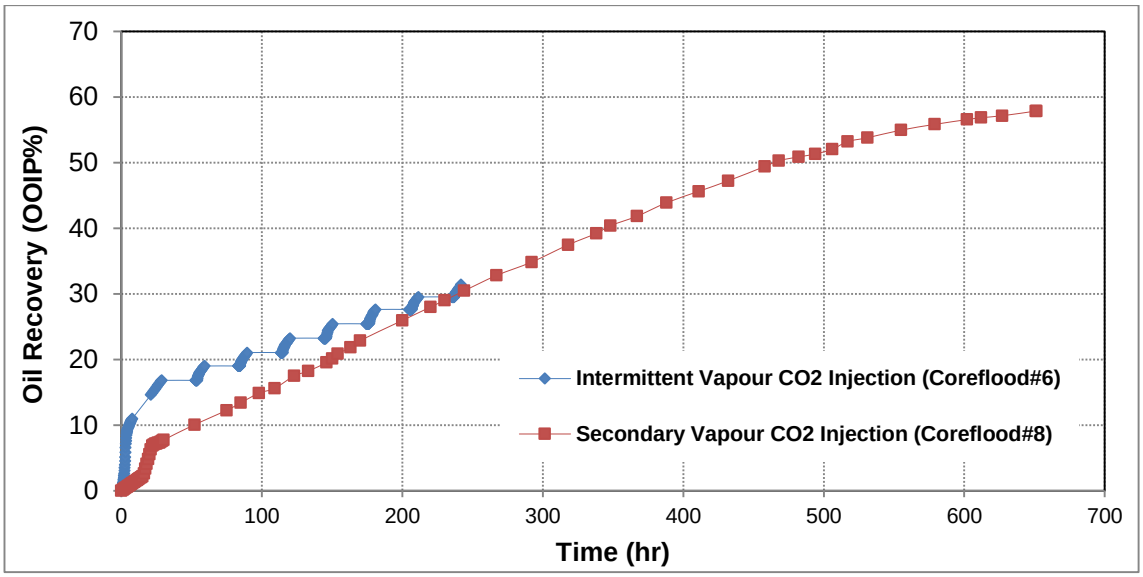


Figure 6-21: Comparison of profiles of oil recovery of intermittent vapour $CO_2$ injection and secondary (continuous) vapour $CO_2$ injection.

### 6.3.3 1st (Tertiary) Waterflood

Around 1 PV of $CO_2$-saturated brine was injected through the core after the period of secondary $CO_2$ injection. The injected water followed the least resistance paths of $CO_2$ in the core and it displaced gas toward the production outlet. A low fraction of the remaining oil in the core was recovered until the breakthrough, Figure 6-22. Oil production rate increased after the breakthrough because of the production of the oil bank ahead of water front. Oil was produced continuously at high water cuts until the end of waterflood. The relatively low amount of oil recovery is mainly attributed to the low saturation of the remaining oil in the core.

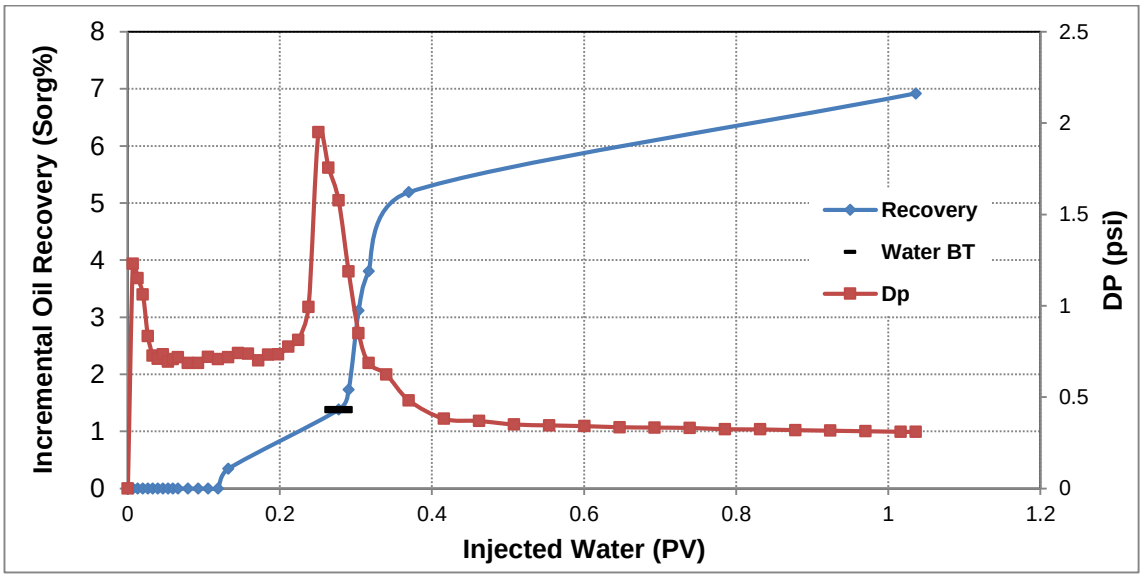


Figure 6-22: Incremental oil recovery and differential pressure across core during the period of waterflood.

***Summary***

Figure 6-23 illustrates the cumulative oil recovery during different periods of Coreflood#8. The breakthrough of $CO_2$ was not affected by reducing the rate of injection of $CO_2$. The importance of the mechanism of solution gas drive in improving oil recovery after the breakthrough of $CO_2$ was discussed. The main mechanism of oil recovery was the dissolution of $CO_2$ in the oil and the resultant oil viscosity reduction. An advantage of low-density $CO_2$ injection compared to dense $CO_2$ injection is that the mechanism of extraction and liberation of methane of oil are less effective. The liberation of methane of oil by dense $CO_2$ leads to an initial increase in the viscosity of the oil which later is compensated by the dissolution of $CO_2$ in oil. However, in the case of low-density $CO_2$ injection, the viscosity of the oil is being reduced from the beginning of the contact of $CO_2$ and live heavy oil. The performance of tertiary waterflood after an extended period of $CO_2$ injection depends on the saturation of remaining oil in place as well as the scheme of injection of $CO_2$.

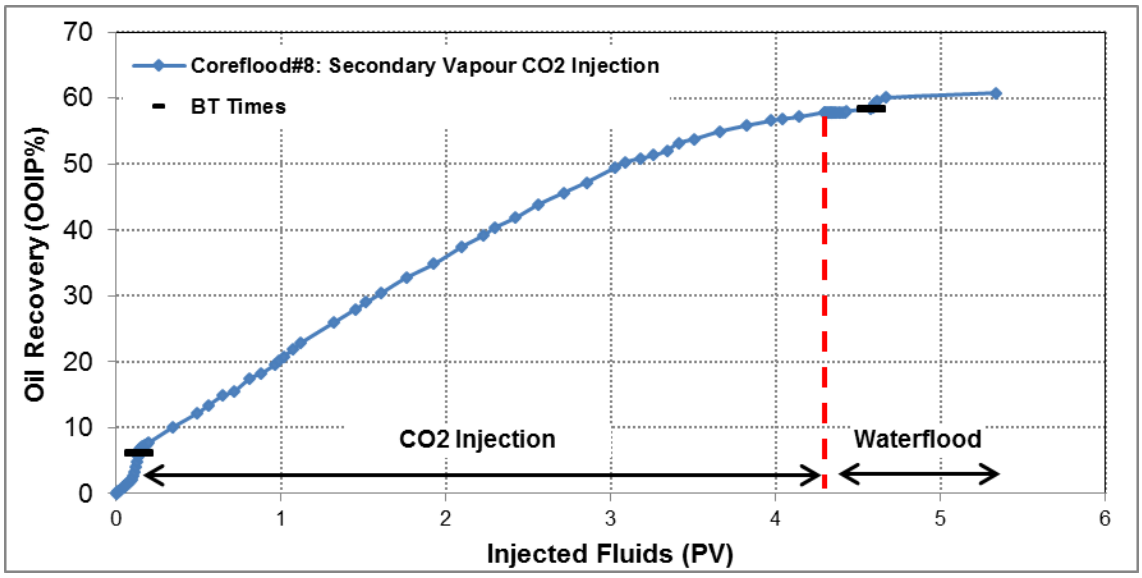


Figure 6-23: Cumulative oil recovery during different periods of Coreflood#8.

## 6.4 Coreflood#9: Water alternating (Vapour) $CO_2$ Injection

It was shown that a period of waterflood after a period of $CO_2$ injection can improve sweep efficiency and hence enhancing oil recovery. This suggests that combining water and $CO_2$ injection in relatively small slugs can further enhance oil recovery. In addition, the combining of water and $CO_2$ injection can reduce the utilisation of $CO_2$. To investigate this, three cycles of water alternating $CO_2$ were injected into the core saturated with live crude 'C'. The experiment was later continued by co-injection of a surfactant solution and $CO_2$ in order to improve recovery factor by in-situ propagation of foam in the core and also by the formation of an emulsion between the surfactant solution and oil in place. A summary of the performance of all the periods of fluid injection in terms of cumulative oil recovery will be shown in Figure 6-32. Table 6-9 shows the conditions and fluids of Coreflood#9.

Table 6-9: Fluids and conditions of Coreflood#9.

| **Coreflood#9** | **Coreflood#7** |
|---|---|
| Crude Oil: Methane-saturated Crude 'C' | Crude Oil: Methane-saturated Crude 'C' |
| Brine: Methane-saturated or $CO_2$-saturated | Brine: Methane-saturated or $CO_2$-saturated |
| Gas: Vapour $CO_2$ | Gas: Vapour $CO_2$ |
| Surfactant: 0.3 wt% Petrostep C1 | Surfactant: -- |
| Temperature: 50° C | Temperature: 50° C |
| Pressure: 600 psi | Pressure: 600 psi |
| Injection Rate: 1 or 7 $cm^3$/hr | Injection Rate: 7 $cm^3$/hr |
| Core Position: Vertical (top to bottom) | Core Position: Vertical (top to bottom) |

***Procedure***

The following were the main steps to conduct Coreflood#9:

1. **Dead Brine Injection:** Core was saturated with brine and the permeability was re-measured. The permeability of the core remained unchanged.
2. **Live Brine Injection:** The live brine was injected through the core to avoid gas transfer from following live oil into the brine.
3. **Live Oil Injection:** The core was flooded with live crude 'C' and an irreducible water saturation of 8% was achieved.
4. **Water alternating $CO_2$ Injection:** 3 cycles of water alternating $CO_2$ injection were performed. In each cycle, water was injected at 7 $cm^3/hr$ while the rate of injection of $CO_2$ was 1 $cm^3/hr$.
5. **Surfactant Pre-flush:** 0.1 PV of surfactant solution was injected into the core.
6. **Co-injection of Surfactant and $CO_2$:** Co-injection of surfactant and $CO_2$ was

started after pre-flush of the core with the surfactant solution. The injection was performed at various rates of injection.

7. **Core Cleaning:** Several cycles of toluene and methanol were injected into the core.

***Results and Discussion***

### 6.4.1 1st (Secondary) Waterflood

The first slug of water alternating $CO_2$ injection was an injection of methane-saturated brine into the core saturated with live crude 'C'. Following the above-mentioned procedure, the injection of water into the core was started. This experiment (Coreflood#9) was performed at the same conditions that the experiment of tertiary (low-density) $CO_2$ injection (Coreflood#7) had been performed. In both experiments, (methane-saturated) brine was the first injection fluid after establishing irreducible water saturation in the core. Figure 6-24 and Figure 6-25 compare the profiles of oil recovery and DP across the core during the period of 1st (secondary) waterflood in both experiments. It is ensured that the results and also the behaviour of the fluids and the rock were repeatable in the coreflood experiments reported in this study.

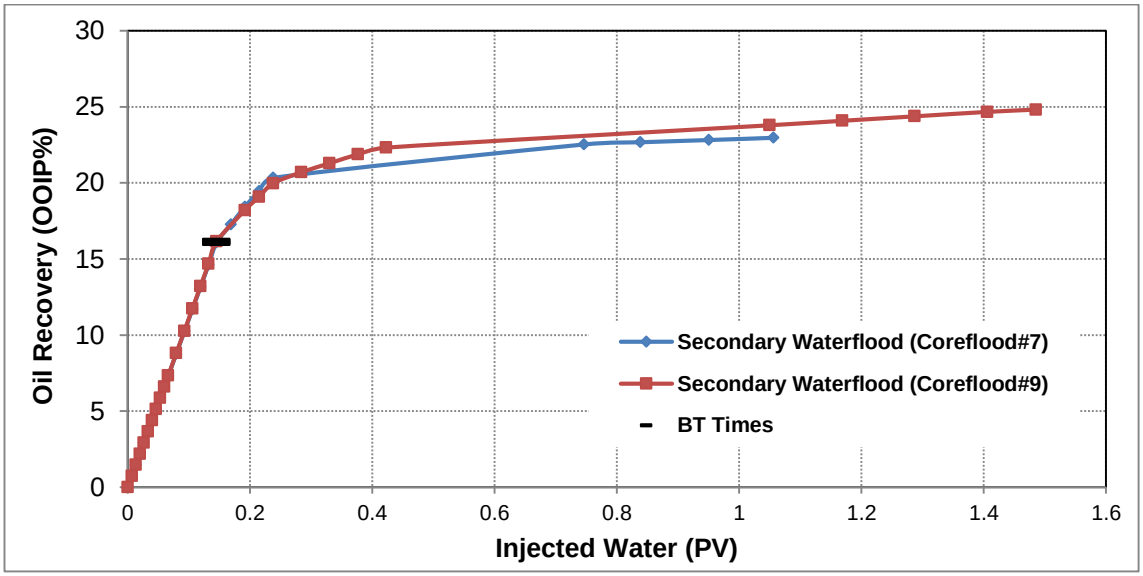


Figure 6-24: Comparison of profiles of oil recovery during the period of secondary waterflood in Coreflood#7 and Coreflood#9.

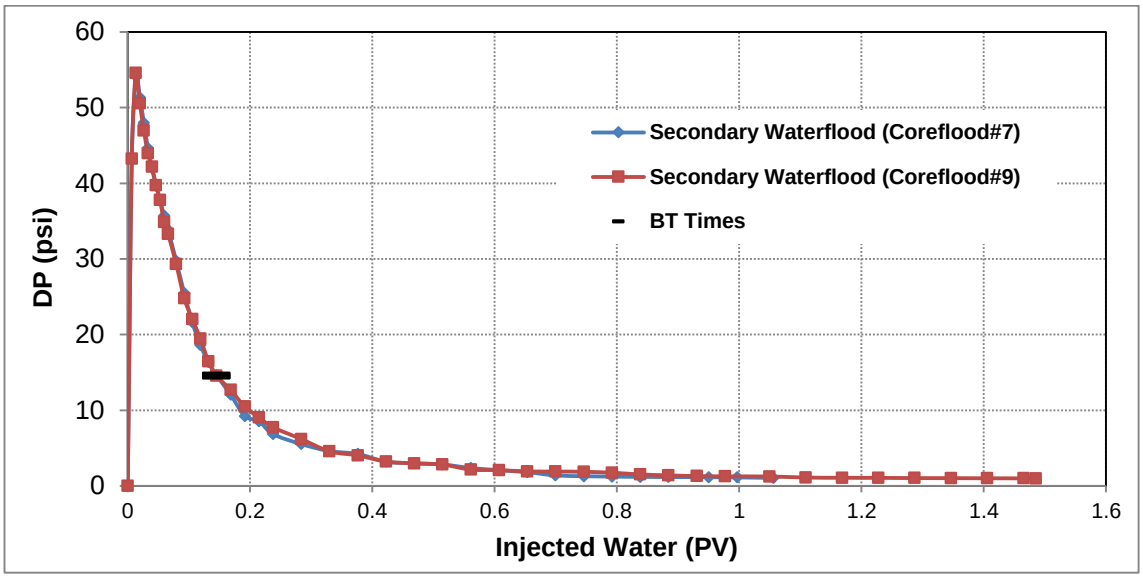


Figure 6-25: Comparison of profiles of differential pressure across the core during the period of secondary waterflood in Coreflood#7 and Coreflood#9.

### 6.4.2 1st (Tertiary) $CO_2$ Injection

After the period of 1st (secondary) waterflood, 1 PV of $CO_2$ was injected at 1 $cm^3/hr$ through the core to evaluate the performance of tertiary injection of vapour $CO_2$ in the recovery of the remaining oil in place. Figure 6-26 compares the profiles of recovery of the remaining oil in the core by tertiary injection of $CO_2$ in Coreflood#7 and Coreflood#9. The main difference in both experiments was the rate of injection of $CO_2$. The injection of $CO_2$ was continued for an almost equal period of time in both runs, as evidence in Figure 6-27. It should be mentioned that the difference in the saturation of the remaining oil in the core was negligible before the beginning of $CO_2$ injection.

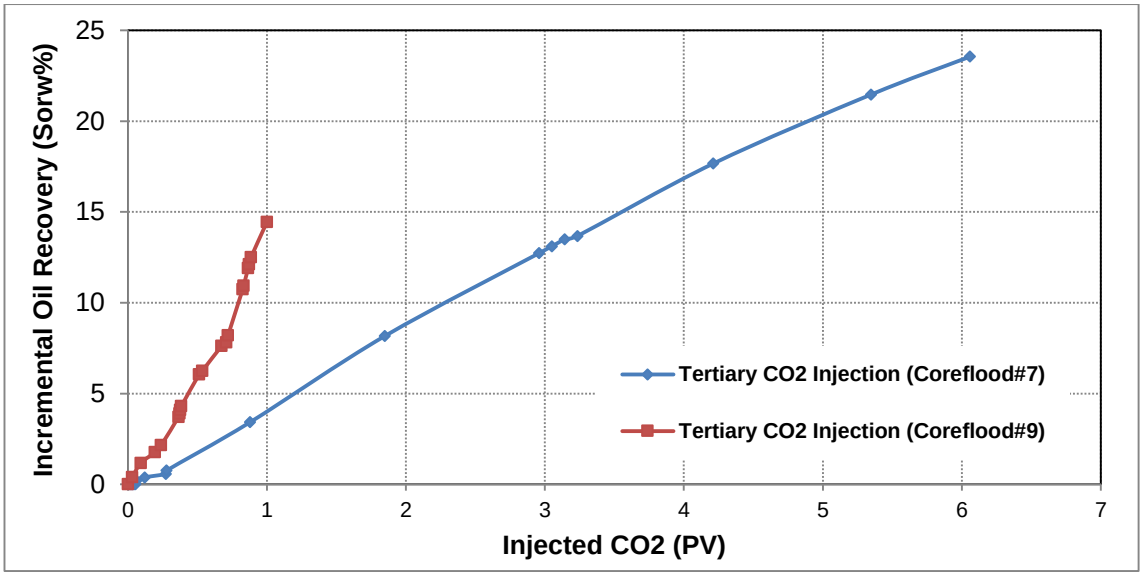


Figure 6-26: Comparison of profiles of incremental oil recovery during the period of tertiary $CO_2$ injection in Coreflood#7 and Coreflood#9.

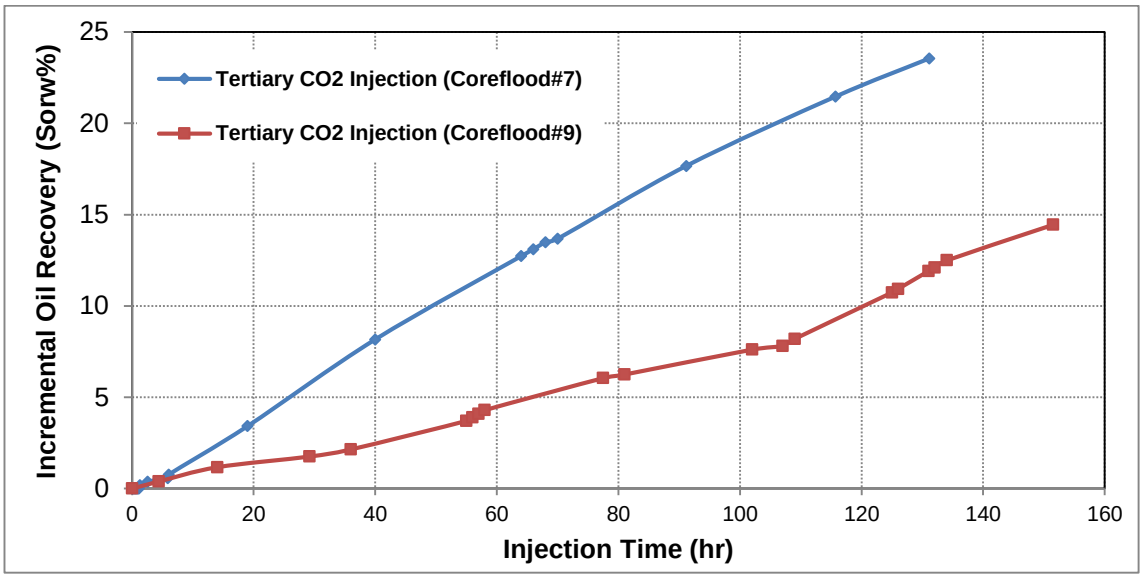


Figure 6-27: Comparison of performance of incremental oil recovery during the period of tertiary $CO_2$ injection in Coreflood#7 and Coreflood#9.

The results of oil recovery reflect that higher amount of oil was recovered by a higher rate of injection of $CO_2$ into the core. However, in the scale of the core used in this study, the volume of $CO_2$ utilised in the run of high-rate of injection is 6 times higher than the volume of $CO_2$ injected at a lower rate. In an actual reservoir, the amount of time for $CO_2$ to contact oil would be significantly higher and hence higher amount of oil can be recovered by increasing the rate of injection of $CO_2$. It should be mentioned that none of the flow rates at which $CO_2$ was injected into the core in these two experiments is considered as the optimum rate of injection. Many factors such as availability of injection gas, injectivity of formation, reservoir heterogeneity, and capacity of production facilities can affect the rate of injection of a gaseous fluid into an oil reservoir (Lake 1989; Moffitt, et al. 2015).

### 6.4.3 Water alternating $CO_2$ Injection

After the 1st period of $CO_2$ injection, two more cycles of water and $CO_2$ injection were performed to improve recovery factor, Figure 6-28. A significant amount of the remaining oil in the core was recovered by ($CO_2$-saturated) waterflood after the 1st period of $CO_2$ injection. The behaviour of this period of waterflood was notably similar to the performance of the period of 2nd waterflood in Coreflood#7. The continuation of the experiment by $CO_2$ injection after the 2nd waterflood improved recovery factor as well. However, the impact was not as significant as it was during the period of 1st $CO_2$ injection perhaps due to the lower saturation of oil in the core and also a lower amount of oil being accessible to $CO_2$ by water-shielding. The performance of 3rd waterflood was significantly poor and hence the run was terminated after only 0.5 PV of injection. The

reasons for poor recovery of waterflood could be due to the presences of established paths of water and $CO_2$ within the core and the low saturation of oil in those paths of interest of water. The distributions of saturation of the fluids in the core at the end of each slug of injection are compared in Figure 6-29 in which the extent of reshuffling of water and $CO_2$ is noted.

It is significant that the oil was still recovered during the 3rd period of $CO_2$ injection. In the MM experiments, it was shown that $CO_2$ can diffuse into the oil surrounded by water. The dissolution of $CO_2$ in oil causes to oil swelling as well as oil viscosity reduction which would improve the mobility of oil in porous media. The ability of $CO_2$ to drive oil toward the production outlet at this stage of the experiment suggests that improving sweep efficiency of $CO_2$ injection by lowering its mobility in porous media may further enhance recovery factor from of the oil.

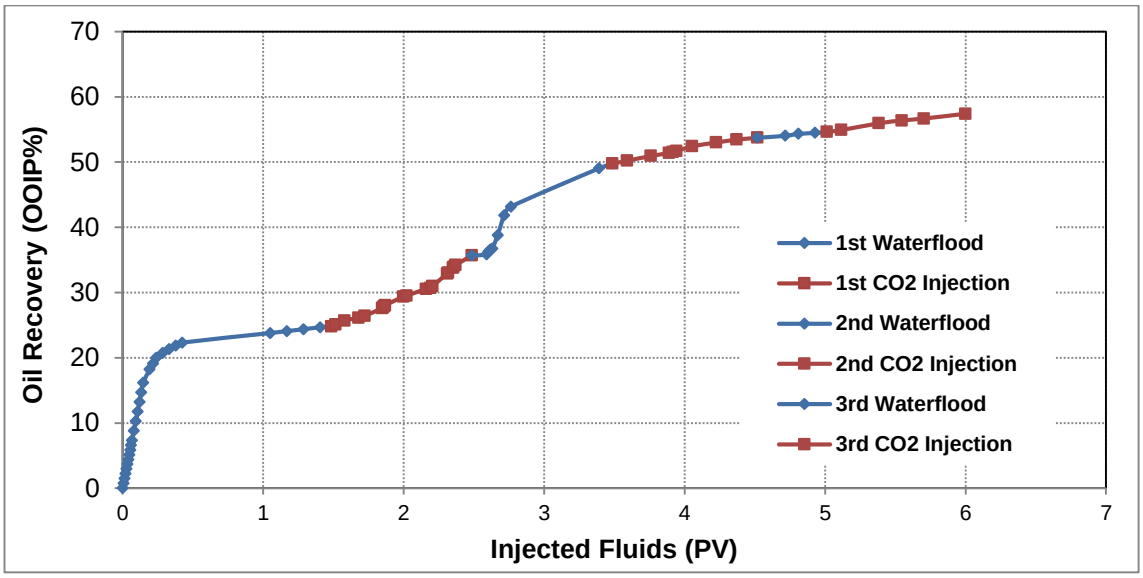


Figure 6-28: Cumulative oil recovery during the different period of water alternating $CO_2$ injection.

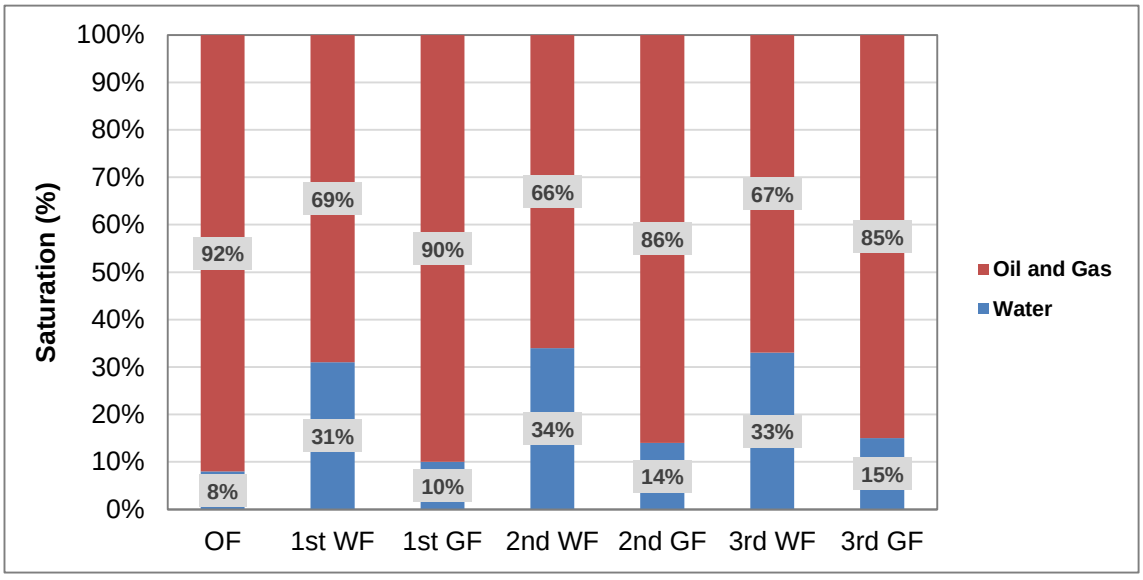


Figure 6-29: Saturation distribution of fluids at the end of each slug of water alternating $CO_2$ injection.

### 6.4.4 Co-injection of Surfactant and $CO_2$

After the last (third) slug of $CO_2$ injection, the cumulative oil recovery of 57% of the initial oil in the core was achieved, meaning that the significant saturation of the remaining oil in place can still be a target of EOR techniques. Although $CO_2$ injection could still recover the remaining oil in the core, the efficiency of this process was relatively low. A solution to reduce the mobility of $CO_2$ in porous media is the combining of $CO_2$ injection with a surfactant solution to form in-situ foam. In a visualisation study, Emadi, et al. (2012) showed that co-injection of (vapour) $CO_2$ and a surfactant solution into a waterflooded porous medium (glass micromodel) caused to in-situ formation of foam and hence sweep of the remaining oil in the system. The oil used in their study was dead crude 'C' and the experiments were performed at 44˚ *C* and 600 *psi*.

Under the same conditions of our low-density (vapour) $CO_2$ injection coreflood experiments, Emadi (2012) performed two coreflood experiments using the same surfactant solution in our study, too. First, the clean core was saturated with the surfactant solution and then $CO_2$ and surfactant were simultaneously injected through the core ($CO_2$ at 4.5 $cm^3/hr$ and surfactant at 2.5 $cm^3/hr$). The behaviour of DP was monitored and recorded during the experiment. After 2 total pore volumes (TPVs) of injection, it was observed that the DP was increased at a constant rate until 6 TPVs of injection and then remained relatively constant until the end of the run (8.3 TPVs). The results indicated that relatively strong and stable foam was formed during the late times of the period of co-injection. The apparent viscosity of the foam was also calculated by using the data of DP across the core. The core was then prepared for the second experiment by cleaning it with toluene and methanol injected in succession. In the second experiment, after a period of secondary waterflood, $CO_2$ and the surfactant were injected simultaneously into the core. The waterflood after 1 PV of injection resulted in the recovery of 19% of the initial oil in the core. 6 TPVs of the co-injection of $CO_2$ and the surfactant ($CO_2$ at 4.5 $cm^3/hr$ and surfactant at 2.5 $cm^3/hr$) improved oil recovery by the production of 56% of the initial oil in place during this period. The DP across the core increased significantly before the breakthrough due to the formation of an oil bank. The production of the oil bank was continued until the breakthrough of $CO_2$ which was accompanied by the reduction of the DP within the core. Later, the DP increased gradually almost until the late times of the period of co-injection. Accordingly, it was concluded that in-situ formation of 'CO2-foam' was the main reason for the rising DP at late times of the run. That is, the formation of foam in the core took place while a significantly high saturation of oil was still in the

core.

In this work, 0.1 PV of the surfactant solution was injected at 7 $cm^3/hr$ into the core after the 3rd slug of $CO_2$ injection. This surfactant pre-flush was conducted to reduce the adsorption of the surfactant on the surface of the rock during the period of co-injection of surfactant and $CO_2$. The injected surfactant displaced $CO_2$ toward the production outlet and a small fraction of oil (less than 1% of the remaining oil in place) was also produced during this period. Then, the co-injection of $CO_2$ and surfactant was started at a total rate of 7 $cm^3/hr$ ($CO_2$ at 4.5 $cm^3/hr$, and surfactant at 2.5 $cm^3/hr$). The co-injection of $CO_2$ and surfactant was continued at a constant total rate until around 5.8 TPVs of injection where the rates of injection (of both fluids) were doubled and continued until 7.4 TPVs of injection. Here, the injection was stopped and the core was shut to charge the storage vessels with the injection fluids. After 24 hours, the co-injection of surfactant and $CO_2$ into the core was continued but at a different total rate of injection of $CO_2$ and surfactant; $CO_2$ at 11.5 $cm^3/hr$ and surfactant at 2.5 $cm^3/hr$. This run was continued at a constant rate until 2.7 TPVs of injection, where the rate of injection of $CO_2$ was increased to 18.5 $cm^3/hr$.

The results of the above-mentioned periods, the profile of incremental oil recovery and the behaviour of DP across the core, are illustrated in Figure 6-30 and Figure 6-31. Unlike the observation made by Emadi (2012), no clear sign of formation of strong foam in the core was noted during the periods of co-injection of $CO_2$ and surfactant in the experiment reported here. The cores used in both studies were taken from the same block of rock and their physical properties were very similar but the core had been exposed to surfactant in the study reported by Emadi (2012) before performing the coreflood experiment with oil. Thus, the significance of adsorption of the surfactant on the surface of rock would have been lower in their study. However, a significant volume of surfactant was utilised in our study which probably eliminates the role of adsorption in opposing the formation of foam in the core. The lower saturation of the oil in porous media usually has positive or no impact on the propagation of foam. However, the core in our study was initially saturated with live (methane-saturated) crude 'C' instead of dead oil in the study reported by Emadi (2012). Furthermore, because of the injection of several cycles of $CO_2$ and $CO_2$-saturated brine, the remaining oil in the core would have been relatively saturated with $CO_2$. The presence of dissolved gas in the oil could affect phase behaviour of the oil and the surfactant solution (i.e. optimal salinity) and this was likely the main reason of no propagation of foam in the coreflood experiment performed in our study. The presence of gas, in particular, $CO_2$ in oil would reduce the IFT between $CO_2$ and the oil. Therefore,

oil would tend to spread between $CO_2$ and the aqueous solution in the pores and this can delay the propagation speed of foam. The spreading behaviour of oil can also cause to fast destabilising of foam in porous media. In spite of the co-injection of $CO_2$ and surfactant into the core, the pressure gradient within the core was lower during this run compared to the 3rd slug of $CO_2$ injection. This observation may also show that the flow paths of the fluids were different in these two runs. In addition, the physical properties of the core effluent such as its colour was indicating that emulsification was significant between oil and the surfactant solution. The emulsion scavenged the surfactant and hence, a lower amount of surfactant was probably available for formation of foam in the core.

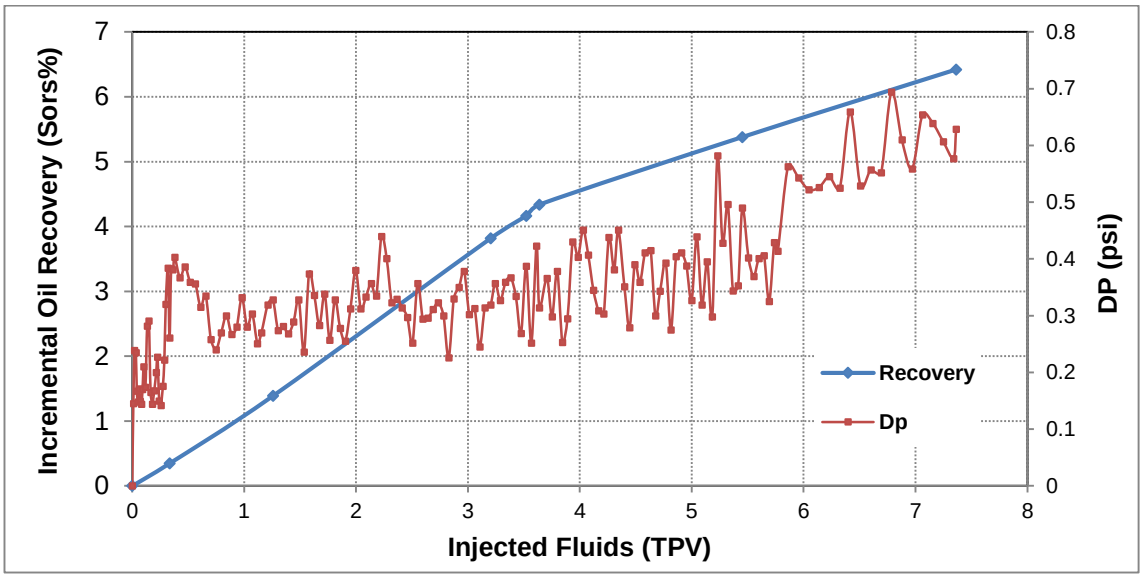


Figure 6-30: Incremental oil recovery and differential pressure across the core during the 1st period of co-injection of $CO_2$ and surfactant. The apparent noisiness of the DP is genuine and is related to the behaviour of flow.

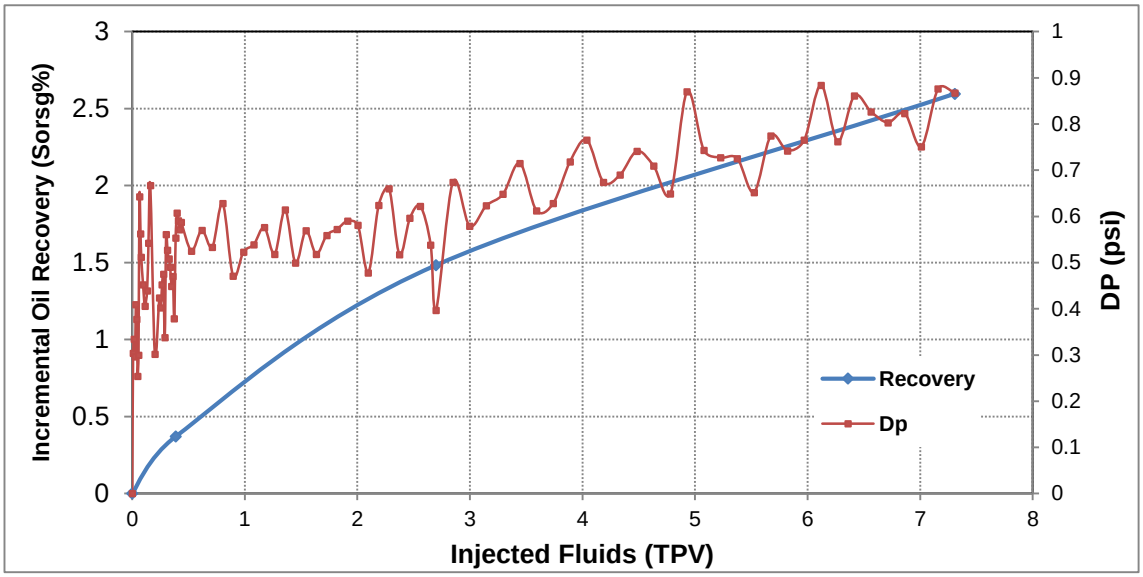


Figure 6-31: Incremental oil recovery and differential pressure across the core during the 2nd period of co-injection of $CO_2$ and surfactant. The apparent noisiness of the DP is genuine and is related to the behaviour of flow.

The results of this study highlight the complexity of the processes in porous media. This becomes even more challenging in the processes that mass transfer plays a key role in determining the performance of them. It is, therefore, important to fully understand these processes and carefully study their underlying mechanisms prior to making decisions on implementation of those processes in actual reservoirs.

***Summary***

Figure 6-32 illustrates the cumulative oil recovery during different stages of Coreflood#9. It was shown that low-density $CO_2$ injection can significantly enhance heavy oil recovery. In addition, a combination of $CO_2$ injection with a higher viscous fluid injection (e.g. water) further improves the sweep efficiency in porous media. It is believed that the remaining oil in the core after three cycles of water and $CO_2$ injection was mainly trapped by capillary forces. Thus, it was aimed to reduce the saturation of oil in the core by co-injection of $CO_2$ and a surfactant solution. The successful coreflood application of the co-injection of $CO_2$ and the surfactant solution used in this experiment has been reported by Emadi (2012) and Farzaneh (2015). However, no sign of strong propagation of foam was observed in this study, mainly due to the presence of dissolved gas (methane and $CO_2$) in the remaining oil in the core.

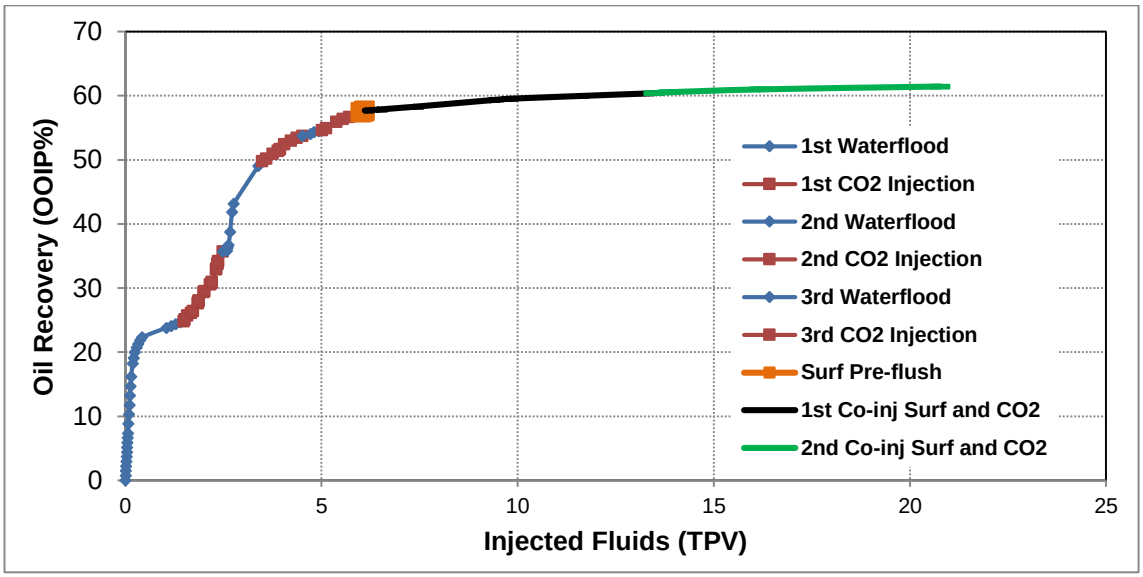


Figure 6-32: Cumulative oil recovery during different periods of Coreflood#9.

## 6.5 Conclusions

Four coreflood experiments were performed at various injection strategies to evaluate the performance of low-density (vapour) $CO_2$ injection for heavy oil recovery. The mechanisms involved in these experiments were investigated and discussed. In addition, the interactions of the fluids in these experiments were compared to the behaviour of the same fluids in the experiments reported in the previous chapters which led to the understanding of the impact of various parameters on the process of heavy oil recovery by $CO_2$ injection. It was shown that the coreflood experiments performed in this study were repeatable. Furthermore, the compositional analysis and the measurement of physical properties of the effluent (e.g. oil, gas) of the coreflood experiments were performed at several stages of the experiments. Based on the results of the experiments reported in this chapter, the following conclusions are drawn:

- The rate of diffusion of $CO_2$ into heavy oil is a significant function of pressure (density of $CO_2$). The speed of dissolution of $CO_2$ in heavy oil decreases by reducing the pressure of the system.
- The mechanism of solution gas drive plays an important role in the process of oil recovery by $CO_2$ injection, particularly after the breakthrough.
- The strength of extraction by $CO_2$ depends on the density of $CO_2$-rich phase. Therefore, this mechanism is less pronounced under the conditions of high-temperature or low-pressure reservoirs.
- The dissolution of $CO_2$ in heavy oil is an important mechanism of oil recovery; whether $CO_2$ is a dense fluid or a low-density gas.
- It is still possible that low-density $CO_2$ can cause to the liberation of methane from heavy oil.
- Under reservoir conditions, the contact of low-density $CO_2$ and heavy leads to the dissolution of $CO_2$ in the oil and hence the viscosity of the oil reduces. However, in the case of dense $CO_2$, initially, the viscosity of the oil increases as a result of the liberation of dissolved gas (methane) from the oil.
- Low-density $CO_2$ is still capable of in-situ improving the physical properties (e.g. viscosity) of heavy oil. However, the impact is significantly lower since the density of $CO_2$ is low.
- Gravity drainage can assist the process of heavy oil recovery by $CO_2$ injection.
- Intermittent injection of $CO_2$, even under the conditions of low-density $CO_2$, showed

considerable potential on improving recovery factor while the utilisation of $CO_2$ was reduced.

- It is crucial to evaluate the performance of any process of gas injection for EHOR under the actual conditions of the reservoirs.
- In a tertiary injection of low-density $CO_2$, the amount of dissolution of $CO_2$ in the water in porous media should be considered for determining the proper amount of $CO_2$ for injection.
- The behaviour of oil recovery of waterflood after an extended period of $CO_2$ injection may depend on the strategy of recovery prior to that waterflood.
- The instability in the flood front is significant in any attempt to displace heavy oil by water or gas injection. For instance, the rate of injection of $CO_2$ does not have notable impacts on the sweep efficiency before the breakthrough.
- Although time is a dominant factor in determining the performance of heavy oil recovery by $CO_2$ injection, viscous forces have also crucial impact on the speed of oil production. Thus, increasing the rate of injection of $CO_2$ would increase the rate of oil production.
- The presence of dissolved gas in heavy oil would affect the performance of co-injection of $CO_2$ and surfactant.
- It is essential to evaluate the phase behaviour of surfactant and oil under reservoir conditions.
- A properly designed and executed low-density (vapour) $CO_2$ injection can recover a significant fraction of heavy oil at reservoir conditions.

# CHAPTER 7: CONCLUSIONS AND RECOMMENDATIONS

## 7.1 Conclusions

This report presents an integrated experimental study on the injection of $CO_2$ for enhanced heavy oil recovery under reservoir conditions. The contribution of this study is divided into two major categories. First, the underlying mechanisms of heavy oil recovery by $CO_2$ injection were investigated and identified in pore-scale as well as macroscale (core-scale). Second, the impacts of various parameters affecting the process of oil recovery were evaluated by developing visualisation (micromodel and visual-cell) and coreflood experiments under different conditions of pressure and temperature. Moreover, the characterization of fluids and the measurements of their PVT properties led to the better translation of the processes of oil recovery in the experiments. $CO_2$ injection under different conditions of pressure and temperature showed considerable potential to improve heavy oil recovery. Table 7-1 summarises the dominant mechanisms of oil recovery during the coreflood experiments. Since the oil is recovered by fluid injection, it is considered that viscous forces have been dominant in all the experiments.

Table 7-1 A summary of the dominant mechanisms during $CO_2$ or VRG injection.

| Coreflood# | Dominant mechanisms | Changes in the recovered oil | Oil recovery (%IOIP) |
|---|---|---|---|
| 1 | Extraction of hydrocarbons<br>Oil viscosity reduction<br>Oil swelling | Improved composition<br>Lower viscosity<br>Lower metal content | 1WF=22<br>1$CO_2$=18<br>2WF=9<br>Total=49 |
| 2 | Extraction of hydrocarbons<br>Oil viscosity reduction<br>Oil swelling<br>Solution gas drive<br>Gravity drainage | Improved composition<br>Lower viscosity<br>Lower metal content | 1$CO_2$=22<br>Intermittent $CO_2$=13<br>1WF=15<br>Total=55 |
| 3 | Oil viscosity reduction<br>Oil swelling<br>Extraction of hydrocarbons<br>Gravity drainage | Improved composition<br>Lower viscosity | 1$CO_2$=19<br>Intermittent $CO_2$=38<br>1WF=6<br>Total=65 |
| 4 | Oil viscosity reduction<br>Oil swelling<br>Extraction of hydrocarbons | Improved composition<br>Lower viscosity | 1WF=24<br>1$CO_2$=18<br>2WF=8<br>Total=50 |
| 5 | Oil viscosity reduction<br>Oil swelling<br>Gravity drainage | Improved composition<br>Lower viscosity | 1VRG=21<br>Intermittent VRG=22<br>2VRG=17<br>1WF=8<br>Total=68 |
| 6 | Oil viscosity reduction<br>Oil swelling<br>Gravity drainage | Lower viscosity | 1$CO_2$=17<br>Intermittent $CO_2$=14<br>1WF=18<br>Total=49 |
| 7 | Oil viscosity reduction<br>Oil swelling | Lower viscosity | 1WF=23<br>1$CO_2$=18<br>2WF=12<br>Total=53 |
| 8 | Oil viscosity reduction<br>Oil swelling<br>Gravity drainage | Lower viscosity | 1$CO_2$=58<br>1WF=3<br>Total=61 |
| 9 | Oil viscosity reduction<br>Oil swelling | Lower viscosity | 1WF=25<br>1$CO_2$=11<br>2WF=14<br>2$CO_2$=4<br>3$CO_2$=3<br>Total=61 |

Based on the results of the experiments and the observations made in this study, the following conclusions are drawn:

- Despite the lower viscosity of $CO_2$ compared to water, $CO_2$ injection can recover a higher amount of heavy oil by a number of mechanisms mainly stemmed from mass transfer between $CO_2$ and oil.
- Higher injectivity is another advantage of $CO_2$ injection compared to waterflood for

heavy oil recovery from sandstone rock.

- The dissolution of $CO_2$ in heavy oil is an important mechanism of oil recovery; whether $CO_2$ is a dense fluid or a low-density gas.
- The mechanisms of solution gas drive and gravity drainage play important roles in the process of oil recovery by $CO_2$ injection, in particular, after the breakthrough.
- A higher quality oil than the original heavy oil in porous media can be recovered by $CO_2$ or VRG injection while waterflood on its own cannot enhance the physical properties of the oil. The extent of in-situ alteration of the quality of recovered oil is a function of injection strategy and it is affected by factors such as gravity.
- Although time is a dominant factor in determining the performance of heavy oil recovery by $CO_2$ injection, viscous forces have also crucial impact on the speed of oil production. Thus, increasing the rate of injection of $CO_2$ would increase the rate of oil production.
- As soon as dense $CO_2$ contacts heavy oil, extraction of hydrocarbons from the oil starts. The extraction of hydrocarbons takes place from the interface of $CO_2$ and oil. Methane in heavy oil is also liberated within the oil-phase far from the interface.
- The liberation of methane of heavy oil by dense $CO_2$ leads to a sudden swelling of the oil. This was the main reason for the increase of core pressure during the shut-in period of intermittent $CO_2$ injection. This phenomenon is somehow similar to the concept of solution gas drive and VRR for optimal viscous and heavy oil recovery.
- Extraction of hydrocarbons by $CO_2$ is a continuous process and eventually the volume of oil will decrease as more light and intermediate components are extracted.
- The strength of extraction by $CO_2$ depends on the density of $CO_2$-rich phase. Therefore, this mechanism is less pronounced under the conditions of high-temperature or low-pressure reservoirs.
- Under reservoir conditions, the contact of low-density $CO_2$ and heavy oil leads to the dissolution of $CO_2$ in the oil and hence the viscosity of the oil reduces. However, in the case of dense $CO_2$, initially, the viscosity of oil increases as a result of the liberation of dissolved gas (methane) from the oil.
- The effect of hydrocarbon extraction by $CO_2$ is not uniformly distributed over components with different carbon numbers.
- Extraction of hydrocarbon components is the main reason of higher quality oil recovery by $CO_2$ injection.
- When dense $CO_2$ contacts heavy oil, an accumulation of light and intermediate

compounds of oil takes place in the oil-rich phase, near the interface of oil and $CO_2$. The dissolution of $CO_2$ in the oil and the resultant oil viscosity reduction and oil swelling would facilitate this process.

- Formation of an oil-rich phase in the $CO_2$-rich stream was observed as a result of $CO_2$ and oil contact in the flow paths of $CO_2$. This oil-rich phase has a relatively lighter colour than the oil in contact with $CO_2$ and it is significantly mobile in porous media but not as fast as a $CO_2$-rich phase.
- The light colour oil-rich phase in the stream of $CO_2$ has a higher concentration of light and intermediate components as well as lower viscosity than the original oil.
- Low-density $CO_2$ is still capable of in-situ improving the physical properties (e.g. viscosity) of heavy oil. However, the impact is significantly lower since the density of $CO_2$ is low.
- $CO_2$ can reach the oil surrounded by water (either initial water or remaining water after a period of waterflood) by dissolving in the water and diffusing from it into the trapped oil.
- The transport of $CO_2$ into oil by the water surrounding the oil is a continuous process. Therefore, at a certain time, the rate of extraction of $CO_2$ from the water by the oil exceeds the rate of $CO_2$ dissolution in the oil which results in the nucleation of $CO_2$ among the oil.
- The growth of $CO_2$-rich phase within the oil surrounded by water results in enlargement of the isolated oil ganglia. The nucleation of dense $CO_2$ within the oil (surrounded by water) leads to the extraction of oil components by $CO_2$ and the volume of $CO_2$-rich phase increases.
- Heavy oil recovered by $CO_2$ injection can have a significantly lower amount of metal elements such as nickel and vanadium.
- Intermittent gas injection in heavy oil reservoirs improves oil recovery while the utilisation of gas is significantly reduced. The improvement is due to the increase in the residence time of gas in porous media.
- A relatively enriched hydrocarbon gas (i.e. VRG) can enhance heavy oil recovery by mechanisms associated with the dissolution of gas in the oil.
- Waterflood after an extended period of $CO_2$ or VRG can recover a considerable amount of the remaining oil in porous media by improving the sweep efficiency.
- It is crucial to evaluate the performance of any process of gas injection for EHOR under the actual conditions of the reservoirs.

- The presence of dissolved gas in heavy oil would affect the performance of co-injection of $CO_2$ and surfactant. Thus, it is essential to evaluate the phase behaviour of surfactant and oil under actual reservoir conditions.
- A properly designed and executed $CO_2$ or VRG injection can recover a significant fraction of heavy oil at reservoir conditions.

## 7.2 Recommendations

The results of the coreflood experiments in this study indicated that viscous fingering is a signature of water or gas injection for displacing heavy oil. Thus, it is crucial to carefully evaluate the impacts of this flow regime on the performance of oil recovery by extending the experiments to a larger scale as well as performing visualisation of the coreflood experiments. The visualisation of the coreflood experiments will lead to a better understanding of the formation of fingers in unstable flow regimes. In addition, the benefit of having high-resolution in-situ maps of the flow and different phases in porous media will significantly assist the quality of the simulation of the experimental processes. That is, it is recommended to perform water or gas injection experiments in horizontal direction since the displacement in actual reservoirs is mainly in the horizontal direction. Therefore, the impacts of gravity on the process of oil recovery would be more pronounced.

Some of the mechanisms discussed in this study had not been reported in detail in the literature. Although the miscibility between $CO_2$ and heavy oil is not generally achievable, the mass transfer between two phases still dominates the process of heavy oil recovery by $CO_2$ injection. It was shown that how the mechanisms associated with mass transfer between oil and $CO_2$ can affect the process of heavy oil recovery. To truly investigate the impacts of these mechanisms on the performance of oil recovery by $CO_2$ injection, it is crucial to understand the properties of the fluids at different stages of the processes. This, however, is a huge challenge and it requires extensive characterization study of the fluids under various stages of an experiment.

Another contribution of the laboratory experimental results is to predict the behaviour of field-scale systems. For this purpose, the experimental data from laboratory must be converted to a different set of input (data) to be able to represent the processes at an appropriate large-scale. The accuracy of the field-scale forecasts will be a crucial function of the data being used as input for the modelling and simulation and that highlights the importance of the process of upscaling. Therefore, it is necessary to conduct experiments to gain information on the impacts of various factors such as time on the process of oil recovery. For example, it is crucial to measure the diffusion coefficient of $CO_2$ into the

oil and to account for the impacts of porous media and viscous fingering on the rate of diffusion.

In addition, to predict the behaviour of a large-scale scheme of $CO_2$ injection for heavy oil recovery, it is essential to take into account all the mechanisms which contribute to the process of oil recovery. Therefore, it is important to develop a proper numerical model which is able to consider all the mechanisms of the process of heavy oil recovery by $CO_2$ injection.

## REFERENCES


Administration, U. E. I., 2013. *Technically Recoverable shale Oil and Shale Gas Resources: An Assessment of 137 Shale Formations in 141 Countries Outside the United States,* Washington, DC: U.S. Energy Information Administration.

Ahmadloo, F., Asghari, K. & Renouf, G., 2010. Performance of Waterflooding in Western Canadian Heavy Oil Reservoirs Using Artificial Neural Network. *Energy & Fuels,* Volume 24, pp. 2520-2526.

Al Ghafri, S., Maitland, G. & Trusler, J., 2014. Experimental and Modeling Study of the Phase Behavior of Synthetic Crude Oil+CO2. *Fluid Phase Equilibria,* 365(01), pp. 20-40.

Al-Murayri, M., Harding, T. & Maini, B., 2011. Impact of Noncondensable Gas on Performance of Steam-Assisted Gravity Drainage. *Journal of Canadian Petroleum Technology,* 50(7-8), pp. 46-54.

Alshmakhy, A. & Maini, B., 2012. Foamy-Oil-Viscosity Measurement. *Journal of Canadian Petroleum Technology,* 51(01), pp. 60-65.

Anderson, W., 1987. Wettability Literature Survey-Part 6: The Effects of Wettability on Waterflooding. *Journal of Petroleum Technology,* 39(12), pp. 1605-1622.

Angstadt, H. & Tsao, H., 1987. Kinetic Study of the Decomposition of Surfactants for EOR. *SPE Reservoir Engineering,* 2(04), pp. 613-618.

Appel, C., L.Q., M., Dean Rhue, R. & Kennelley, E., 2003. Point of Zero Charge Determination in Soils and Minerals via Traditional Methods and Detection of Electroacoustic Mobility. *Geoderma,* 113(01), pp. 77-93.

Asakawa, K., 2005. *A Generalized Analysis of Partitioning Interwell Tracer Tests,* Austin, Texas: The University of Texas at Austin, PhD Thesis.

Asghari, K. & Nakutnyy, P., 2008. *Experimental Results of Polymer Flooding of Heavy Oil Reservoirs,* Calgary, Alberta: Canadian International Petroleum Conference, 17-19 June.

Atkinson, H., 1927. *Recovery of Petroleum from Oil Bearing Sands.* USA, Patent No. US1651311 A.

Attanucci, V., Asbsen, K., Hejl, K. & Wright, C., 1993. *WAG Process Optimization in the Rangely CO2 Miscible Flood,* Houston: SPE Annual Technical Conference and Exhibition, 3-6 October.

Badamchizadeh, A., Maini, B. & Yarranton, H., 2008. *Applicability of CO2-Based Vapex Process to Recover Athabasca Bitumen,* Calgary, Canada: International Thermal

Operations and Heavy Oil Symposium, 20-23 October.

Behbahani, T., Ghotbi, C., Taghikhani, V. & Shahrabadi, A., 2012. Investigation on Asphaltene Deposition Mechanisms during CO2 Flooding Processes in Porous Media: A Novel Experimental Study and a Modified Model Based on Multilayer Theory for Asphaltene Adsorption. *Energy & Fuels,* 26(08), pp. 5080-5091.

Berg, L., Stensen, J., Crapez, B. & Quale, A., 2002. *SWAG Injectivity Behaviour Based on Siri Field Data,* Tulsa, OK: SPE/DOE Improved Oil Recovery Symposium, 13-17 April.

Bijeljic, B., Muggeridge, A. & Blunt, M., 2002. *Effect of Composition on Waterblocking for Multicomponent Gasfloods,* San Antonio, Texas: SPE Annual Technical Conference and Exhibition, 29 September-2 October.

Bracho, L. & Oquendo, O., 1991. *Steam-Solvent Injection, Well LSJ-4057, Tia Juana Field, Western Venezuela,* Bakersfield, California: SPE International Thermal Operations Symposium, 7-8 February.

Bryan, J. & Kantzas, A., 2009. Potential for Alkali-Surfactant Flooding in Heavy Oil Reservoirs Through Oil-in-Water Emulsification. *Journal of Canadian Petroleum Technology,* 48(02), pp. 37-46.

Bryan, J., Mai, A. & Kantzas, A., 2008. *Investigation Into the Processes Responsible for Heavy Oil Recovery by Alkali-Surfactant Flooding,* Tulsa, Oklahoma: SPE Symposium on Improved Oil Recovery, 20-23 April.

Buckley, J. & Jianxin, W., 2002. Crude Oil and Asphaltene Characterization for Prediction of Wetting Alteration. *Journal of Petroleum Science and Engineering,* 33(1-3), pp. 195-202.

Buckley, S. & Leverett, M., 1942. Mechanism of Fluid Displacement in Sands. *Transactions of the AIME,* 146(01), pp. 107 - 116.

Butler, R. & McNab, G., 1981. Theoretical Studies on the Gravity Drainage of Heavy Oil During In Situ Steam Heating. *Journal of Canadian Petroleum Technology,* 59(04), pp. 455-460.

Butler, R. & Mokrys, I., 1989. Solvent Analog Model of Steam-Assisted Gravity Drainage. *AOSTRA Journal of Research,* 5(17), pp. 17-32.

Butler, R. & Stephens, D., 1981. The Gravity Drainage of Steam-heated Heavy Oil to Parallel Horizontal Wells. *Journal of Canadian Petroleum Technology,* pp. 90-96.

Campbell, B. & Orr, F., 1985. Flow Visualization for CO2/Crude-Oil Displacements. *SPE Journal,* 25(05), pp. 665-678.

Cao, G. et al., 2007. *Technical Breakthrough in PCPs' Scaling Issue of ASP Flooding in*

*Daqing Oilfield*, Anaheim, California: SPE Annual Technical Conference and Exhibition, 11-14 November.

Carig, F., 1971. *The Reservoir Engineering Aspects of Waterflooding.* 01 ed. New York: Society of Petroleum Engineering Monograph Series.

Caudle, B. & Dyes, A., 1958. Improving Miscible Displacement by Gas-Water Injection. *Petroleum Transactions, AIME,* Volume 213, pp. 281-284.

Century, J., 2008. Tar Sands: Key Geological Risks and Opportunities. *The Leading Edge,* 27(09), pp. 1202-1204.

Chopra, S., Lines, L., Schmitt, D. & Batzle, M., 2010. *Heavy Oils: Reservoir Characterization and Production Monitoring.* 1st ed. s.l.:Society of Exploration Geophysicists.

Christensen, J., Stenby, E. & Skauge, A., 2001. Review of WAG Experience. *SPE Reservoir Evaluation & Engineering,* 4(02), pp. 97-106.

Clifford, P. & Sorbie, K., 1985. *The Effects of Chemical Degradation on Polymer Flooding,* Phoenix, Arizona: SPE Oilfield and Geothermal Chemistry Symposium, 9-11 March.

Cuthiell, D., Mccarthy, C., Kissel, G. & Cameron, S., 2006. *The Role of Capillarity in VAPEX,* Calgary, Canada: Canadian International Petroleum Conference, 13-15 June.

Danesh, A., 1998. *PVT and Phase Behaviour of Petroleum Reservoir Fluids.* Edinburgh, Scotland: Elsevier.

Das, S. & Butler, R., 1998. Mechanism of the Vapour Extraction Process for Heavy Oil and Bitumen. *Journal of Petroleum Science and Engineering,* 21(1-2), pp. 43-59.

Deans, H., 1978. *Using Chemical Tracers to Measure Fractional Flow and Saturation In-Situ,* Tulsa, OK: SPE Symposium on Improved Methods of Oil Recovery, 16-17 April.

Deasault, M., 2001. *Comparing Venezuelan and Canadian Heavy Oil and Tar Sands,* Calgary: Petroleum Society's Canadian International Petroleum Conference.

Delgado, D., Vittoratos, E. & Kovscek, A., 2013. *Optimal Voidage Replacement Ratio for Viscous and Heavy Oil Reservoirs,* Monterey, California: SPE Western Regional & AAPG Section Meeting, 19-25 April.

Dong, M. & Huang, S., 2002. Flue Gas Injection for Heavy Oil Recovery. *Journal of Canadian Petroleum Technology,* 41(09), pp. 44-50.

Doorwar, S. & Mohanty, K., 2011. *Viscous Fingering during Non-Thermal Heavy Oil Recovery,* Denver, USA: SPE Annual Technical Conference and Exhibition, 30 October-2 November.

Doorwar, S. & Mohanty, K., 2015. *Viscous Fingering Function for Unstable Immiscible*

*Flows,* Houston, USA: SPE Reservoir Simulation Symposium, 23-25 February.

Dunn, S., Nenniger, E. & Rajan, V., 1989. A Study of Bitumen Recovery by Gravity Drainage Using Low Temperature Soluble Gas Injection. *Canadian Journal of Chemical Engineering,* 67(06), pp. 978-991.

Dyes, A., 1954. Production of Water-Driven Reservoirs Below Their Bubblepoint. *Journal of Petroleum Technology,* 6(10), pp. 31-35.

Emadi, A., 2012. *Enhanced Heavy Oil Recovery by Water and Carbon Dioxide Flood,* Edinburgh, UK: Heriot-Watt University, PhD Thesis.

Emadi, A. et al., 2011. *Visual Investigation of Extra-heavy Oil Recovery by CO2/N2 Foam Injection,* Cambridge, UK: 16th European Symposium on Improved Oil Recovery, 12-14 April.

Emadi, A., Sohrabi, M., Jamiolahmady, M. & Ireland, S., 2012. *Visualization of Oil Recovery by CO2-Foam Injection; Effect of Oil Viscosity and Gas Type,* Tulsa, OK, USA: SPE Improved Oil Recovery Symposium, 14-18 April.

Fabbri, C. et al., 2013. *Secondary Polymer Flooding in Extra-Heavy Oil: Gaining Information on Polymer-Oil Relative Permeabilities,* Kuala Lumpur, Malaysia: SPE Enhanced Oil Recovery Conference, 2-4 July.

Farooq, U., Tweheyo, M., Sjöblom, J. & Øye, G., 2011. Surface Characterization of Model, Outcrop, and Reservoir Samples in Low Salinity Aqueous Solutions. *Journal of Dispersion Science and Technology,* 32(04), pp. 519-531.

Farouq Ali, S. & Meldau, R., 1999. *Practical Heavy Oil Recovery.* Calgary: University of Calgary.

Farzaneh, S., 2015. *Investigation of Enhanced Heavy Oil Recovery by CO2 Flood Under Various Injection Strategies,* Edinburgh, UK: Heriot-Watt University, PhD Thesis.

Fathi, S., Austad, T. & Strand, S., 2011. Water-Based Enhanced Oil Recovery (EOR) by "Smart Water": Optimal Ionic Composition for EOR in Carbonates. *Energy & Fuels,* 25(11), pp. 5173-5179.

Fayers, F., Jouaux, F. & Tchelepi, H., 1994. An Improved Macroscopic Model for Viscous Fingering and Its Validation for 2D and 3D Flows. I. Non-gravity Flows. *In Situ,* 18(01), pp. 43-78.

Feng, A. et al., 2012. *Study of Surfactant-Polymer Flooding in Heavy Oil Reservoirs,* Calgary: SPE Heavy Oil Conference Canada, 12-14 June.

Firoozabadi, A., 2001. Mechanisms of Solution Gas Drive in Heavy Oil Reservoirs. *Journal of Canadian Petroleum Technology,* 40(03), pp. 15-20.

Flaaten, A., Nguyen, Q., Pope, G. & Zhang, J., 2009. A Systematic Laboratory Approach

to Low-Cost, High-Performance Chemical Flooding. *SPE Reservoir Evaluation & Engineering,* 12(05), pp. 713-723.

Fletcher, A., Weston, S., Haynes, A. & Clough, M., 2013. *The Successful Implementation of a Novel Polymer EOR Pilot in the Low Permeability Windalia Field,* Kuala Lumpur, Malaysia: SPE Enhanced Oil Recovery Conference, 2-4 July.

Garcia, J. & Pruess, K., 2003. *Flow Instabilities During Injection of CO2 into Saline Aquifers,* LBNL, Berkeley: Proceedings Tough Symposium.

Ghasemi, M. & Whitson, C., 2015. *Compositional Variation in SAGD,* Houston: SPE Annual Technical Conference and Exhibition, 28-30 September.

Glover, C., Puerto, M., Maerker, J. & Sandvik, E., 1979. Surfactant Phase Behavior and Retention in Porous Media. *SPE Journal,* 19(03), pp. 183-193.

Goyal, K. & Kumar, S., 1989. Steamflooding for Enhanced Oil Recovery. In: E. Donaldson, G. Chilingarian & T. Yen, eds. *Enhanced Oil Recovery, II — Processes and Operations.* The Netherlands: Elsevier, pp. 317-349.

Greenkorn, R., 1962. Experimental Study of Waterflood Tracers. *Journal of Petroleum Technology,* 14(01), pp. 87-92.

Gupta, R. & Mohanty, K., 2010. Temperature Effects on Surfactant-Aided Imbibition Into Fractured Carbonates. *SPE Journal,* 15(03), pp. 588-597.

Gupta, S. & Trushenski, S., 1979. Micellar Flooding-Compositional Effects on Oil Displacement. *SPE Journal,* 19(02), pp. 116-128.

Hagedorn, K. & Orr, F., 1994. Component Partitioning in CO2/Crude Oil Systems: Effects of Oil Composition on CO2 Displacement Performance. *SPE Advanced Technology Series,* 2(02), pp. 177-184.

Haghighat, P. & Maini, B., 2010. Role of Asphaltene Precipitation in VAPEX Process. *Journal of Canadian Petroleum Technology,* 49(03), pp. 14-21.

Halevy, E. & Nir, A., 1958. *Use of Radioisotopes in the Study of Underground Flow, Part II. The Characteristics of the Tracer Pulse Shape.* Geneva, Second United Nations International Conference on the Peaceful Uses of Atomic Energy, pp. 162-165.

Hamouda, A. & Alipour Tabrizy, V., 2013. The Effect of Light Gas on Miscible CO2 Flooding to Enhance Oil Recovery from Sandstone and Chalk Reservoirs. *Journal of Petroleum Science and Engineering,* 108(01), pp. 259-266.

Head, I., Jones, D. & Larter, S., 2003. Biological Activity in the Deep Subsurface and the Origin of Heavy Oil. *Nature,* Volume 426, pp. 344-352.

Hill, H. et al., 1974. *The Behavior of Polymers in Porous Media,* Tulsa, Oklahoma: SPE Improved Oil Recovery Symposium, 22-24 April.

Hirasaki, G., 1982. Ion Exchange With Clays in the Presence of Surfactant. *SPE Journal*, 22(02), pp. 181-192.

Hirasaki, G., Miller, C. & Puerto, M., 2011. Recent Advances in Surfactant EOR. *SPE Journal*, 16(04), pp. 889-907.

Holm, L. & Josendal, V., 1974. Mechanisms of Oil Displacement by Carbon Dioxide. *Journal of Canadian Petroleum Technology*, 26(12), pp. 1427-1438.

Homsy, G., 1987. Viscous Fingering in Porous Media. *Annual Review of Fluid Mechanics*, 19(01), pp. 271-311.

Huh, C., Lange, E. & Cannella, W., 1990. *Polymer Retention in Porous Media*, Tulsa, OK: SPE/DOE Enhanced Oil Recovery Symposium, 22-25 April.

Hwang, J., Park, S., Deo, M. & Hanson, F., 1995. Phase Behavior of CO2/Crude Oil Mixtures in Supercritical Fluid Extraction System: Experimental Data and Modeling. *Industrial & Engineering Chemistry Research*, 34(04), pp. 1280-1286.

Idem, R. & Ibrahim, H., 2002. Kinetics of CO2-Induced Asphaltene Precipitation from Various Saskatchewan Crude Oils during CO2 Miscible Flooding. *Journal of Petroleum Science and Engineering*, 35(3-4), pp. 233-246.

Jadhunandan, P. & Morrow, N., 1995. Effect of Wettability on Waterflood Recovery for Crude-Oil/Brine/Rock Systems. *SPE Reservoir Engineering*, 10(01), pp. 40-46.

Jayasekera, A. & Goodyear, S., 2000. The Development of Heavy Oil Field in the United Kingdom Continental Shelf: Past, Present, and Future. *SPE Reservoir Evaluation & Engineering*, 3(05), pp. 371-379.

Jennings, H. J., 1975. A Study of Caustic Solution-Crude Oil Interfacial Tensions. *SPE Journal*, 15(03), pp. 197-202.

Jerauld, G., 1997. General Three-Phase Relative Permeability Model for Prudhoe Bay. *SPE Reservoir Engineering*, 12(04), pp. 255-263.

Kaczmarczyk, R., Herbas, J. & Castillo, J., 2013. *Approximations of Primary, Secondary and Tertiary Recovery Factor in Viscous and Heavy Oil Reservoirs*, Aberdeen, UK: SPE Offshore Europe Oil and Gas Conference and Exhibition, 3-6 September.

Kim, T., Vittoratos, E. & Kovscek, A., 2015. *An Experimental Investigation of Viscous Oil Recovery Efficiency as a Function of Voidage Replacement Ratio*, Grove, California: SPE Western Regional Meeting, 27-30 April.

Klins, M., 1984. *Carbon Dioxide Flooding: Basic Mechanisms and Project Design.* 1st ed. Boston: D. Reidel Publishing Company.

Koliander, W. & Kunar-Schreferl, G., 2000. *The Metal Content of Crude Oils and Its Influence on Crude Oil Processing*, Calgary, Canada: 16th World Petroleum Congress,

11-15 June.

Kumar, M., Hoang, V., Satik, C. & Rojas, D., 2008. High-Mobility-Ratio Waterflood Performance Prediction: Challenges and New Insights. *SPE Reservoir Evaluation & Engineering*, 11(01), pp. 186-196.

Laidler, K. & Meiser, J., 1982. *Physical Chemistry.* 1st ed. Menlo Park, California: Benjamin/Cummings Publishing Company.

Lake, L., 1989. *Enhanced Oil Recovery.* 1st ed. Englewood Cliffs: Prentice Hall.

Larter, S. et al., 2003. The controls on the Composition of Biodegraded Oils in the Deep Subsurface - Part 1: Biodegradation Rates in Petroleum Reservoirs. *Organic Geochemistry,* 34(04), pp. 601-613.

Lee, A. & Eakin, B., 1964. Gas-Phase Viscosity of Hydrocarbon Mixtures. *SPE Journal,* Volume 4, pp. 247-249.

Li, H., Zheng, S. & Yang, D., 2013. Enhanced Swelling Effect and Viscosity Reduction of Solvent(s)/CO2/Heavy-Oil Systems. *SPE Journal,* 18(04), pp. 695-707.

Li, K. et al., 2014. Novel Method for Characterizing Single-Phase Polymer Flooding. *SPE Journal,* 19(04), pp. 695-702.

Lillico, D. et al., 2001. Gas Bubble Nucleation Kinetics in a Live Heavy Oil. *Colloids and Surfaces,* 192(1), pp. 25-38.

Liu, Q., Dong, M. & Ma, S., 2006. *Alkaline/Surfactant Flood Potential in Western Canadian Heavy Oil Reservoirs,* Tulsa, Oklahoma: SPE/DOE Symposium on Improved Oil Recovery, 22-26 April.

Luo, P. & Gu, Y., 2005. *Effects of Asphaltene Content and Solvent Concentration on Heavy Oil Viscosity,* Calgary, Canada: SPE International Thermal Operations and Heavy Oil Symposium, 1-3 November.

Luo, P., Zhang, Y., Wang, X. & Huang, S., 2012. Propane-Enriched CO2 Immiscible Flooding for Improved Heavy Oil Recovery. *Energy & Fuels,* 26(04), pp. 2124-2135.

Maerker, J., 1975. Shear Degradation of Partially Hydrolyzed Polyacrylamide Solutions. *SPE Journal,* 15(04), pp. 311-322.

Mai, A. & Kantzas, A., 2009. Heavy Oil Waterflooding: Effects of Flow Rate and Oil Viscosity. *Journal of Canadian Petroleum Technology,* 48(03), pp. 42-51.

Manichand, R. & Seright, R., 2014. Field vs. Laboratory Polymer-Retention Values for a Polymer Flood in the Tambaredjo Field. *SPE Reservoir Evaluation & Engineering,* 17(03), pp. 314-325.

Martinez-Palou, R. et al., 2011. Transportation of Heavy and Extra-heavy Crude Oil by Pipeline: A Review. *Journal of Petroleum Science and Engineering,* 75(3-4), pp. 274-

282.

McGuire, P. et al., 2005. *Viscosity Reduction WAG: An Effective EOR Process for North Slope Viscous Oils,* Irvine, USA: SPE Western Regional Meeting, 30 March-1 April.

Menzie, D. & Nielsen, R., 1963. A Study of the Vaporization of Crude Oil by Carbon Dioxide Repressuring. *Journal of Petroleum Technology,* 15(11), pp. 1247-1252.

Meyer, R. F. & Attanasi, E. D., 2003. *Heavy Oil and Natural Bitumen--Strategic Petroleum Resources,* Virginia: U.S. Geological Survey.

Miller, J. & Jones, R., 1981. *A Laboratory Study to Determine Physical Characteristics of Heavy Oil After CO2 Saturation,* Tulsa, Oklahoma: SPE/DOE Enhanced Oil Recovery Symposium, 5-8 April.

Mitchell, D. & Speight, J., 1973. The Solubility of Asphaltenes in Hydrocarbon Solvents. *Fuel,* 52(02), pp. 149-152.

Moffitt, P., Pecore, D., Trees, M. & Salts, G., 2015. *East Vacuum Grayburg San Andres Unit, 30 Years of CO2 Flooding: Accomplishments, Challenges and Opportunities,* Houston, USA: SPE Annual Technical Conference and Exhibition, 28-30 September.

Mokrys, I. & Butler, K., 1993. *In-Situ Upgrading of Heavy Oils and Bitumen by Propane Deasphalting: The Vapex Process,* Oklahoma City, USA: SPE Production Operations Symposium, 21-23 March.

Mumgan, N., 1981. Carbon Dioxide Flooding-Fundamentals. *Journal of Canadian Petroleum Technology,* 20(01), pp. 87-92.

Nelson, R., Lawson, J., Thigpen, D. & Stegemeier, G., 1984. *Cosurfactant-Enhanced Alkaline Flooding,* Tulsa, OK: SPE Enhanced Oil Recovery Symposium, 15-18 April.

Nghiem, L., Sammon, P. & Kohse, B., 2001. *Modeling Asphaltene Precipitation and Dispersive Mixing in the VAPEX Process,* Houston, USA: SPE Reservoir Simulation Symposium, 11-14 February.

Nguyen, T. & Farouq Ali, S., 1993. *Immiscible Carbon Dioxide Floods, Using Impure Gas in the WAG Mode,* Calgary, Alberta: Petroleum Society of Canada Annual Technical Meeting, May 9 - 12.

Nguyen, T. & Farouq Ali, S., 1998. Effect of Nitrogen on the Solubility and Diffusivity of Carbon Dioxide into Oil and Oil Recovery by the Immiscible WAG Process. *Journal of Canadian Petroleum Technology,* 37(02), pp. 24-31.

NIST, 2014. *Thermophysical Properties of Fluid Systems.* [Online] Available at: http://webbook.nist.gov/chemistry/fluid/ [Accessed 05 February 2014].

Orr, F. & Silva, M., 1987. Effect of Oil Composition on Minimum Miscibility Pressure-Part 2: Correlation. *SPE Reservoir Engineering,* 2(04), pp. 479-491.

Owen, E. W., 1975. *Trek of the Oil Finders: A History of Exploration for Petroleum.* 1st ed. Tulsa, OK: American Association of Petroleum Geologists.

Pan, H. et al., 2014. *Phase Behavior Modeling and Flow Simulation for Low-Temperature CO2 Injection*, Amsterdam, The Netherlands: SPE Annual Technical Conference and Exhibition, 27-29 October.

Prats, M., 1982. *Thermal Recovery.* Richardson, Texas: Society of Petroleum Engineers.

Pulkrabek, W. W., 1997. *Engineering Fundamentals of the Internal Combustion Engine.* New Jersey: Prentice Hall.

Qazvini Firouz, A. & Torabi, F., 2014. Utilization of Carbon Dioxide and Methane in Huff-n-Puff Injection Scheme to Improve Heavy Oil Recovery. *Fuel,* Volume 117, pp. 966-973.

Quale, E., Crapez, B., Stensen, J. & Berge, L., 2000. *SWAG Injection on the Siri Field - An Optimized Injection System for Less Cost,* Paris: SPE European Petroleum Conference, 24-25 October.

Ratnakar, R. & Dindoruk, B., 2015. Measurement of Gas Diffusivity in Heavy Oils and Bitumens by Use of Pressure-Decay Test and Establishment of Minimum Time Criteria for Experiments. *SPE Journal,* 20(05), pp. 1167-1180.

Reid, R., Prausnitz, J. & Sherwood, T., 1977. *The Properties of Gases and Liquids.* 3rd ed. New York: McGraw-Hill.

Riazi, M. R. & Whitson, C. H., 1993. Estimating Diffusion Coefficients of Dense Fluids. *Industrial & Engineering Chemistry Research*, pp. 3081-3088.

Riebeek, H., 2011. *Earth Observatory.* [Online] Available at: http://earthobservatory.nasa.gov/Features/CarbonCycle/printall.php [Accessed 05 May 2016].

Robinson, D. & Peng, D., 1978. *The Characterization of the Heptanes and Heavier Fractions for the GPA Peng-Robinson Programs.* Tulsa, OK: Gas Processors Association.

Romanowski, L. & Thomas, K., 1985. *Hot-gas Injection in Asphalt Ridge Tar Sand,* Laramie, WY: National Energy Technology Laboratory.

Romm, J., 2006. *Hell and High Water: Global Warming - The Solution and the Politics - and What We Should Do.* New York: HarperCollins.

Samuelson, M. & Constien, V., 1996. *Effects of High Temperature on Polymer Degradation and Cleanup,* Denver, Colorado: SPE Annual Technical Conference and Exhibition, 6-9 October.

Sandrea, R., 2012. *Evaluating production potential of mature US oil, gas shale plays.*

[Online] Available at: http://www.ogj.com [Accessed 02 January 2016].

Sankur, V. & Emanuel, A., 1983. *A Laboratory Study of Heavy Oil Recovery With CO2 Injection,* Ventura, California: SPE California Regional Meeting, 23-25 March.

Sarathi, P., 1999. *In-situ Combustion Handbook - Principles and Practices.* Tulsa, OK: U.S. Department of Energy .

Sayegh, S. & Maini, B., 1984. Laboratory Evaluation Of The CO2 Huff-N-Puff Process For Heavy Oil Reservoirs. *Journal of Canadian Petroleum Technology,* 23(03), pp. 29-36.

Sayegh, S., Rao, D., Kokal, S. & Najman, J., 1990. Phase Behaviour and Physical Properties of Lindbergh Heavy Oil/CO2 Mixtures. *Journal of Canadian Petroleum Technology,* 29(06), pp. 31-39.

Schmidt, G., Ruedy, R., Miller, R. & Lacis, A., 2010. Attribution of the Present-day Total Greenhouse Effect. *Journal of Geophysical Research,* 115(D20), pp. 1-6.

Seright, R., Fan, T., Wavrik, K. & Balaban, R., 2011. New Insights Into Polymer Rheology in Porous Media. *SPE Journal,* 16(01), pp. 35-42.

Seyyedsar, S., Ghazanfari, M. & Taghikhani, V., 2014. Experimental Investigation of Simultaneous Water and CO2 (SWACO2) Injection for Oil Recovery in Immiscible and Near-miscible Conditions: A Comparative Study. *The Canadian Journal of Chemical Engineering,* 92(10), pp. 1791-1797.

Sharma, M., Kuo, J. & Yen, T., 1987. Further Investigation of the Surface Charge Properties of Oxide Surfaces in Oil-bearing Sands and Sandstones. *Journal of Colloid and Interface Science,* 115(01), pp. 9-16.

Shook, G., Pope, G. & Asakawa, K., 2009. *Determining Reservoir Properties and Flood Performance From Tracer Test Analysis*, New Orleans, USA: SPE Annual Technical Conference and Exhibition, 4-7 October.

Simon, R., Rosman, A. & Zana, E., 1978. Phase Behaviour Properties of CO2-Reservoir Oil Systems. *SPE Journal,* 18(01), pp. 20-26.

Sirvastava, M. & Nguyen, Q., 2010. *Application of Gas for Mobility Control in Chemical EOR in Problematic Carbonate Reservoirs,* Tulsa, OK: SPE Improved Oil Recovery Symposium, 24-28 April.

Skauge, A. et al., 2012. *2-D Visualisation of Unstable Waterflood and Polymer Flood for Displacement of Heavy Oil,* Tulsa, Oklahoma: SPE Improved Oil Recovery Symposium, 14-18 April.

Skauge, T. et al., 2014. *Polymer Flood at Adverse Mobility Ratio in 2D Flow by X-ray Visualization,* Muscat, Oman: SPE EOR Conference at Oil and Gas West Asia, 31 March-

2 April.

Sohrabi, M., Danesh, A. & Jamiolahmady, M., 2008. Visualisation of Residual Oil Recovery by Near-miscible Gas and SWAG Injection Using High-pressure Micromodels. *Transport in Porous Media,* 74(02), pp. 239-257.

Sohrabi, M. & Emadi, A., 2012. *Novel Insights into the Pore-Scale Mechanisms of Enhanced Oil Recovery by CO2 Injection,* Copenhagen, Denmark: EAGE Annual Conference & Exhibition incorporating SPE Europec, 4-7 June.

Southwick, J. & Manke, C., 1988. Molecular Degradation, Injectivity, and Elastic Properties of Polymer. *SPE Reservoir Engineering,* 3(04), pp. 1193-1201.

Speight, J., 2011. *An Introduction to Petroleum Technology, Economics, and Politics.* 1st ed. Canada: John Wiley & Sons and Scrivener Publishing.

Speight, J., Long, R. & Trowbridge, T., 1984. Factors Influencing the Separation of Asphaltenes from Heavy Petroleum Feedstocks. *Fuel,* 63(05), pp. 616-620.

Srivastava, R., Huang, S. & Dong, M., 1999. Asphaltene Deposition During CO2 Flooding. *SPE Production & Facilities,* 14(04), pp. 235-245.

Stephenson, D., Graham, A. & Luhning, R., 1993. Mobility Control Experience in the Joffre Viking Miscible CO2 Flood. *SPE Reservoir Engineering,* 8(03), pp. 183-188.

Svrcek, W. & Mehrotra, A., 1982. Gas Solubility, Viscosity and Density Measurements for Athabasca Bitumen. *Journal of Canadian Petroleum Technology,* 21(04), pp. 31-38.

Sydansk, D. & Seright, S., 2007. When and Where Relative Permeability Modification Water-Shutoff Treatments Can Be Successfully Applied. *SPE Production & Operations,* 22(02), pp. 236-247.

Talbi, K. & Maini, B., 2008. Experimental Investigation of CO2-based VAPEX for Recovery of Heavy Oils and Bitumen. *Journal of Canadian Petroleum Technology,* 47(04), pp. 29-36.

Tang, G.-Q. & Kovscek, A., 2011. High-Resolution Imaging of Unstable, Forced Imbibition in Berea Sandstone. *Transport in Porous Media,* Volume 86, pp. 647-664.

Targac, G. et al., 2005. *Unlocking the Value in West Sak Heavy Oil,* Calgary, Canada: SPE International Thermal Operations and Heavy Oil Symposium, 1-3 November.

Terwilliger, P. et al., 1951. An Experimental and Theoretical Investigation of Gravity Drainage Performance. *Journal of Petroleum Technology,* 3(11), pp. 285-296.

Thomas, S., 2008. Enhanced Oil Recovery - An Overview. *Oil & Gas Science and Technology,* 63(01), pp. 9-19.

Totten, G. E., 2004. A timeline of Highlights from the Histories of ASTM Committee D02 and the Petroleum Industry. *ASTM Standardization News,* pp. 18-27.

Unatrakarn, D., Asghari, K. & Condor, J., 2011. Experimental Studies of CO2 and CH4 Diffusion Coefficient in Bulk Oil and Porous Media. *Energy Procedia*, Volume 4, pp. 2170-2177.

Uren, L. & Fahmy, E., 1927. Factors Influencing the Recovery of Petroleum from Unconsolidated Sands by Waterflooding. *Transactions of the AIME*, 77(01), pp. 318-335.

Urquhart, R., 1986. Heavy Oil Transportation - Present and Future. *Journal of Canadian Petroleum Technology*, 25(02), pp. 68-71.

Vazquez, D. & Mansoori, G., 2000. Identification and Measurement of Petroleum Precipitates. *Journal of Petroleum Science and Engineering*, 26(1-4), pp. 49-55.

Vermeulen, T., 2011. *Knowledge Sharing Report - CO2 Liquid Logistics Concept (LLSC): Overall Supply Chain Optimization*, The Hague, The Netherlands: Tebodin Netherlands B.V.

Vignes, A., 1966. Diffusion in Binary Solutions. *Industrial & Engineering Chemistry Fundamentals*, pp. 189-199.

Vittoratos, E., Coates, R. & West, C., 2011. *Optimal Voidage Replacement Ratio for Communicating Heavy Oil Waterflood Wells*, Kuwait City: SPE Heavy Oil Conference and Exhibition, 12-14 December.

Vittoratos, S. & West, C., 2010. *Optimal Heavy Oil Waterflood Management May Differ from that of Light Oils*, Muscat, Oman: SPE EOR Conference at Oil & Gas West Asia, 11-13 April.

Wang, S., Chen, S. & Li, Z., 2016. Characterization of Produced and Residual Oils in the CO2 Flooding Process. *Energy & Fuels*, 30(01), pp. 54-62.

Welge, H., 1952. A Simplified Method for Computing Oil Recovery by Gas or Water Drive. *Journal of Petroleum Technology*, 4(04), pp. 91-98.

Wellington, S., 1983. Biopolymer Solution Viscosity Stabilization - Polymer Degradation and Antioxidant Use. *SPE Journal*, 23(06), pp. 901-912.

Willhite, G., 1986. *Waterflooding.* Richardson, Texas: Society of Petroleum Engineers.

Wu, D. et al., 2001. *Emulsification and Stabilization of ASP Flooding Produced Liquid*, Anaheim, California: SPE Annual Technical Conference and Exhibition, 11-14 November.

Wu, Y., Pruess, K. & Chen, Z., 1993. Buckley-Leverett Flow in Composite Porous Media. *SPE Advanced Technology Series*, 1(02), pp. 36-42.

Yang, D., Tontiwachwuthikul, P. & Gu, Y., 2005. Interfacial Tensions of the Crude Oil + Reservoir Brine + CO2 Systems at Pressures up to 31 MPa and Temperature of 27 and 58 C. *Journal of Chemical and Engineering Data*, 50(04), pp. 1242-1249.

Yildiz, H. & Morrow, N., 1996. Effect of brine composition on recovery of Moutray crude oil by waterflooding. *Journal of Petroleum Science and Engineering,* 14(03), pp. 159-168.

Yin, Y. & Yen, A., 2000. *Asphaltene Deposition and Chemical Control in CO2 Floods,* Tulsa, Oklahoma: SPE/DOE Improved Oil Recovery Symposium, 3-5 April.

Zaitoun, A., Bertin, H. & Lasseux, D., 1998. *Two-Phase Flow Property Modifications by Polymer Adsorption,* Tulsa, Oklahoma: SPE/DOE Improved Oil Recovery Symposium, 19-22 April.

Zaitoun, A., Kohler, N. & Montemurro, M., 1992. *Control of Water Influx in Heavy-Oil Horizontal Wells by Polymer Treatment,* Washington, DC: SPE Annual Technical Conference and Exhibition, 4-7 October.

Zanganeh, P. et al., 2011. Asphaltene Deposition during CO2 Injection and Pressure Depletion: A Visual Study. *Energy & Fuels,* 26(01), pp. 1412-1419.

Zemel, B., 1995. *Tracers in the Oil Field.* Amsterdam, The Netherlands: Developments in Petroleum Science, Elsevier Science.

Zhang, G., Yu, J., Du, C. & Lee, R., 2015. *Formulation of Surfactants for Very Low/High Salinity Surfactant Flooding without Alkali,* The Woodlands, Texas: SPE International Symposium on Oilfield Chemistry, 13-15 April.

Zhang, K. et al., 2015. *Future Trends for Tight Oil Exploitation,* Cairo, Egypt: SPE North Africa Technical Conference and Exhibition, 14-16 September.

Zhao, L., 2007. Steam Alternating Solvent Process. *SPE Reservoir Evaluation & Engineering,* 10(02), pp. 185-190.

Zheng, C. et al., 2000. Effects of Polymer Adsorption and Flow Behaviour on Two-Phase Flow in Porous Media. *SPE Reservoir Evaluation & Engineering,* 3(03), pp. 216-223.